ANA LAURA ALMEIDA DOS
SANTOS

Planárias terrestres (Platyhelminthes, Geoplanidae) do Chile: taxonomia integrativa e descoberta de novos táxons endêmicos

Land planarians (Platyhelminthes, Geoplanidae) from Chile: integrative taxonomy and discovery of new endemic taxa

v. único

SÃO PAULO

2021

ANA LAURA ALMEIDA DOS
SANTOS

Planárias terrestres (Platyhelminthes, Geoplanidae) do Chile: taxonomia integrativa e descoberta de novos táxons endêmicos

Land planarians (Platyhelminthes, Geoplanidae) from Chile: integrative taxonomy and discovery of new endemic taxa

v. único

Versão original

Tese submetida ao Programa de Pós-Graduação do Museu de Zoologia da Universidade de São Paulo em cumprimento parcial aos requisitos para a obtenção do título de Doutor em Ciências (Sistemática, Taxonomia Animal e Biodiversidade).

Orientador: Prof. Dr. Fernando Jesús Carbayo Baz

SÃO PAULO

2021

Catalogação na Publicação
Serviço de Biblioteca e Documentação
Museu de Zoologia da Universidade de São Paulo

Santos, Ana Laura Almeida dos
Planárias terrestres (Platyhelminthes, Geoplanidae) do Chile: taxonomia integrativa e descoberta de novos táxons endêmicos. = Land planarians (Platyhelminthes, Geoplanidae) from Chile: integrative taxonomy and discovery of new endemic taxa. / Ana Laura Almeida dos Santos; orientador Fernando Jésus Carbayo Baz. São Paulo, 2021.
235p.

Tese submetida ao Programa de Pós-Graduação do Museu de Zoologia Museu de Zoologia da Universidade de São Paulo, em cumprimento parcial aos requisitos para obtenção do título de doutor em Ciências (Sistemática, Taxonomia Animal e Biodiversidade).
Versão original
Volume único

1. Platyhelminthes – Geoplanidae - Chile 2. Geoplanidae - taxonomia. I. Carbayo B., Fernando Jésus, orient. II. Título.

CDU 595.123(83)

CRB-8 3805

ALMEIDA DOS SANTOS, Ana Laura

Land Planarians (Platyhelminthes, Geoplanidae) from Chile: integrative taxonomy and discovery of new endemic taxa

Planárias terrestres (Platyhelminthes, Geoplanidae) do Chile: taxonomia integrativa e descoberta de novos táxons endêmicos

Tese submetida ao Programa de Pós-Graduação do Museu de Zoologia da Universidade de São Paulo em cumprimento parcial aos requisitos para a obtenção do título de Doutor em Ciências (Sistemática, Taxonomia Animal e Biodiversidade).

Data de aprovação: _____/_____/_____

COMISSÃO JULGADORA

Prof. Dr._____ Instituição:_____

Decisão: _____ Assinatura:_____

Prof. Dr._____ Instituição:_____

Decisão: _____ Assinatura:_____

Prof. Dr._____ Instituição:_____

Decisão: _____ Assinatura:_____

Prof. Dr._____ Instituição:_____

Decisão: _____ Assinatura:_____

Prof. Dr._____ Instituição:_____

Decisão: _____ Assinatura:_____

Dedico essa tese ao meu filho, à minha mãe e à memória do meu pai, com todo amor, carinho e gratidão.

AGRADECIMENTOS

À minha mãe Nilda, ao meu filho Ri e ao meu companheiro Jur pelo amor, cuidado, força, carinho e apoio. Estendo esses agradecimentos à todos os membros da minha família, em especial, aos meus entes do estado da Paraíba por serem tão bons, simples, acolhedores, generosos e amáveis. Agradeço à minha amiga Vitória Albino e à toda a sua sua família, pela acolhida e gentileza de sempre.

Aos meus colega de laboratório, e em especial aos amigos Ana Paula Goulart Araújo, Beatriz Santos, Bianca Luján, Ítalo Silva, Karine Gobetti, Khatarine Camelo, Marcos Silva e Laura Bolonhezi por toda generosidade e o apoio.

Ao meu orientador, Prof. Dr. Fernando Carbayo por sua massiva contribuição em tudo o conteúdo que compreende esta tese e à Domingo Lago-Barcia pela revisão de inglês do artigo que compreende o primeiro capítulo dessa tese.

Ao professor Pudim por toda a sua generosidade e humanidade. Por ser sempre prestativo e ajudar tanto os alunos em suas pesquisas. Agradeço-o por tornar o ambiente descontraído e agradável e por nos enriquecer sempre com suas conversas de variados assuntos, qque sempre acrescetam muito em conhecimento. A conclusão dessa tese se deve muito a você, Prof. Pudim, e aos maravilhosos amigos Ana Paula Goulart Araújo, Beatriz Santos, Bianca Luján, Marcos Silva e Maytê Suguimoto, pela força e sustentação que me forneceram. Tenho muita sorte e me considero muito privilegiada em ter convivido e aprendido com vocês. Sou grata do fundo do meu coração. Obrigada por existirem!

Aos meus amigos Gislaine Banchetti, Viviane Capetine, Luis Henrique Marins e Andréia de Lira, pois são muito responsáveis por eu ter conseguido concluir este doutorado. Vocês são maravilhosos! Muito obrigada por tudo o que fizeram por mim! Amos vocês! Aos amigos Amanda Cseh, Ana Cristina Machado, Gabi, Denis.

À Ana Claudia Elias, por toda a força e consolo que me deu durante o longo período de hospitalização do meu pai e seu falecimento no fim do meu primeiro ano de doutorado. Agradeço também à todas as muitas outras pessoas que também me deram forças nesse momento dor.

À todos os professores da educação básica pública do país, que tem passado por um momento (de pandemia) muito desafiador em sua função de bem formar

cidadãos. Em especial, agradeço aos meus professores do ensino básico, Vera Lúcia, João Paulo, Deise, Meire, Sergio, Jovem, Rose, Alberto, Danielle, Gilson, Sandro, e muitos outros, os quais não vou me recordar de citá-los aqui, mas sou igualmente grata. Transformaram os rumos da minha vida e os de muitos outros estudantes em sua fase inicial de formação. Gratidão.

Aos técnicos do laboratório de histologia da EACH-USP, Geison Castro da Silveira e Lucas Beltrami, pelas preparações histológicas dos espécimes que estudei na execução desse projeto. Agradeço aos técnicos Beatriz Vieira Freire, Manuel Antunes Junior e Sabrina Baroni, do laboratório de Biologia Molecular do Departamento de Zoologia do IB-USP, por toda a dispnibilidade em prestar eventuais auxílos durante meu trabalho de obtenção de sequências nucleotídicas para este projeto.

Ao Prof. Dr. Tiago Francoy por sua gentil colaboração com a parte molecular do artigo que compõe o primeiro capítulo dessa tese. Agradeço à Dra. Marta Álvares-Prezas por sua intensa e generosa colaboração com toda a parte molecular desse projeto. Agradeço a Laura Bolonhezi pela colaboração no estudo taxonômico de uma das espécies novas apresentadas aqui.

Aos Profs. Drs. Luis Paulo de Moura Andrioli e Pedro Dias, por terem me permitido trabalhar em seus laboratórios (EACH-USP) de biologia molecular na fase inicial desse projeto. Agradeço aos Profs. Drs. Marcelo Duarte, Ricardo Pinto-da-Rocha e Pedro Gnaspini por suas contribuições quanto membros da minha banca de qualificação. Ao Dr. José Grau por envio de material biológico de duas das espécies estudadas nessa tese. Ao Dr. Ronald Sluys e José Grau, que colaboram comigo e com meu orinetador na proposta de um novo gênero de planária.

À Agência USP Mulheres pelo acolhimento e ao Instituto de Psicologia da USP, que realizou gratuitamente atendimentos psicológicos gratuitos à toda a comunidade USP durante a pandemia causada pela Covid-19, em especial ao Murilo, quem me atendeu.

Ao MZUSP e aos seus funcionários pela gentileza e prestatividade, à EACH-USP, onde meu projeto foi desenvolvido, e ao IB-USP, onde realizei grande parte dos trabalhos de DNA. O presente trabalho foi realizado com apoio da Coordenação de Aperfeiçoamento de Pessoal de Nível Superior - Brasil (CAPES) - Código de Financiamento 001. (Proc. 88882.378126/2019-01).

“*Nada é permanente, exceto a mudança*.”

Heráclito de Éfeso.

RESUMO

Geoplanidae compreende mais de 900 espécies e está dividida em quatro subfamílias: Bipaliinae Stimpson, 1857 (cosmopolita), Geoplaninae Stimpson, 1857 (neotropical), Microplaninae Pantin, 1853 (cosmopolita) e Rhynchodeminae Graff, 1896 (cosmopolita). Grande parte dos estudos taxonômicos de planárias terrestres do continente sul americano trata de espécies ao Leste dos Andes, especialmente das regiões sul e sudeste do Brasil, e da Argentina. A diversidade de planárias de países ao Oeste dos Andes, como o Chile, ainda é pouco conhecida. As 28 espécies conhecidas do Chile pertencem a Rhynchodeminae (1), Timyminae (2) e a Geoplaninae (25). As 14 espécies dos gêneros *Geoplana, Pasipha e Pseudogeoplana* têm posição taxonômica incerta. As demais espécies pertencem aos gêneros *Gusana* (2); *Liana* (1), *Pichidamas* Bulnes (1), *Inakayalia* (3) e *Polycladus* (1), todos endêmicos, exceto *Inakayalia*, que também ocorre nos Andes argentinos. Nesta tese, é conduzido o estudo morfológico e molecular de 20 espécimes recentemente coletados, que resultou na descrição de 15 novas espécies, e na redescrição de outra. Para esta abordagem integrativa, lâminas histológicas foram examinadas ao microscópio, e foram sequenciados os genes mitocondrial COI e nuclear rDNA 28S. Filogenias foram otimizadas usando máxima verossimilhança e inferência bayesiana. Ainda, as espécies de *Gusana* estudadas foram delimitadas com um método baseado nas distâncias genéticas. O Capítulo 1 da tese, já publicado, é um estudo sobre *Timyma*, antes considerado como um relicto sul-americano de um táxon Gondwânico. Os resultados mostram que *Timyma* é grupo irmão de Geoplaninae e é filogeneticamente distante de Bipaliinae. Este relacionamento contradiz a hipótese de *Timyma* como táxon Gondwânico e indica que a cabeça em forma de leque evoluiu independentemente em *Timyma* e em Bipaliinae. Consequentemente, *Timyma* é rediagnosticado e uma nova subfamília é proposta para o gênero. O Capítulo 2 trata da descrição de quatro novas espécies de *Gusana* e o gênero é rediagosticado. No Capítulo 3, são descritas 10 novas espécies e é testado seu posicionamento filogenético na família Geoplanidae. As filogenias apontam que as espécies chilenas mais os representantes de Geoplaninae, formam um grupo monofilético. Por sua vez, este grupo está dividido em 9 clados principais com 1-4 gêneros, 6 dos quais são gêneros novos aqui propostos. Um dos clados principais

abriga todas as espécies de Geoplaninae ocorrentes ao Leste dos Andes mais uma espécie do Chile. Os outros 8 clados principais são exclusivos do Chile, excetuando *Inakayalia*, que ocorre também nos Andes argentinos. Um clado principal acomoda Timyminae, que é recuperado como irmão de um dos oito clados principais, e não como irmão de Geoplaninae. Cada um destes nove clados e cada um dos novos gêneros pode ser diagnosticado por sinapomorfias morfológicas putativas. Em vista da divergência entre as árvores filogenéticas e a classificação atual, uma nova classificação de Geoplaninae é proposta, Geoplaninae é rediagnosticada, Geoplaninae e Timyminae são rebaixadas a tribo e sete novas tribos são propostas. Este estudo expande consideravelmente o conhecimento da diversidade taxonômica e morfológica das planárias terrestres neotropicais e ilustra a importância da taxonomia integrativa para a classificação dos organismos.

Palavras-chave: Platelmintos terrestres. Taxonomia integrativa. Morfologia. Histologia. Sistemática filogenética

ABSTRACT

Geoplanidae comprises approximately 900 species and is divided into four subfamilies: Bipaliinae Stimpson, 1857 (cosmopolitan), Geoplaninae Stimpson, 1857 (neotropical), Microplaninae Pantin, 1853 (cosmopolitan), and Rhynchodeminae Graff, 1896 (cosmopolitan). A substantial part of the taxonomic studies of land planarians from South American dealt with species from the East of the Andes, especially from the southern and southeastern regions of Brazil, and from Argentina. The diversity of Geoplanidae from West of the Andes, such as Chile, is still little known. The 28 known species described from Chile belong to Rhynchodeminae (1), Timyminae (2) and Geoplaninae (25). Within Geoplaninae, the 14 species of the genera *Geoplana*, *Pasipha* and *Pseudogeoplana* have uncertain taxonomic position. The other species are housed in the genera *Gusana* (2); *Liana* (1), *Pichidamas* (1), *Inakayalia* (3) and *Polycladus* (1), all endemic, except *Inakayalia*, which occurs in the Argentinean Andes. In this thesis, the morphological and molecular studies of 20 recently collected specimens resulted in the description of 15 new species, and the redescription of 1 species. For this integrative approach, histological slides were examined under the microscope and the mitochondrial COI and nuclear rDNA 28S genes were sequenced. Phylogenies were inferred using maximum likelihood and Bayesian inference as optimality criteria. Furthermore, the *Gusana* species studied here were delimited with a genetic distances method. Chapter 1 of the thesis, already published, is a study on *Timyma*, taxon considered as a South American relict of the Gondwana. The results show that *Timyma* is the sistergroup of Geoplaninae and is phylogenetically distant from Bipaliinae. This relationship contradicts the hypothesis of *Timyma* as a Gondwanic taxon and indicates that the semilunate headplate evolved independently in *Timyma* and Bipaliinae. Consequently, *Timyma* is re-diagnosed and a new subfamily is proposed for the genus. Chapter 2 deals with the description of four new species of *Gusana* and a re-diagnosis of the genus. In Chapter 3, 10 new species are described and their phylogenetic position in the Geoplanidae family is tested. The phylogenies indicate that these species plus the representatives of Geoplaninae, form a monophyletic group. In turn, this group is divided into 9 main clades with 1-4 genera each, 6 of which are new genera proposed here. One of the main clades houses all species of Geoplaninae

occurring East of the Andes plus one species from Chile. The other 8 main clades are exclusive to Chile, except for *Inakayalia*. One main clade accommodates Timyminae, which is sister to one of the other eight main clades. Each of these clades and each of the new genera can be diagnosed by putative morphological synapomorphies. In view of the divergence between the phylogenetic trees and the current classification, a new classification of Geoplaninae is proposed and Geoplaninae is re-diagnosed. Furthermore, Geoplaninae and Timyminae are down-ranked to tribe and seven new tribes are proposed. This study considerably expands the knowledge of the taxonomic and morphological diversity of neotropical Geoplanidae and illustrates the integrative taxonomy importance for the classification of living organisms.

Keywords: Land flatworms. Integrative taxonomy. Morphology. Histology. Phylogenetic systematics.

SUMÁRIO

INTRODUÇÃO GERAL

a) Planárias terrestres: classificação e riqueza.

As planárias terrestres (Geoplanidae, Platyhelminthes) são vermes de vida livre denominados tricládidos por apresentarem intestino organizado em três ramos principais. Estes animais possuem forma do corpo variando entre achatado dorso-ventralmente e subcilíndrico, e comprimento que varia de poucos milímetros até, excepcionalmente, um metro (especialmente em espécies asiáticas). Esses animais são sensíveis à luz e perdem os líquidos corpóreos com muita facilidade. Uma solução adaptativa que contorna essas limitações é o hábito noturno de vida; durante o dia, se abrigam embaixo de troncos caídos na floresta e embaixo de rochas (Carbayo, 2005). São hermafroditas, de reprodução sexuada, e predadores de pequenos invertebrados, tais como: minhocas, opiliões, lesmas, nemertinos, etc. (Cseh *et al.*, 2017).

As planárias terrestres são animais de baixa vagilidade e, rios, montanhas, áreas desmatadas, entre outros, são barreiras geográficas para sua dispersão (Álvarez-Presas *et al.*, 2011). Tais características tornam as planárias terrestres modelos potenciais para o estudo de Biogeografia (Sunnucks *et al.*, 2006; Alvarez-Presas *et al.*, 2011).

Esses organismos são Platelmintos da ordem Tricladida Lang, 1881. Tricladida é dividida em três subordens: Maricola Hallez, 1892, Cavernicola Sluys, 1990 e Continenticola Carranza et al., 1998, sendo esta última composta por planárias de água doce e planárias terrestres. Dentro de Continenticola há duas superfamílias, Planairoidea e Geoplanoidea, esta última abarca algumas espécies de planárias de água doce e todas as espécies de planárias terrestres. E, finalmente, a família Geoplanidae Stimpson, 1857 é exclusiva de planárias terrestres.

Existem formalmente cinco subfamílias em Geoplanidae: Bipaliinae Stimpson, 1857, Geoplaninae Stimpson, 1857, Microplaninae Pantin, 1853, Rhynchodeminae Graff, 1896 e Timyminae Almeida & Carbayo, 2021 (in Almeida et al., 2021), entre as quais se distribuem cerca de 900 espécies (Carbayo, *et. al.*, 2013). As subfamílias Bipaliinae, Microplaninae e Rhynchodeminae possuem distribuição cosmopolita,

enquanto que a subfamília Geoplaninae é exclusiva da região Neotropical, com representantes nas regiões à leste e à oeste da Cordilheira dos Andes (Carbayo, *et al.,* 2013; Grau & Carbayo, 2010, Froehlich, 1957; Winsor *et al.* 1998).

A subfamília Geoplaninae, com 346 espécies nominais (http://planarias.each.usp.br; acesso em 19 junho 2021), foi principalmente estudada por Schirch (1929), Riester (1938), Hyman (1939, 1941, 1955, 1957, 1962), Marcus (1951), Du Bois Reymond-Marcus (1951a), Froehlich (1955a, b, 1956a, b, 1959, 1967), E. M. Froehlich (1955, 1978), E. M. Froehlich e Froehlich (1972), Carbayo e Leal-Zanchet (2003), Leal-Zanchet e Souza (2003), Carbayo *et. al.*, (2013), Negrete & Brusa (2012, 2018), Negrete *et al*., (2010, 2011, 2014, 2015, 2016, 2019, 2020).

Apesar dos esforços realizados pelos pesquisadores, os estudos taxonômicos de planárias terrestres no continente Sul Americano são principalmente oriundos das porções sul e sudeste da Mata Atlântica brasileira e, em menor quantidade, proveniente do território Argentino. Pouco se conhece dessa fauna em outros países da América do sul, especialmente da porção oeste dos Andes, como o Chile.

As planárias terrestres chilenas conhecidas pela Ciência compreendem 28 espécies (Grau & Carbayo, 2010, Bulnes & Carbayo, 2018, Almeida *et al*., 2021), de ocorrência registrada desde as proximidades do rio Huasco (28º S), na região do Atacama, até o Parque Nacional Laguna San Rafael (46º S). Estas espécies estão alocadas na subfamília Rhynchodeminae, Timyminae e, principalmente em Geoplaninae.

b) Histórico de estudo das planárias terrestres do Chile.

A fauna de planárias terrestres do Chile, com 28 espécies, é proveniente de coletas apenas esporádicas. Muitas descrições de espécies foram realizadas a partir apenas de aspectos externos da morfologia dos indivíduos, ou, quando incluindo informações de microanatomia interna, apresentando informações taxonomicamente importantes de forma incompleta, especialmente em ocasiões em que espécimes-tipo são imaturos (Grau & Carbayo, 2010).

O estudo da fauna de planárias terrestres chilena teve início durante o século XIX, com o famoso naturalista inglês Charles Darwin, que atracou na costa do Chile durante uma expedição a bordo do navio HMS Beagle. Darwin examinou e descreveu quatro espécies de planárias: *Planaria elongata*, *Planaria maculata*, *Planaria pallida* e *Planaria semilineata* (Darwin, 1844). Apenas descreveu o aspecto externo dos animais. Atualmente, as quatro espécies estão alocadas no gênero *Pseudogeoplana* Ogren & Kawakatsu, 1990. Este gênero foi proposto para espécies insuficientemente conhecidas para uma classificação inequívoca (Ogren & Kawakatsu, 1990).

Charles Blanchard descreveu outra espécie chilena, *Polycladus gayi* Blanchard, 1845, espécie consideravelmente grande e que causou confusão, pois o autor inverteu a posição da cabeça com a da cauda e, assim, considerou erroneamente que os poros do corpo se situavam na metade anterior do corpo (Moseley, 1877).

Ainda no final do século XIX, Ludwig von Graff (1899) realizou um profundo estudo taxonômico de espécies de vários países do mundo. Graff estudou e descreveu, com riqueza de detalhes, nove espécies de planárias do Chile, a saber, *Geoplana albopunctata*, *Geoplana chilensis*, *Geoplana cruciata*, *Geoplana lata*, *Geoplana nobilis*, *Geoplana pardalina*, *Geoplana platei*, *Geoplana reticulata* e *Geoplana sagittata,* a partir de espécimes que recebeu de doação (Graff, 1899). Nenhuma destas espécies está atualmente em *Geoplana*. *Geoplana chilensis* foi transferida para *Pasipha*; *Geoplana cruciata, Geoplana lata* e *Geoplana platei* foram transferidas para *Gusana* e, as demais espécies foram alocada em *Pseudogeoplana.* Nesse trabalho, Graff ainda revisou algumas descrições de Darwin e estudou também a morfologia interna de *Polycladus gayi*.

Ernest Marcus estudou, entre planárias marinhas e de água doce, uma planária terrestre do Chile. Todos esses espécimes são oriundos de coletas realizadas pela Universidad Sueca de Lund durante uma expedição naquele país (1948-1949). A espécies chilena *Amaga ruca* (Marcus, 1954) foi, recentemente, reestudada e transferida para o novo gênero *Wallmapuplana* Negrete *et al.*, 2020.

C. G. Froehlich (1967) fez algumas considerações biogeográficas sobre as planárias terrestres. Para Froehlich, as espécies chilenas paralelas ao gênero *Artioposthia* Graff,

1896 são particularmente interessantes para fins biogeográficos porque apresentam características morfológicas tidas como primitivas na época. Uma destas características é a presença de testículos ventrais, como ocorre nas espécies da região Australiana, e não dorsais, como é típico em Geoplaninae, táxon restrito à região Neotropical. Para o autor, isso seria uma evidência da antiga união entre América do Sul, Austrália e Nova Zelândia e, portanto a fauna das Geoplanidae do continente Sul Americano teria duas origens geográficas distintas: neotropical e australiana (C. G. Froehlich, 1967).

Um dos trabalhos mais completos sobre taxonomia de planárias do Chile foi realizado por E. M. Froehlich (1978), onde foram descritas sete espécies novas, outras duas espécies antes conhecidas foram redescritas e três gêneros novos e endêmicos do Chile foram propostos: *Gusana* Froehlich, 1978*, Liana* Froehlich, 1978 e *Timyma* Froehlich, 1978*.* Trabalhos mais atuais e também esporádicos contribuem vagarosamente para o conhecimento dessa fauna (Grau & Carbayo, 2010; Grau & Carbayo, 2011; Grau *et al.*, 2012; Bulnes et al., 2018, Negrete et al., 2020, Almeida et al., 2021).

c) Composição da fauna chilena de planárias terrestres.

As planárias terrestres (Platyhelminthes, Geoplanidae) do Chile compreendem 28 espécies, distribuídas em três subfamílias. Geoplaninae Stimpson, 1857, de distribuição exclusivamente neotropical, é a subfamília com mais representantes do Chile, com quatro espécies em três gêneros endêmicos: *Gusana*, *Liana* e *Pichidamas*. Ocorrem também no Chile uma espécie de Caenoplanini Ogren & Kawakatsu, 1991 (Rhinchodeminae Graff, 1896, subfamília de distribuição cosmopolita), e duas espécies de *Timyma*, alocadas na recém proposta subfamília Timyminae Almeida *et al.*, 2021, conhecida apenas do Chile.

Outras cinco espécies chilenas que antes estavam alocadas em *Geoplana* Stimpson, 1857, foram, após uma revisão do gênero (Almeida *et al*., 2019), retiradas de *Geoplana* e permanecem sob o status de *incertae sedis*. Além destas, são registradas para o Chile outras 9 espécies de planárias de *Pseudogeoplana* Ogren & Kawakatsu, 1990, grupo

que comporta espécies insuficientemente conhecidas em termos morfológicos e que, portanto, impossibilita uma classificação inequívoca. As subfamílias Bipaliinae Stimpson, 1857 e Microplaninae Pantin, 1953 não têm representantes no Chile.

Apesar dos esforços em se conhecer as planárias terrestres do Chile, muitas descrições carecem de informações morfológicas taxonomicamente importantes e, por isso, são insuficientes para a devida identificação. Considerando a quantidade atual de espécies conhecidas e coletas preliminares, estima-se que o número real para aquele país seja muito superior ao que se conhece (Grau & Carbayo, 2010).

Em expedições recentes realizadas no Chile, principalmente em dezembro de 2010, por Carbayo e colaboradores, foi coletada uma quantidade expressiva de espécimes, incluindo animais de regiões não exploradas previamente com esta finalidade. Análises preliminares apontaram que muitos dos animais representam novos táxons. Estes animais foram fixados à maneira de facilitar estudos morfológicos e moleculares, e descortinam uma oportunidade excepcional para ampliar o conhecimento taxonômico e sistemático das planárias neotropicais. Através do estudo destes animais, nossos objetivos são ampliar o conhecimento sobre a diversidade morfológico-taxonômica e propor hipóteses de relacionamento filogenético entre Geoplaninae.

Os resultados desse estudo reforçam o que já supunham Grau & Carbayo (2012), de que a riqueza de espécies chilenas conhecidas pela Ciência é subestimada em relação a sua real condição. Essa tese está dividida em três capítulos. No capítulo I, é redescrita *Timyma juliae* Froehlich, 1978, e descrita uma nova espécie do gênero. A partir de dados moleculares, também é inferida uma hipótese de relacionamento filogenético de *Timyma* com as demais Geoplanidae e proposta uma nova subfamília. Este trabalho já está publicado e, aqui, apresentamos a versão aceita para publicação no periódico *Zoologia Scripta*. No capítulo II, apresentamos quatro espécies novas de *Gusana* e suas relações filogenéticas com as demais Geoplaninae. No capítulo III, apresentamos uma hipótese de relacionamento filogenético entre as espécies chilenas e a demais Geoplanidae, descrevemos uma espécie nova de *Pichidamas*, e mais nove espécies novas distribuídas em sete novos gêneros aqui propostos. Os gêneros são alocados em um total de nove novas tribos de Geoplaninae. Esta visão ampliada da diversidade morfológica e taxonômica implicou, também, na rediagnose de

Geoplaninae, a proposição de Geoplanini para a maior parte das espécies ao Leste dos Andes, e o re-ranquamento de Timyminae, que passa a ser considerada tribo.

REFERÊNCIAS GERAIS

Almeida, A.L.; Marques, F.P.L. & Carbayo, F. 2019. 'Endless forms most beautiful': taxonomic revision of the planarian *Geoplana vaginuloides* (Darwin, 1844) and discovery of numerous congeners (Platyhelminthes: Tricladida). *Zoological Journal of the Linnean Society*. 185 (1): 1-65. doi:10.1093/zoolinnean/zly022.

Almeida, A. L, Francoy T. M, Álvarez-Presas M. & Carbayo F. 2021. Convergent evolution: A new subfamily for bipaliin-like Chilean land planarians (platyhelminthes). Zool Scr. 2021; 00:1–9. https://doi.org/10.1111/zsc.12479

Álvarez-Presas, M., Carbayo, F., Rozas, J., & Riutort, M. (2011). Land planarians (Platyhelminthes) as a model organism for finescale phylogeographic studies: Understanding patterns of biodiversity in the Brazilian Atlantic Forest hotspot. Journal of Evolutionary Biology, 24, 887–896. https://doi. org/10.1111/j.1420-9101.2010.02220.x

Blanchard, É. (1847). Sur lórganisation des vers. Chapitre IV. A*nnales des Sciences Naturelles. Troiseéme Série Zoologie*, 8: 119-149.

Boll, P. K. & Leal-Zanchet, A. M. 2018. Diversity out of simplicity: interaction behavior of land planarians with co-occurring invertebrates.

Bulnes, V. N.; Grau, J. H. & Carbayo, F. 2018. A new Chilean genus and species of land planarian (Platyhelminthes: Tricladida, Geoplaninae) with cephalic retractor muscle and adenodactyl. *Jornal of Natural History,* 56: 2553-2566.

Carbayo, F. 2005. Procedimentos de campo e laboratório para a caracterização das planárias terrestres neotropicais (Platyehlminthes: Tricladida). *Caderno La Salle XI*. 2 (1): 131-144.

Carbayo, F. & Leal-Zanchet, A. M. 2003. Two new genera of geoplaninid land planarians (Platyhelminthes: Tricladida: Terricola) of Brazil in the ligh of cephalic

specializations. *Invertebrate Systematics*, 17: 449–468.

Carbayo, F.; Álvarez-Presas, M.; Olivares, C. T.; Marques, F. P. L.; Froehlich, E. M. & Riutort, M. 2013. Molecular phylogeny of Geoplaninae (Platyhelminthes) challenges current classification: proposal of taxonomic actions. *Zoologica Scripta* 42: 508-528.

Carranza, S., Ruiz-Trillo, I., Littlewood, D. T. J., Riutort, M. & Baguña, J. 1998a. A reappraisal of the phylogenetic and taxonomic position of land planarians (Platyhelminthes, Turbellaria, Tricladida) inferred from 18S rDNA sequences. Pedobiologia, 42, 433–440.

Carranza, S., Littlewood, D. T. J., Clough, K. A., Ruiz-Trillo, I., Baguña, J. & Riutort, M. 1998b. A robust molecular phylogeny of the Tricladida (Platyhelminthes: Seriata) with a discussion on morphological synapomorphies. Proceedings of the Royal Society of London. Series B: Biological Sciences, 265, 631–640.

Cseh, A., Carbayo, F. &Froehlich, E. M. 2017. Observations on food preference of Neotropical land planarians (Platyhelminthes), with emphasis on Obama anthropophila, and their phylogenetic diversification. Zoologia (Curitiba), 34: 1984-4689. https://doi.org/10.3897/zoologia.34.e12622.

Darwin C. 1844. Brief descriptions of several terrestrial planariae and of some remarkable marine species, with an account of their habits. Ann. Mag. Nat. Hist. 14: 241–251.

Froehlich, C.G. 1955. Sobre morfologia e taxonomia das Geoplanidae. Boletim da Faculdade de Filosofia, Ciências e Letras da Universidade de São Paulo, São Paulo, Sér. Zoologia, 19 (16): 289-369.

Froehlich, C. G. (1955c). Notas sobre geoplanas brasileiras. *Papeis Avulsos do Departamento de Zoologia*, 12, 189–198.

Froehlich, C. G. (1956). Tricladida Terricola das regiões de Teresópolis e Ubatuba. Papéis Avulsos do Departamento de Zoologia 12(16), 313-344.

Froehlich, C. G. (1956b). Planáarias Terrestres do Paraná. Dusenia, 7, 173–196.

Froehlich, G. C. 1959. On geoplanids from Brazil. *Bol. Fac. Fil. Ci. Letras, Univ. São Paulo,* Zool., 22: 201-265.

Froehlich, C. G. 1967. A contribution to the zoogeography of neotropical land planarians. Acta Zool. Lilloana, 23: 153-167.

Froehlich, E. M. & Froehlich, C. G. (1972). Land planarians from the Amazonian Region. Papeis Avulsos do Departamento de Zoologia, 26, 29–45.

Froehlich, E. M. 1978. On a collection of chilean land planarians. Boletim de Zoologia, Universidade de São Paulo, 3: 7-80.

Graff, L. von. 1896. Ueber das System und die geographische Verbreitung der Landplanarien. *Verhandl Deutsch Zoolog Ges*, 6: 75-93.

Graff, L. V. (1899). Monographie der Turbellarien. II. Tricladida terricola (Landplanarien). Engelmann.

Grau, J. H., & Carbayo, F. (2010). Panorama de la diversidad de planarias terrestres (Platyhelminthes: Tricladida) de Chile. Boletín de Biodiversidad de Chile, 2, 41–54.

Grau JH, Carbayo F. 2011. A new land planarian species of *Geoplana* (Platyhelminthes, Tricladida, Geoplanidae) from the Valdivian temperate rainforest of southern Chile. Zoosyst. Evol. 87:327–334.

Grau, J., Sluys, R. Froehlich, E. M. & Carbayo, F. 2012. Reflections on the genus Amaga Ogren and Kawakatsu 1990, and description of a new genus of land planarian (Platyhelminthes: Tricladida: Geoplanidae). Jour. of Nat. Hist,, 46: 1529-1546.

Hyman, L. H. 1939. Land planarians from the Hawaiian Islands. Archives de Zoologie Expérimentale et Genérale, 80, 116-124.

Hyman, L. H. 1941. Terrestrial flatworms from the Canal Zone, Panama. American Museum Novitates, 1105, 1–11.

Hyman, L. H. 1955. Miscellaneous marine and terrestrial flatworms from South America. American Museum Novitates, 1742, 1–33.

Hyman, L. H. 1957. A few turbellarians from Trinidad and the Canal Zone, with corrective remarks. American Museum Novitates, 1862, 1–8.

Hyman, L. H. 1962. Some land planarians from Caribbean countries. American Museum

Novitates, 2110, 1–25.

Leal-Zanchet, A. M. & Carbayo, F. 2001. Two new species of Geoplanidae Platyhelminthes, Tricladida, Terricola) from Brazil. Journal of Zoology, 253, 433–446.

Leal-Zanchet, A. M & Souza, S. A. 2003. Redescrição de Choeradoplana iheringi Graff (Platyhelminthes, Tricladida, Terricola). *Revista Brasileira de Zoologia,* 20(3): 523-530.

Leal-Zanchet, A. M. & Froehlich, E. M. 2006. A species complex in the genus Notogynaphallia Ogren and Kawakatsu (Platyhelminthes: Tricladida: Terricola) with a taxonomic revision of homonyms of Geoplana marginata Schultze & Müller and a reinterpretation of Notogynaphallia caissara (Froehlich) anatomy. Belgian Journal of Zoology, 136, 81–100.

Lemos, V. S. & Leal-Zanchet, A. M. 2008. Two new species of Notogynaphallia Ogren & Kawakatsu (Platyhelminthes: Tricladida: Terricola) from Southern Brazil. Zootaxa, 1907, 28-46

Marcus, E. 1951. Turbellaria brasileiros (9). Boletins da Faculdade de Filosofia, Ciências e Letras da Universidade de São Paulo, Série Zoologia 16: 5–215.

Marcus, E., 1954. Reports of the Lund University Chile Expedition 1948-1949. II. Turbellaria. Acta Universitet Lund, 49: 1-115.

Moseley, H. N., 1877. Notes on the structure of several forms of land planarians, with a description of two new genera and several new species, and a list of all species at present known. Quarterly Journal of Microscopical Science, 17: 273-292.

Negrete, L. H. L., Brusa, F. & Carbayo, F. 2010. A new peruvian land planarian species of the genus Gigantea (Platyhelminthes, Tricladida, Geoplanidae). Zootaxa, 2422: 43-52.

Negrete, L. & Brusa, F. 2012. Choeradoplana crassiphalla sp. nov. (Platyhelminthes: Tricladida: Geoplanidae): A new species of land planarian from the Atlantic Forest of Argentina. *Studies on Neotropical Fauna and Environment*, 47: 227-237.

Negrete, L. & Brusa, F. 2016. Land flatworms of the genus Pasipha (Platyhelminthes, Geoplanidae) in Argentina, with description of three new species. Zootaxa, 4137(4): 187-210.

Negrete, L. & Brusa, F. 2016. First report of the genus Cratera (Platyhelminthes, Geoplanidae) in Argentina, with description of a new species and comments on the species of the genus. ZooKeys, 610: 1-12. DOI: 10.3897/zookeys.610.9465

Negrete, L. H. L., Brusa, F. & Winsor, L. 2011. The blue land planarian Caenoplana coerulea, an invader in Argentina. Revista Mexicana de Biodiversidad, 82: 287-291.

Negrete, L. H. L., Brusa, F. & Damborenea, C. 2012. A new species of Geoplana (Platyhelminthes: Tricladida: Geoplanidae) from the Western Amazon basin with comments on the land planarian fauna from Peru. *Zootaxa*, 3358: 55-67.

Negrete, L. H. L., Colpo, K. D. & Brusa. 2014. Land planarian assemblages in protected areas of the interior atlantic forest: Implications for conservation. 9(3): e90513. https://doi.org/10.1371/journal.pone.0090513.

Negrete, L., Leal-Zanchet, A.M. & Brusa, F. 2015. A new species of *Notogynaphallia*(Platyhelminthes, Geoplanidae) extends the known distribution of land planarians in Chacoan province (Chacoan subregion), South America. *Zool. Stud.* 54, 58. https://doi.org/10.1186/s40555-015-0136-5

Negrete, L., H. L., Gira, R. D., & Brusa, F. 2019. Two new species of land planarians (Platyhelminthes, Tricladida, Geoplanidae) from protected areas in the southern extreme of the Paranaense Rainforest, Argentina. Zoologischer Anzeiger 279, 38–51. doi:10.1016/j.jcz.2019.01.002

Negrete, L., Álvarez-Presas, M., Riutort, M. and Brusa, F. 2020. Integrative taxonomy of land planarians (Platyhelminthes: Geoplanidae) from the Andean-Patagonian Forests from Argentina and Chile, with the erection of two new genera. Journal of Zoological Systematics and Evolutionary Research 00, 1-25. doi: 10.1111/jzs.12444

Negrete, L., Amaral, S. V., Ribeiro, G. G., Gonçalves, J. W., Valiati, V. H., Damborenea, C., Brusa, F. & Leal-Zanchet, A. M. 2020. Far away, so close! Integrative taxonomy reveals a new genus and species of land flatworm (Platyhelminthes: Geoplanidae) from southern South America, Zoological Journal of the Linnean Society, 189(3): 722–744,

https://doi.org/10.1093/zoolinnean/zlz131

Ogren, R. E. & Kawakatsu, M. 1990. Index to the species of the family Geoplanidae (Turbellaria, Tricladida, Terricola) Part I: Geoplaninae. *Bulletin of Fujis Women's College*. 29: 79-166.

Ogren, R. E. & Kawakatsu, M. 1991. Index to the species of the family Geoplanidae (Turbellaria, Tricladida, Terricola) Part II: Caenoplaninae and Pelmatoplaninae. *Bulletin of Fujis Women's College*. 29: 35-58.

Pantin, C. F. A. (1953). On the name of the ground fluke Fasciola terrestris O. F. Müller, On Othelosoma symondsi Gray, and on the genus Amblyplana von Graff. Journal of the Linnean Society Zoology, 42, 207–218 https://doi.org/10.1111/j.1096-3642.1953.tb02539.x

Riester, A. 1938. Beiträge zur Geoplaniden-Fauna Brasiliens. Abhandlungen der Senckenbergischen Naturforschenden Gesellschaft 441: 1–88.

Schirch, P. 1929. Sobre as planárias terrestres do Brasil. Boletim do Museu Nacional, Rio de Janeiro, 5(1): 27-38.

Ball, I. R. & Sluys, R. 1990. Turbellaria: Tricladida: Terricola. In: Dindal DL (ed) Soil biology guide. John Wiley & Sons, New York, pp 137–153.

Sluys R. & Riutort M. 2018. Planarian Diversity and Phylogeny. *Methods Mol Biol.* 1774:1-56. doi: 10.1007/978-1-4939-7802-1_1. PMID: 29916154.

Stimpson, W. 1857. Prodromus descriptionis animalium evertebratorum quæ in Expeditione ad Oceanum, Pacificum Septentrionalem a Republica Federata missa, Johanne Rodgers Duce, observavit er descripsit. Pars I. Turbellaria Dendrocœla. *Proceedings of the Academy of Natural Sciences of Philadelphia*. 9:19-31.

Sunnucks, P., Blacket, M. J., Taylor, J. M., Sands, C. J., Ciavaglia, S. A., Garrick, R. C., Tait, N. N., Rowell, D. M. & Pavlova, A. 2006. A tale of two flatties: different responses of two terrestrial flatworms to past environmental climatic fluctuations at Tallaganda in montane southeastern Australia. Molecular Ecology, 15, 4513–4531.

Winsor, L., Johns, P. M., & Yeates, G. W. 1998. Introduction, and ecological and systematic background, to the Terricola (Tricladida). Pedobiologia, 42, 389–404.

Chapter 1

Convergent evolution: a new subfamily for bipaliin-like Chilean land planarians (Platyhelminthes)

Convergent evolution: A new subfamily for bipaliin-like Chilean land planarians (Platyhelminthes)

Ana Laura Almeida[1,2], Tiago Mauricio Francoy[2], Marta Álvarez-Presas[3], Fernando Carbayo[1,2]

[1] Museu de Zoologia da Universidade de São Paulo, Avenida Nazaré, 481, CEP 04263-000, Ipiranga, São Paulo, SP, Brazil

[2] Laboratório de Ecologia e Evolução, Escola de Artes, Ciências e Humanidades, Universidade de São Paulo - USP, Av. Arlindo Bettio, 1000, CEP 03828-000, São Paulo, SP, Brazil

[3] School of Biological Sciences, University of Bristol, 24 Tyndall Avenue, BS8 1TQ, Bristol, UK

Running title: Convergent evolution in land planarians

Almeida et al.

Abstract

Almeida et al. (2020). Convergent evolution: A new subfamily for bipaliin-like Chilean land planarians (Platyhelminthes). *Zoologica Scripta*, 00, 000-000.

The monotypic genus of land planarians *Timyma* (Rhynchodeminae, Geoplanidae) has been suggested to be a relict that could reflect a pre-Tertiary Antarctic connection between South America and Australia and New Zealand. Two species belonging to this genus, *T. juliae* E. M. Froehlich, 1978 and *T. olmuensis* Almeida & Carbayo sp. n. are (re)described herein. Both species present ventral testes and a semilunate headplate, the same as the members of the Oriental subfamily Bipaliinae. *Timyma olmuensis* Almeida & Carbayo sp. n. is studied by means of an integrative approach. Two nuclear gene fragments (28S, EF) and a mitochondrial gene fragment (COI) were sequenced. Phylogenetic analyses pointed out that *Timyma* is the sister-group of the Neotropical Geoplaninae, and is phylogenetically distant from Bipaliinae, contradicting the hypothesis of *Timyma* as a South American relict of a Gondwanan taxon. These results indicate that the headplate evolved independently in *Timyma* and Bipaliinae. Morphological data reinforces this view. Accordingly, Timyminae subfam. n. is proposed for *Timyma* and a new diagnosis for the genus is proposed.

Fernando Carbayo, Laboratório de Ecologia e Evolução, Escola de Artes, Ciências e

Humanidades, Universidade de São Paulo - USP, Av. Arlindo Bettio, 1000, CEP 03828-000, São Paulo, SP, Brazil, +55 11 994967360, email: baz@usp.br

Introduction

The Chilean biota possesses a compelling challenge regarding its origin and phyletic relationships with regards to transoceanic and trans-Andean lineages (Nelson & Ladiges, 2001; Crisci et al., 1991; Roig-Juñent, 2000). Some taxons exhibit affinities with other Neotropical members, while other groups are more closely related to New Zealand and Tasmanian taxa (e. g., Kunzmann, 2007; Milner et al., 2015; Fachin et al., 2018; Burckhardt, 2009). Vicariance events are the most confident explanations for disjunct distributions of organisms that present a low vagilility, such as the land planarians, or Geoplanidae Stimpson, 1857 (Platyhelminthes, Tricladida) (Sluys, 1995; Winsor et al., 1998). Land planarians from Chile also were proposed to be composed of two main biogeographic groups. A Neotropical group would have evolved in South America, and another group would have arisen from a Notogeic-related lineage (Froehlich, 1967). The Neotropical subfamily Geoplaninae is characterised by the dorsal position of the testes, whereas the Notogeic-related fauna is represented by two groups, both having ventral testes, namely *Timyma* Froehlich, 1978, and an undescribed genus paralleling *Artioposthia* Graff, 1896 (Froehlich, 1967), the latter considered to be heterogeneous (Winsor, 1991). The representatives of this undescribed genus exhibits adenodactyls, which are known from Australasian taxa. This trait would represent additional evidence of its relationship with the Notogeic organisms (Froehlich, 1967).Froehlich (1967) suggested that *Timyma* might be a relict with affinities to a Notogeic and Oriental group that would reflect a pre-Tertiary Antarctic connection between South America and Australia and New Zealand. The morphological knowledge on this taxon, and its systematic position, is deficient. *Timyma juliae* Froehlich, 1978 was described from two preserved specimens collected in a relictual hygrophilous cloud-forest in the Parque Nacional Bosque Fray Jorge and donated to her (Froehlich, 1978). Froehlich was surprised by the body shape of the preserved specimens. The anterior region of the body ended abruptly, and at first glance, she believed the cephalic region was lost due to trauma (Froehlich, 1978). Under careful examination, Froehlich noted that the shape of the cephalic region

resembled that of the Oriental group Bipaliidae Stimpson, 1857 (currently Bipaliinae), but this latter group presented a narrow creeping sole, whereas, in *Timyma,* the sole was wide. She also noted similarities between *Timyma* and Bipaliinae with regards to the sensory border, comprising sensory pits (sensory furrows) and sensorial papillae (epidermal papillae) (Froehlich, 1978). However, these papillae are transversely arranged in *Timyma*, whereas in Bipaliinae, they are vertical (Froehlich, 1978). Despite the hypothesized affinities of *Timyma* with bipaliins, Froehlich (1978) placed the genus in Geoplanidae. At that time, Geoplanidae was a large group embracing all land planarians with the exception of the currently named Rhynchodeminae Graff, 1896 and Bipaliinae.

Timyma was diagnosed as follows: "*Geoplanidae with elongated body ending abruptly in a wide anterior extremity. Longitudinal cutaneous musculature weak and longitudinal parenchymal musculature absent. Sensory border circling the anterior end and restricted to it. Ventral testes opening directly into the efferent ducts [sperm ducts] which run over the central nerve plate. Without adhesive musculo-glandular organs or sensory papillae. Copulatory apparatus without adenodactyls*." (Froehlich, 1978). Later, in a series of taxonomic revisions of land planarians, Ogren & Kawakatsu (1990a, b, 1991) divided Geoplanidae into the groups Geoplaninae, Pelmatoplaninae Ogren & Kawakatsu, 1991, and Caenoplaninae Ogren & Kawakatsu, 1991, and transferred *Timyma* to the latter group (currently Caenoplanini). Nonetheless, they acknowledged that "*this genus may differ somewhat from other genera assigned here [to Caenoplanini] in that the subcutaneous longitudinal muscle is relatively less well developed and weaker. Future comparisons may reveal a more appropriate grouping as more histological details become known about the species in the Geoplanidae. The genus* Timyma *belongs in Section 2 of the Caenoplaninae because of its weak tegumentary longitudinal muscle and lack of the parenchymal ring zone*." (Ogren & Kawakatsu, 1991, p. 31). Finally, Sluys et al. (2009) changed the hierarchical level of Geoplanidae, Bipaliidae, Rhynchodemidae to the level of subfamily, among other taxonomic actions and Caenoplaninae as a tribe within Rhynchodeminae. Currently, *Timyma* is a member of the Caenoplanini (Rhynchodeminae). These erratic taxonomic changes in *Timyma* demonstrate the need for a comprehensive systematic review of the genus. In this paper, (a) *T. juliae* is redescribed and a new species of *Timyma,*

recently discovered in Chile, is described; (b) the systematic position of the genus is addressed through a novel molecular phylogentic framework; and (c) the semilunate headplate of *Timyma* and Bipaliinae are reinterpreted in the light of the morphological analysis and the inferred phylogenetic relationships.

Material and methods

Fieldwork and morphological protocols The representatives of *Timyma* were found in 2010 by active searching during the day and night in forested areas of the Parque Nacional Bosque Fray Jorge (30º 30’ S, 71º 35’ W, Coquimbo Region) and Parque Nacional La Campana (32°58'52" S 71°07'59" W, Olmué, Valparaíso Region), in Chile (Fig. 1). They were photographed and subsequently killed in boiling water, immediately fixed in 97% ethanol and stored at -20°C. In 2018, a small body portion of an individual of each species was removed for DNA studies and the remaining main body portion was cut into several pieces, dehydrated, cleared in clove oil, and infiltrated and embedded in Paraplast® Tissue Embedding Medium. Tissue blocks were sectioned at 4-7 µm intervals using a retracting rotary microtome and the produced sections were glued with albumin-glycerol (1:1) onto glass slides, and subsequently stained following Cason (1950). Stained sections were dehydrated, cleared in xylene, and mounted in synthetic balsam (Synth). Sections were studied with an Olympus BX51 optical compound microscope. The pharynges and copulatory apparatuses were reconstructed with the aid of a camera lucida attached to the microscope. Photomicrographs were taken with a DP72 digital camera attached to the microscope, and subsequently edited with GIMP (GNU Image Manipulation Program 2.8.16; The GIMP team www.gimp.org, 1995-2016). Colour descriptions of the body of live or fixed specimens follow online RAL palette colors (© RAL gemeinnützige GmbH, available at https://www.ral-farben.de/uebersicht-ral-classic-farben.html?&L=1) through comparison with digital images of the specimens on a computer screen. Unless stated differently, figures were orientated so that the anterior extremity of the body is to the left. The holotype of the new species is deposited in the Museo Nacional de Historia Natural (MNHNCL), Santiago, Chile. Specimens of *T. juliae* are deposited in the Museu de Zoologia da Universidade de São Paulo (MZUSP), Brazil.

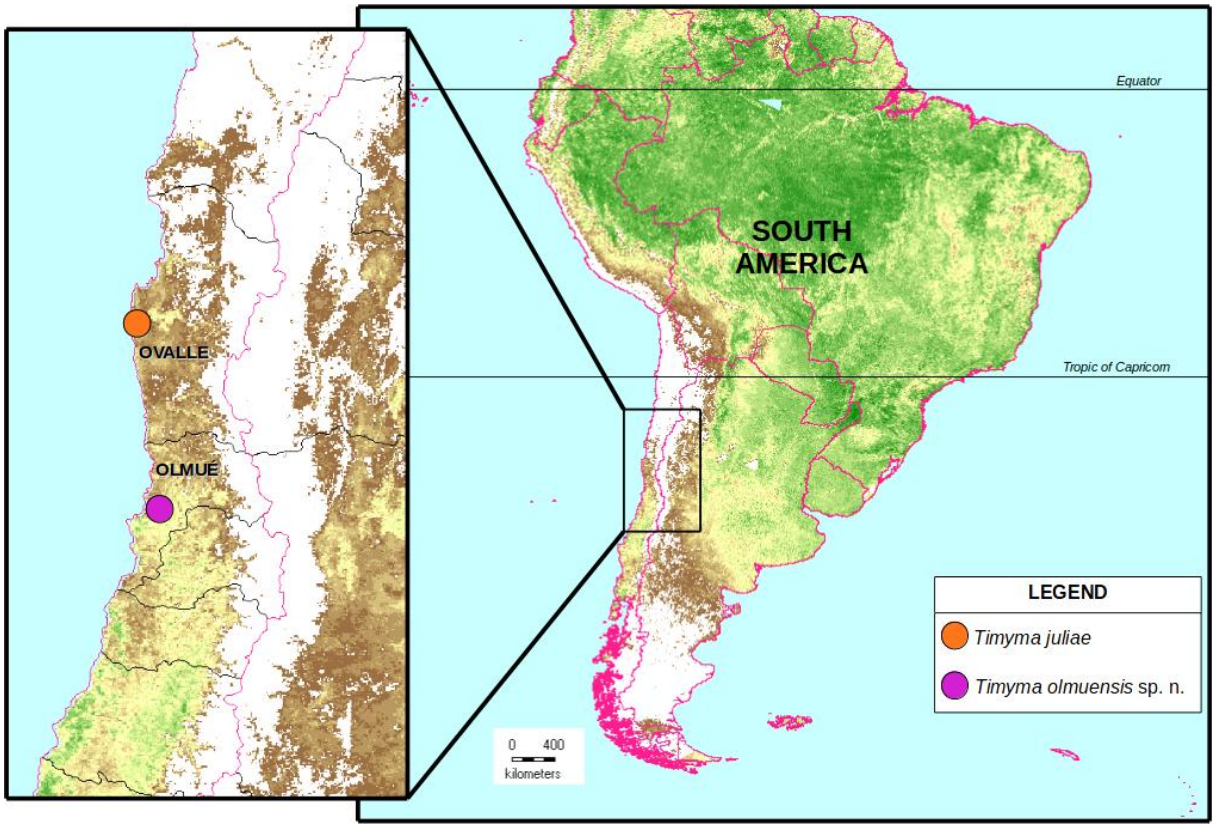

Fig. 1. Distribution map of *Timyma*.

Molecular protocol. Genomic DNA extractions of two specimens (one of *T. olmuensis* Almeida & Carbayo sp. n.; one of *T. juliae*) were performed with Wizard® Genomic DNA Purification kit (Promega, Madison, WI, USA) following Álvarez-Presas *et al.* (2011). Polymerase Chain Reaction (PCR) was used to amplify partial sequences of the nuclear regions of the ribosomal 28S (28S) and the Elongation Factor 1-alpha promoter (EF) genes, and a fragment of the mitochondrial Cytochrome Oxidase I gene (COI). Amplifications were performed in a 20 µl volume containing 1µl of DNA at a concentration of 50 ng/µl, 4 µl of 5x Phusion® Buffer GC (Thermo Scientific) mM Tris–HCl (pH 8.4), 50 mM KCl, 1 µl of lM dNTPs, 1.0–3.0 mM MgCl2, 1 µl of lM of each primer, and 0.2 µl of Phusion® High-Fidelity DNA Polymerase (Thermo Scientific). General PCR conditions included initial denaturation for 3 min at 98°C, 35 cycles of denaturation for 10 sec at 98°C, annealing for 30 sec at specific temperatures (Table S1), extension for 1 min at 72ºC, and a final extension for 5 min at 72°C. Amplification and sequencing were performed with the primer sets described in Table S1. PCR products were purified using an Agencourt AMPure XP DNA Purification and Cleanup kit (Beckman Coulter Inc.). Products were subsequently cycle-sequenced directly from

both forward and reverse directions using ABI Big-Dye Sequence Terminator (v. 3.1), cleaned with ethanol precipitation, and sequenced on an ABI Prism Genetic Analyzer (3131XL) automated sequencer (Applied Biosystems/ThermoFisher). Sequences were assembled into contigs using the Consed/Phred/Phrap package (Ewing & Green 1998; Ewing *et al.,* 1998; Gordon *et al*., 1998, 2001). Additional sequences were obtained from the GenBank database (https://www.ncbi.nlm.nih.gov/genbank). These sequences belong to representatives of most of the genera of the Neotropical Geoplaninae, plus representatives of the three other land planarian subfamilies. Representatives of the freshwater family Dugesiidae were used as outgroup (Álvarez-Presas *et al*., 2008; Álvarez-Presas & Riutort, 2014) (Table 2). These data include the only two Chilean, undescribed species of land planarians that have DNA sequences available in the GenBank database, (i. e., *Polycladus* sp. and *Gusana* sp.). These two representatives here are referred to as “Western Geoplaninae”, whereas the remaining members of the group are named "Eastern Geoplaninae". Whenever available, only gene sequences from the same individual were concatenated. The obtained sequences and those from GenBank were aligned with the online version of MAFFT (Katoh *et al*., 2019) using the G-INS-i iterative refinement method with 1000 cycles. Aligned sequences were visualized and edited with BioEdit (Hall, 1999). The online resource by Bikandi *et al*. (2004; http://insilico.ehu.es) was used to find the reading frame of the gene COI by translating the nucleotides into amino acids using the equinoderm and flatworm mitochondrial genetic code, whereas for the EF the standard genetic code was used. Ambiguously aligned positions in the 28S alignment were excluded from the analyses by applying GBlocks v 0.91b (Talavera & Castresana, 2007: http://molevol.cmima.csic.es/castresana/Gblocks_server.html), with the following settings: half allowed gap positions, a minimum length of a block of 5 nucleotides, 36 as the minimum number of sequences for a conserved position, 36 as the minimum number of sequences for a flanking position, and 4 as the maximum number of contiguous nonconserved positions. Since the COI gene has been discovered to be saturated in other datasets including Tricladida (Álvarez-Presas *et al*., 2008), a saturation test for this gene was performed with the software DAMBE (Xia, 2018).

Phylogenetic analyses

Five datasets were considered to infer general phylogenies and evaluate the stability of the phylogenetic position of *Timyma*: 28S dataset, EF dataset, COI dataset, 3-gene concatenated dataset (3-gene), and 3-gene concatenated dataset without third codon position of COI gene (3-gene-no3).The best scheme for partitioning and substitution models was obtained with the software PartitionFinder version 2.1.1 (Lanfear et al., 2016) under the model selection AICc (Hurvich and Tsai, 1989) , with branch length unlinked and greedy algorithm (Lanfear *et al.*, 2012) available on the CIPRES Science Gateway platform (Miller *et al*., 2010). Phylogenies were inferred for the five datasets using Maximum Likelihood (ML) on the software IQ-Tree (Nguyen *et al*., 2015). 1000 ultrafast bootstrap replicates were performed per analysis. The partition scheme and substitution models obtained with PartitionFinder2 were applied for the analyses of the concatenated datasets. Both concatenated datasets were also analysed with Bayesian Inference (BI) method using the software MrBayes v. 3.2 (Ronquist *et al.*, 2012) as implemented in CIPRES - Cyberinfrastructure for Phylogenetic Research (Miller *et al*., 2010). Analyses were run with the partitions and substitution models indicated by PartitionFinder described above. Two runs of Markov Chain Monte Carlo (MCMC) with twelve chains each for 150 million generations were run, sampling every 10 000 generations. 25% of the topologies were ignored as 'burn-in'. In order to check that both runs converged, the congruence of the topologies and model parameters of both runs were compared using the standard deviation of the split frequencies (SD < 0.01). Final summary trees and posterior probabilities were produced and viewed on the software FigTree v. 1.4.2 (http://tree.bio.ed.ac.uk/software/figtree/).

Results

Molecular analyses

Among the two representatives of *Timyma juliae* and *Timyma olmuensis* Almeida & Carbayo sp. n., only sequences of the holotype of the latter species were obtained before tissue was depleted. Therefore, only DNA sequences of this specimen were used in further analyses. Sequence alignments resulted in matrices with 56-to-71 terminals (including the one of *Timyma olmuensis* Almeida & Carbayo sp. n.), varying according to the availability of sequences in the GenBank for each molecular marker.

The 28S dataset, with 71 terminals and 1376 base pairs (pb) was shortened to 1234 bp after applying GBlocks. EF dataset included sequences of 56 terminals with a length of 612 bp; COI included 678 bp sequences of 65 terminals. Both of the concatenated datasets included 70 terminals, the 3-gene dataset being 2524 bp long and the 3-gene-no3, 2298 bp in length.For the concatenated 3-gene dataset, PartitionFinder indicated four partitions and the GTR substitution model with gamma-distributed rate variation across sites and a proportion of invariable sites (GTR + I + Γ) for the partitions: 28S, first and second codon position of COI, first and second position of EF, third codon position of COI and third codon position of EF. For the concatenated 3-gene-no3 dataset, PartitionFinder indicated three partitions and the GTR substitution model with gamma-distributed rate variation across sites and a proportion of invariable sites (GTR + I + Γ) for the partitions: 28S, first and second codon position of COI, first and second position of EF, third codon position of EF.

Results of the DAMBE analyses show that the third codon position of COI alignment is saturated (Iss 0.815 x Iss.cSym 0.721. P = 0.0005). For this reason, all the analyses were repeated using the concatenated 3-gene-no3 dataset, which still showed substantial saturation, but appropriate for analysis (Iss 0.640 x Iss.cSym 0.685. P = 0.34) (Fig. 1S).

Under ML, both concatenated datasets produced tree topologies congruent with previously accepted phylogenies for Geoplanidae in that they retrieved the subfamilies and the genera as monophyletic with high statistical support (ultrafast bootstrap, UFBoot). In these trees the clades Eastern and Western (*Polycladus + Gusana*) Geoplaninae share a sister-group relationship, being *Timyma* sister to Geoplaninae, and these clades are highly supported. In turn, Rhynchodeminae is sister to this large group with low support. The remaining two subfamilies Bipaliinae and Microplaninae Pantin, 1953 are either sister to each other (3-gene dataset, Fig. 2) or Bipaliinae is the basal lineage of Geoplanidae (3-gene-no3 dataset, Fig. S2), both with high support. The latter topology was also retrieved under ML with 28S dataset (Fig. S3). Phylogenetic inference from the COI dataset only recovered one of the four subfamilies, namely Geoplaninae, showing polyphyletism for some genera inside the group (Fig. S4). In the phylogenies inferred with the EF dataset, only the subfamilies Microplaninae and Bipaliinae were recovered as monophyletic (Fig. S5). Bayesian trees inferred from the concatenated datasets, also retrieved all subfamilies and genera as monophyletic with

high Posterior Probability (PP). The phylogenetic position of *Timyma* was recovered as either the sister clade of the Western Geoplaninae (3-gene dataset; Fig. S6), or as the sister clade to *Polycladus* (3-gen-no3 dataset; Fig. S7), but none of the positions of *Timyma are* statistically supported, nor the relationships among the subfamilies. The relationships between the subfamilies also vary. Inferences from the 3-gene dataset retrieved the clade composed of Geoplaninae and *Timyma* as sister to Bipaliinae + Microplaninae, being Rhynchodeminae the basal subfamily. On the other side, BI from the 3-gene-no3 dataset the group including Geoplaninae and *Timyma* is sister to Rhynchodeminae, and in turn, this large clade is sister to Bipaliinae + Microplaninae.

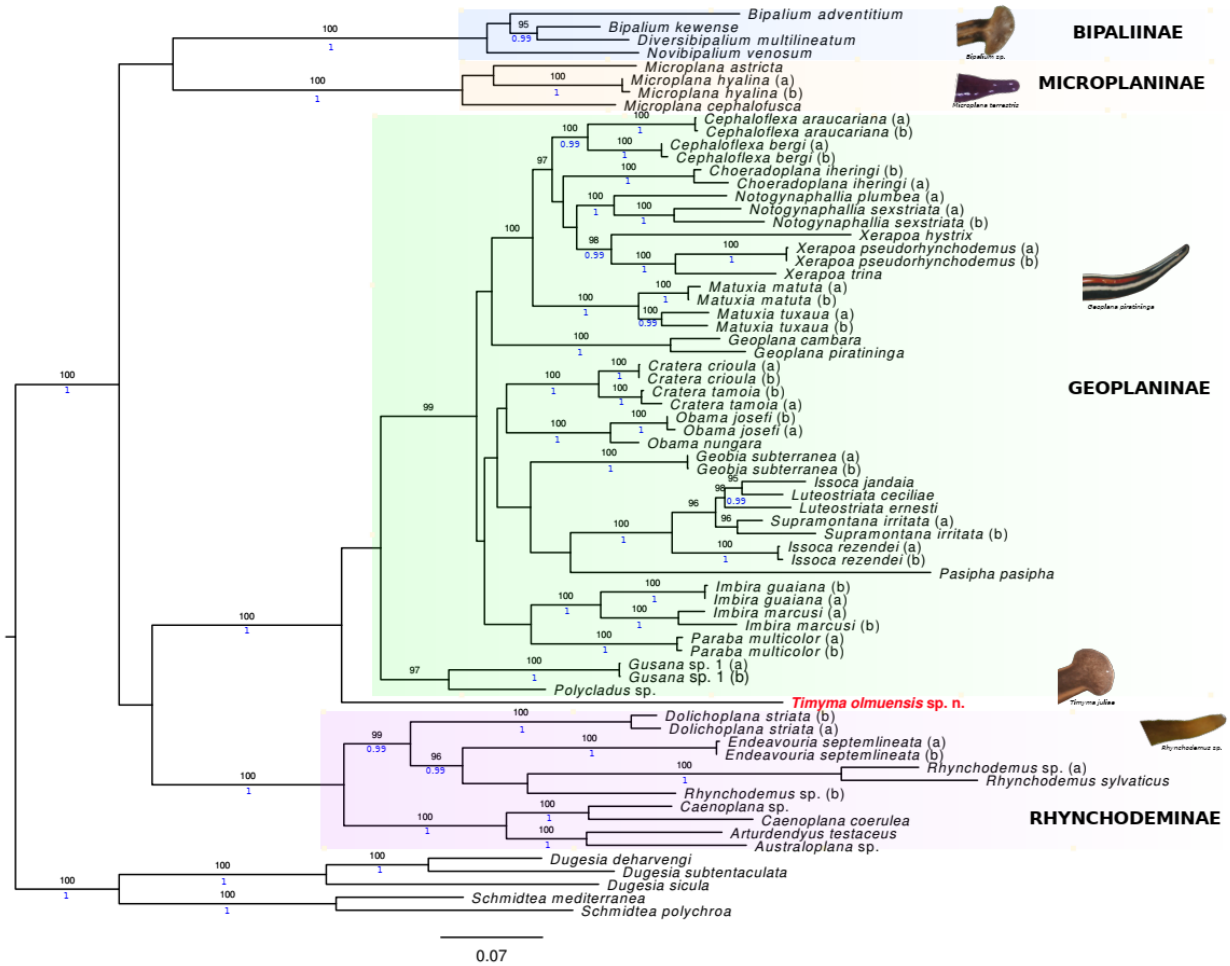

Fig. 2. Phylogenetic tree inferred from the concatenated three genes (28S rDNA + COI + EF) under maximum likelihood as the optimality criteria. Numbers at the nodes correspond to ultrafast bootstrap values of the maximum likelihood analysis (in black) and those of Bayesian posterior probability (in blue) (see also Figure S6). Bipaliinae and Timyminae subfam. n. converged on the same the semilunate headplate.

Systematic account

Order Tricladida Lang, 1881

Suborder Continenticola Carranza, Littlewood, Clough, Ruiz-Trillo, Baguñà & Riutort, 1998

Geoplanidae Stimpson, 1857

Timyminae subfam. n., Almeida & Carbayo

Zoobank registration: urn:lsid:zoobank.org:act:36825DCD-92ED-47E3-A46D-EDE2123C0C62

Type genus. *Timyma* Froehlich 1978, here designated.

Etymology. The genus name was derived from the Brazilian Tupi words *tim (nose)* + *ym (without)* (E. M. Froehlich, com. pess.; see also Bueno, 2008). It is assumed that the gender is female. Timyminae is formed by adding the suffix -inae to stem of the name of the type genus after dropping the putative gender suffix (Art. 19 of the ICZN,1999).

Diagnosis. Timyminae is characterized by the semilunate headplate and subcylindrical body. The eyes contour the headplate and body margins. The sensory border is ventro-marginal, and is provided with sensory papillae and sensory pits. The ventral nerve plate is well developed occupying most of the body width. The width of the creeping sole is three quarters of body width. The cutaneous musculature is tripartite, and 3-6% of body height in thickness. There are two parenchymatic muscle layers, a supraintestinal and a subintestinal constituted by scattered transverse fibers. The testes are ventrally located.

***Timyma* Froehlich, 1978**

New diagnosis of *Timyma*. Timyminae with mouth approximately in midbody. Without parenchymatic longitudinal muscle. Pharyngeal pouch extends posteriorly beyond copulatory apparatus. Outer pharyngeal musculature tripartite, with an outer longitudinal muscle layer, a mid-circular, and an inner longitudinal muscle layer. Prostatic vesicle extrabulbar. Penis papilla absent. Distal section of male atrium narrowed. Ovovitelline ducts emerge from the ventral aspect of ovaries, and subsequently ascend laterally to the female atrium to join dorsally to it. Female genital canal dilated to form an ootype projected from dorso-posterior aspect of the female

atrium. Without adhesive musculo-glandular organs. Copulatory apparatus without adenodactyls.

Taxonomic remarks

Redescription of *Timyma juliae* Froehlich, 1978 (Fig 3, Figs S8-S13) is available in Supplementary material section.

Fig. 3. A. *Timyma juliae* Froehlich, 1978. Living specimen MZUSP PL 2265. Body is ca. 14 mm in length.

Fig. 4. *Timyma olmuensis* Almeida & Carbayo, sp. n. Living holotype. Body is ca. 13 mm in length.

Description of *Timyma olmuensis* Almeida & Carbayo, sp. n. (Fig 4, Figs S14-S17) is available in Supplementary material section. Zoobank registration. urn:lsid:zoobank.org:act:6636381E-83B7-4DF9-B722-2CABD4F1207B

Our redescription of *T. juliae* agrees with the original description, with the exception of the intrabulbar portion of the prostatic vesicle, which we interpreted as the ejaculatory duct. *Timyma olmuensis* Almeida & Carbayo sp. n. is readily distinguished from *T. juliae* in the external aspect in that its dorsum displays a yellowish background with four brown gray stripes (*vs*. two ochre brown submarginal bands on a predominantly gray brown color in *T. juliae*). The copulatory apparatus of the new species differs from that of *T. juliae* in that in the new species (a) the prostatic vesicle penetrates the anterior aspect of the penis bulb (*vs*. ventro-anterior in *T. juliae*); (b) the male atrium is not folded (*vs*. folded); and (c) the female atrium is located above the gonopore canal (*vs*. posterior to it).

Discussion

As demonstrated in previous studies, mitochondrial genes (COI in this case) are too variable to solve deep phylogenetic relationships within Geoplanidae, whereas the substitution rates in the gene 28S are adequate for the family level and permit the analysis of deeper relationships (Álvarez-Presas *et al.*, 2008). Apparently, EF behaves the same way as the mitochondrial genes at this level, and it lacks sufficient resolution. However, concatenated genes produced better resolved phylogenies than the ones obtained from the individual genes alone, as stated in Álvarez-Presas & Riutort (2014). This situation, where genes with different resolutions provide a more robust tree when concatenated, may be explained by the influence that each gene has at different levels of a tree (Baldauf *et al*., 2000) or simply by the fact that longer sequences would result in smaller variances (Gadagkar *et al*., 2005).

Our results do not support the current classification of *Timyma* within Rhynchodeminae (Caenoplanini) under any optimization criteria or any molecular dataset. From the phylogenies it is also evident that *Timyma* is not a close relative of Bipaliinae. Molecular data suggest that this genus is sister to Geoplaninae. In its

external appearance, live specimens of *Timyma* are bipaliin-like organisms and with their fan-like or semilunate headplate, the species can be confused with members of Bipaliinae (Fig. 5). The diagnosis of Bipaliinae reads: "*Elongate body, with a laterally expanded headplate. This region is surrounded by a sensory margin with sensory grooves, and above numerous eyes. Creeping sole beginning at the base of the headpiece*" (Graff, 1899: 409). Later, this diagnosis was complemented by Ogren & Kawakatsu (1987): "*the copulatory organs are simple, without accessory ducts, or copulatory bursa, while the male and female exit ducts are separated by a fold of tissue before they enter the common genital antrum*". *Timyma* mismatches this diagnosis in that it does not present the fold separating male and female atria, and the common atrium.

Fig. 5. Living specimen of the alien *Bipalium kewense* Moseley, 1878, found in Caraguatatuba, State of São Paulo, Brazil. Inset. detail of the semilunate headplate. Body is ca. 180 mm in length.

There are further morphological attributes in Bipaliinae that eventually could segregate *Timyma* from Bipaliinae. One of these attributes is the parenchymatic musculature, as reported by Winsor (1983) for most Bipaliinae. In *Timyma*, there are only two parenchymatic muscle layers, namely a supra-intestinal and a sub-intestinal,

both constituted by scattered transverse fibers. In contrast, in *Bipalium kewense* (best studied species among all bipaliin members) the parenchymatic muscular system is more elaborated. The main differences are found in the presence of a ring zone of longitudinal and transverse muscle fibers around the intestine in *B. kewense*, a pair of ventral plates of subneural longitudinal muscles, and a muscular specialization in the region of the creeping sole (Winsor, 1983). The following further traits position *Timyma* apart from Bipaliinae: (a) The creeping sole occupies 3/4th of the body width in *Timyma* (*vs*. 1/4th in Bipaliinae); (b) eyes are large (31-50 µm) (*vs*. 14.8-18.5 µm in *Bipalium*); these eyes are distributed in an irregular row (*vs*. in multiple rows, eventually crowded on the sides of the neck region in *Bipalium* (Winsor, 1983)); (d) the sensory margin of *Timyma* is ventro-marginal (*vs*. laterally positioned in *Bipalium*; Fernandes *et al*., 2001); and (e) the main nerve system is a plate (*vs*. a pair of cords). From these divergent morphological details and the molecular phylogeny it is clear that *Timyma* is not a member of Bipaliinae. Instead, a striking convergent evolution of the semicircular headplate should be assumed (Figs. 3-5). In *B. kewense*, the head plays an important role in detecting earthworms, its prey (Barnwell, 1966). It is postulated here that a similar function exists for the expanded head of *Timyma*, albeit nothing is known about the behavior and feeding preferences of *Timyma*.

The morphological features of *Timyma* also preclude this genus from fitting into the remaining three subfamilies, none of them presenting a semicircular headplate. Furthermore, Rhynchodeminae houses species with only a pair of eyes (however eyes are numerous in many rhynchodemins); Microplaninae encompasses species with the cutaneous longitudinal musculature poorly developed and fibers of this musculature are not aggregated into large bundles. In Geoplaninae the testes are dorsally located. Thus, from the morphological viewpoint, *Timyma* can no longer be maintained in Rhynchodeminae, and should be placed in a new taxon, namely Timyminae subfam. n. In view of the expanded knowledge of the morphology of the genus, we also suggest a new diagnosis of *Timyma* (see *Taxonomic account*).

Froehlich (1967) substantiated his view of *Timyma* as a relict with affinities to a Notogeic and South East Asian biota on the fact that the testes are in a ventral position in the body. As a consequence of the phylogenetic relationships inferred here, however, the most plausible scenario is that *Timyma* evolved from a South American

ancestor with ventral testes, and the lineage originating Geoplaninae would have evolved dorsal testes.

Furthermore, in the phylogenetic analyses, the Asian-distributed Bipaliinae was never retrieved as sister to *Timyma*. Thus, two independent events had resulted in a strikingly similar semilunate headplate in *Timyma* and Bipaliinae.

Up to now, twenty-seven species of land planarians are known from Chile. Seven of them are allocated in five endemic genera. The remaining species are insufficiently known and in need of a thorough taxonomic revision (see Froehlich, 1959; Grau & Carbayo, 2010; Carbayo *et al*., 2013). The actual richness of species and endemic genera might be far larger. This viewpoint is reinforced by the historical biogeographic isolation of this country and the fact that the land planarian fauna of Chile has has to date, scarcely been
prospected.

The phylogenetic scenario revealed here does not need to invoke neither vicariance or dispersal events to explain the presence of *Timyma* in South America. Further targeted field work may result in the re-discovery of the undescribed genus reported by Froehlich (1967). In this hopeful situation, a new test of a close relationship among the Chilean and Notogeic land planarian fauna may tell another story.

Acknowledgements

To Corporación Nacional Forestal (Chile) for licensing field work (#27/2010). To Fernando Portella de Luna Marques (USP) and Francisco Cádiz for their help with sampling. Ítalo Silva de Oliveira Sousa, Geison Castro da Silveira, and Lucas Beltrami for histological processing. Bianca Lujan, Beatriz Vieira Freire, Manuel Antunes Junior and Sabrina Baroni (USP) are thanked for their kind assistance during molecular work. Domingo Lago-Barcia (USP) kindly read a draft of the manuscript. ALA thanks National Council for the Improvement of Higher Education - CAPES (Proc. 88882.378126/2019-01) for a PhD fellowship. FC has financial support from São Paulo Research Foundation - FAPESP (Proc. 2019/12357-7). Two anonymous referees are sincerely thanked for their helpful corrections and suggestions.

References

Álvarez-Presas, M., Carbayo, F., Rozas, J. & Riutort M. (2011). Land planarians (Platyhelminthes) as a model organism for finescale phylogeographic studies: understanding patterns of biodiversity in the Brazilian Atlantic Forest hotspot. *Journal of Evolutionary Biology,* 24, 887-896. https://doi.org/10.1111/j.1420-9101.2010.02220.x

Álvarez-Presas, M., Baguñà, J. & Riutort, M. (2008). Molecular phylogeny of land and freshwater planarians (Tricladida, Platyhelminthes): From freshwater to land and back. *Molecular Phylogenetics and Evolution,* 47, 555–568. https://doi.org/10.1016/j.ympev.2008.01.032

Álvarez-Presas, M. & Riutort, M. (2014). Planarian (Platyhelminthes, Tricladida) diversity and molecular markers: a new view of an old group. *Diversity* 6: 323-338. https://doi.org/10.3390/d6020323

Baldauf, S. L, Roger, A. J., Wenk-Siefert, I. & Doolittle, W. F. (2000). A Kingdom-Level Phylogeny of Eukaryotes Based on Combined Protein Data. *Science,* 290, 972-977. https://doi.org/10.1126/science.290.5493.972

Barnwell, G. M. (1966). The role of encephalization in the feeding behavior of a land planarian, Bipalium kewense. *Journal of Biological Psychology,* 8, 41-47.

Bueno, S. (1998). *Dicionário Vocabulário Tupi-Guarani Português*. São Paulo: Editora Vida Livros.

Burckhardt, D. (2009). Taxonomy and phylogeny of the Gondwanan moss bugs or Peloridiidae (Hemiptera, Coleorrhyncha). *Deutsche Entomologische Zeitschrift,* 56(2), 173– 235. https://doi.org/10.1002/mmnd.200900019

Carbayo, F., Álvarez-Presas, M., Olivares, C. T., Marques, F. P. L., Froehlich, E. M. & Riutort M. (2013). Molecular phylogeny of Geoplaninae (Platyhelminthes) challenges current classification: proposal of taxonomic actions. *Zoologica Scripta,* 42(5), 508–528. https://doi.org/10.1111/zsc.12019

Cason, J. E. (1950). A rapid one-step Mallory-Heidenhain stain for connective tissue. *Stain Technology,* 25(4), 225-226.

Crisci, J. V., Cigliano, M. M., Morrone, J. J. & Roig-Junent, S. A. (1991). Historical biogeography of Southern South America. *Systematic Zoology,* 40, 152–171. https://doi.org/10.1093/sysbio/40.2.152

Ewing, B. & Green, P. (1998). Base-calling of automated sequencer traces using Phred II. Error probabilities. *Genome Research,* 8, 186–194.

Ewing, B., Hillier, L., Wendl, M. C. & Green, P. (1998). Basecalling of automated sequencer traces using Phred I. Accuracy assessment. *Genome Research,* 8, 175-185. ttps://doi.org/10.1101/gr.8.3.175

Fachin, D. A., Santos, C. M. d. & Amorim, D. d. S. (2018). First two species of Austroleptis Hardy (Diptera: Brachycera: Austroleptidae) from Brazil. *Zootaxa,* 4369(4), 557– 574. https://doi.org/10.11646/zootaxa.4369.4.6

Fernandes, M. C., Alvares, E. P., Gama, P. & Silveira, M. (2001). The sensory border of the land planarian Bipalium kewense (Tricladida, Terricola). *Belgian Journal of Zoology,* 131(Supplement 1), 173-178.

Froehlich, C. G. (1959). On geoplanids from Brazil. *Boletins da Faculdade de Filosofia, Ciências e Letras, Universidade de São Paulo, Série Zoologia,* 22, 201-265. https://doi.org/10.11606/issn.2526-3382.bffclzoologia.1959.120326

Froehlich, C. G. (1967). A contribution to the zoogeography of neotropical land planarians. *Acta Zoologica Lilloana,* 23, 153-162.

Froehlich, E. M. (1978). On a collection of Chilean land planarians. *Boletins de Zoologia da Universidade de São Paulo,* 3, 7-80. https://doi.org/10.11606/issn.2526-3358.bolzoo.1978.121651

Gadagkar, S. R., Rosenberg, M. S. & Kumar, S. (2005). Inferring species phylogenies from multiple genes: concatenated sequence tree versus consensus gene tree. *Journal of Experimental Zoology. Part B, Molecular and developmental evolution,* 304(1), 64-74. https://doi.org/10.1002/jez.b.21026

Gordon, D., Abajian, C. & Green, P. (1998). Consed: a graphical tool for sequence finishing. *Genome Research,* 8, 195-202.

Gordon, D., Desmarais, C. & Green P. (2001). Automated finishing with autofinish. *Genome Research,* 11, 614-625. https://doi.org/10.1101/gr.171401

Graff, L. v. (1896). Über das system und die geographische Verbreitung der Landplanarien. *Verhandlungen der deutschen zoologischen Gesellschaft,* 6, 75–93.

Graff, L. v. (1899). *Monographie der Turbellarien. II. Tricladida terricola (Landplanarien)*. Leipzig: Engelmann.

Grau, J. H. & Carbayo, F. (2010). Panorama de la diversidad de planarias terrestres (Platyhelminthes: Tricladida) de Chile. *Boletín de Biodiversidad de Chile,* 2, 41-54.

Hall, T. A. (1999). BioEdit: a user-friendly biological sequence alignment editor and analysis program for Windows 95/98/NT. *Nucleic Acid Symposium Series,* 41, 95–98.

Hurvich, C. M. & Tsai, C. L. (1989). Regression and time-series model selection in small samples. *Biometrika,* 76, 297–307. https://doi.org/10.1093/biomet/76.2.297

ICZN. (1999). *International Code of Zoological Nomenclature*. 4th Ed. The International Trust for Zoological Nomenclature. Available at https://www.iczn.org/. Accessed: 05/08/2020.

Katoh, K., Rozewicki, J. & Yamada, K. D. (2019). MAFFT online service: Multiple sequence alignment, interactive sequence choice and visualization. *Briefings in Bioinformatics,* 20(4), 1160–1166. https://doi.org/10.1093/bib/bbx108

Kunzmann, L. (2007). Araucariaceae (Pinopsida): Aspects in palaeobiogeography and palaeobiodiversity in the Mesozoic. *Zoologischer Anzeiger,* 246, 257–277. https://doi.org/10.1016/j.jcz.2007.08.001

Lanfear, R., Calcott, B., Ho, S. Y. & Guindon, S. (2012). PartitionFinder: combined selection of partitioning schemes and substitution models for phylogenetic analyses. *Molecular Biology and Evolution,* 29(6), 1695-1701.

https://doi.org/10.1093/molbev/mss020

Lanfear, R., Frandsen, P. B., Wright, A. M., Senfeld, T. & Calcott, B. (2016). PartitionFinder 2: new methods for selecting partitioned models of evolution for molecular and morphological phylogenetic analyses. *Molecular Biology and Evolution,* 34(3), 772-773. https://doi.org/10.1093/molbev/msw260

Miller, M. A., Pfeiffer, W. & Schwartz, T. (2010). Creating the CIPRES Science Gateway for Inference of Large Phylogenetic Trees. In Proceedings of the Gateway Computing Environments Workshop (GCE) (pp. 1–8). New Orleans, LA. https://doi.org/10.1109/GCE.2010.5676129

Milner, M. L., Weston, P. H., Rossetto, M. & Crisp, M. D. (2015). Biogeography of the Gondwanan genus Lomatia (Proteaceae): vicariance at continental and intercontinental scales. *Journal of Biogeography,* 42, 2440–2451. https://doi.org/10.1111/jbi.12588

Nelson, G. & Ladiges, P. Y. (2001). Gondwana, vicariance biogeography and the New York School revisited. *Australian Journal of Botany,* 49, 389–409. https://doi.org/10.1071/BT00025

Nguyen, L.-T., Schmidt, H. A., Haeseler, A. v. & Minh, B. Q. (2015). IQ-TREE: A fast and effective stochastic algorithm for estimating maximum likelihood phylogenies. *Molecular Phylogenetics and Evolution,* 32, 268-274. https://doi.org/10.1093/molbev/msu300

Ogren, R. E. & Kawakatsu, M. (1987). Index to the species of the genus Bipalium (Turbellaria, Tricladida, Terricola). *Bulletin of the Fuji Women's College,* 25(2), 79-119.

Ogren, R. E. & Kawakatsu, M. (1990a). Index to the species of the family Geoplanidae (Turbellaria, Tricladida, Terricola) Part I: Geoplaninae. *Bulletin of Fuji Women's College,* 28(1), 79-166.

Ogren, R. E. & Kawakatsu, M. (1990b). Index to the species of the family Geoplanidae (Turbellaria, Tricladida, Terricola). Part II: Caenoplaninae and Pelmatoplaninae. *Bulletin of the Fuji Women's College,* 29(2), 25-102.

Pantin, C. F. A. (1953). On the name of the ground fluke Fasciola terrestris O. F. Müller, On *Othelosoma symondsi* Gray, and on the genus Amblyplana von Graff. *Journal of The Linnean Society - Zoology,* 42, 207-218. https://doi.org/10.1111/j.1096-3642.1953.tb02539.x

Roig-Juñent, S. (2000). The subtribes and genera of the Tribe Broscini (Coleoptera: Carabidae): Cladistic analysis, taxonomic treatment, and biogeographical considerations. *Bulletin of the American Museum of Natural History,* 255, 1-90. https://doi.org/10.1206/0003-0090(2000)255<0001:TSAGOT>2.0.CO;2

Ronquist, F., Teslenko, M., Mark, P. v. d., Ayres, D.L., Darling, A., Höhna, S., ... Huelsenbeck, J. P. (2012). MrBayes 3 2, efficient Bayesian phylogenetic inference and model choice across a large model space. *Systematic Biology*, 61, 539–542. https://doi.org/10.1093/sysbio/sys029

Sluys, R. (1995). Platyhelminthes as paleogeographical indicators. *Hydrobiologia,* 305, 49-53.

Sluys, R., Kawakatsu, M., Riutort, M. & Baguñà, J. (2009). A new higher classification of planarian flatworms. *Journal of Natural History,* 43(29-30), 1763–1777. https://doi.org/10.1080/00222930902741669

Stimpson, W. (1857). Prodromus descriptionis animalium evertebratorum quae in Expeditione ad Oceanum, Pacificum Septentrionalem a Republica Federata missa, Johanne Rodgers Duce, observavit et descripsit. Pars 1. Turbellaria Dendrocoela. *Proceedings of the Academy of Natural Science of Philadelphia,* 9, 19–31. https://doi.org/10.5962/bhl.title.51447

Winsor, L. (1991). A provisional classification of Australian terrestrial geoplanid flatworms (Tricladida: Terricola: Geoplanidae). *The Victorian Naturalist,* 108(2), 42-49.

Winsor, L. (1983). A revision of the cosmopolitan land planarian Bipalium kewense Moseley, 1878. (Turbellaria: Tricladida: Terricola). *Zoological Journal of the Linnean Society,* 79, 61-100. https://doi.org/10.1111/j.1096-3642.1983.tb01161.x

Winsor, L., Johns, P. M. & Yeates, G. W. (1998). Introduction, and ecological and systematic background, to the Terricola (Tricladida). *Pedobiologia,* 42, 389–404.

Xia, X. (2018). DAMBE7: New and improved tools for data analysis in molecular biology and evolution. *Molecular Biology and Evolution,* 35, 1550–1552. https://doi.org/10.1093/molbev/msy073

Supplementary material of the manuscript Almeida et al. *Convergent evolution: A new subfamily for bipaliin-like Chilean land planarians (Platyhelminthes).* Zoologica Scripta.

CONTENTS

Supplementary material

Manuscript title: Convergent evolution: A new subfamily for bipaliin-like Chilean land planarians (Platyhelminthes)

Ana Laura Almeida, Tiago Mauricio Francoy, Marta Álvarez-Presas, Fernando Carbayo.

Table S1. Primers used for the amplification and sequencing of the DNA fragments.

Target Locus	Primer name (Orientation)	Utilization	Annealing temperature	Primer Sequence (5' to 3')	Reference
28S rDNA	LSU 5F (Forward)	Amplification and sequencing	56-58ºC	TAGGTCGACCCGCTGAAYTTAAGCA	Littlewood et al. (1997)
	Rob1 (Forward)	Sequencing	-	GTCCAATAGCAAACAAGTCCCG	Heneberg et al. (2013)
	LSU 330F (Forward)	Sequencing	-	CAAGTACCGTGAGGGAAAGTTG	Williams & Ozawa (2006)
	Rob2 (Reverse)	Sequencing	-	CACGYACTRTTTACCTC	Chisholm et al., (2001)
	EC-D2 (Reverse)	Sequencing	-	CCTTGGTCCGTGTTTCAAGACGGG	Littlewood et al. (1997)
	LSU 1500R (Reverse)	Amplification and sequencing	56-58ºC	GCTATCCTGAGGGAAACTTCG	Tkach et al. (1999)
EF-1α	EFPlatF (Forward)	Amplification and sequencing	48ºC	GATTGCYCCWGGYCATCG	Carbayo et al. (2013)
	EFPlatR (Reverse)	Amplification and sequencing	48ºC	RGCRATWGAYTCGTGRTGC	Carbayo et al. (2013)
COI	BarS (Forward)	Amplification and sequencing	45ºC	GTTATGCCTGTAATGATTG	Álvarez-Presas et al. (2011)
	FlatwormCOIF (Forward)	Sequencing	-	GAGCAACAACATAATAAGTATCATG	Sunnucks et al. (2006)
	COIR (Reverse)	Amplification and sequencing	45ºC	CCWGTYARMCCHCCWAYAGTAAA	Lázaro et al. (2009)

REFERENCES CITED IN TABLE S1

Carbayo F, Álvarez-Presas M, Olivares CT, Marques FPL, Froehlich EM, Riutort M. 2013. Molecular phylogeny of Geoplaninae (Platyhelminthes) challenges current classification: proposal of taxonomic actions. *Zoologica Scripta* **42(5):** 508–528.

Chisholm LA, Morgan JAT, Adlard RD, Whittington ID. 2001. Phylogenetic analysis of the Monocotylidae (Monogenea) inferred from 28S rDNA sequences. *International Journal for Parasitology* **31:** 1253-1263. DOI: 10.1016/s0020-7519(01)00223-5

Heneberg P, Literák I. 2013. Molecular phylogenetic characterization of Collyriclum faba with reference to its three host-specific ecotypes. *Parasitology International* **62:** 262-267.**Álvarez-Presas M, Carbayo F, Rozas J, Riutort M. 2011.** Land planarians (Platyhelminthes) as a model organism for finescale phylogeographic studies: understanding patterns of biodiversity in the Brazilian Atlantic Forest hotspot. *Journal of Evolutionary Biology* **24:** 887-896.

Lázaro EM, Sluys R, Pala M, Stocchino GA, Baguñà J, Riutort M. 2009. Molecular barcoding and phylogeography of sexual and asexual freshwater planarians of the genus *Dugesia* in the Western Mediterranean (Platyhelminthes, Tricladida, Dugesiidae). *Molecular Phylogenetics and Evolution* **52:** 835-845.

Littlewood DTJ, Rohde K, Chough KA. 1997. Parasite speciation within or between host species? - Phylogenetic evidence from site-specific polystome monogeneans. *International Journal for Parasitology* **27:** 1289-1297.

Sunnucks P, Blacket MJ, Taylor JM, Sands CJ, Ciavaglia SA, Garrick RC, Tait NN, Rowell DM, Pavlova A. 2006. A tale of two flatties: different responses of two terrestrial flatworms to past environmental climatic fluctuations at Tallaganda in montane southeastern Australia. *Molecular Ecology* **15:** 4513-4531.

Tkach, V.; Grabda-Kazubska, B.; Pawlowski, J. & Swiderski, Z. 1999. Molecular and morphological evidence for close phylogenetic affinities of the genera Macrodera, Lepdophallus, Metaleptophallus and Paralepoderma (Digenea, Plagiorchiata). *Acta Parasitologica* **44:** 170-179.

Williams ST, Ozawa T. 2006. Molecular phylogeny suggests polyphyly of both the turban shells (family Turbinidae) and the superfamily Trochoidea (Mollusca: Vetigastropoda). *Molecular Phylogenetics and Evolution* **39:** 33-51. https://doi.org/10.1016/j.ympev.2005.12.017

Family	**Subfamily**	**Terminal name**	**Formal species name**	**28S rDNA - Accession Number**	**COI – Accession Number**	**EF1-α – Accession Number**
Dugesidae Ball, 1974		*Dugesia deharvengi*	*Dugesia deharvengi* Kawakatsu & Mitchell, 1989	KF907824	KF907820	-
		Dugesia subtentaculata	*Dugesia subtentaculata* (Draparnaud, 1801)	MK712520	MK712622	KJ599690
		Dugesia sicula	*Dugesia sicula* Lepori, 1948	DQ665969	KF308800	KJ599689
		Schmidtea mediterranea	*Schmidtea mediterranea* Benazzi, Baguna, Ballester & del Papa, 1975	MG457267	JF837062	KJ599709
		Schmidtea polychroa	*Schmidtea polychroa* (Schmidt, 1861)	DQ665993	FJ647021	AJ250914
Geoplanidae Stimpson, 1857	Bipaliinae Stimpson, 1857	*Bipalium adventitium*	*Bipalium adventitium* Hyman, 1943	AF022758	AF178306	KJ599681
		Bipalium kewense	*Bipalium kewense* Moseley, 1878	KJ659703	KJ659609	-
		Diversibipalium multilineatum	*Diversibipalium multilineatum* (Makino & Shirasawa, 1983)	KU245357	KU245358	KU872709
		Novibipalium venosum	*Novibipalium venosum* (Kaburaki, 1922)	DQ665981	DQ666048	KJ599694
	Geoplaninae Stimpson, 1857	*Cephaloflexa araucariana* (a)	*Cephaloflexa araucariana* Carbayo & Leal-Zanchet, 2003	KC608436	KC608319	KC614539
		Cephaloflexa araucariana (b)	*Cephaloflexa araucariana* Carbayo & Leal-Zanchet, 2003	KC608433	KC608316	KC614536
		Cephaloflexa bergi (a)	*Cephaloflexa bergi* Graff, 1899	KC608355	KC608240	KC614474
		Cephaloflexa bergi (b)	*Cephaloflexa bergi* Graff, 1899	KC608353	KC608238	KC614472
		Choeradoplana iheringi (a)	*Choeradoplana iheringi* Graff, 1899	KC608437	KC608320	KC614540
		Choeradoplana iheringi (b)	*Choeradoplana iheringi* Graff, 1899	MF802624	MF802642	MF802673
		Cratera crioula (a)	*Cratera crioula* (Froehlich, 1955)	KC608441	KC608324	KC614544
		Cratera crioula (b)	*Cratera crioula* (Froehlich, 1955)	KC608440	KC608323	KC614543
		Cratera tamoia (a)	*Cratera tamoia* (Froehlich, 1955)	KC608369	KC608254	KC614484

		Cratera tamoia (b)	*Cratera tamoia* (Froehlich, 1955)	KC608361	KC608246	KC614478
		Geobia subterranea (a)	*Geobia subterranea* Schultze & Müller, 1857	KC608340	KC608225	KC614464
		Geobia subterranea (b)	*Geobia subterranea* Schultze & Müller, 1857	KC608370	KC608255	KC614485
		Geoplana cambara	*Geoplana cambara* Almeida & Carbayo, 2018	KC608377	KC608262	KC614492
		Geoplana piratininga	*Geoplana piratininga* Almeida & Carbayo, 2018	KC614479	KC608247	KC608362
		Gusana sp. 1 (a)	*Gusana* sp. Froehlich, 1978	KC608448	KC608331	KC614549
		Gusana sp. 1 (b)	*Gusana* sp. Froehlich, 1978	KC608449	KC608332	-
		Imbira guaiana (a)	*Imbira guaiana* Leal-Zanchet & Carbayo, 2001	KC608431	KC608314	-
		Imbira guaiana (b)	*Imbira guaiana* Leal-Zanchet & Carbayo, 2001	KC608344	KC608229	KC614467
		Imbira marcusi (a)	*Imbira marcusi* Carbayo et al., 2013	KC608406	KC608291	KC614516
		Imbira marcusi (b)	*Imbira marcusi* Carbayo et al., 2013	KC608356	KC608241	-
		Issoca jandaia	*Issoca jandaia* Froehlich, 1954	KC608385	KC608270	KC614498
		Issoca rezendei (a)	*Issoca rezendei* (Schirch, 1929)	KC608378	KC608263	KC614493
		Issoca rezendei (b)	*Issoca rezendei* (Schirch, 1929)	KC608363	KC608248	KC614480
		Luteostriata ceciliae	*Luteostriata ceciliae* (Froehlich & Leal-Zanchet, 2003)	KC608438	KC608321	KC614541
		Luteostriata ernesti	*Luteostriata ernesti* (Leal-Zanchet & Froehlich, 2006)	KC608430	KC608313	KC614534
		Matuxia matuta (a)	*Matuxia matuta* Froehlich, 1954	KC608392	KC608277	KC614504
		Matuxia matuta (b)	*Matuxia matuta* Froehlich, 1954	KC608391	KC608276	KC614503
		Matuxia tuxaua (a)	*Matuxia tuxaua* Froehlich, 1954	KC608419	KC608302	KC614525
		Matuxia tuxaua (b)	*Matuxia tuxaua* Froehlich, 1954	KC608368	KC608253	-
		Notogynaphallia plumbea (a)	*Notogynaphallia plumbea* (Froehlich, 1956)	KC608420	KC608303	KC614526
		Notogynaphallia sexstriata (a)	*Notogynaphallia sexstriata* (Graff, 1899)	KC608372	KC608257	KC614487
		Notogynaphallia sexstriata (b)	*Notogynaphallia sexstriata* (Graff, 1899)	KC608347	KC608232	KC614470
		Obama josefi (a)	*Obama josefi* Carbayo & Leal-Zanchet, 2001	KT714098	KU564143	KU564191
		Obama josefi (b)	*Obama josefi* Carbayo & Leal-Zanchet, 2001	KC608435	KC608318	KC614538
		Obama nungara	*Obama nungara* Carbayo, Alvarez-Presas, Jones & Riutort, 2016	KT714094	KT714108	KT714112

		Paraba multicolor (a)	*Paraba multicolor* Graff, 1899	KC608386	KC608271	KC614499
		Paraba multicolor (b)	*Paraba multicolor* Graff, 1899	KC608415	KC608299	KC614521
		Pasipha pasipha	*Pasipha pasipha* (Marcus, 1951)	KC608410	-	KC608295
		Polycladus sp.	*Polycladus* sp. Blanchard, 1845	KC608343	KC608228	-
		Supramontana irritata (a)	*Supramontana irritata* Carbayo & Leal-Zanchet, 2003	KC608451	KC608334	KC614551
		Supramontana irritata (b)	*Supramontana irritata* Carbayo & Leal-Zanchet, 2003	KC608439	KC608322	KC614542
		Xerapoa hystrix	*Xerapoa hystrix* Froehlich, 1954	KC608418	-	KC614524
		Xerapoa pseudorhynchodemus (a)	*Xerapoa pseudorhynchodemus* (Riester, 1938)	KC608352	KC608237	-
		Xerapoa pseudorhynchodemus (b)	*Xerapoa pseudorhynchodemus* (Riester, 1938)	KC608350	KC608235	-
		Xerapoa trina	*Xerapoa trina* Marcus, 1951	KC608365	KC608250	-
	Microplaninae Pantin, 1953	*Microplana astricta*	*Microplana astricta* Sluys, Álvarez-Presas & Mateos, 2017	KU872619	KU867128	KU872666
		Microplana cephalofusca	*Microplana cephalofusca* Sluys, Álvarez-Presas & Mateos, 2017	KU872620	KU867133	KU872667
		Microplana hyalina (a)	*Microplana hyalina* Vila-Farré & Sluys, 2011	KU872630	KU867167	KU872679
		Microplana hyalina (b)	*Microplana hyalina* Vila-Farré & Sluys, 2011	KU872631	KU867168	KU872680
	Rhynchodeminae Graff, 1896 > Caenoplanini Ogren & Kawakatsu, 1991	*Arturdendyus testaceus*	*Arturdendyus testaceus* (Hutton, 1880)	DQ665952	MN990643	KC614560
		Australoplana sp.	*Australoplana* sp. Winsor, 1991	DQ665955	DQ666028	# KC614558
		Caenoplana coerulea	*Caenoplana coerulea* Moseley, 1877	DQ665961	DQ666030	-
		Caenoplana sp.	*Caenoplana* sp. Moseley, 1877	DQ665964	DQ666031	# KJ599685
		Endeavouria septemlineata (a)	*Endeavouria septemlineata* (Hyman, 1939)	KC608348	KC608233	KC614471

		Endeavouria septemlineata (b)	*Endeavouria septemlineata* (Hyman, 1939)	KC608337	KC608222	KC614461
	Rhynchodeminae Graff, 1896 > Rhynchodemini Heinzel, 1929	*Dolichoplana striata* (a)	*Dolichoplana striata* Moseley, 1877	KC608341	KC608226	KC614465
		Dolichoplana striata (b)	*Dolichoplana striata* Moseley, 1877	KJ659698	KJ659679	-
		Rhynchodemus sp. (a)	*Rhynchodemus* sp. Leidy, 1851	KJ659697	KJ659676	-
		Rhynchodemus sp. (b)	*Rhynchodemus* sp. Leidy, 1851	KJ599733	-	KJ599706
		Rhynchodemus sylvaticus	*Rhynchodemus sylvaticus* (Leidy, 1851)	KJ659706	KJ659686	-
	Timyminae	*Timyma olmuensis* sp. n.	*Timyma olmuensis* sp. n.	MW354692*	MW331438*	MW363878*

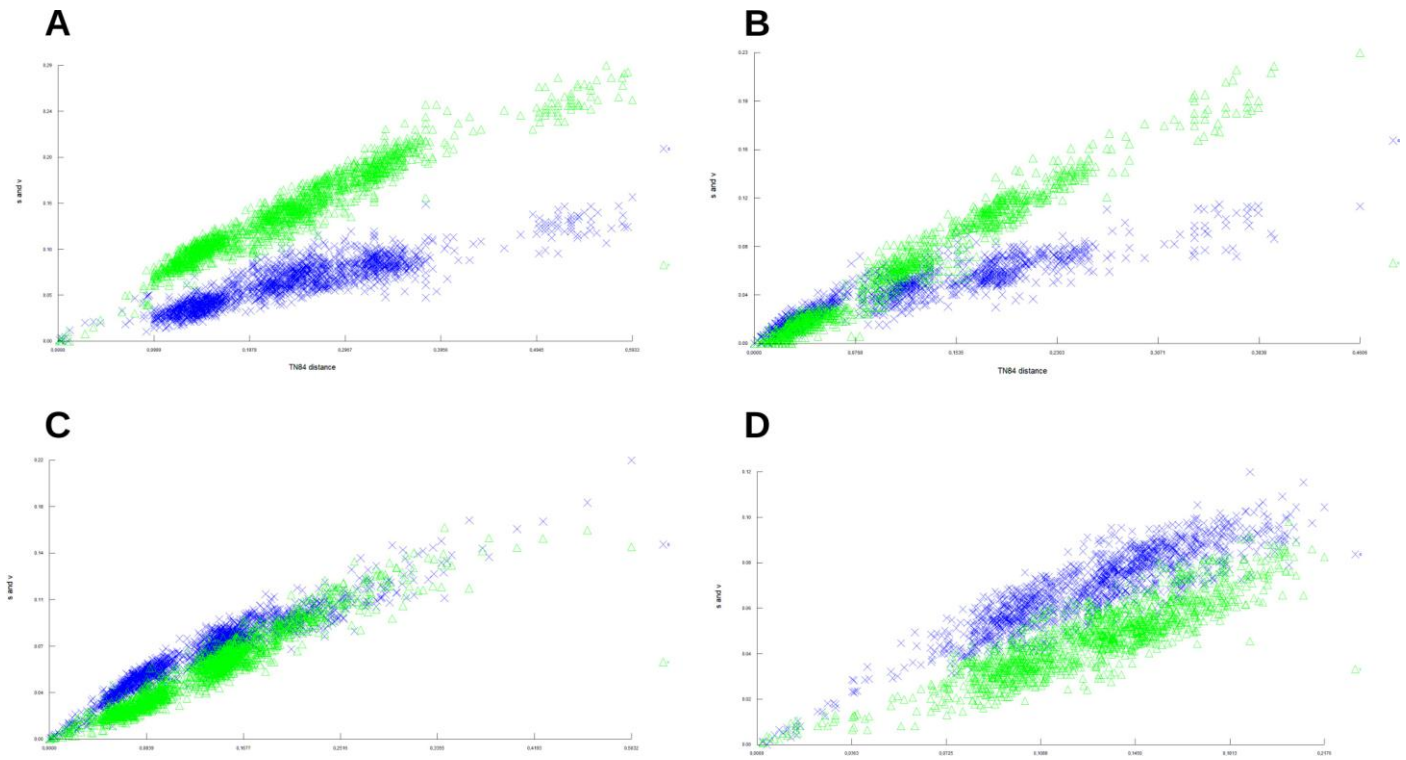

Fig. S1. Scatterplot of the transitions (s) and transversions (v) plotted against F84 distance. - A. COI gene using all the positions of each codon from the sequenced fragment. - B. COI gene using only first and second positions of each codon from the sequenced fragment. - C. 28S gene using all the positions from the sequenced fragment. - D. Elongation Factor 1-alpha gene using all the positions of each codon from the sequenced fragment.

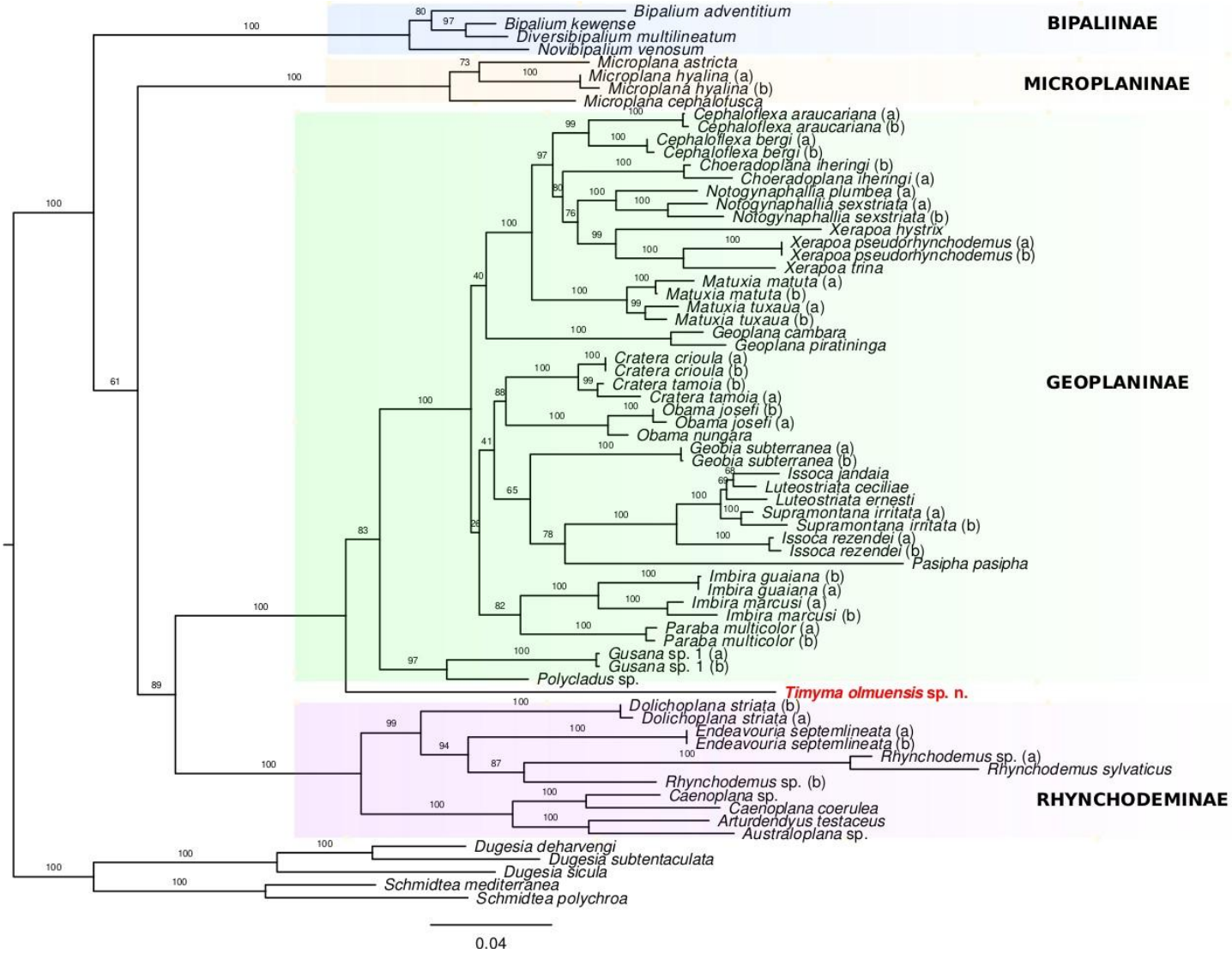

Fig. S2. Phylogenetic tree inferred from the concatenated three genes (28S rDNA + COI + EF) without the third codon position of COI gene, under maximum likelihood as the optimality criteria. Numbers at the nodes correspond to ultrafast bootstrap values.

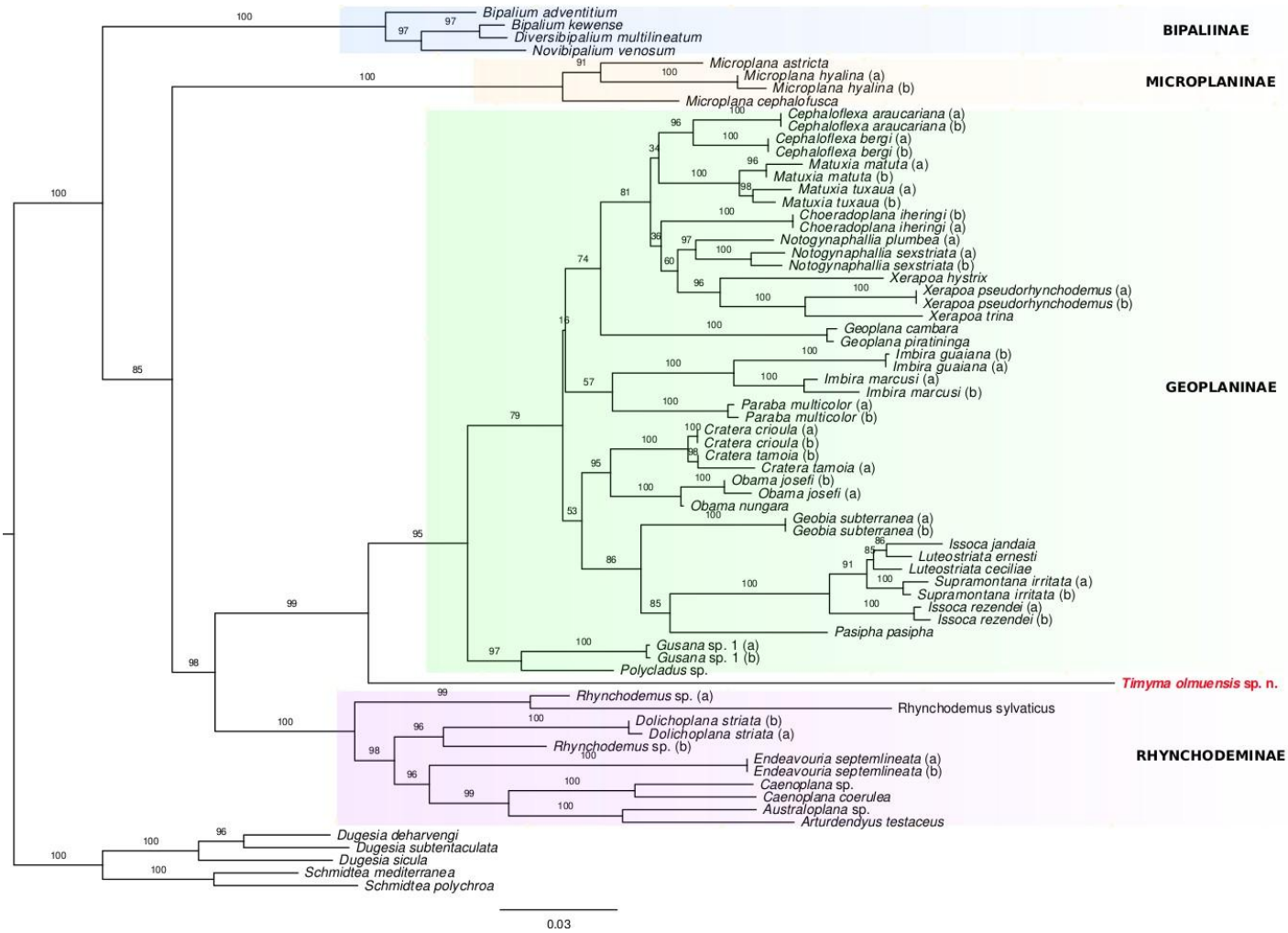

Fig. S3. Phylogenetic tree inferred from the 28S rDNA gene, under maximum likelihood as the optimality criteria. Numbers at the nodes correspond to ultrafast bootstrap values.

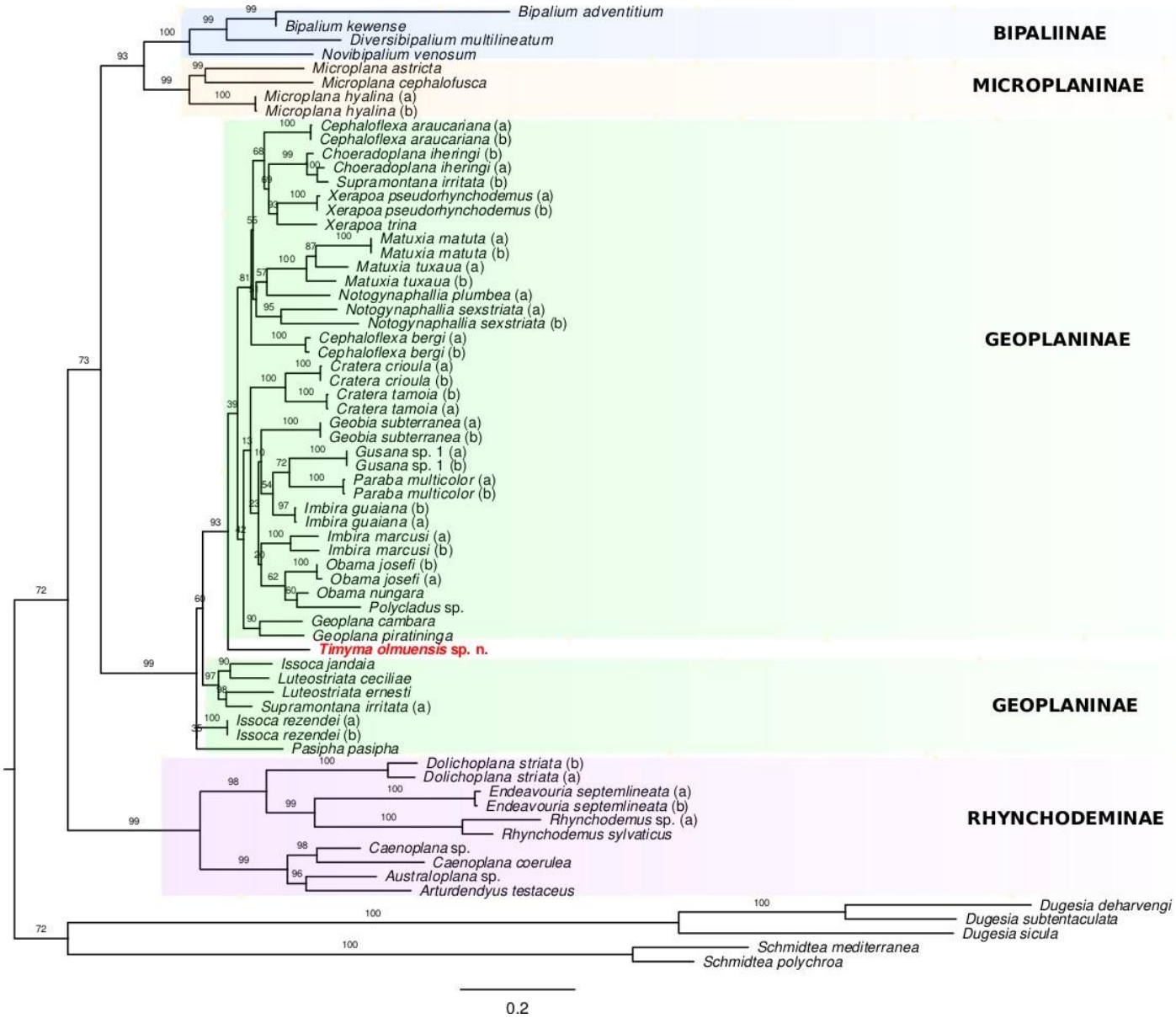

Fig. S4. Phylogenetic tree inferred from the COI gene, under maximum likelihood as the optimality criteria. Numbers at the nodes correspond to ultrafast bootstrap values.

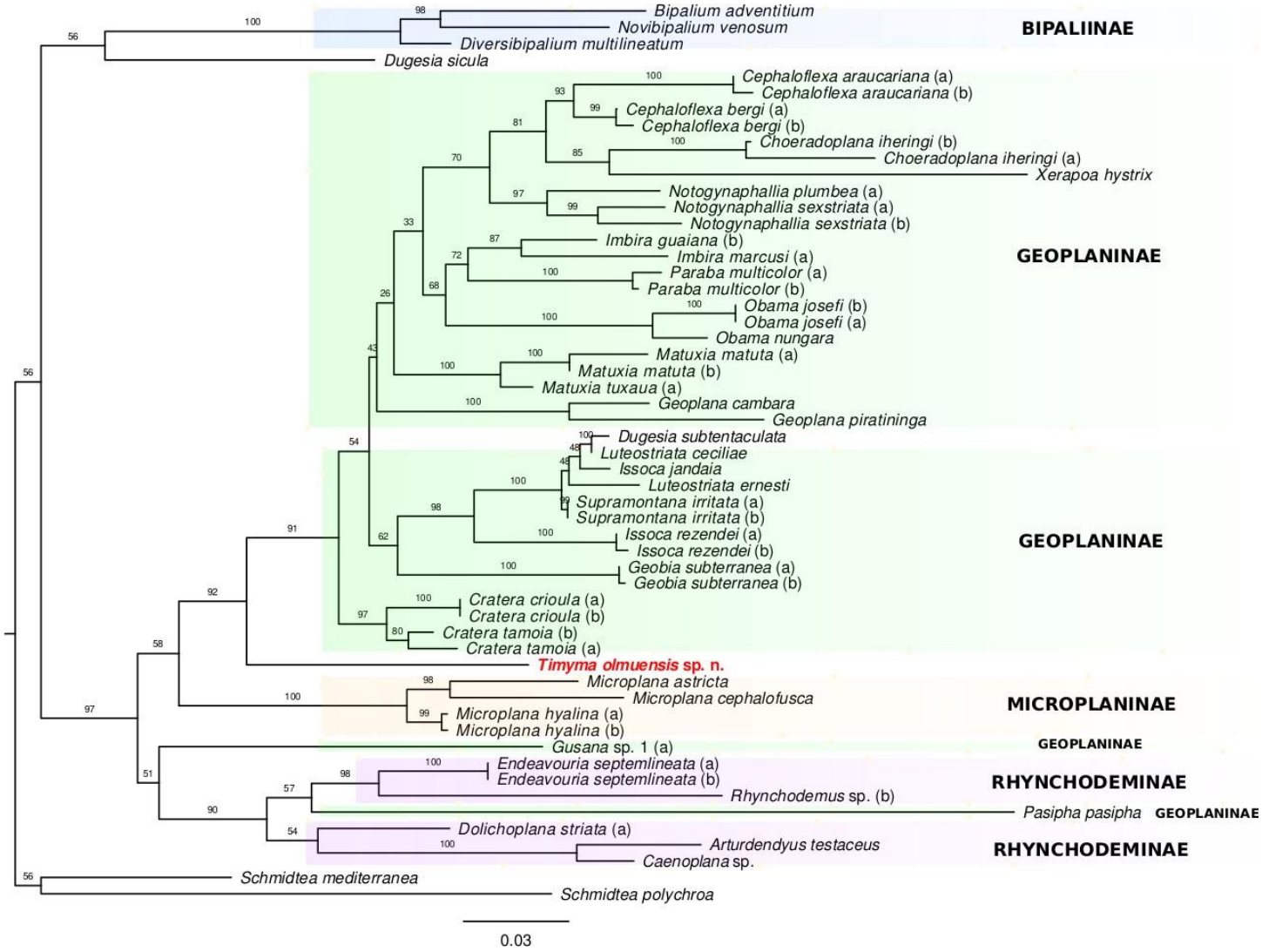

Fig. S5. Phylogenetic tree inferred from the elongation factor 1-alpha gene, under maximum likelihood as the optimality criteria. Numbers at the nodes correspond to ultrafast bootstrap values.

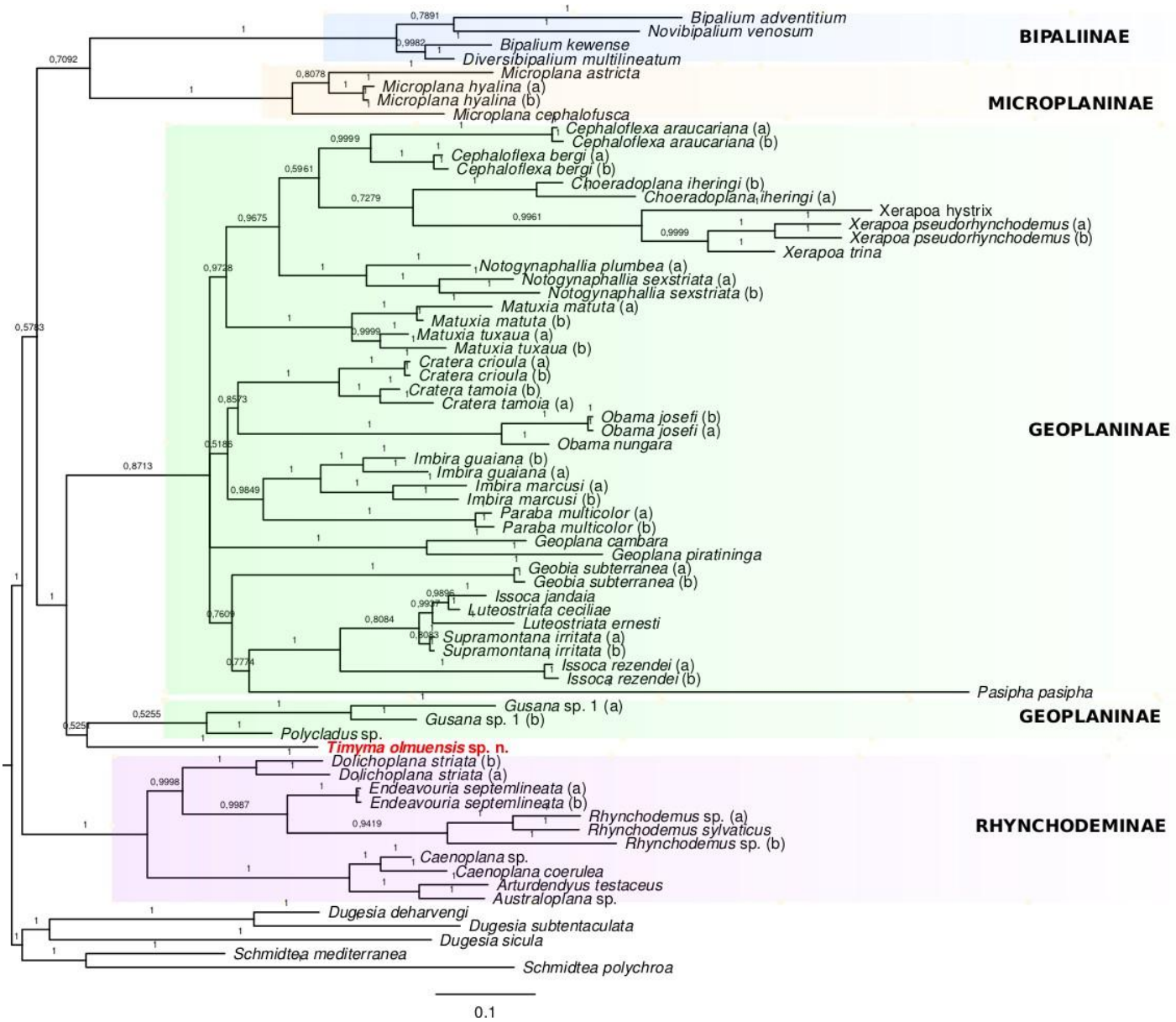

Fig. S6. Phylogenetic tree inferred by Bayesian inference from the concatenated three genes (28S rDNA + COI + EF). Numbers at the nodes correspond to posterior probabilities.

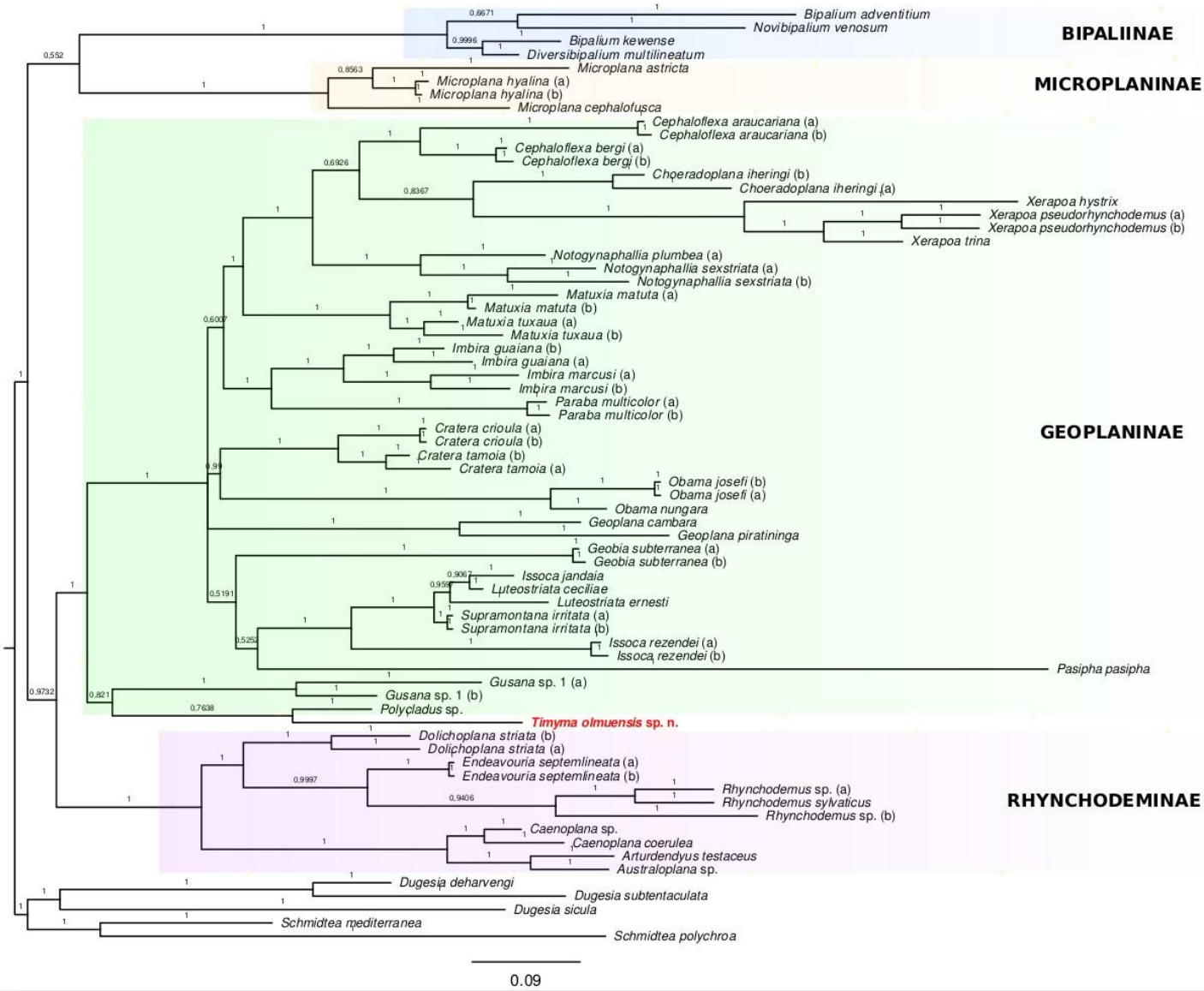

Fig. S7. Phylogenetic tree inferred by Bayesian inference from the concatenated three genes (28S rDNA + COI + EF) without the third codon position of COI gene. Numbers at the nodes correspond to posterior probabilities.

Redescription of *Timyma juliae* Froehlich, 1978 (Fig 3, Figs S8-S13)

Material examined. Two type specimens from Chile, Región de Coquimbo, Provincia del Limarí, Parque Nacional Bosque de Fray Jorge, Coord. -30.6625, -71.6826. 22 May 1962, F. Di Castri. ***Holotype***: Horizontal sections of cephalic region on 7 slides (labeled S348-S353, S356, respectively); sagittal sections of pharynx and copulatory apparatus on 5 slides (S343-S347); horizontal sections of posterior tip on 2 slides (S354-S355). ***Paratype***, sexually immature. F. Di Castri, 22 May 1962. Sagittal sections of the entire specimen on 5 slides (S342, S357-S360). ***Other material***. Same data as for the type material. **MZUSP PL 2265** (Field code, F4716), sexually mature. F. Carbayo, 03 December 2010. Transverse sections of cephalic region on 7 slides; horizontal sections of ovarian region on 4 slides; transverse sections of pre-pharyngeal region on 4 slides; sagittal sections of pharynx and copulatory apparatus on 11 slides. **MZUSP PL 2263** (Field code, F4493). Francisco Cádiz, 15 January 2010. Transverse sections of the anterior half of the body on 5 slides. Collected only this body portion. **MZUSP PL 2266** (Field code, F4735), sexually mature. F. Carbayo, 04 December 2010. Transverse sections of cephalic region on 3 slides; sagittal sections of pharynx and copulatory apparatus on 4 slides. **MZUSP PL 2264** (Field code, F4706), sexually mature. F. Carbayo, 03 December 2010. Horizontal sections of cephalic region on 2 slides; sagittal sections of copulatory apparatus on 3 slides.

Type locality. Parque Nacional Bosque de Fray Jorge, in hygrophilous cloud-forest surrounded by a semi arid landscape. Región de Coquimbo, Chile.
Distribution. Only known from the type locality.
Diagnosis. Species of *Timyma* with a dorsum provided with two ochre brown submarginal bands on a predominantly gray brown color. The prostatic vesicle enters the ventro-anterior aspect of the penis bulb. The male atrium with large folds. The female atrium is located posteriorly to the gonopore canal.

Description
External morphology. The live specimens measured approximately 14 mm in length and 3 mm in width (Fig. S8A-C). The body is relatively short and tubby, with a semilunate headplate and a

pointed posterior extremity. Contracted, the cephalic region is blunt (Fig. S8B). The preserved specimens measured approximately 11-14 mm long and 2-3 mm wide, and the cephalic region, representing 8.5% of the body length, became blunt and slightly wider than the ‘neck’ behind, resembling a spatula (Fig. S8D). The gray brown (RAL 8019) dorsal side is broken by a ochre brown (RAL 8001) submarginal band (with 12.5% of body width) at each side of the body, and extending posteriorly from the 'neck' to the posterior tip of the body where they merge. The ventral surface is whitish (Fig. S8C).

The eyes, measuring between 31-50 µm in diameter, are distributed in an irregular row contouring the cephalic region (Fig. S8D). Posteriorly they are located along the ferruginous submarginal bands to the posterior end of the body. Eyes in these bands are encircled by a halo. The relative position of the mouth : body length, is 40-54.5%; that of gonopore : body length, 50-77% (n=3).

Internal morphology. Histological examination was done mostly on sections of the type specimens and MZUSP PL2265, since the sections are of high quality. The sensory border is crenulated and contours the ventro-marginal region the cephalic region. This border consists of sensory papillae and sensory pits. Sensory papillae are epidermal projections 8-10 µm high and 30 µm wide, and are lined with a non ciliated epithelium. The sensory papillae are arranged in a single row. The space between two contiguous papillae is seen as a vertical slit (Fig. S8E). Parenchymatic glands producing erythrophil secretions penetrate the papillae and discharge their contents through epithelium.

Sensory pits are less numerous than the epidermal papillae and extend posteriorly 200 µm behind the papillae. Where sensory papillae and sensory pits coexist, the latter are located between the papillae (Fig. S9C-D). Sensory pits are funnel-shaped and 10-20 µm deep. They are distributed into 2-3 irregular rows. The parenchyma underlying sensory pits is stained red, so giving the pit the appearance of being an opening of gland cells.

Creeping sole occupying approximately 76% of the ventral surface, and just behind the cephalic region measures 74%. The dorsal and ventral epidermis of the body are pierced by abundant gland cells producing erythrophil granules. The epidermal cells of the dorsum and margins of the body contain numerous rhabdites. The creeping sole is pierced by glands producing fine cyanophil granules. An epidermal band flanking the inner side of the sensory margin is pierced by cells producing erythrophil, amorphous secretion. Glandular margin is absent. The main nervous system is organized in a plate.

The cutaneous musculature comprises three layers, namely a subepithelial circular muscle, followed

by two diagonal layers of decussate muscles, and then an innermost well developed layer of longitudinal muscles (Fig. S9A). The longitudinal muscles are composed of bundles of 4-6 fibers each, dorsally and ventrally and a thickness relative to body height in the pre-pharyngeal region ranges between 4-6%.

The parenchymatic muscle layers are very weak, and only comprise supraintestinal and subintestinal transverse muscles. The histological sections of the cephalic region with best quality are transverse. In the transverse sections of the cephalic region, the cutaneous and parenchymatic muscle systems apparently reflect those of the pre-pharyngeal region, but are even weaker, with the exception of the subintestinal transverse parenchymatic muscle, here more developed (Fig. S9B). Parenchymatic dorso-ventral and diagonal muscle fibers are also relatively abundant in the very anterior tip of the body (Fig. S9C).

The mouth is situated at a distance from the root of the pharynx equivalent to 20.6% of the pharyngeal pouch length, or 50% of pharyngeal length (Fig. S10A, see also Figs S11, S12C-D, S13). The pharyngeal pouch extends behind the copulatory apparatus passing dorsally to it. A short esophagus is present; esophagus : pharynx ratio is 8%. The pharynx is cylindrical (Fig. S10A).

The entire pharyngeal epithelium is pierced by gland cells producing cyanophil granules. Additionally, the distal epithelium of the pharynx is pierced by the ducts of glands secreting erythrophil granules. The outer pharyngeal musculature consists of a subepithelial longitudinal muscle (5 µm thick), followed by a circular muscle (20 µm thick), and a third longitudinal muscle (17.5 µm). The inner pharyngeal musculature consists of a subepithelial circular muscle (22.5 µm), followed by a longitudinal muscle (12.5 µm, Fig. S10B).

The testes are 200-300 µm diameter, and are distributed into 1-2 rows at each side of the body. They are ventrally located between the subintestinal parenchymal muscle and the intestinal branches (Fig. S10C). The anteriormost testes are placed at a distance equivalent to 20% of body length; the posteriormost testes at a distance equivalent to 44% of body length, i.e, lateral to the pharyngeal root.

In their distal course, the sperm ducts are lateral to the penis bulb, and bent anteriorly and medially to open laterally into the proximal half of the prostatic vesicle. The sperm ducts are lined with a squamous epithelium and are filled with a mass of spermatozoa. The prostatic vesicle is a tubular, and slightly sinuous. It is extrabulbar, and attached to the ventro-anterior portion of the penis bulb. The prostatic vesicle is lined with an irregular, ciliated epithelium which varies from cuboidal to columnar. This epithelium is pierced by two types of gland cells producing erythrophil and

cyanophil granules, respectively. The prostatic vesicle is surrounded by a 7-8 µm thick circular muscle. The prostatic vesicle penetrates the ventral aspect of the penis bulb to communicate with the ejaculatory duct (Figs S11-S12). The ejaculatory is a sinuous duct running dorsally to open into the male atrium through a small papilla-like fold projected from the ventro-anterior section of this atrium (Figs S11-S12). The ejaculatory duct is lined with a cuboidal, seemingly non ciliated epithelium, and is pierced by gland cells producing cyanophil granules. A 3.5-µm-thick circular muscle surrounds the epithelium of this duct. A penis papilla is absent.

The male atrium is relatively long and presents 4-5 large, transverse folds, the posterior most being the largest (Figs S11-S12). This atrium is lined with a cuboidal-to-columnar epithelium, the free surface of it is irregular along the anterior half of the atrium. The epithelium of this atrium is pierced by two types of gland cells producing cyanophil and erythrophil granules, respectively, and is underlain by a 2.5-µm-thick circular muscle, followed by a 5-µm-thick longitudinal muscle. Dorsal to the gonopore canal, a fold separates male from female atrium.

The ovaries are ovoid (Fig. S13A), and have a maximum diameter of 220 µm along the longitudinal body axis. The ovaries are located at a distance from the anterior tip of the body corresponding to 18-19% of the body length, and lay between the intestine and the nerve plate. The ovovitelline ducts emerge from the ventral aspect of the ovaries and run ventrally above the nerve plate (Fig. S13A). Before reaching the gonopore, these ducts ascend dorso-posteriorly (postflex condition with dorsal approach) to join the ootype dorsally to the female atrium (Fig. S12). The ootype is a slightly dilated cavity that communicates with the dorsal section of the female atrium (Figs S12, S13B-D). The female atrium is globular, and lined with a pseudostratified epithelium (40-100-µm high) which fills most of its space (Figs S12, S13B-D). This epithelium is not ciliated, but in some ventral sections seems to bear cilia. The epithelium is underlain by a 5-µm-thick longitudinal muscle, followed by a 15-µm-thick circular muscle. A longitudinal muscle coat (25-µm-thick) envelops the female atrium.

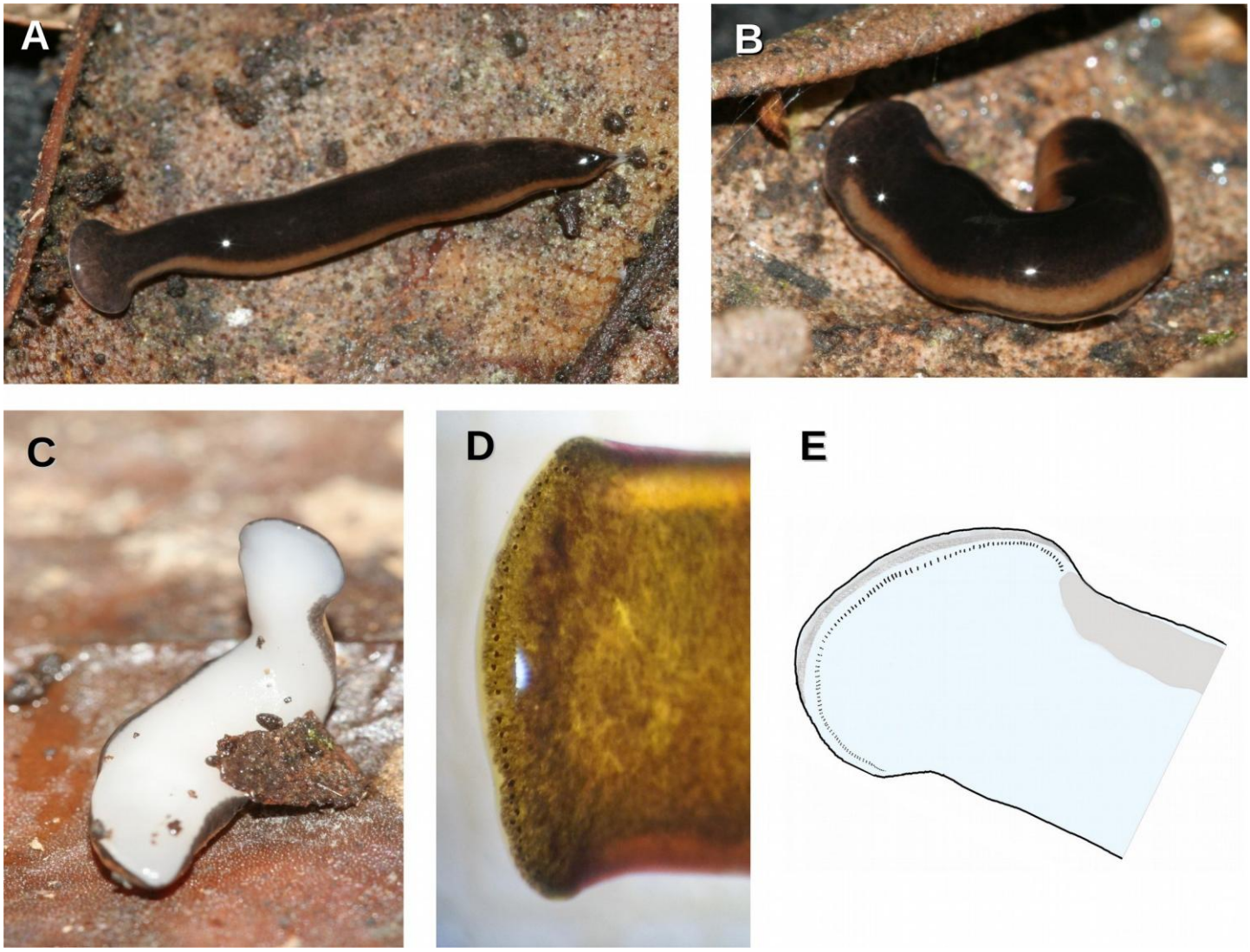

Fig. S8. *Timyma juliae* E. M. Froehlich, 1978. - A-C. Live specimens in dorsal (A, B, specimen MZUSP PL2264) and ventral (C, specimen MZUSP PL2266) view. - D. Cephalic region of specimen MZUSP PL2266 in clove oil showing eyes. - E. Diagrammatic representation of a ventral view of the cephalic region of the specimen MZUSP PL2265 showing vertical slits between sensory papillae.

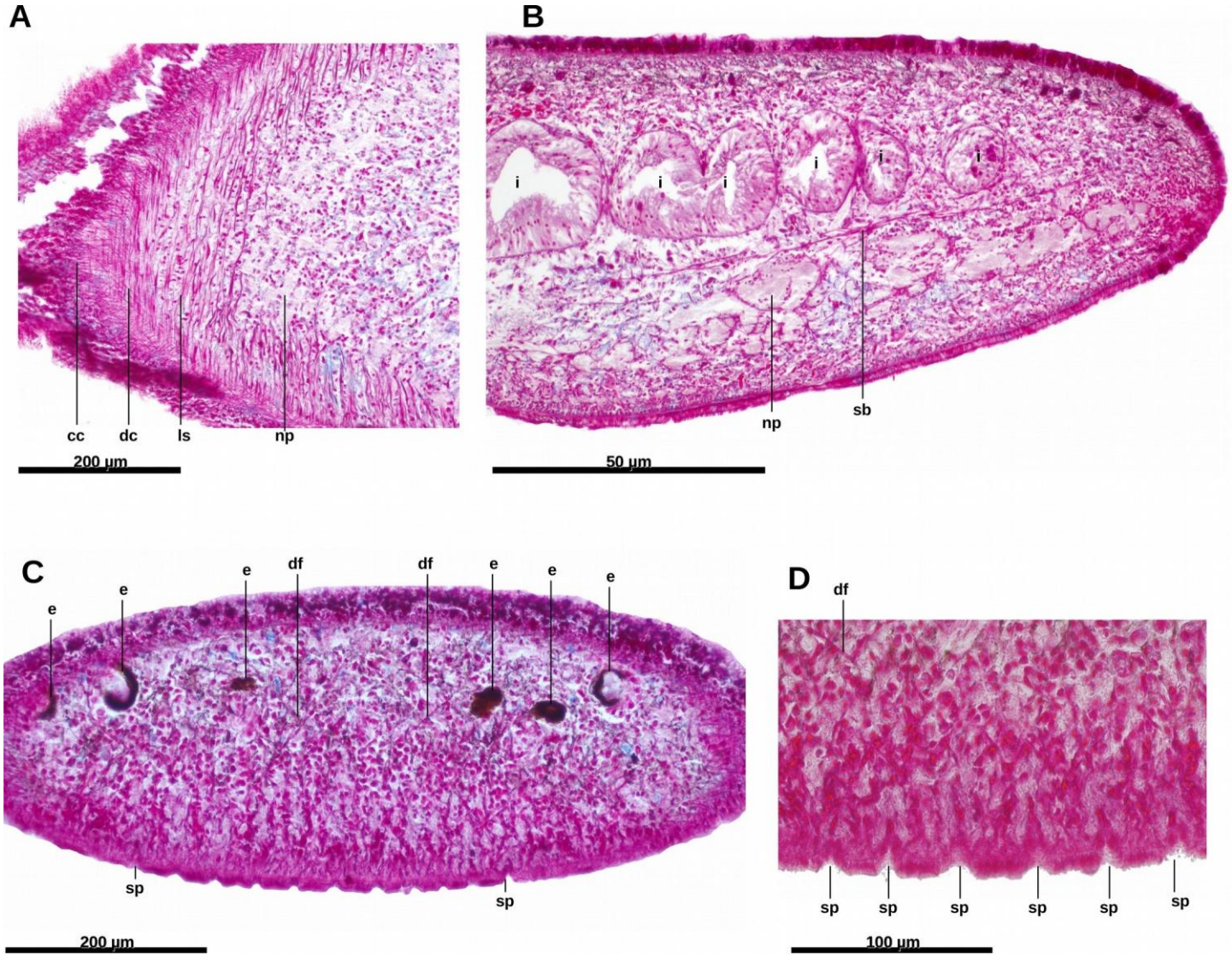

Fig. S9. *Timyma juliae* E. M. Froehlich, 1978. Photomicrographs of histological sections of specimen MZUSP PL2265. - A. Horizontal section of near dorsal epidermis. - B. Transverse section of the cephalic region. - C-D. Transverse sections of the very anterior region of the body showing sensory papillae and sensory pits.

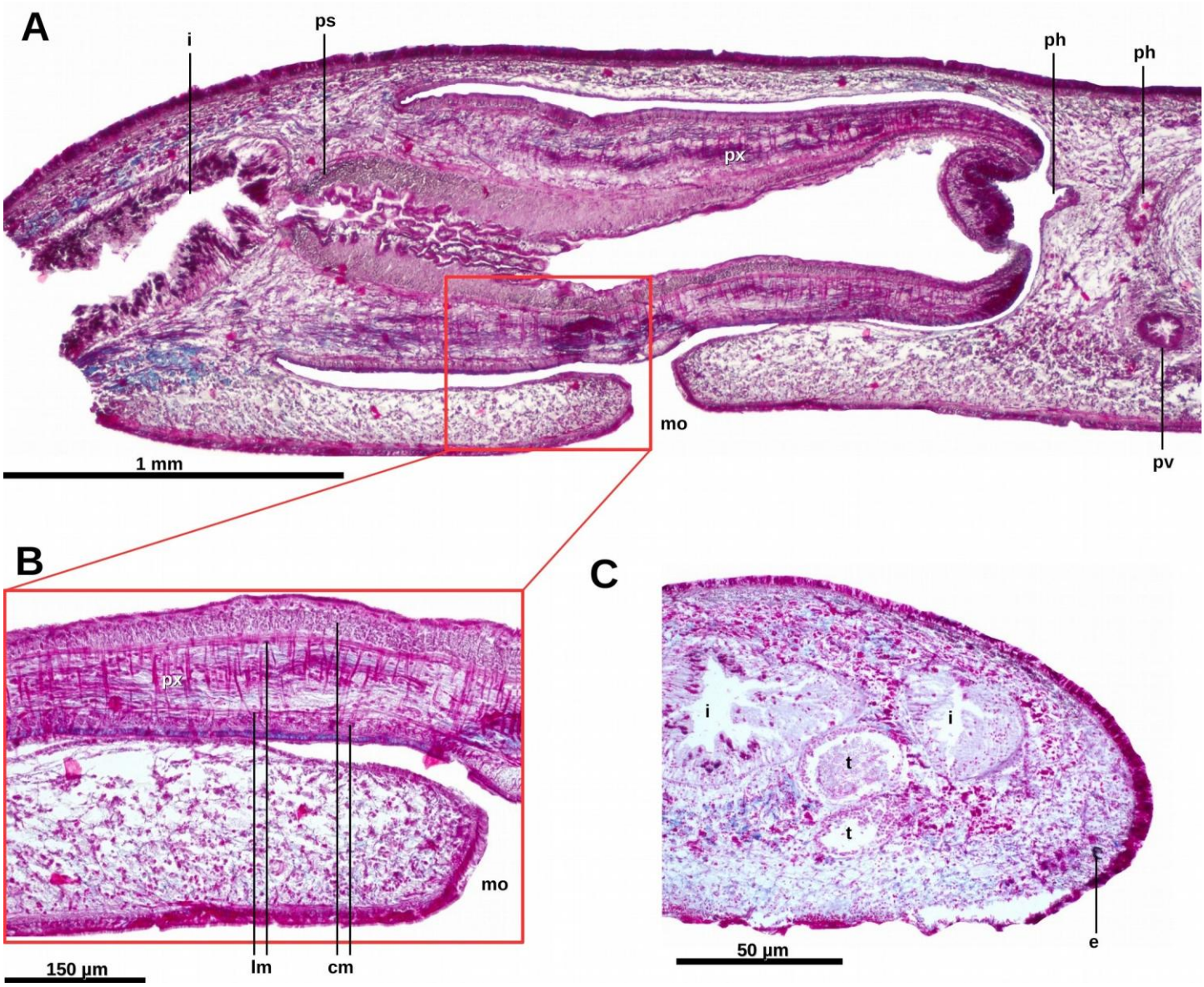

Fig. S10. *Timyma juliae* E. M. Froehlich, 1978. Photomicrographs of histological sections of specimen MZUSP PL2265. - A-B. Sagittal sections of the pharynx. - C. Transverse section of the pre-pharyngeal region showing the ventral testes.

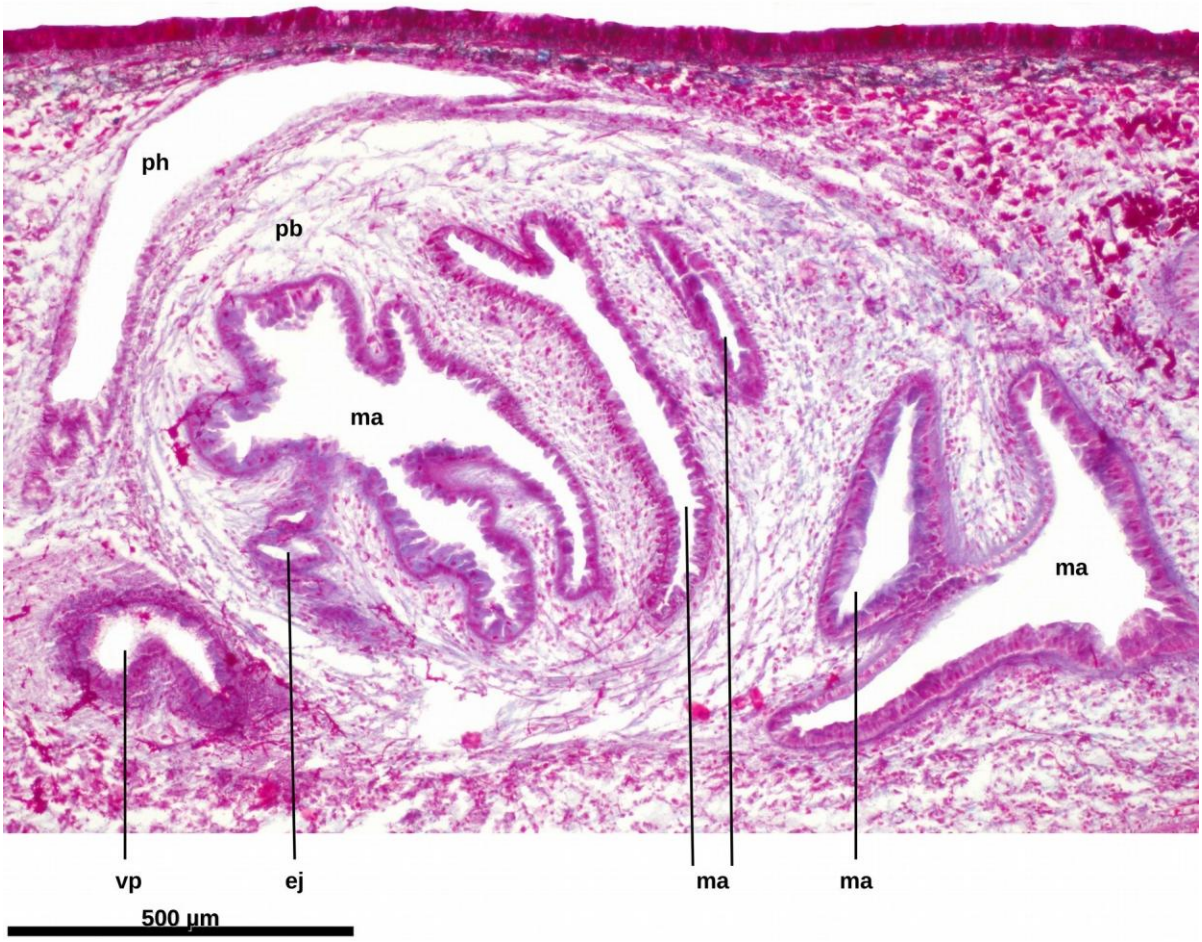

Fig. S11. *Timyma juliae* E. M. Froehlich, 1978. Photomicrograph of a sagittal section of the male copulatory apparatus of specimen MZUSP PL2265.

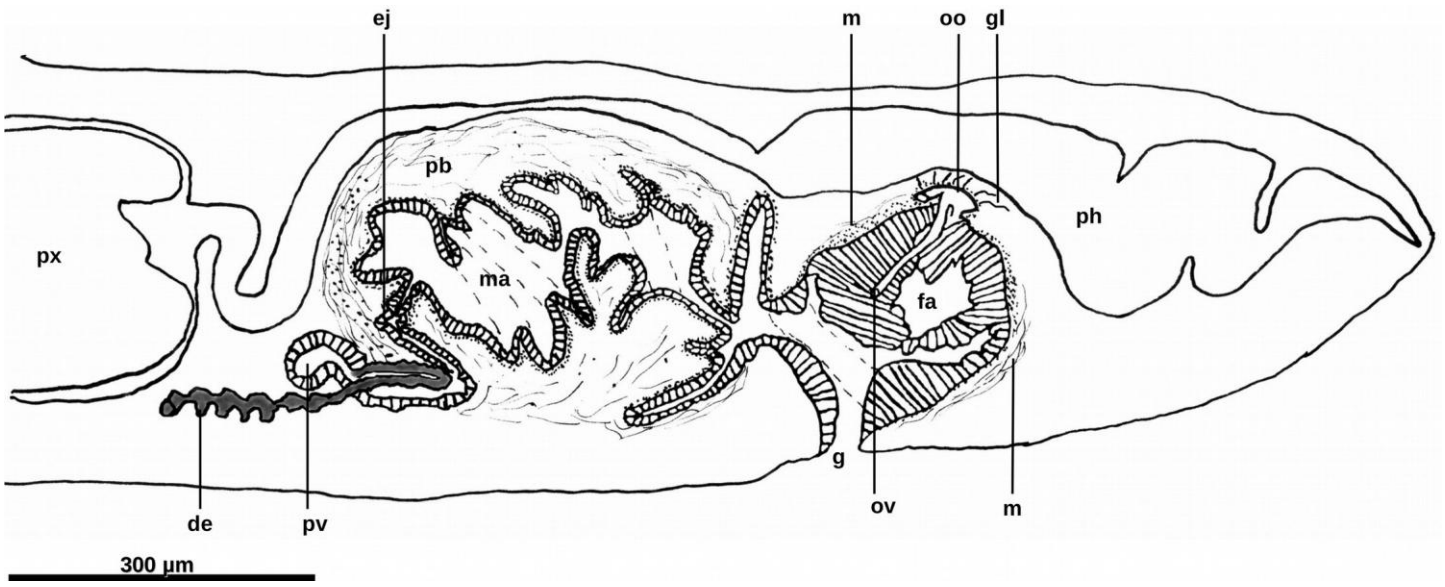

Fig. S12. *Timyma juliae* E. M. Froehlich, 1978. Diagrammatic representation of the copulatory apparatus and distal portion of the pharyngeal pocket of specimen MZUSP PL2265.

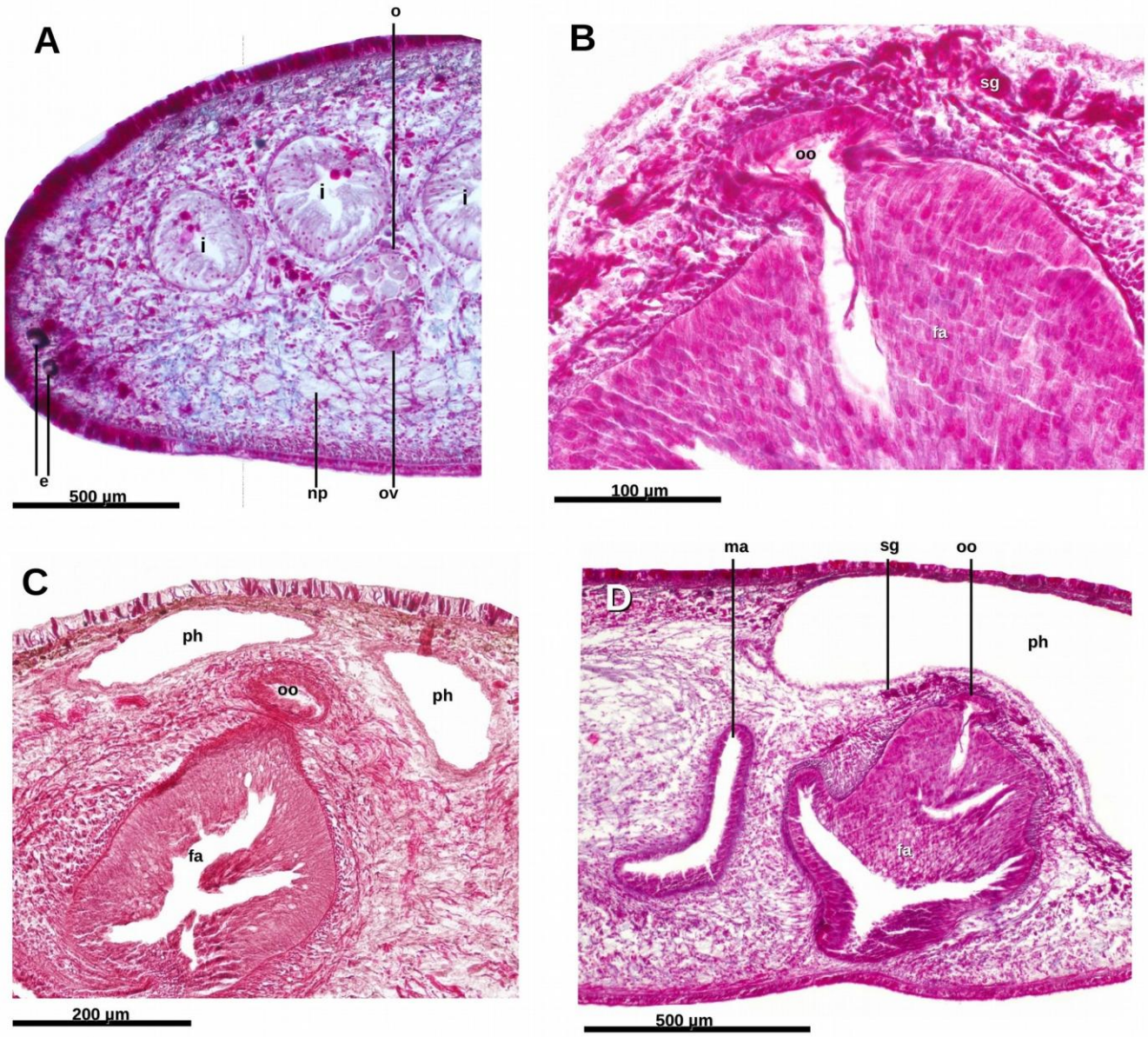

Fig. S13. *Timyma juliae* E. M. Froehlich, 1978. Photomicrographs of histological sections. - A. Transverse section at the level of an ovary of specimen MZUSP PL2265. - B-D. Sagittal sections of the female atrium of specimen MZUSP PL2265 (B, D) and holotype (C).

***Timyma olmuensis* Almeida & Carbayo sp. n.** (Fig 4, Figs S14-S17)
Zoobank registration. urn:lsid:zoobank.org:act:6636381E-83B7-4DF9-B722-2CABD4F1207B

***Holotype* MNHNCL PLAT-15018** (field code, F4817). Chile, Valparaíso Region, Olmué, Parque Nacional La Campana, Coord. -32.98133, -71.33060, F. Carbayo, 06 December 2010. Transverse sections of cephalic region and ovaries on 12 slides; horizontal sections of a body portion behind on 5 slides; transverse sections of pre-pharyngeal region and anterior portion of the pharynx on 3 slides; sagittal sections of pharynx and incompletely developed copulatory apparatus on 16 slides.
***Type locality*.** Parque Nacional La Campana, Olmué, Valparaíso Region, Chile.
Etymology. The specific epithet is a reference to the geographical origin of the species, Olmué. It is assumed that the gender of the name *Timyma* is female.
Diagnosis. Species of *Timyma* with a dorsum provided with four brown gray stripes on a yellowish background. The prostatic vesicle enters the anterior aspect of the penis bulb. The male atrium is not folded. The female atrium is located above the gonopore canal.

Description
External morphology. The shape of the live (Fig. S14A-B) and preserved (Fig. S14C) holotype is as in the type species of the genus. The living holotype was approximately 13 mm in length. Preserved, it measured approximately 14.5 mm long and 2 mm wide. The dorsal side is sulfur yellow (RAL 1016) with two paramedian bands and two lateral bands (each with 17% of body width) of brown gray color (RAL 7013) (Fig. S14A). A ventromarginal, darker band (with 9% of body width) extends on each side of the body. Ventrally, the median region is whitish, external to which is a brown gray band (with 1/4 th of the body width) on each side (Fig. S14B-C).
The size of eyes and their distribution along the body are as in the type species of the genus. The relative position of the mouth : body length, is 46%; that of gonopore : body length, 64%.
Internal morphology. The sensory border is similar to that of the type species of the genus, excepting for the following differences: (a) the parenchymatic erythrophil glands that penetrate the papillae were not seen opening through the lining epithelium of the papilla; (b) the subapical portion of the lining epithelium of the papillae is translucent, maybe caused by paucity of gland cells (Fig. S15A-B); epithelial cells of sensory papillae appear to possess short cilia; (c) the inner side of the sensory margin is pierced by very scarce glands producing erythrophil, amorphous secretion (Fig. S15A-B).

The creeping sole occupies approximately 70% of the ventral surface. The cutaneous musculature is as that of the type species of the genus in terms of organization (Figs S15C-D, S16A-B). The longitudinal cutaneous muscles are composed of bundles of 4-6 fibers each, dorsally and ventrally. The relative thickness of the cutaneous musculature is approximately 3% of body height; the suboptimal quality of these sections hampered accurate measurements. The organization of the parenchymatic musculature (Fig. S16A-B) is as in the type species of the genus in terms of organization and relative development.

The pharyngeal pouch extends behind the copulatory apparatus passing over it (Fig. S17C-D). Only the distal portion of pharynx is available, the shape of which is compatible with a cylindrical type. Outer and inner pharyngeal musculature (Fig. S16C) as in *T. juliae*. in terms of organization and relative development.

The testes are 80-105 µm in diameter. They are ventrally located between the subintestinal parenchymal muscle layer and the intestinal branches, and are distributed in one single row at each side of the body (Fig. S15E). The anteriormost testes are placed at a distance equivalent to 24.5% of body length; the posteriormost testes at a distance equivalent to 43% of body length, i.e, lateral to pharyngeal root.

The holotype is not fully mature. The sperm ducts are not developed (Fig. S17D). The prostatic vesicle is an extrabulbar, horizontal tube located anterior to the penis bulb. The prostatic vesicle is lined with a cuboidal-to-columnar, ciliated epithelium. Gland cells producing erythrophil granules concentrate around the prostatic vesicle, only few of which pierce the epithelium of this vesicle (Fig. S17C-D). This epithelium is underlain by a circular muscle (6-7.5 µm thick). The prostatic vesicle penetrates the anterior aspect of the penis bulb to communicate with the ejaculatory duct. The ejaculatory duct is horizontal and slightly sinuous, and opens into a funnel-shaped cavity of the anterior region of the male atrium. The ejaculatory duct is lined with a cuboidal epithelium, apparently not ciliated, and is surrounded by a thin circular muscle. Penis papilla absent.

The male atrium is divided into two sections (Figs S16D, S17C-D): a dorso-proximal, funnel-shaped region broadly communicating with an elongateregion running from beneath the funnel-shaped section to the gonopore canal. These regions are differentiated by means of their lining epithelia. That of the funnel-shaped region is composed of cells having various heights so that the free surface of the epithelium is sinuous. This epithelium is pierced by gland cells producing cyanophil granules. The distal portion is lined with a squamous-to-columnar epithelium, which is pierced by gland cells producing cyanophil granules. The entire male atrium is surrounded by

circular muscle (5 µm thick in anterior half), followed by a longitudinal one (7.5 µm) of longitudinal fibers. Both layers are half as thick in the distal portion of the atrium.

The ovaries are incompletely mature, and ovoid, with a maximum diameter of 100 µm along the longitudinal body axis. The ovaries are located at a distance from the anterior tip of the body corresponding to 14% of the body length, and lie between the intestine and the nerve plate. The oviducts are incompletely developed. They emerge from the ventral portion of the ovaries (Fig. S17A) and run a short distance before disappearing. These oviducts reappear as short ducts joining each other and the short female genital canal. The distal section of this canal is dilated to form an ootype which subsequently opens into the postero-dorsal region of the female atrium. The female genital canal is lined with a cuboidal-to-columnar epithelium which is crossed by gland cells producing erythrophil granules. Shell glands are not developed.

The female atrium is relatively short, funnel-shaped and located above the genital canal. The female atrium is lined with a 25-23 µm high, pseudostratified epithelium (Fig. S17B). This epithelium is pierced by two types of gland cells producing cyanophil and erythrophil granules, respectively. The epithelium is underlain by a 2.5-µm-thick longitudinal muscle, followed by a 40-42.5-µm-thick circular muscle. A longitudinal muscle coat (7.5-µm-thick) envelops the female atrium.

Fig. S14. *Timyma olmuensis* Almeida & Carbayo sp. n. Live holotype in dorsal (A) and ventral (B) views. Ventral view of the preserved holotype on millimetre graph paper.

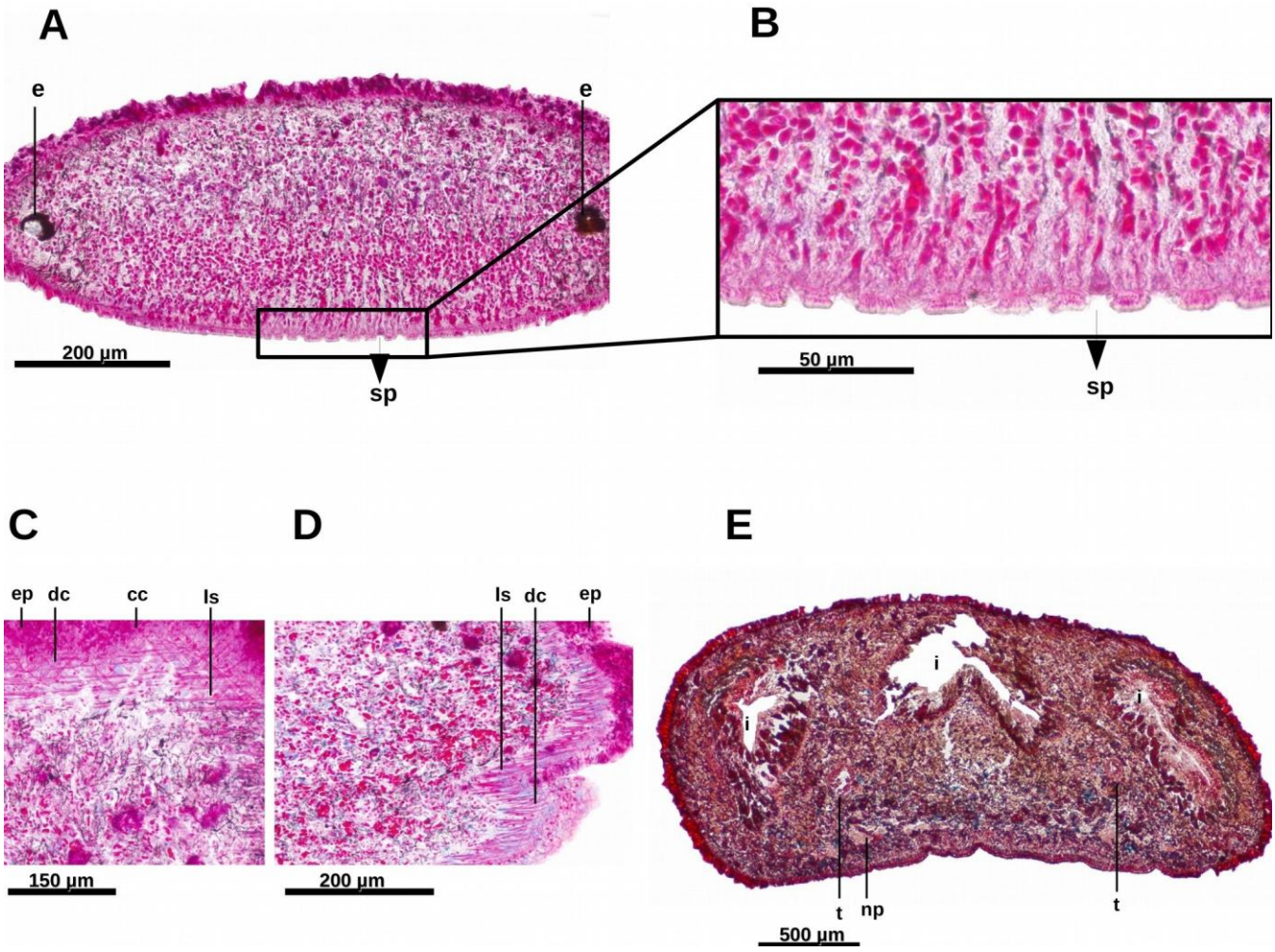

Fig. S15. *Timyma olmuensis* Almeida & Carbayo sp. n. Photomicrographs of histological sections of the holotype. - A-B. Transverse sections of the very anterior region of the body showing sensory papillae and sensory pits. - C-D. Horizontal section of near dorsal (C) and ventral (D) epidermis. E. Transverse section of the pre-pharyngeal region showing the ventral testes.

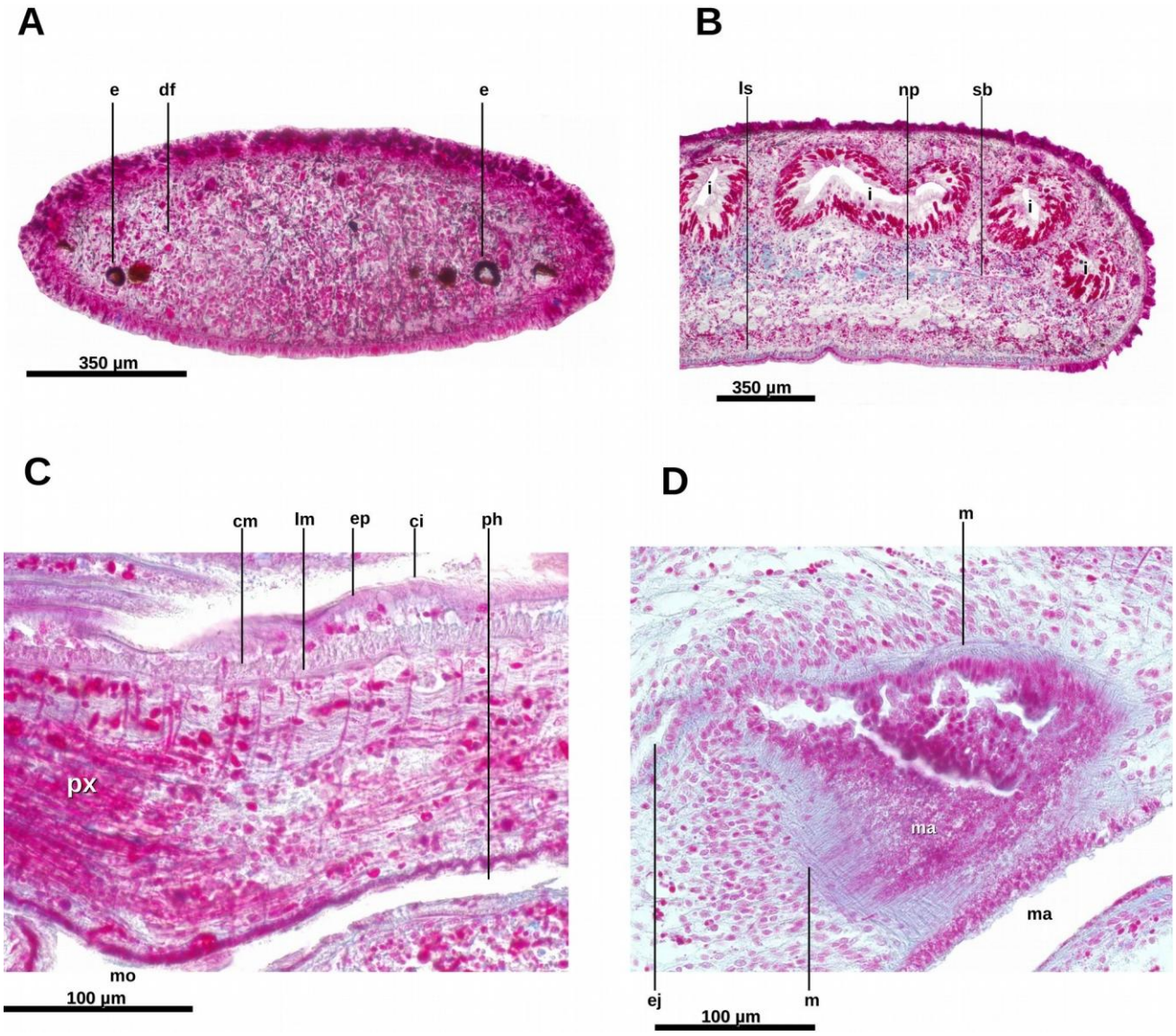

Fig. S16. *Timyma olmuensis* Almeida & Carbayo sp. n. Photomicrographs of histological sections of the holotype. - A. transverse section of the anterior extremity of the body showing eyes. - B. Transverse section of the cephalic region. - C. Sagittal section of a detail of the pharynx. - D. Sagittal section of the funnel-shaped portion of the male atrium.

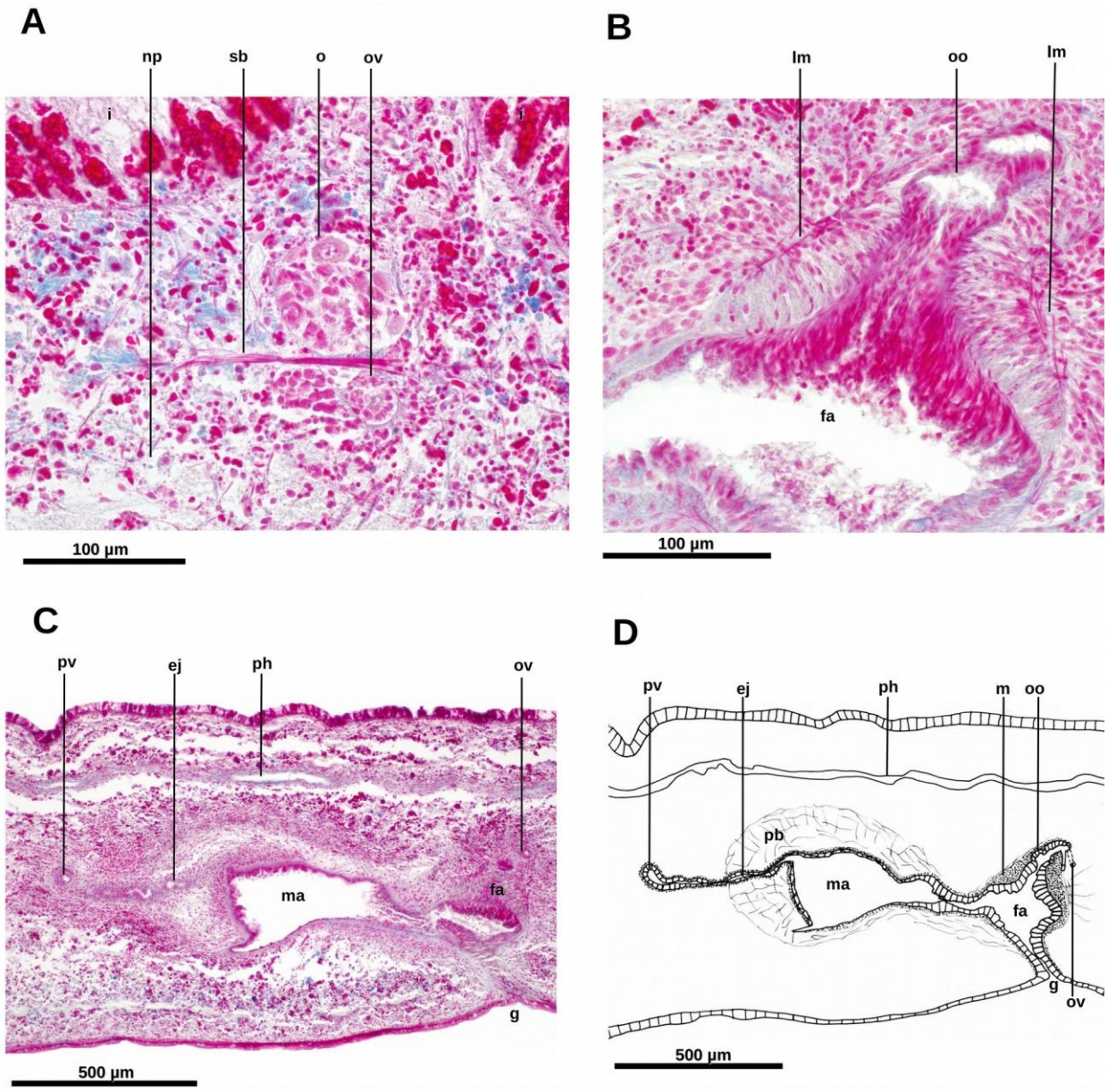

Fig. S17. *Timyma olmuensis* Almeida & Carbayo sp. n. Holotype. - A. Photomicrograph of a transverse section showing an ovary. - B-C. Photomicrographs of sagittal sections showing a detail of the female atrium and ootype (B) and the copulatory apparatus. - D. Diagrammatic Diagrammatic representation of the copulatory apparatus and a portion of the pharyngeal pocket.

Chapter 2

Integrative taxonomy increases biodiversity knowledge of *Gusana* (Platyhelminthes, Tricladida) with the description of four new Chilean species

Integrative taxonomy increases biodiversity knowledge of *Gusana* (Platyhelminthes, Tricladida) with the description of four new Chilean species

Ana Laura Almeida[1], Marta Álvarez-Presas[2], Laura Bolonhezi[3] & Fernando Carbayo[1,3]

[1] Museu de Zoologia da Universidade de São Paulo, Avenida Nazaré, 481, CEP 04263-000, Ipiranga, São Paulo, SP, Brazil
[2] School of Biological Sciences, University of Bristol, 24 Tyndall Avenue, BS8 1TQ, Bristol, UK
[3] Laboratório de Ecologia e Evolução, Escola de Artes, Ciências e Humanidades, Universidade de São Paulo - USP, Av. Arlindo Bettio, 1000, CEP 03828-000, São Paulo, SP, Brazil

Abstract

The Chilean land planarian genus *Gusana* (Platyhelminthes, Tricladida, Geoplaninae) comprises three species described in the 19th century. Four new species of the genus are herein described using integrative taxonomy. The seven species are very similar in attributes such as the body shape, the dorsal color pattern, and the internal organs, namely the type of pharynx and the shape and relative size of the components of the copulatory apparatus. The monophyletic status of the genus is demonstrated through the maximum likelihood and Bayesian inference optimality methods with cytochrome C oxidase I gene data. In addition, a molecular species delimitation method, based on pairwise genetic distances, applied to a total of six individuals of the four species points to the cohesiveness of morphological and molecular data.

Keywords: Geoplanidae, Flatworms, morphology, Neotropical, Phylogeny, Systematics, ASAP

Introduction

In recent years, progress in the knowledge on the taxonomy and morphological diversity of the Neotropical land planarians (Geoplanidae, Tricladida, Platyhelminthes) has focused particularly on organisms from the eastern Andes, mainly Argentina (e.g., Negrete et al., 2019 and references therein) and Brazil (e.g., Boll et al., 2019). In contrast, the organisms from the western Andes remain largely understudied.

The Chilean diversity of land planarians currently comprises 28 species. They are distributed into the subfamilies Rhynchodeminae Graff, 1896 (1 species), Timyminae Almeida et al., 2021 (2), and Geoplaninae Stimpson, 1857 (25). The latter two groups are exclusively Neotropical.

The Chilean geoplanins are housed into the genera "*Geoplana*" Stimpson, 1857 (4 species, quotation marks mean species without a close phylogenetic relationship with members of the genus quoted; see Carbayo et al. (2013)), *Gusana* Froehlich, 1978 (3), *Liana* Froehlich, 1978 (1), "*Pasipha*" Ogren & Kawakatsu, 1990 (2), *Polycladus* Blanchard, 1847 (1), *Pseudogeoplana* Ogren & Kawakatsu, 1990 (9), *Inakayalia* Negrete et al., 2020 (3), and *Wallmapuplana* Negrete et al., 2020 (1). *Pseudogeoplana* is a collective group for species with insufficient morphological information for their classification (Ogren & Kawakatsu, 1990).

In her comprehensive work on the taxonomy of Chilean land flatworms, E. M. Froehlich described or redescribed ten species and proposed three new genera (E. M.

Froehlich, 1978), including *Gusana* Froehlich, 1978. Currently this genus houses three species, namely *Gusana cruciata* (Graff, 1899), *Gusana lata* (Graff, 1899), and *Gusana platei* (Graff, 1899). The taxonomic history of the species is a mixed picture that follows.

***Geoplana cruciata* Graff, 1899**. Graff described the species from two specimens collected nearby Tumbes (Concepción Province, Biobío Region). The specimens remain unsectioned in the Berlin Museum. E. M. Froehlich (1978) examined three specimens with a 'rather high body of uncommon shape'. The specimens were collected in 1961-1964 in Nahuelbuta, Mancera Island, and Lago Calafquén, respectively. The worm from Nahuelbuta was incompletely mature, whereas the other two animals were immature. Despite the differences observed in the color pattern of the body concerning *Gu. cruciata*, the author considered the animals conspecific with this species. E. M. Froehlich proposed the new genus *Gusana* for this species, given the distinct external and internal features.

***Geoplana lata* Graff, 1899**. The type of material, collected in Corral, Valdivia Province, Los Ríos Region), consists of a single, unsectioned individual housed in the Museum of Zoology of Hamburg. Later on, C. G. Froehlich (1967) reported that 'two species from Chile, *Gu. lata* Graff and *Gu. cruciata* Graff, have in common a small, short but broad body (preserved), a large male atrium but a very small penis papilla, and the female genital canal arriving from below". The author did not provide field details on the specimens he studied nor other morphological accounts.

In her 1978's paper, E. M Froehlich (1978) also studied three specimens (seemingly those regarded by C. G. Froehlich (1967) as members of *Gu. lata*) collected in 1961 in Lake Todos los Santos, Malleco Province, La Araucanía Region. The author identified them as *Microplana ruca* Marcus, 1954 (E. M. Froehlich, 1978), a species subsequently transferred to *Amaga* Ogren & Kawakatsu, 1990 (Ogren & Kawakatsu, 1990). Recently, *Amaga ruca* was reallocated in *Wallmapuplana* Negrete et al., 2020 and designated as the type species of the genus.

***Geoplana platei* Graff, 1899**. Graff described this species from only one individual collected nearby Corral. The unsectioned individual is deposited in the Museum of Zoology of Hamburg. E. M. Froehlich wondered whether *Gu. platei* were conspecific with *Gu. cruciata*, given that "both the form of the body and the color pattern are very similar", but did not take any taxonomic action. The author also "suspected that *Geoplana platei* which approaches *Gusana cruciata* by the shape and locality, and that was described by Graff as possessing a sensory border clearly visible, is another species to be assigned to *Gusana*" (E. M. Froehlich, 1978, p 10). The species was later reallocated in *Gusana* by Ogren & Kawakatsu (1990).

In order to contribute to expanding the knowledge of the diversity of the genus, here we describe four new species of *Gusana* from individuals collected during a sampling trip in 2010. We also explore molecular data to demonstrate the monophyletic status of the genus and to test the morphological species independently with a statistical molecular species delimitation method.

Material and methods

The specimens were found in 2010 by active searching during the day and night in forested areas of the Parque Hualpén, Parque Nacional Conguillío, Parque Nacional Nahuelbuta, and Monumento Natural Cerro Ñielol, in Chile (Fig. 1). They were photographed and subsequently killed and fixed in 92% ethanol and stored at -20° C. In 2017, a small body portion of each individual was removed for DNA studies. The remaining main body portion was gradually rehydrated to 80% ethanol and maintained in this fluid for some months to reduce tissue hardness. Complementarily, specimens MNHNCL PLAT-15030, MNHNCL PLAT-15032, and MZUSP PL 2278, which were still hard, were immersed in Sandison solution for three days to soften the body (Sandison, 1955).

The specimens were cut into several pieces, dehydrated, cleared in clove oil, and infiltrated and embedded in Paraplast® Tissue Embedding Medium. Tissue blocks were sectioned at 7 µm intervals using a retracting rotary microtome, and the produced sections were glued with albumin-glycerol (1:1) onto glass slides and subsequently stained following Cason (1950). Stained sections were dehydrated, cleared in xylene, and mounted in synthetic balsam (Synth). Sections were studied with an Olympus BX51 optical compound microscope. Diagrams of the copulatory apparatuses were drawn with the aid of a camera lucida attached to the microscope. Photomicrographs were taken with a DP72, a digital camera attached to the microscope, and subsequently edited with GIMP (GNU Image Manipulation Program 2.8.16; The GIMP team www.gimp.org, 1995-2016) to provide a whitish background or sharpness. Color descriptions of the body of live or fixed specimens follow online RAL palette colors (© RAL gemeinnützige GmbH, available at https://www.ral-farben.de/uebersicht-ral-classic-farben.html?&L=1) through comparison with digital images of the specimens on a computer screen. Unless stated differently, figures were orientated so that the anterior extremity of the body is to the left. The holotype of each new species is deposited in the Museo Nacional de Historia Natural (MNHNCL), Santiago, Chile. The paratypes are deposited in the Museu de Zoologia da Universidade de São Paulo (MZUSP), Brazil.

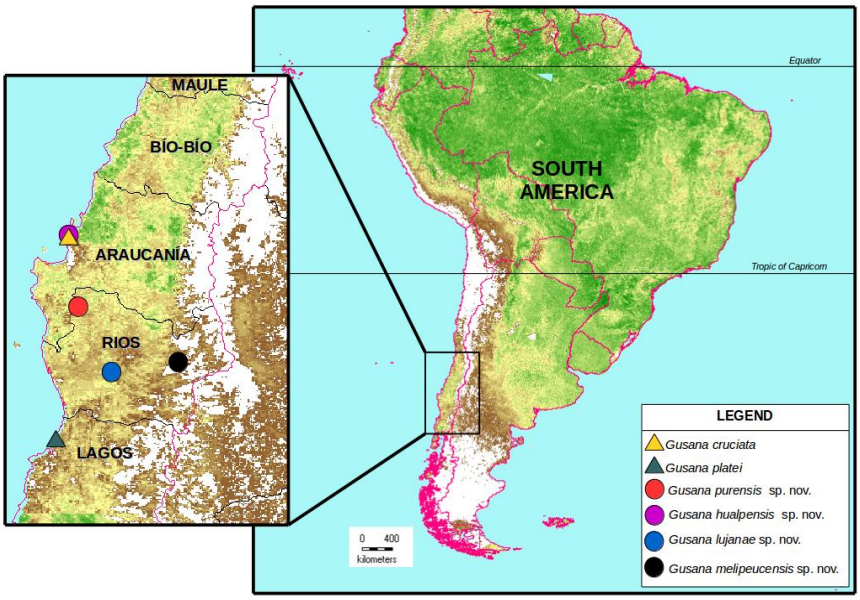

Fig. 1. Distribution map of *Gusana*.

Molecular methods

DNA extraction, amplification, and sequencing

Genomic DNA extractions of four specimens of *Gusana* (Table 1) were performed with an ammonium acetate protocol according to Fetzner, J. (1999). Polymerase Chain Reaction (PCR) was used to amplify partial sequences of the ribosomal 28S rDNA gene (herein 28S) and a fragment of the mitochondrial Cytochrome Oxidase I gene (COI). Amplifications were performed in a 25 µl volume containing 3 µl of DNA at a concentration of 50 ng/µl, 2.5 µl of 5x Phusion® Buffer HF (Thermo Scientific) mM Tris–HCl (pH 8.4), 50 mM KCl, 1 µl of lM dNTPs, 2 mM MgCl2, 1 µl of lM of each primer, 0.15 µl of GoTaq® DNA Polymerase (Promega), and 15.35 µl of ultrapure water. General PCR conditions included initial denaturation for 3 min at 94°C, 35 cycles of denaturation for 30 sec at 94°C, annealing for 30 sec at specific temperatures (Table 2), extension for 1 min at 72ºC, and a final extension for 3 min at 72°C. Amplification and sequencing were performed with the primer sets described in Table 2. PCR products were purified using an Agencourt AMPure XP DNA Purification and Cleanup kit (Beckman Coulter Inc.). Products were subsequently cycle-sequenced using BigDye Terminator v3.1 Cycle Sequencing Kit, cleaned with ethanol precipitation, and sequenced on an ABI 3730 DNA Analyzer automated sequencer (Life Technologies-Applied Biosystems). Sequence *reads* were assembled in contigs using the Consed/Phred/Phrap package (Ewing & Green 1998; Ewing et al. 1998; Gordon et al. 1998, 2001).

Table 1. Individuals used in the study with their corresponding sequence's GenBank accession numbers. Sequences generated for this study are indicated with *.

Subfamily	**Terminal name**	**Formal species name**	**28S rDNA – Accession Number**	**COI – Accession Number**
Geoplaninae Stimpson, 1857	*Cratera crioula* (1)	*Cratera crioula* (Froehlich, 1955)	KC608441	KC608324
	Cratera crioula (2)	*Cratera crioula* (Froehlich, 1955)	KC608440	KC608323
	Cratera tamoia (1)	*Cratera tamoia* (Froehlich, 1955)	KC608369	KC608254
	Cratera tamoia (2)	*Cratera tamoia* (Froehlich, 1955)	KC608361	KC608246
	Geobia subterranea (1)	*Geobia subterranea* Schultze & Müller, 1856	KC608340	KC608225
	Geobia subterranea (2)	*Geobia subterranea* Schultze & Müller, 1856	KC608370	KC608255
	Geoplana cambara	*Geoplana cambara* Almeida & Carbayo, 2019	KC608377	KC608262
	Geoplana Piratininga	*Geoplana piratininga* Almeida & Carbayo, 2019	KC614479	KC608247
	Gusana hualpensis sp. n. (1)	*Gusana hualpensis* sp. n.	KC608448	KC608331
	Gusana hualpensis sp. n. (2)	*Gusana hualpensis* sp. n.	KC608449	KC608332
	Gusana melipeucensis sp. n.	*Gusana melipeucensis* sp. n.	MW854310*	MW865707*

	Gusana lujanae sp. n. (1)	*Gusana lujanae* sp. n.	MW854313*	MW865709*
	Gusana lujanae sp. n. (2)	*Gusana lujanae* sp. n.	MW854312*	MW865708*
	Gusana purensis sp. n.	*Gusana purensis* sp. n.	MW854311*	MW881250*
	Imbira guaiana (1)	*Imbira guaiana* (Leal-Zanchet & Carbayo, 2001)	KC608431	KC608314
	Imbira guaiana (2)	*Imbira guaiana* (Leal-Zanchet & Carbayo, 2001)	KC608344	KC608229
	Imbira marcusi	*Imbira marcusi* Carbayo et al., 2013	KC608406	KC608291
	Obama josefi (1)	*Obama josefi* (Carbayo & Leal-Zanchet, 2001)	KT714098	KU564143
	Obama josefi (2)	*Obama josefi* (Carbayo & Leal-Zanchet, 2001)	KC608435	KC608318
	Obama nungara	*Obama nungara* Carbayo, Álvarez-Presas, Johnes & Riutort, 2016	KT714094	KT714108
Rhynchodeminae Graff, 1896	*Dolichoplana striata*	*Dolichoplana striata* Moseley, 1877	KJ659698	KJ659679
	Endeavouria septemlineata	*Endeavouria septemlineata* (Hyman, 1939)	KC608348	KC608233

Table 2. List of primers used to amplify and sequencing the DNA fragments.

Gene region	**Primer name**	**Utilization**	**Sequence (5' to 3')**	**Reference**	**Annealing temperature**
28S rDNA	LSU 5F (Forward)	Amplification and sequencing	TAGGTCGACCCGCTGAAYTTAAGCA	Littlewood *et al.* (1997)	56-58ºC
	Rob1 (Forward)	Sequencing	GTCCAATAGCAAACAAGTCCCG	Heneberg et al. (2013)	-
	LSU 330F (Forward)	Sequencing	CAAGTACCGTGAGGGAAAGTTG	Williams & Ozawa (2006)	-
	Rob2 (Reverse)	Sequencing	CACGYACTRTTTACCTC	Chisholm et al., (2001)	-
	ECD-2 (Reverse)	Sequencing	CCTTGGTCCGTGTTTCAAGACGGG	Littlewood *et al.* (1997)	-
	LSU 1500R (Reverse)	Amplification and sequencing	GCTATCCTGAGGGAAACTTCG	Tkach *et al.* (1999)	56-58ºC
COI	BarS (Forward)	Amplification and sequencing	GTTATGCCTGTAATGATTG	Álvarez-Presas *et al.* (2011)	45ºC
	FlatwormCOIF (Forward)	Sequencing	GAGCAACAACATAATAAGTATCATG	Sunnucks *et al.* (2006)	-
	COIR (Reverse)	Amplification and sequencing	CCWGTYARMCCHCCWAYAGTAAA	Lázaro *et al.* (2009)	45ºC

Molecular analyses

Two different datasets were used for the phylogenetic and molecular species delimitation analyses. The phylogenetic inference was performed using a concatenated dataset (named *Concatenated* dataset) combining sequences from 22 specimens corresponding to the 28S and COI genes (Table 1). For the molecular species delimitation analysis, we used a dataset containing only COI sequences named *COIdel*. Individual gene phylogenies were inferred using the *COIdel* dataset as well. COI sequences were aligned using the translation to amino acids (Echinoderm and Flatworm mitochondrial translation table number 9) as a guide. The 28S sequences were aligned using the online version of the software MAFFT (v7; Katoh & Standley,

2014), selecting the "AUTO" option. In order to remove those sites ambiguously aligned, we used the software TrimAl (Capella-Gutiérrez et al., 2009) with the option "automated1". Both alignments were concatenated using the software BioEdit (Hall, 1999). The phylogenetic inference was approached with two different methods: (1) Maximum Likelihood (ML) implemented in the software IQtree2 (Minh et al. 2020), with 10,000 ultrafast bootstrap replicates (UFB), partition by gene (for the *Concatenated* dataset), and the "TESTMERGE" option, that implements the greedy algorithm of PartitionFinder (Lanfear et al., 2017) to reduce over-parameterization and increase model fit; and (2) Bayesian Inference (BI) implemented in the software MrBayes v3.2.7a (Ronquist et al., 2012) applying the GTR+G model in 2 independent runs for 5 million generations, which convergence was checked according to the average standard deviation of split frequencies value (below 0.01). 25% of the stored trees were removed as burn-in.

The molecular species delimitation was tested using a new approach named Assemble Species by Automatic Partitioning (ASAP), a tool designed to propose partitions of species hypotheses using pairwise genetic distances calculated between DNA sequences without phylogenetic reconstruction (Puillandre et al., 2021). The *COIdel* dataset was uploaded to the website (https://bioinfo.mnhn.fr/abi/public/asap/asapweb.html), selecting the Kimura (K80) method for the calculation of genetic distance.

Abbreviations used in figures

(ce) common muscular coat

(cm) cutaneous musculature

(co) common glandular ovovitelline duct

(dc) diagonal cutaneous muscles

(dd) diagonal double muscle layer

(de) dorsal epidermis

(f) fold

(dp) diagonal parenchymatic muscle

(e) eye

(ej) ejaculatory duct

(ep) epithelium

(es) esophagus

(fa) female atrium

(fg) female genital canal

(g) gonopore

(gl) gland cells

(i) intestine

(lc) normal longitudinal cutaneous muscle

(lo) longitudinal muscle

(lsp) sunken longitudinal cutaneous muscle

(lu) pharyngeal lumen

(m) muscle

(ma) male genital atrium

(mo) mouth

(nc) cutaneous peripheral nerve net

(np) nervous plate

(oo) ootype

(o) ovary

(ov) ovovitelline duct

(ci) circular muscle

(ph) pharyngeal pouch

(pp) penis papilla

(pv) prostatic vesicle

(px) pharynx

(sb) sensory border

(sd) sperm duct

(sg) shell glands

(sh) sphincter

(sp) supraintestinal transverse muscles

(spi) sensory pit

(st) spermatophore

(stm) subintestinal transverse muscles

(t) testis

(ve) ventral epidermis

(vi) vitellaria

Results

Molecular results

Phylogenies

The final datasets (both *Concatenated* and *COIdel*) include 22 specimens, 6 of them belonging to the genus *Gusana*. Two species from the Rhynchodeminae subfamily (*Dolichoplana striata* Moseley, 1877 and *Endeavouria septemlineata* (Hyman, 1939)) were used as outgroup (Table 1). The final length of the *COIdel* dataset is 679 bp, while the *Concatenated* dataset is 1959 bp long.

Gusana is a robust monophyletic group (ML: 98% Ultra Fast Bootstrap, UFB; BI: 0.99 Posterior Probability, PP) for both optimality methods with the *COIdel* dataset (Fig. S1-S2, Suppl. mat.). The internal relationships of the genus are identical for both optimality methods, but the statistical robustness of these relationships is low. Both methods (ML and BI) show identical topologies when the *Concatenated* dataset is analyzed, with maximum support for *Gusana* as a monophyletic group. However, only one internal group, namely *Gu. purensis + Gu. lujanae*, has statistical support (Fig. 2).

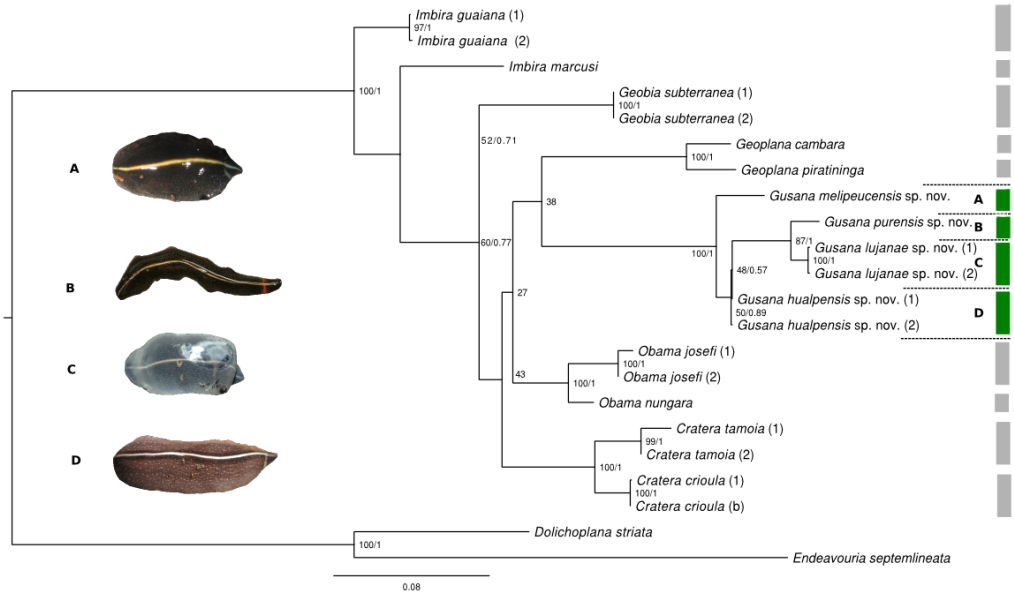

Fig. 2. Phylogenetic tree inferred from the Concatenated dataset (28S rDNA+COI genes) under Maximum Likelihood as the optimality criteria. Numbers at the nodes correspond to ultrafast bootstrap (UFB) values of the ML (left) and to the Bayesian Posterior Probability (PP) (right). Scale bar represents number of substitutions per site.

Molecular species delimitation (ASAP)

The number of putative species retrieved by the 10 best partition schemes produced through ASAP ranges from 2 to 16 (Fig. 3). The best composite score (named asap-score) is 1.5, and it corresponds to a partition with 12 putative species. This partition groups all the *Gusana* specimens in the same MOTU (Molecular Operational Taxonomic Unit). The second best asap-score (2.5) is chosen as the best partition scheme, showing 15 different putative species, with the genus *Gusana* represented by 4 different MOTUs.

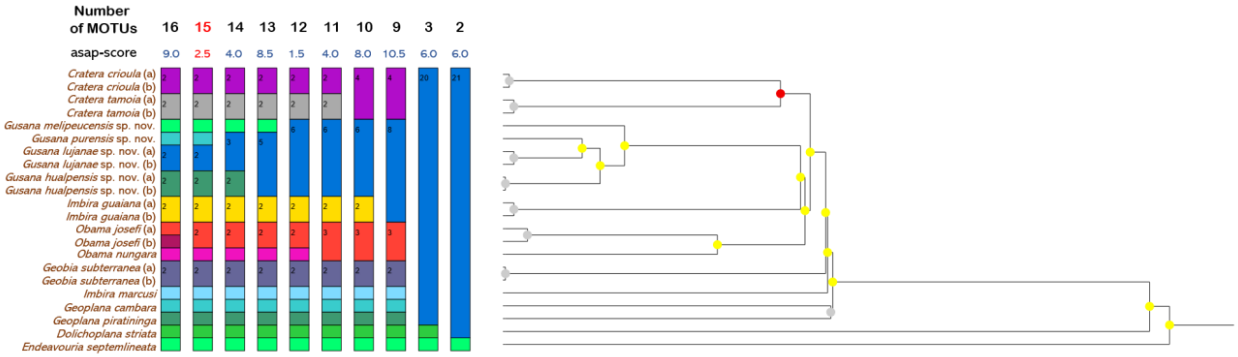

Fig. 3. ASAP partition results. Each coloured bar corresponds to a partition given the asap-score value (indicated in brackets on the top of the bar). Colours on the nodes of the dendrogram correspond to the probability of non-panmictic species. The darker the colour, the higher the probability. Grey colour corresponds to non-calculated probabilities.

Morphological results and taxonomic account

Order Tricladida Lang, 1881

Suborder Continenticola Carranza, Littlewood, Clough, Ruiz-Trillo, Baguñà & Riutort, 1998

Family Geoplanidae Stimpson, 1857

Subfamily Geoplaninae Stimpson, 1857

Genus *Gusana* Froehlich, 1978

***Gusana hualpensis* Carbayo, sp. nov.**

Synonymy

Gusana sp. Carbayo et al. 2013: p. 11, fig. 3.

Material examined. *Holotype* MNHNCL PLAT-15029 (Field code, F4421). CHILE. Concepción Province, Biobío Region: Parque Hualpén (Coord. -36.7961, -73.1524), Francisco Cádiz, 18.i.2010. Horizontal sections of cephalic region on 17 slides; sagittal sections of pharynx and copulatory apparatus on 80 slides. *Paratype* MZUSP PL 1089 (Field code, F4428). CHILE. Concepción Province, same locality and the same date as holotype. Transverse sections of the cephalic region on 10 slides; sagittal sections of the pharynx and copulatory apparatus on 19 slides.

Distribution Only known from the type locality, Parque Hualpén, Concepción Province, Biobío Region, Chile.

Etymology The specific epithet is a reference to the geographical origin of the species, Hualpén Park.

Diagnosis Species of *Gusana* with a whitish dorsal mid stripe bounded on either side by a stripe darker than the general body dark color; a light stripe traverses the cephalic region, dorsally and ventrally. The ejaculatory duct runs horizontally. Prostatic vesicle inverted U-shaped in lateral view.

Description.

External aspect. The animals measured approximately 20 mm in length at crawling. At rest, the body is broad and lanceolate. The cephalic region is triangular with a pointed tip; the posterior extremity is rounded. The dorsum is convex, the ventral side flat. The

preserved specimens measured 15 mm in length, 7-7.5 mm in width, and 1.6-2.2 mm in height.

The general color of the dorsum is dark with a whitish mid stripe and an anterior transverse whitish stripe (Fig. 4A). The latter is located at the end of the anterior 1/15th of the body and may be discontinuous. The width of these stripes is 1/25th of the body width. The dark color is constituted of olive-grey pigment (RAL 6003), darker external to the mid stripe. Numerous whitish speckles are arranged in numerous minute longitudinal striae over the dorsum. The ventral side is light grey with graphite grey (RAL 7024) dots grouped into a pair of paramedian stripes and a tenuous pair of lateral stripes (Fig. 4B). A transverse whitish stria at the end of the anterior 1/15th of the body is continued from the dorsal one resembling a whitish necklace.

The eyes are monolobulated and 35-50 µm in diameter. They are distributed in a single row along the entire body margins. Anterior to the necklace, the eyes are inside clear halos (Fig. 4C). The sensory border is a grey, ventro-marginal line, 0.1 mm in width contouring the anterior 1/5th of the body. The sensory pits are 13-15 µm deep and are distributed along a ventro-lateral row, from the very anterior tip, where the row is uniserial. Behind, they increase up to 6 pits in a row (Fig. 5A). The pits extend posteriorly along 29% of the body length. The relative position of the mouth: body length ranges between 53-57%; that of gonopore: body length, 70-73%.

Internal morphology. The creeping sole occupies approximately 95% of the body width. The cells of the dorsal epidermis contain numerous rhabdites and are pierced by two types of gland cells, producing erythrophil and xanthophil granules, respectively, dorsally and ventrally. There is a poorly defined glandular margin constituted by gland cells producing erythrophil granules. The main nervous system is a plate.

The cutaneous musculature comprises three layers along the body length, namely a subepithelial, one-fiber-thick circular muscle, followed by a double 5-µm-thick layer with diagonal fibers, and then a well-developed innermost longitudinal muscle. This longitudinal muscle is divided dorsally and ventrally into a normal layer (28-30 µm thick dorsally, 28-30 µm ventrally) and a layer sunken into the parenchyma, internally to the cutaneous nerve net (400-420 µm thick dorsally, 100-120 µm ventrally). Muscle fibers of this longitudinal layer are arranged into loose bundles with

2-7 fibers each, dorsally and 3-10 fibers ventrally (Fig. 5 B-E). The cutaneous musculature thickness relative to body height at the pre-pharyngeal region ranges between 17.1-22.9%, or 3.5-3.9%, considering the normal portion only. In the cephalic region, these muscle layers maintain this organization and are thinner towards the anterior extremity of the body.

Three parenchymatic muscle layers present: a dorsal loose layer (20 µm thick) of decussate fibers, part of which are mixed with fibers of the dorsal sunken longitudinal cutaneous muscle; a supraintestinal layer of transverse fibers (70 µm thick), and a subintestinal layer (80 µm thick) of transverse fibers (Fig. 5B).

The mouth is situated at the end of the pharyngeal pouch (Fig. 5F). The pharyngeal pouch is very close to the prostatic vesicle. The esophagus: pharynx ratio is 13%. The pharynx is cylindrical (Fig. 5F). The epithelium of the distal portion of the pharynx is pierced by three types of gland cells producing xanthophil, erythrophil, and cyanophil granules, respectively. The outer pharyngeal musculature consists of a 5-µm-thick subepithelial longitudinal muscle, followed by a 40-µm-thick circular muscle, and an innermost 25-µm-thick longitudinal muscle. The inner pharyngeal musculature consists of a single subepithelial 50-µm thick muscle of circular and longitudinal mixed fibers (Fig. 5G).

The testes are approximately 370 µm diameter and are distributed into 4-6 rows at each side of the body. They are dorsally located between the supraintestinal parenchymatic muscle and the intestine (Fig. 5D). The anteriormost testes are 18% of the body length (and 5% behind ovaries) from the anterior extremity; posteriormost testes 46% of the body length (and 6%, anterior to pharyngeal root).

The dilated distal section of the sperm ducts is bent dorsally and medially to open laterally into the anterior third of the prostatic vesicle (Fig. 6A). An 8-µm-thick circular muscle surrounds these ducts. The prostatic vesicle is extrabulbar, and its main, anterior portion kidney-shaped. The distal portion of the vesicle is inclined downwards as it narrows to cross the ventro-anterior section of the penis bulb and subsequently opening into the ejaculatory duct (Fig. 6A, C). The penis bulb is shifted to a postero-dorsal position above the male atrium. The prostatic vesicle is lined with columnar, ciliated epithelium, which is crossed by numerous gland cells producing coarse erythrophil granules. Three well-developed muscle layers surround the

prostatic vesicle: a subepithelial longitudinal muscle (25 µm thick), followed by a circular muscle (25 µm thick), and an ectalmost longitudinal muscle (100 µm thick) (Fig. 6B-C).

The proximal portion of the ejaculatory is located anterior to the penis papilla and is spiral-shaped. The distal portion of this duct is straight and opens at the tip of the penis papilla (Fig. 6A). This duct is lined with cuboidal, ciliated epithelium and is surrounded by a circular muscle (10 µm thick).

The penis papilla is horizontal and finger-shaped, with a pointed tip. It is located closer to the ventral epidermis than to the dorsal, occupies the anterior half of the male atrium, and is lined with a squamous epithelium with sunken nuclei. This epithelium is underlain by a circular muscle (20 µm thick), followed by a longitudinal one (20 µm).

The male atrium is four times longer than the female atrium and is divided into two halves. The anterior half is twice as long as its height and houses the penis papilla. The distal half is spacious (Fig. 6A-C), and a large dorsal fold projects ventro-posteriorly. This large fold merges with a thin ventral fold projecting from halfway along the ventral wall of the atrium.

The male atrium is lined with a squamous-to-cuboidal epithelium and is pierced by two types of gland cells producing fine weakly erythrophil granules and cyanophil granules. The thin ventral fold is pierced by numerous glands producing strongly erythrophil granules. This epithelium of the male atrium is underlain by a circular muscle (20 µm thick), followed by a longitudinal one (20 µm thick). A transverse annular fold narrows the communication of the male and female atria. The columnar epithelium of this fold is pierced by glands producing erythrophil granules and is underlain by a longitudinal muscle (10 µm thick) followed by a circular one (30 µm thick), giving rise to a moderately developed sphincter (Fig. 6A, D). Fibers of both muscle layers are partially intermingled with each other. The male atrium is twice as long as the female atrium.

The ovaries are ovoid, with a maximum diameter of 200 µm in the antero-posterior axis of the body. The ovaries are 13% of the body length behind the anterior tip of the body. The ovovitelline ducts emerge from the dorso-lateral portion of the ovaries and run immediately above the nerve plate. These ducts ascend dorsally

behind the female atrium to join the common glandular ovovitelline duct (Fig. 6A). The distal portion of the ovovitelline ducts receives shell glands. The common glandular ovovitelline duct runs dorso-anteriorly to open into the female genital canal, which enters the dorso-posterior region of the female atrium. The female atrium is funnel-shaped and is inclined towards the gonopore canal (Fig. 6D).

The common glandular ovovitelline duct is lined with columnar, ciliated epithelium (10 µm high). The female genital canal is lined with a columnar (25 µm high) epithelium and is surrounded by a 20-µm thick circular muscle. The female atrium is lined with a columnar, 25-µm high epithelium. Two types of gland cells pierce the female atrial epithelium, one type being scarce and producing fine erythrophil granules and a second one producing granules weakly cyanophil. A 30-µm-thick layer of crisscrossed fibers underlies the epithelium of the female atrium..

Remarks. Currently, three species of *Gusana* are known, namely *Gu. cruciata,* and *Gu. platei*. *Gusana cruciata*, *Gu. platei*, and the four new species are similar to each other in the general shape and color pattern of the body. *Gusana hualpensis* resembles *Gu. cruciata*, and *Gu. hualpensis* in that they present a light mid stripe and a 'necklace'. However, the light mid stripe is whitish in *Gu. hualpensis*, whereas this stripe is yellowish in the other three species.

Concerning the copulatory apparatus, only *Gu. hualpensis* and *Gu. hualpensis* present a female genital canal not angled, but only in *Gu. hualpensis* the common glandular ovovitelline duct is relatively short.

Fig. 4. *Gusana hualpensis* Carbayo, sp. nov. Paratype. (A): living specimen in the sampling site. (B): ventral view of the preserved specimen on graph paper. (C): dorsal view of the preserved anterior extremity.

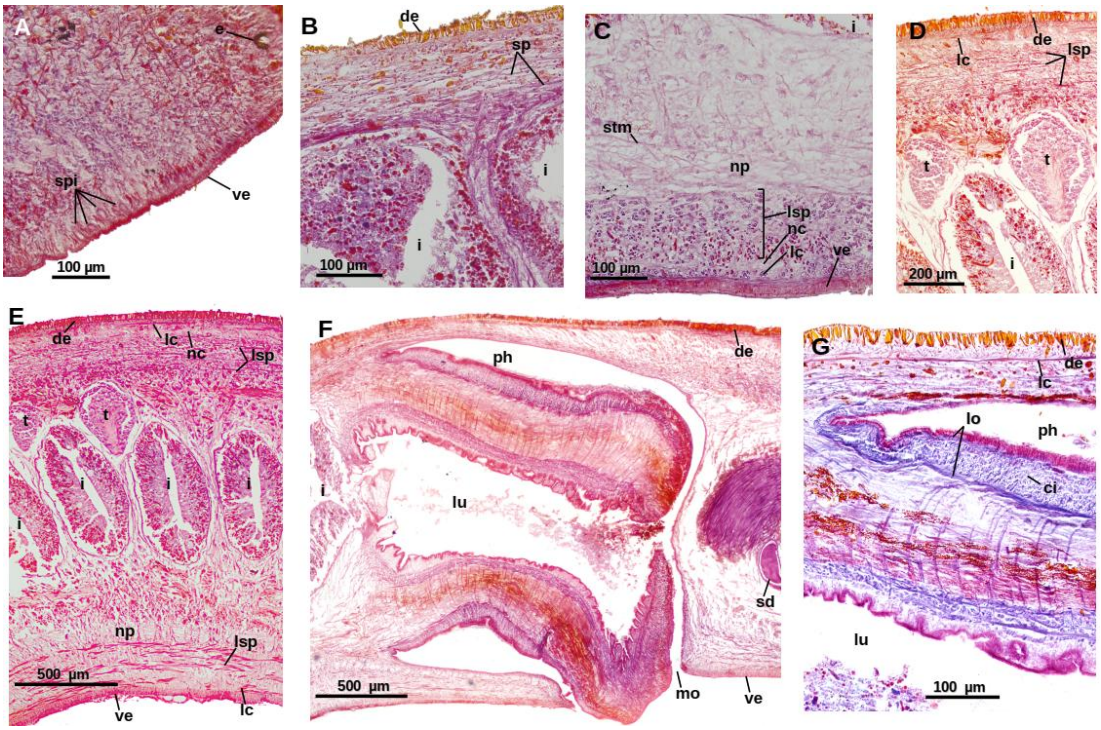

Fig 5. *Gusana hualpensis* Carbayo, sp. nov. Photomicrographs. (A): transverse section of the cephalic region of the paratype. (B): transverse section of the antero-dorsal region of the paratype. (C): transverse section of the antero-ventral region of the paratype. (D-E): sagittal sections of the pre-pharyngeal region of the holotype. (F): sagittal section of the pharynx of the holotype. (G): sagittal section of the dorsal pharyngeal insertion of the paratype.

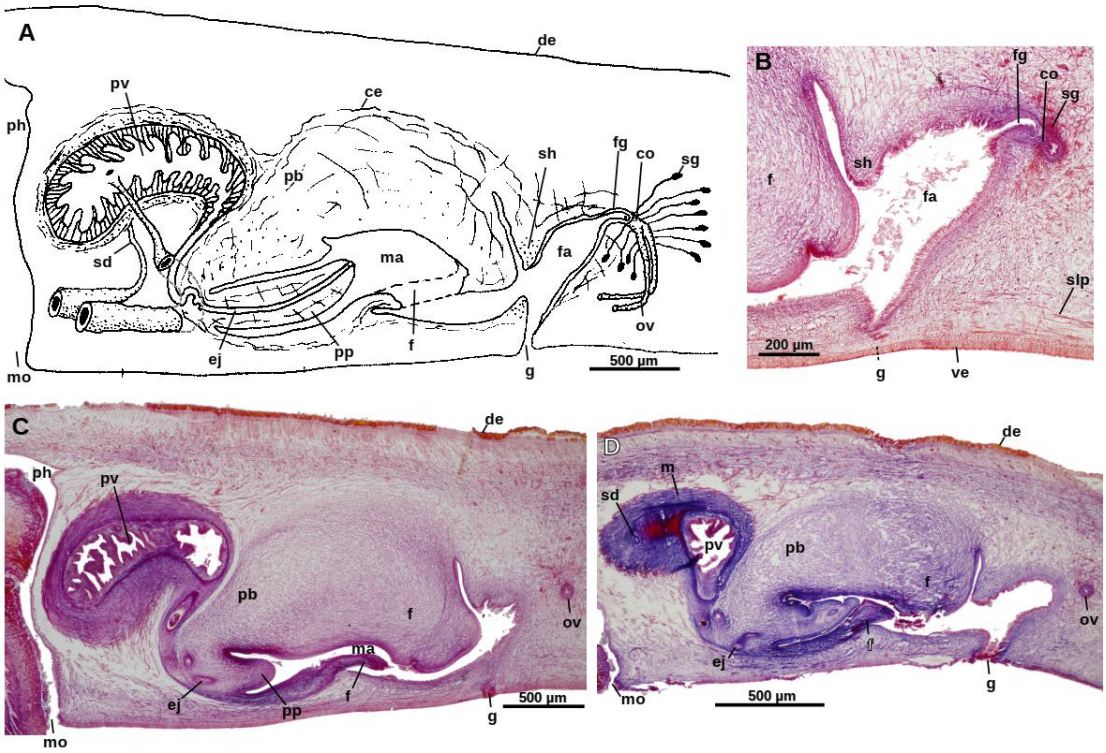

Fig. 6. *Gusana hualpensis* Carbayo, sp. nov. (A): sagittal reconstruction of the copulatory apparatus of the holotype. (B): distal region of the male atrium and female atrium of the holotype. (C): photomicrograph of a sagittal section of the copulatory apparatus of the holotype. (D): photomicrograph of a sagittal section of the copulatory apparatus of the paratype.

Gusana lujanae Almeida & Carbayo, sp. nov.

Material examined

Holotype MNHNCL PLAT-15032 (Field code, F4507). CHILE. La Araucanía Region: Cautín Province, Temuco, Monumento Natural Cerro Ñielol (Coord. -38.7228, -72.5846), Francisco Cádiz, 19.i.2010. Transverse sections of the cephalic region on 12 slides (very anterior extremity damaged when alive); horizontal sections of the ovarian region on 10 slides; transverse sections of the pre-pharyngeal region on 7 slides; sagittal sections of the pharynx and copulatory apparatus on 26 slides.

Paratype MZUSP PL 2278 (Field code, F4505). CHILE. La Araucanía Region, same locality and the same date as holotype. Horizontal sections of the cephalic region on 16 slides; horizontal sections of the ovarian region on 16 slides; transverse sections of the pre-pharyngeal region on 14 slides; sagittal sections of the pharynx and copulatory apparatus on 33 slides.

Distribution. Only known from Monumento Natural Cerro Ñielol, Temuco, Cautín Province, La Araucanía Region, Chile.

Etymology. The specific epithet is a homage to Bianca Lujan (USP) for her friendship.

Diagnosis. Species of *Gusana* with a transverse light stripe on the ventral cephalic region only. Communication of the common ovovitelline duct with the female genital canal is angled. The male atrium is three times longer than the female atrium.

Description. External aspect. The size of the living specimens is not available. The preserved specimens measured 13.5-16 mm in length, 6-6.5 mm in width, and 1.6 mm in height. The body is broad and relatively short. In dorsal view, the body is lanceolate with the cephalic region triangular and pointed; the posterior extremity is rounded. The dorsal color of the preserved specimens is black green (RAL 6012), mottled with clear speckles and a whitish-to-yellowish thin median stripe (1/36th of body width; Fig. 7A-B). An additional tenuous pair of paramedian stripes of the same whitish-to-yellowish color may be present (Fig. 7B). The margins of the body are greyish. The ventral cephalic region is black grey (RAL 7021) with a whitish transverse stripe (Fig. 7E). The remaining ventral surface is light grey (RAL 7035) with dark specks that are more densely distributed along the paramedian zones (Fig. 7C) only, or also along the lateral zones (Fig. 7D). The ventral body margins are whitish.

The eyes are monolobulated and 64-80 µm in diameter. They are distributed in a

single row, contouring the entire body margins. The sensory border (Fig. 7E) is a grey, ventro-marginal line, 0.1 mm in width, contouring the anterior 8% of the body. The sensory pits are 50 µm deep and are distributed along the sensory margin from the very anterior tip of the body along 32% of the body length (Fig. 7F-I). These pits are arranged in 1-2 rows on each side of the body. The relative position of the mouth: body length is 57%. The relative position of the gonopore: body length, 82%.

Internal morphology. The creeping sole occupies the entire ventral surface. The dorsal epidermal cells contain numerous rhabdites. The epithelium is also pierced by two types of gland cells, producing erythrophil and xanthophil granules, respectively, dorsally and ventrally. In the pre-pharyngeal region, the erythrophil type is scarce in the dorsal epithelium, whereas the xanthophil type is rare in the ventral one. A glandular margin is absent. The nervous system is organized in a plate.

The cutaneous musculature comprises three layers: a subepithelial 3-µm-thick circular layer, a double layer (12 µm) with diagonal fibers, and a well-developed innermost longitudinal layer. The longitudinal layer is divided dorsally and ventrally into a normal layer (6-12 µm thick dorsally, 30-70 µm ventrally) and a layer sunken into the parenchyma, internally to the cutaneous nerve net (95-150 µm thick dorsally, 160-190 µm ventrally) (Fig. 8). The muscle fibers of the normal layer are arranged into poorly defined bundles with 4-16 and 6-18 fibers each, dorsally and ventrally, respectively, whereas these values for the sunken longitudinal layer are 3-6 and 10-18 fibers, respectively (Figs. 8C-E; 9A-C). The sunken ventral fibers are not gathered into bundles towards the body margins(Fig. 8A-B). The cutaneous musculature thickness relative to body height at the pre-pharyngeal region ranges between 21-23%, or 4.5-5.1% considering only the normal portion.

There are three parenchymatic muscle layers: a dorsal layer (100 µm thick) of decussate fibers that are mixed with fibers of the dorsal sunken longitudinal cutaneous muscle (Fig. 9A-B); a supraintestinal layer of transverse fibers (150 µm thick) also mixed with fibers of the dorsal sunken longitudinal cutaneous muscle; and a subintestinal layer (90 µm thick) of transverse fibers. Some transverse fibers extend among the components of the nerve plate into the ventral sunken cutaneous layer (Fig. 8B).

The mouth is situated more or less at the end of the pharyngeal pouch. The

pharyngeal pouch is very close to the prostatic vesicle (Fig. 9D). The esophagus: pharynx ratio is 13%. The pharynx is cylindrical, with the dorsal insertion slightly shifted posteriorly (Fig. 9D). The epithelium of the distal portion of the pharynx is pierced by three types of gland cells producing xanthophil, erythrophil, and cyanophil granules, respectively. The outer pharyngeal musculature consists of a subepithelial longitudinal muscle (5 µm thick), followed by a circular muscle (35 µm thick), and a longitudinal muscle (20 µm thick). The inner pharyngeal musculature consists of a single subepithelial layer (120 µm thick) of circular and longitudinal mixed fibers (Fig. 9F).

The testes are approximately 350 µm in diameter and are located between the supraintestinal parenchymatic muscle layer and the intestine (Fig. 8A-B, D). They are distributed into 3-4 dorsal rows at each side of the body. The anteriormost testes are 12.5% of the body length from the anterior extremity; posteriormost testes 43% of the body length, so being shortly anterior to the pharyngeal root.

The distal section of the sperm ducts is bent antero-dorsally to open laterally into the anterior third of the prostatic vesicle (Fig. 10A). Sperm are present in the distal portion of the sperm ducts, lined with a cuboidal, ciliated epithelium. This epithelium is crossed by gland cells producing cyanophil granules and is surrounded by a 10-µm-thick circular muscle.

The prostatic vesicle is extrabulbar and located anteriorly to the penis bulb. The anterior portion of this vesicle is roughly cylindrical and inclined postero-dorsally. The posterior portion vertically descends as it narrows to cross the ventro-anterior section of the penis bulb and subsequently to open into the ejaculatory duct (Fig. 10A-B). The penis bulb is shifted to a postero-dorsal position above the male atrium. The prostatic vesicle is lined with a columnar, ciliated epithelium producing amorphous erythrophil secretion and is crossed by numerous gland cells producing coarse erythrophil granules. The prostatic vesicle is surrounded by three muscle layers: a subepithelial longitudinal layer (40 µm thick), followed by a circular layer (100 µm thick), and an ectalmost longitudinal layer (180 µm thick) (Fig. 10A).

The anterior portion of the ejaculatory duct is spiral and anterior to the penis papilla (Fig. 10B). The posterior portion of this duct is straight and runs along the penis papilla to open at its tip (Fig. 10A, C). This duct is lined with cuboidal, ciliated

epithelium and is surrounded by a circular muscle (15 µm thick).

The horizontal penis papilla is cylindrical, with a pointed tip. This papilla is located closer to the ventral epidermis than to the dorsal one and occupies the anterior half of the male atrium (Fig. 10A). The papilla is lined with a squamous epithelium pierced by numerous gland cells producing fine erythrophil granules. This epithelium is underlain by a circular muscle (30 µm thick), followed by a longitudinal one (30 µm).

The male atrium is three times longer than the female atrium and is elongated, narrower in its anterior half. It is provided with a large fold projecting ventro-posteriorly from its dorsal side and ventrally merges with a smaller fold situated halfway along the ventro-lateral wall of the atrium (Fig. 10A, C, E). The anterior half is located closer to the ventral epidermis than to the dorsal one. The male atrium is lined with a squamous-to-cuboidal epithelium that is pierced by gland cells producing erythrophil granules. Additionally, the anterior half is pierced by gland cells producing cyanophil granules, whereas the dorso-distal section of the atrium is crossed by cells containing amorphous xanthophil secretion. The epithelium of this atrium is underlain by a circular muscle, followed by a longitudinal muscle, both being 50-90-µm-thick.

A fold located dorsally to the gonopore canal narrows the communication between the male and the female atrium. This fold is lined with a columnar epithelium that is pierced by gland cells producing erythrophil secretion. The musculature underlying this epithelium of this fold consists of a dense and thick circular muscle which is continued from the musculature underlying the ventro-distal section of the male atrium, giving rise to a well-developed sphincter (Fig. 10A, C, E). The male atrium is three times as long as the female atrium (Fig. 10A).

A structure seemingly being a spermatophore is embedded in the dorsal wall of the male atrium of both specimens (Fig. 10A, C-E). The spermatophore is comma-shaped and ranges between 370-400 µm in length and 200-220 µm in width. The pointed extremity of the spermatophore is located deep in the stroma. Most of the spermatophore is composed of an amorphous xanthophil mass. Fine cyanophil granules and strands of erythrophil granules are mixed with the xanthophil mass. These three substances are produced by the respective gland cells located in the stroma around the spermatophore. The epithelial lining of the male atrium lacks where

the spermatophore is attached, and small lumps of sperm are attached to the free surface of the spermatophore or embedded in it.

The ovaries are ovoid, with a maximum diameter of 320 µm in the antero-posterior axis of the body. The ovaries are located 12.5% of the body length behind the anterior tip of the body. The ovovitelline ducts emerge from the dorso-lateral portion of the ovaries and run ventrally above the nerve plate. Behind the female atrium, these ducts ascend dorso-posteriorly and subsequently bend dorso-anteriorly to join the common ovovitelline duct The distal portion of it is dilated to form the ootype. A short distal segment of the ovovitelline ducts and the common ovovitelline duct receive shell glands (Fig. 10A, F). The ootype lies external to the common muscle coat. The communication of the ootype with the female genital canal is angled. This 135-µm-long canal enters the dorso-posterior region of the female atrium. The female atrium is a spacious cavity narrowed by the dorsal fold separating the female from the male atrium. This female atrium is oriented towards the gonopore canal.

The common glandular ovovitelline duct and the ootype are lined with columnar, ciliated epithelium (10 µm high), crossed by shell glands and glands producing erythrophil granules. The female genital canal is lined with a 37-µm-high columnar epithelium, and the apical portion of its cells is inclined towards the female atrium. A circular, 20-µm thick circular muscle surrounds this canal.

The female atrium is lined with a 35-µm-high columnar epithelium, the free surface of which is undulate. This epithelium is pierced by two types of gland cells producing erythrophil and fine xanthophil granules, respectively. This epithelium is underlain by a 5-µm-thick circular layer of thin muscle fibers, followed by a 25-µm thick longitudinal muscle with radial and circular fibers interspersed (Fig. 10E-G).

Remarks. *Gusana lujanae* distinguishes readily from all species of the genus in that it does not present a necklace but a clear transverse stripe on the ventral side. Concerning the internal organs, *Gu. lujanae* differs from most species in the genus in having the communication of the common ovovitelline duct with the female genital canal angled, as in *Gu. purensis*. However, in *Gu. purensis*, the ratio male atrium length: female atrium length is 9 : 1 (vs. 3 : 1 in *Gu. lujanae*).

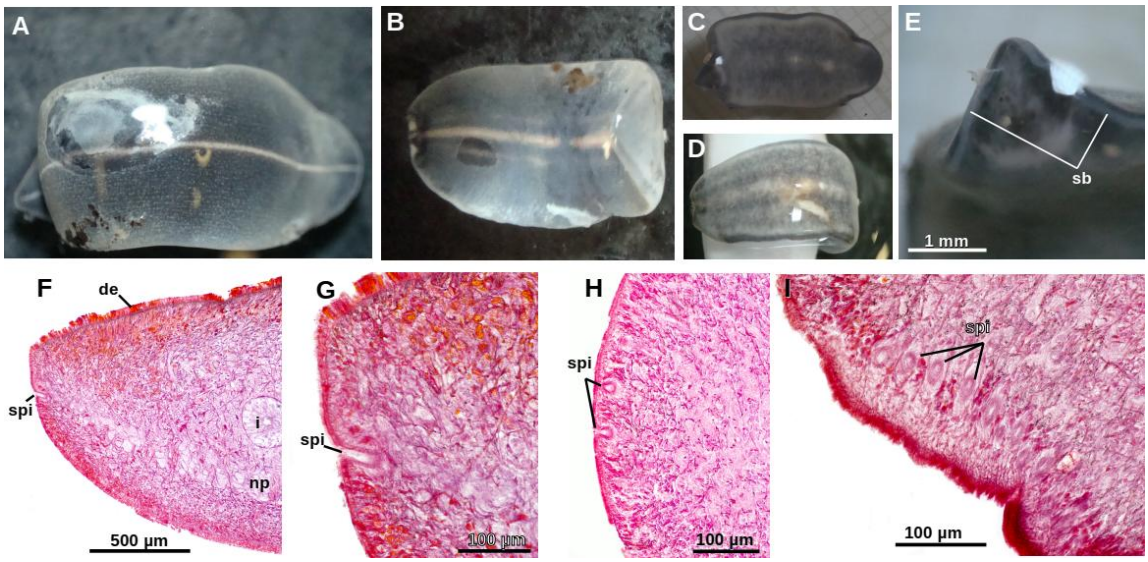

Fig. 7. *Gusana lujanae* Almeida & Carbayo, sp. nov. (A): dorsal view of the preserved paratype. (B): dorsal view of the preserved holotype. (C): ventral view of the preserved paratype on graph paper. (D): ventral view of the preserved paratype. (E): Ventral view of the anterior extremity of the body of the preserved paratype. (F-H): photomicrograph of a transverse section of the cephalic region of the paratype. (I): transverse-to-sagittal section of the cephalic region of the paratype.

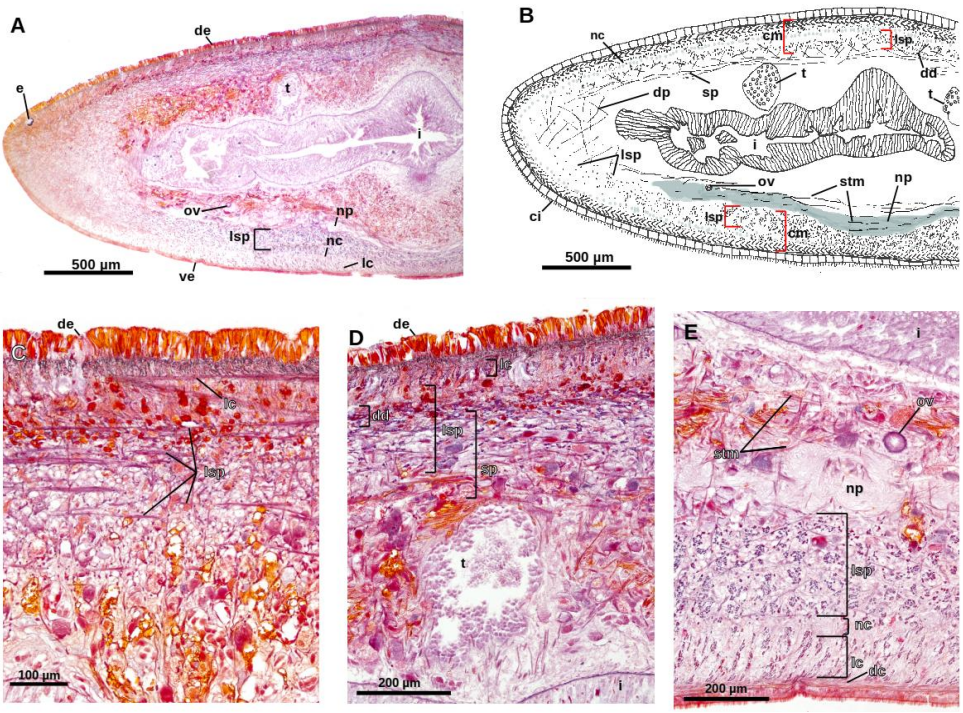

Fig. 8. *Gusana lujanae* Almeida & Carbayo, sp. nov. Paratype. (A): photomicrograph of a transverse section of the pre-pharyngeal region. (B): diagrammatic representation of a transverse section of the pre-pharyngeal region. (C): photomicrograph of a dorsal portion of the pharyngeal region in a sagittal section. (D): photomicrograph of the dorsal portion of a transverse section of the pre-pharyngeal region. (E): photomicrograph of a ventral portion of a transverse section of the pre-pharyngeal region.

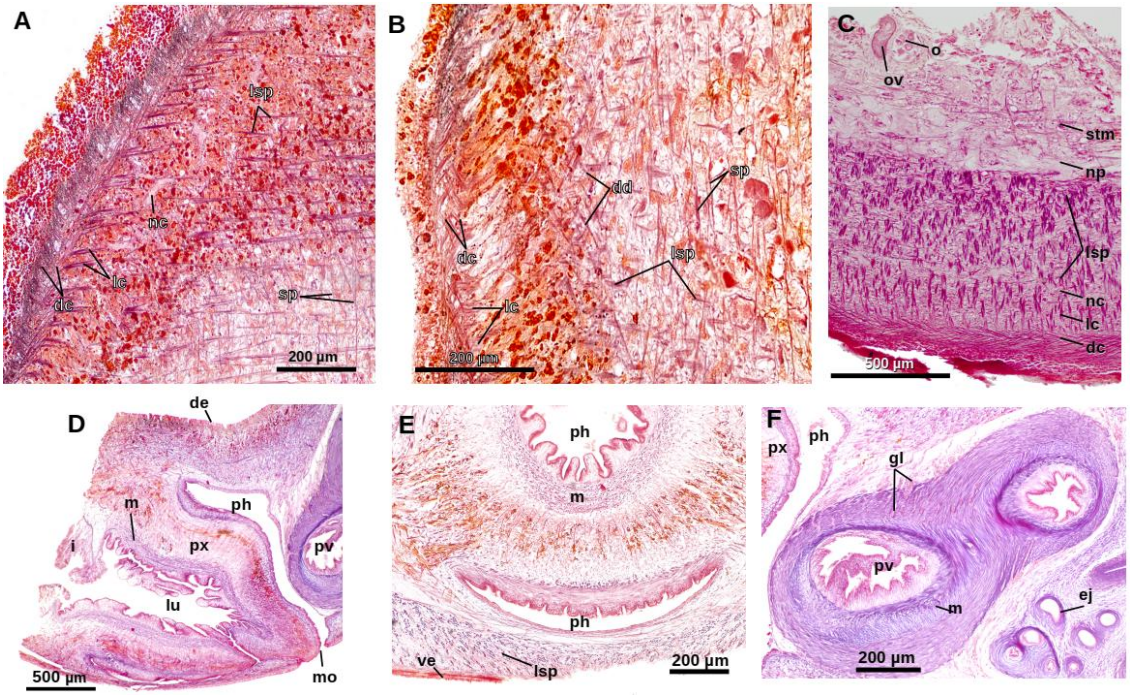

Fig. 9. *Gusana lujanae* Almeida & Carbayo, sp. nov. Photomicrographs. (A-B): horizontal sections of the dorsal portion of the body of the paratype. (C): transverse section of the ventral portion of the ovarian region of the paratype. (D): sagittal section of the pharynx of the holotype. (E): transverse section of the esophagus of the paratype. (F): sagittal section showing the prostatic vesicle and ejaculatory duct of the holotype.

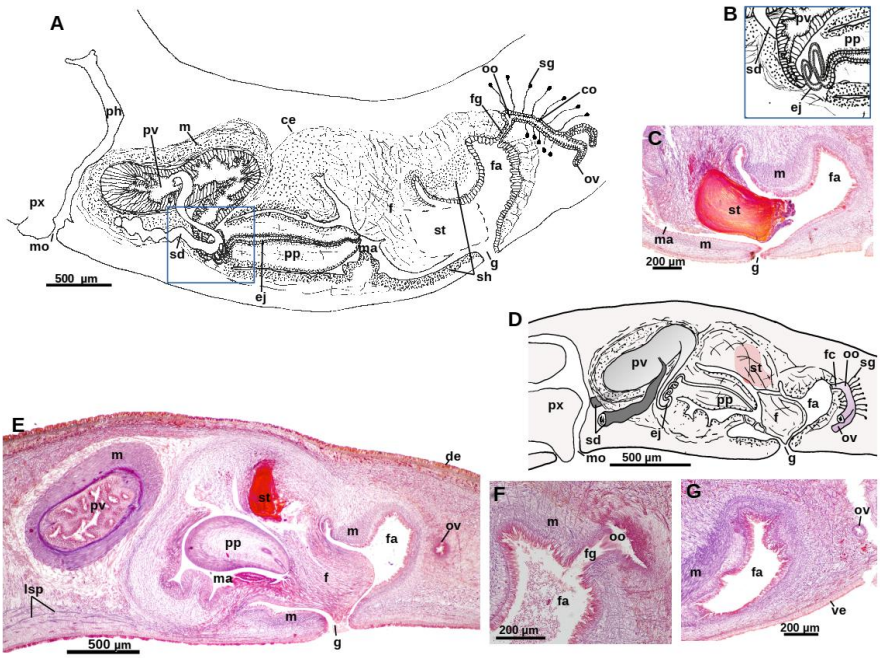

Fig. 10. *Gusana lujanae* Almeida & Carbayo, sp. nov. (A): sagittal reconstruction of the copulatory apparatus of the holotype. (B): portion of the ejaculatory duct hidden behind the prostatic vesicle in Fig 15A. (C): spermatophore attached to the fold of the male atrium of the holotype. (D): sagittal reconstruction of the copulatory apparatus of the paratype. (E): photomicrograph of a sagittal section of the copulatory apparatus of the paratype. (F-G): female genital canal and female atrium of the holotype.

***Gusana melipeucensis* Almeida & Carbayo, sp. nov.**

Material examined *Holotype* MNHNCL PLAT-15030 (Field code, F4430). CHILE. La Araucanía Region: Cautín Province, Melipeuco, Parque Nacional Conguillío (Coord. -38.6501, -71.6493), F. Cádiz, 24.i.2010. Transverse-to-sagittal sections of the cephalic region on 3 slides; horizontal sections of the ovaries region on 2 slides; transverse sections of the pre-pharyngeal region on 7 slides; sagittal sections of the pharynx and copulatory apparatus on 10 slides.

Distribution. Only known from the type locality, Parque Nacional Conguillío, Melipeuco, Cautín Province, La Araucanía Region, Chile.

Etymology. The specific epithet is a reference to the geographical origin of the species, Melipeuco.

Diagnosis. Species of Gusana with a transverse light stripe in the cephalic region, dorsally and ventrally. Sperm ducts open into the proximal region of the prostatic vesicle.

Description.

External aspect. The size of the living animal is not available. Preserved, it measured nine millimeters in length, 3.5 mm in width, and 0.7 mm in height. At rest, the body is lanceolate, broad, and relatively short. The cephalic region is pointed with a triangular shape; the posterior extremity is rounded. The dorsum is convex, the ventral side flat. The predominant color of the dorsum is black grey (RAL 7021) with clear speckles (Fig. 11A). A longitudinal mid stripe (1/18th of the body width) runs along the entire length of the body. This mid stripe is whitish in the cephalic region and yellowish with a brownish outline along the remaining body length (Fig. 11A-B). In the cephalic region, there is a transverse white stripe that extends ventrally (Fig. 11C). The margins of the body are greyish (Fig. 11B). The ventral side of the preserved animal is greyish except a poorly defined brownish, paramedian band on each side of the body and a lateral, irregular stripe of the same color (Fig. 11C). Around the mouth and the gonopore, the ventral side is whitish.

The monolobulated eyes are 45-50 µm in diameter. They contour the anterior tip of the body and extend marginally at the end tip of the body. The sensory pits are distributed along the greyish sensory margin. This margin runs from the very anterior tip (Fig. 11B) to 26.5% of the body length behind. These pits are either 55-80 µm deep

simple invaginations or, less frequently, 2 or 3 invaginations, each 28-37-µm deep and 35-µm wide, converge into a single pit (Fig. 12A-B). Shortly behind the anterior tip of the body, the pits are organized into several rows in the same transverse plane. The number of rows is difficult to determine due to the plane of the sections. The relative position of the mouth: body length is 61%; that of the gonopore: body length is 72%.

Internal morphology. The creeping sole occupies the entire ventral surface. The dorsal epidermal cells contain numerous rhabdites (Fig. 12C-D). Two types of gland cells, producing xanthophil and erythrophil granules, respectively, pierce the dorsal and ventral epidermis. A glandular margin is absent. The central nervous system is organized as a ventral plate.

The cutaneous musculature comprises a subepithelial layer (2.5 µm) of circular fibers, followed by a double layer (5 µm) of diagonal fibers, and a layer of longitudinal fibers, which exhibits a portion sunken into the parenchyma, dorsally and ventrally (Fig. 12A-D). Dorsally, the normal and sunken portions are 15 µm and 75 µm thick, respectively; ventrally, 25.5 µm and 92.5 µm, respectively. The muscle fibers of the normal layer are arranged into poorly defined bundles, each with 4-10 fibers dorsally and 6-20 ventrally (Fig. 12C-F). The muscle fibers of the sunken longitudinal muscle are not gathered in evident bundles, and towards the body margins, the fibers are scattered (Fig. 12C). The cutaneous musculature thickness relative to body height at the pre-pharyngeal region is 23%, or 5.5-6.0% if the normal portion is considered only. Towards the anterior tip of the body, the musculature exhibits similar organization as in the pre-pharyngeal region, although it is relatively weaker.

The parenchymatic muscle layers are organized as follows: a dorsal layer (90 µm thick) of decussate fibers mixed with those of the dorsal sunken longitudinal cutaneous muscle (Fig. 12F); a supraintestinal layer (30-455 µm thick) of transverse fibers; and a subintestinal layer (50 µm thick) of transverse fibers. Additionally, transverse fibers are running among the components of the nervous plate and the sunken ventral portion of the longitudinal cutaneous muscle.

The mouth is situated at a distance from the root of the pharynx, equivalent to 90% of the length of the pharyngeal pouch. The pharyngeal pouch is attached to the prostatic vesicle (Figs. 13, 14A). The esophagus: pharynx ratio is 23%. The pharynx is cylindrical. The epithelium of the distal portion of the pharynx is pierced by two types

of gland cells producing xanthophil and cyanophil granules, respectively. The outer pharyngeal musculature consists of a subepithelial layer (7.5 µm thick) of longitudinal fibers, followed by a layer (70 µm thick) of spaced circular fibers, and a layer (10 µm thick) of longitudinal fibers. The inner pharyngeal musculature consists of a subepithelial layer (75 µm thick) of circular and longitudinal fibers interwoven.

The testes are pear-shaped and approximately 250 µm in diameter. They are distributed into 1-2 rows on each side of the body. They are dorsally located between the supraintestinal parenchymatic muscle layer and the intestine (Fig. 12C). The anteriormost testes are located at a distance from the anterior extremity 28% of the body length; posteriormost testes 61%, therefore they are lateral to the pharyngeal root.

The sperm ducts run ventrally. Their distal portion, which contains sperm, bends anteriorly and penetrates the thick muscle coat of the prostatic vesicle. The sperm ducts traverse this muscle vertically to open laterally into the proximal portion of the prostatic vesicle (Fig. 13). The sperm ducts are lined with a cuboidal epithelium, which is surrounded by a 5-µm-thick circular muscle.

The prostatic vesicle is extrabulbar and located anteriorly to the penis bulb. This vesicle is inverted-U-shaped in lateral view (Fig. 13). The anterior half of the vesicle is wider than the posterior, the latter being slightly lateral to the penis bulb. The prostatic vesicle penetrates the ventro-anterior section of the penis bulb to open into the ejaculatory duct (Fig. 14B). The penis bulb is shifted to a postero-dorsal position above the male atrium. The prostatic vesicle is lined with columnar, ciliated epithelium, crossed by numerous gland cells of two types producing coarse xanthophil and erythrophil granules, respectively. The prostatic vesicle is surrounded by three distinct muscle layers: a subepithelial longitudinal muscle (40 µm thick), followed by a circular muscle (40 µm thick), and an ectalmost longitudinal muscle (75 µm thick).

The ejaculatory duct is canalicular; its anterior half runs upwards and loops before continuing backwards into the penis papilla to open at its tip (Fig. 13). The ejaculatory duct is lined with a cuboidal, ciliated epithelium, crossed by numerous gland cells producing fine erythrophil granules, and is surrounded by a circular muscle (5 µm thick).

The penis papilla is cylindrical and inclined towards the gonopore. This papilla

occupies the anterior half of the male atrium. The papilla is lined with a squamous epithelium, pierced by numerous gland cells producing fine erythrophil granules, especially around its insertion. The epithelium of the penis papilla is underlain by a circular muscle (12.5 µm thick), followed by a longitudinal muscle (17.5 µm).

The male atrium is nine times longer than the female atrium and is elongated and provided with a large fold projected posteriorly from the dorso-left side of the atrial wall. This fold merges with a ventro-lateral fold projected from the distal half of the atrium (Figs. 13, 14B-C). The male atrium is lined with a cuboidal epithelium which in some parts presents small weakly stained vesicles detaching from it. The epithelium of the male atrium is pierced by gland cells producing fine erythrophil granules. Additionally, the distal portion of the male atrium is pierced by gland cells producing xanthophil granules. The musculature underlying the epithelium of the male atrium is constituted by a subepithelial circular muscle (20-µm thick), followed by a longitudinal muscle (15-µm thick). Muscle fibers underlining the large fold's epithelium are scattered and apparently oriented diagonally. The male atrium is twice as long as the female atrium.

The ovaries are ovoid, with a maximum diameter of 300 µm along latero-lateral axis of the body. The ovaries are 22% of the body length behind the anterior tip of the body. The ovovitelline ducts emerge from the dorso-anterior portion of the ovaries and run ventrally above the nerve plate. Behind the gonopore, these ducts ascend dorso-posteriorly, and their distal section widens to open into a dilated common ovovitelline duct or ootype (Fig. 13). Dilated sections of the ovovitelline ducts and ootype receive shell glands and are surrounded by a 12.5-µm thick muscle of thin circular and longitudinal fibers. This common duct continues with the female genital canal, which is gradually narrower as it runs dorso-anteriorly to open into the dorso-posterior section of the female atrium (Fig. 14D). This canal is lined with a squamous-to-cuboidal epithelium and is surrounded by an 8-µm thick muscle consisting of crisscrossed fibers.

The female atrium is funnel-shaped (Figs. 13, 14C) and is lined with a 35-µm high, columnar, non-ciliated epithelium. In some sections, the epithelium is apparently stratified. This epithelium is pierced by gland cells producing xanthophil granules and is underlain by a 160-µm-thick layer of mainly longitudinal and circular muscle fibers.

Remarks. The external appearance of *Gusana hualpensis* resembles only that of *Gu. hualpensis* in the light dorsal mid stripe and the whitish necklace. However, in *Gu. hualpensis*, there is a pair of dark paramedian stripes bordering the mid stripe, whereas in *Gu. hualpensis*, the pigment is evenly black greyish or presents a clearer stripe. Concerning the copulatory apparatus, *Gusana hualpensis* distinguishes it from its congeners in that it is the only species in which the sperm ducts open in the proximal region of the prostatic vesicle.

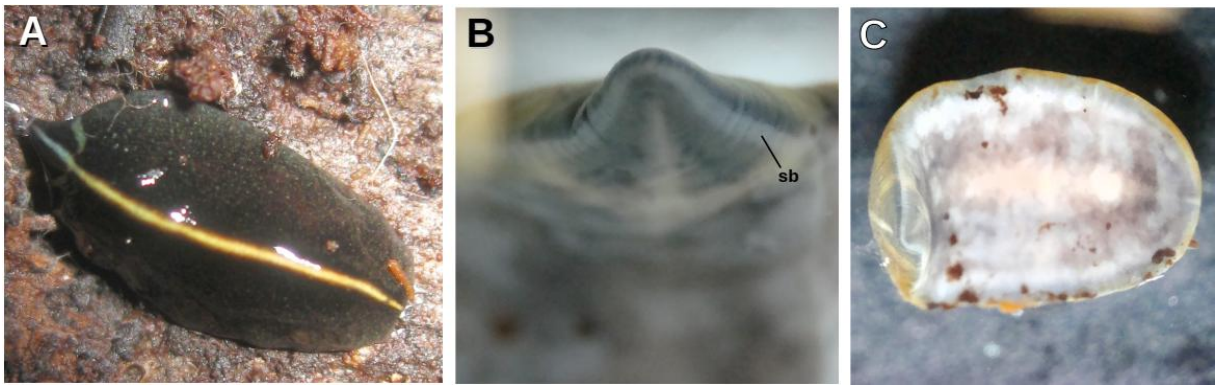

Fig. 11. *Gusana melipeucensis* Almeida & Carbayo, sp. nov. (A): living specimen in the sampling site. (B): ventral view of the preserved specimen. (C): fronto-ventral view of the anterior extremity.

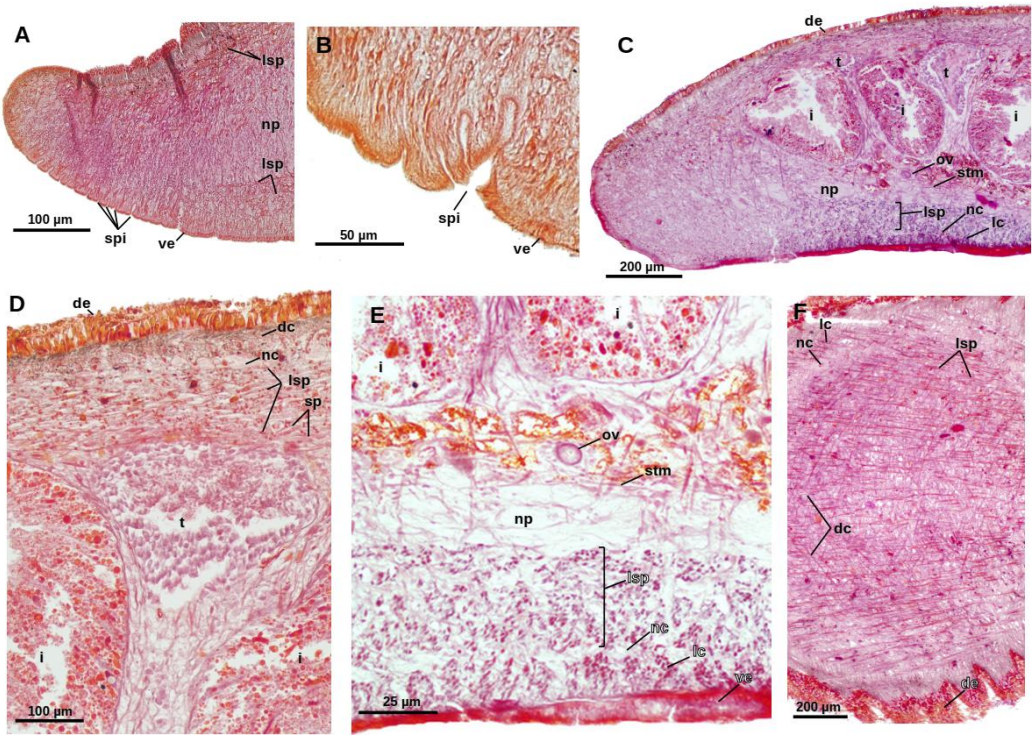

Fig. 12. *Gusana melipeucensis* Almeida & Carbayo, sp. nov. Photomicrographs. (A-B): transverse-to-sagittal sections of the cephalic region. (C): transverse section of the pre-pharyngeal region. (D): dorsal portion of a transverse section of the pre-pharyngeal region. (E): ventral portion of a transverse section of the pre-pharyngeal region. (F): dorsal portion of a horizontal section of the ovarian region.

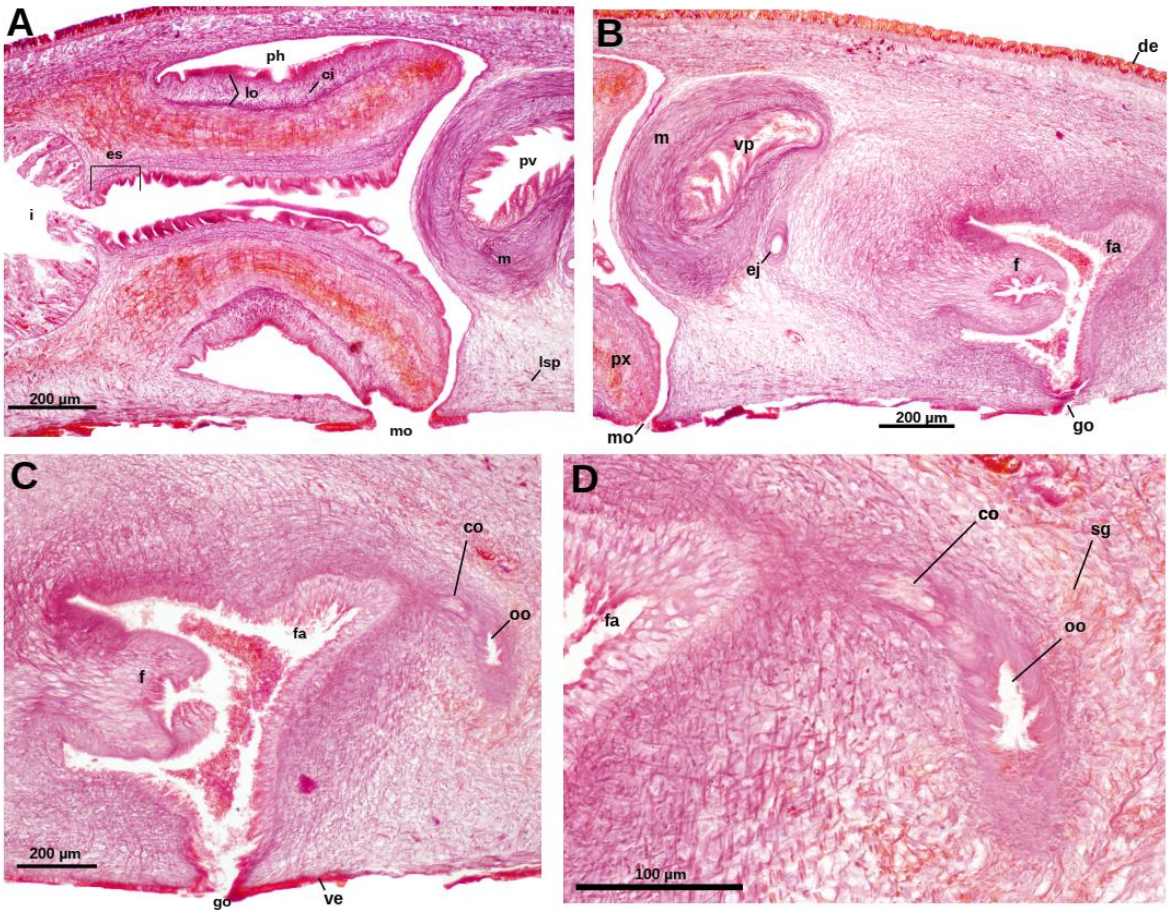

Fig. 13. *Gusana melipeucensis* Almeida & Carbayo, sp. nov. Photomicrographs of sagittal sections. (A) pharynx. (B): general view of the copulatory apparatus. (C): distal fold of the male atrium and female atrium. (D): female genital canal and female atrium.

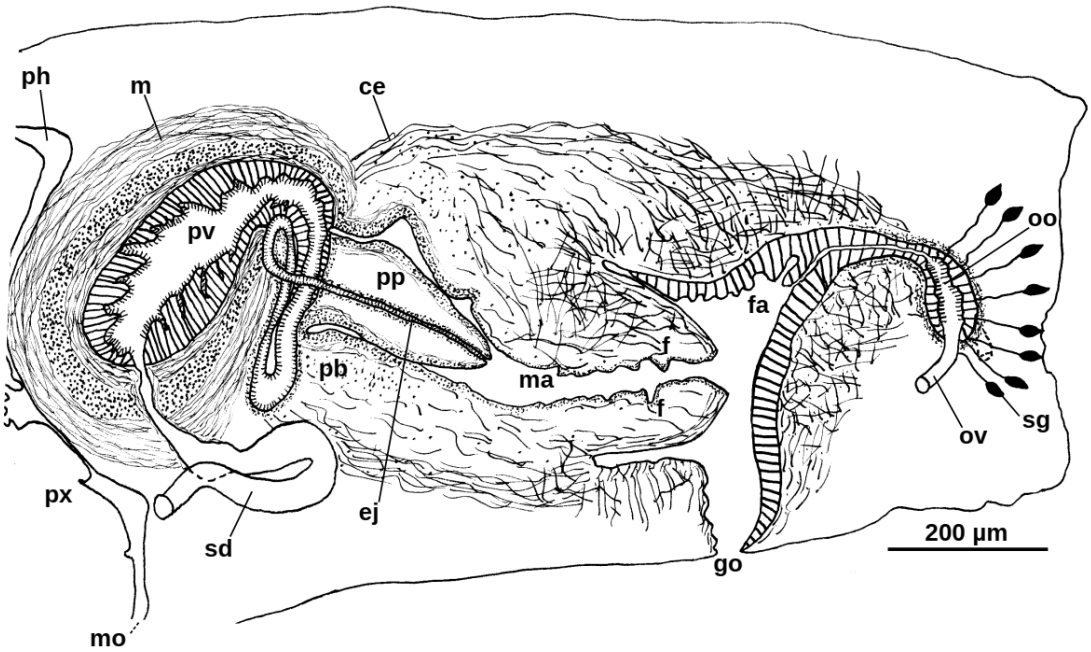

Fig. 14. *Gusana melipeucensis* Almeida & Carbayo, sp. nov.): sagittal reconstruction of the copulatory apparatus of the holotype

Gusana purensis Bolonhezi, Almeida & Carbayo, sp. nov.

Material examined

Holotype MNHNCL PLAT-15031 (Field code, F4889). CHILE. La Araucanía Region: Malleco Province, Purén, Parque Nacional Nahuelbuta (Coord. -37.8275, -73.0097), F. Carbayo, 11.xii.2010: transverse sections of the cephalic region on 5 slides; horizontal sections of the ovarian region on 2 slides; transverse sections of the post-ovarian region on 6 slides; sagittal sections of the pharynx and copulatory apparatus on 6 slides.

Distribution. Only known from the type locality, Parque Nacional Nahuelbuta, Purén, Malleco Province, La Araucanía Region, Chile.

Etymology. The specific epithet is a reference to the geographical origin of the species, Purén.

Diagnosis. Species of *Gusana* with a transverse reddish stripe in the cephalic region, dorsally and ventrally. The male atrium is nine times longer than the female atrium.

Description.

External aspect. The living animal was not measured. Preserved, it measured 12 mm in length, 4 mm in width, and 1.2 mm in height. The body of the preserved specimen is lanceolate, broad, and relatively short, with a triangular and pointed cephalic region and a rounded posterior extremity. The dorsum of the living animal is convex, the ventral side flat. The predominant color of the dorsum is black brown (RAL 8022) with clear speckles, which are absent in the cephalic region (1/12th of the body length) (Fig. 15A-B). A longitudinal sulfur yellow (RAL 1016) mid stripe (1/20th of the body width) almost reaches both body extremities. Between the cephalic region and the remaining body is a transverse red orange (RAL 2001) stripe that extends ventrally so resembling a 'necklace'. The margins of the body are light grey (RAL 7035). The ventral side is light grey with brownish irregular dots, except the midline (Fig. 15B). This ventral side is whitish around the mouth and the gonopore.

The eyes, monolobulated, are 45-60 µm in diameter, each encircled by a halo.

They contour the anterior tip of the body and extend marginally until the posterior extremity of the body. The sensory pits are distributed along the greyish sensory margin. These pits are 35-42 µm deep, simple invaginations, and are arranged in a single row in the anterior tip. At a distance of 12% of the body length, they arrange in 2-3 rows (Fig. 16A). Groups of two pits may open in transverse wrinkles (Fig. 16B). The relative position of the mouth: body length is 56%; that of the gonopore: body length is 72.9%.

Internal morphology. The creeping sole occupies the entire ventral surface. The dorsal epidermal cells contain numerous rhabdites (Fig. 16C). Three types of gland cells, producing xanthophil, coarse cyanophil, and fine cyanophil granules, respectively, pierce the dorsal epidermis. The latter type also pierces the ventral epithelium, which is stained reddish. Additionally, two types of gland cells producing erythrophil and xanthophil granules pierce the ventral epithelium. These relatively scarce two types are more densely distributed towards the body margins. A glandular margin is absent.

The cutaneous musculature comprises a subepithelial layer (2.5 µm) of circular fibers, followed by a double layer (5-7.5 µm) of diagonal fibers, and a layer of longitudinal fibers, the latter exhibiting a portion sunken into the parenchyma, dorsally and ventrally (Fig. 16C-E). Dorsally, the normal and sunken portions are 30-32 µm and 134-153 µm thick, respectively; ventrally, 42-48 µm and 140-150 µm, respectively (Fig. 16C-D). The muscle fibers of the normal layer are arranged into poorly defined bundles with 4-10 and 6-20 fibers each, dorsally and ventrally, respectively, whereas these values are 4-9 and 8-18 fibers for the sunken longitudinal layer, respectively. Towards the body margins, the sunken ventral fibers are not gathered into bundles. The cutaneous musculature thickness relative to the body height at the pre-pharyngeal region is 16%, or 6.8% if the normal portion is considered only. Towards the anterior tip of the body, the cutaneous musculature exhibits similar organization as in the pre-pharyngeal region, although it is relatively weaker.

The parenchymatic muscle layers are organized in a dorsal layer (85-100 µm thick) of decussate fibers mixed with fibers of the dorsal sunken longitudinal cutaneous muscle; a supraintestinal layer (120-260 µm thick) of transverse fibers, and

a subintestinal layer (50-80 µm thick) of transverse fibers (Fig. 16D). Additionally, transverse fibers run among the components of the nervous plate.

The mouth is situated at the end of the pharyngeal pouch (Fig. 16E). The pharyngeal pouch is attached to the prostatic vesicle. The esophagus: pharynx ratio is 20%. The pharynx is cylindrical. The epithelium of the distal portion of the pharynx is pierced by three types of gland cells producing erythrophil, xanthophil, and cyanophil granules, respectively. The outer pharyngeal musculature consists of a subepithelial longitudinal muscle (10 µm thick), followed by a circular muscle (42 µm thick), and a longitudinal muscle (17 µm thick) (Fig. 16E-F). The inner pharyngeal musculature consists of a layer (70 µm thick) of circular and longitudinal fibers interwoven.

The testes are pear-shaped and 330-380 µm in diameter (Fig. 16C). They are distributed into 2-3 rows on each side of the body. They are dorsally located between the supraintestinal parenchymatic muscle layer and the intestine. The anteriormost testes are 21% of the body length from the anterior extremity; posteriormost testes approximately 49% of the body length.

The sperm ducts run ventrally. Their distal portion, which contains sperm, bends dorsally to penetrate the thick muscle of the prostatic vesicle and subsequently opens laterally into the mid-region of this vesicle (Fig. 17A). The sperm ducts are lined with a cuboidal epithelium, surrounded by a 50-µm-thick circular muscle.

The prostatic vesicle is extrabulbar and anterior to the penis bulb. The vesicle is more or less inverted-U-shaped in lateral view (Fig. 17A), with its anterior half wider than the distal, the latter running ventrally to penetrate the ventro-anterior section of the penis bulb. The penis bulb is shifted to a postero-dorsal position above the male atrium (Fig. 17A-C). The prostatic vesicle is lined with a columnar, ciliated epithelium, which is crossed by numerous gland cells producing coarse erythrophil granules. The prostatic vesicle is surrounded by three well-developed muscle layers: a subepithelial longitudinal muscle (20 µm thick), followed by a circular muscle (42 µm thick), and an ectalmost longitudinal muscle (80 µm thick).

The anterior section of the ejaculatory duct is helicoidal and ascending,

whereas the portion running within the penis papilla is straight and opens at the tip of the papilla (Fig. 17A). The ejaculatory duct is lined with a cuboidal epithelium, crossed by gland cells producing cyanophil granules, and some gland cells producing erythrophil granules. A 5-14-µm thick circular muscle surrounds the ejaculatory duct.

The penis papilla is conical and is located in a ventral position concerning the body height, occupying the anterior 2/5th of the male atrium (Fig. 17A-C). This papilla is lined with a squamous-to-cuboidal epithelium, pierced by gland cells producing erythrophil granules and by scarce cells producing cyanophil granules. The epithelium of the penis papilla is underlain by a circular muscle (12.5 µm thick), followed by a longitudinal muscle (15 µm).

The male atrium is narrow and elongate, provided with a dorsal and large fold that merges with a smaller fold projecting from the midventral region of the atrium (Fig. 17A-C). This atrium is nine times longer than the female atrium. The anterior half of the male atrium is lined with a squamous-to-cuboidal epithelium. This epithelium is pierced by gland cells producing erythrophil granules. Additionally, the ventral portion of the anterior half receives scarce cells producing xanthophil granules. The distal half of the male atrium is lined with a cuboidal-to-columnar epithelium pierced by three types of gland cells producing cyanophil, xanthophil, and erythrophil granules, respectively. The latter type of gland cell is particularly abundant in the midventral fold (Fig. 17B). The musculature underlying the epithelium of the male atrium is composed of a subepithelial 30-70-µm-thick circular muscle, followed by a 15-50-µm-thick longitudinal muscle, both muscles being thinner in the midregion of the male atrium. An annular fold narrows the distalmost section of the male atrium, the epithelium of which is pierced by abundant gland cells producing erythrophil granules and by irregularly distributed cells producing cyanophil granules. This epithelium is surrounded by a 50-110-µm-thick circular muscle forming a sphincter (Fig. 17A, C). The male atrium is three times as long as the female one.

The ovaries are rounded and 300-350 µm in diameter. The ovaries are located at a distance from the anterior tip, 21% of the body length. The ovovitelline ducts emerge from the dorsal surface of the ovaries and run above the nerve plate. Behind

the female atrium, these ducts ascend dorso-posteriorly to open into the ootype. A short distal section of each ovovitelline duct and the ootype receive shell glands. The communication of the ootype with the female genital canal is angled (Fig. 17A), and the latter opens into the dorso-posterior portion of the female atrium. This canal is lined with squamous-to-cuboidal epithelium and is surrounded by an 8-µm thick muscle consisting of crisscrossed fibers.

The female atrium is more or less funnel-shaped (Fig. 17A, D) and is lined with a columnar epithelium which becomes cuboidal towards the gonopore. This epithelium is pierced by three types of gland cells producing xanthophil, erythrophil, and cyanophil granules, respectively, the latter type being present only in the converging region with the female genital canal. An 18-25-µm-thick layer of muscle of circular and longitudinal fibers surrounds the epithelium of the female atrium. Radial fibers are also present (Fig. 17D).

Remarks. In the external aspect, *Gusana purensis* distinguishes readily from all species of the genus by means of its reddish necklace. Regarding the internal organs, *Gusana purensis* differs from its congeners in that the ratio male atrium length: female atrium length is 9 :1 (vs. 4 : 1 or less in the remaining species).

Fig. 15. *Gusana purensis* Bolonhezi, Carbayo & Almeida, sp. nov. Holotype. Dorsal (A) and partially ventral (C) views of the living holotype. Scale bars not available.

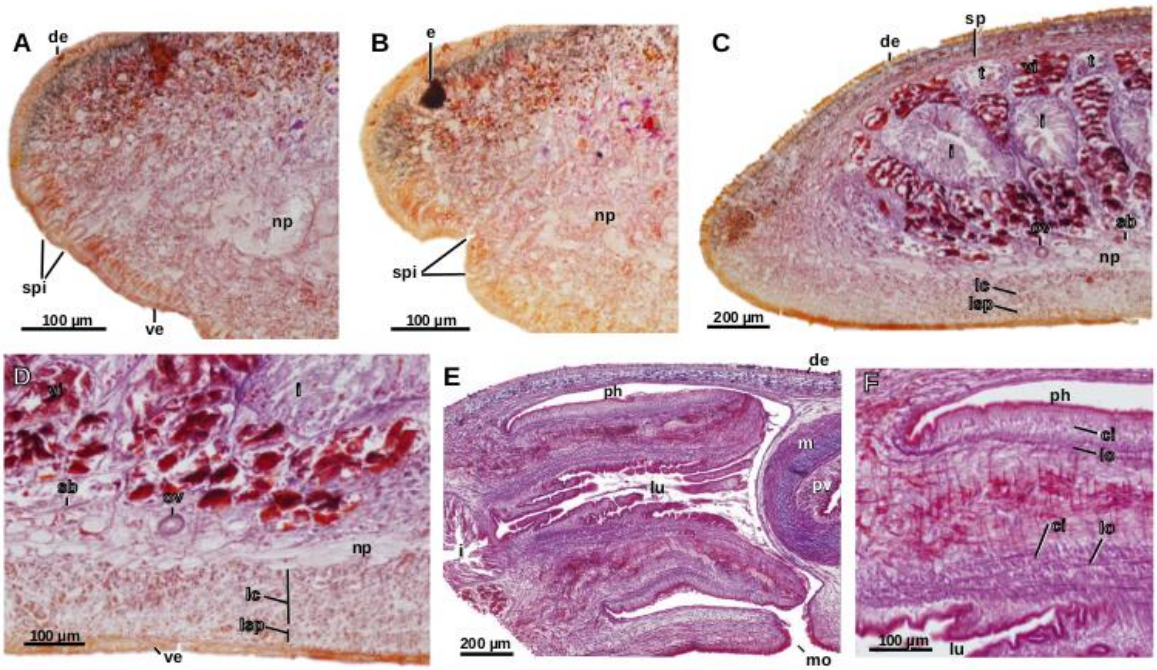

Fig. 16. *Gusana purensis* Bolonhezi, Carbayo & Almeida, sp. nov. Photomicrographs of the holotype. A-B: transverse sections of the cephalic region showing sensory pits. C-D: transverse sections of the pre-pharyngeal region. E-F: sagittal sections of the pharynx.

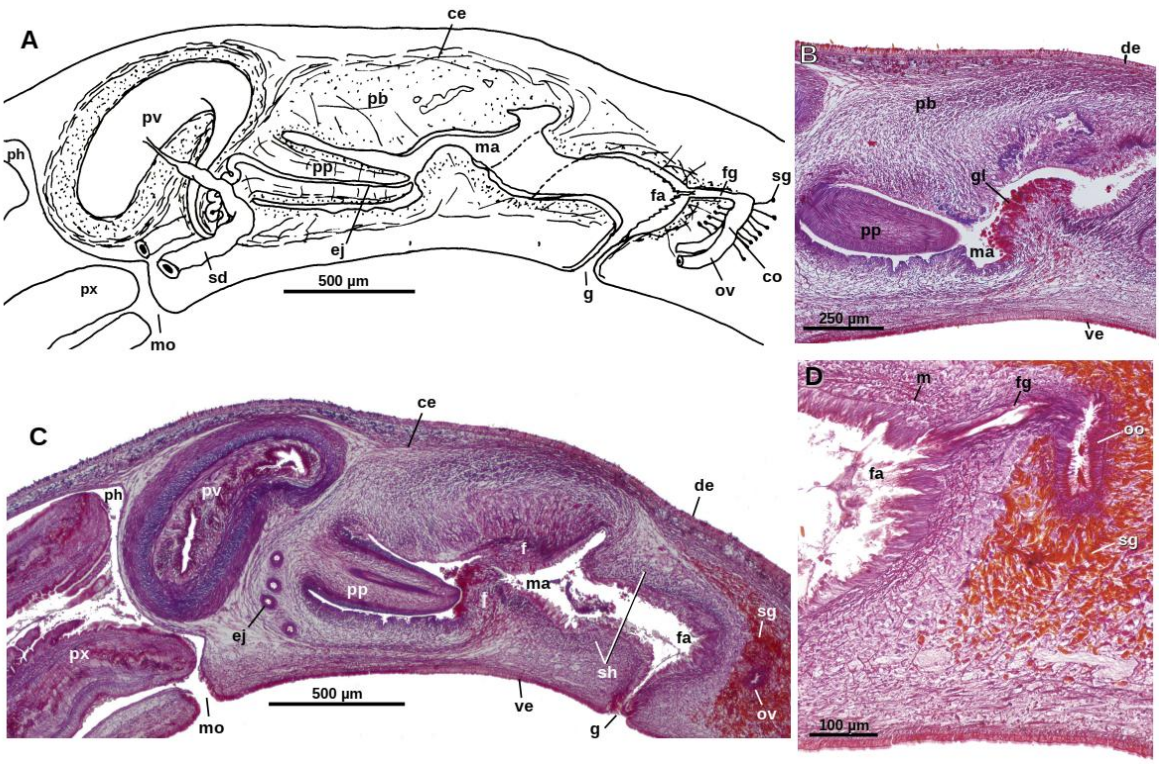

Fig. 17. *Gusana purensis* Bolonhezi, Carbayo & Almeida, sp. nov. Holotype. (A): Diagrammatic

reconstruction of the copulatory apparatus of the holotype. (B-D): photomicrographs of sagittal sections of the male atrium (B), copulatory apparatus (C), and female atrium (D).

Discussion

Molecular accuracy. Previous molecular phylogenetic trees included only two individuals of *Gusana*, namely those of *Gu. hualpensis* (see Carbayo et al. 2013; Negrete et al., 2020) and the number and/or nature of the genes were different from the present paper. Therefore, our results cannot appropriately be compared with previous studies. It might well be this situation that best explains the different sister-group relationships of *Gusana* concerning Carbayo's et al. (2013) and Negrete's et al. (2020) studies. Here is noted again the relevance of the genes used and the taxonomic representation for molecular phylogenies. Nonetheless, the phylogenetic trees inferred here, which count six terminals of four species of *Gusana,* allowed us to give evidence of the monophyly of the genus.

ASAP is a single-marker species delimitation method that relies on pairwise genetic distances to assign specimens to species (Puillandre et al., 2021). As a result, an asap-score is computed with the combination of the probabilities of groups to be panmictic species and the barcode gap widths. As other molecular species delimitation methods (e. g., ABGD), ASAP outputs more than one partition, ranked in this case by their asap-scores. The lower the asap-score, the better the partition. However, the partition with the best asap-score not always needs to be the only one considered, but also the subsequent ones (Puillandre et al., 2021). This new molecular species delimitation method highlights the need for the integrative taxonomy concept in this kind of analysis. When single markers are used, several partition schemes can be meaningful for the same dataset. Here is when the combination of the morphological data and the genetic distances tells the putative true story and allows selecting one of the partitions as the most plausible. One of the partitions that might be the best under the asap-score ranking would cluster together species that are considered separated lineages under morphological criteria. For that reason, and in an integrative taxonomic context, the best partition scheme in the present analysis corresponds to the second-best asap-score and not to the first. In this partition, the genus *Gusana* (main focus of

the work) is represented by 4 different MOTUs, matching each a morphotype with a characteristic set of morphological traits that give them a particular identity and deserve to be named a new species.

Systematics. With this contribution, the number of species of *Gusana* has increased from two to six. The general shape and color pattern of the body of the six species are markedly similar to each other and different from those of other land planarians. This similarity led E. M. Froehlich (1978) (a) to suggest the conspecificity of *Gu. platei* and *Gu. cruciata* (see E. M. Froehlich, 1978), and (b) to conclude that three specimens studied by her are *Gu. cruciata*, despite their minor differences in the color of the dorsum among them and concerning the syntypes. A thorough study of the type material of these species is needed.

Another interesting characteristic of *Gusana* is the close resemblance of the internal morphology of the congeners. Indeed, the species differ from each other only in details of the relative size (e. g., male atrium, common glandular ovovitelline duct) and position (e. g., sperm ducts) of the organs. The original diagnosis of *Gusana* reads:

> "*Geoplanidae [currently Geoplaninae] with a broad, foliaceous body, tapering very abruptly to the anterior end. Anterior end triangular. Creeping sole broad, with more than half the body width. Subepidermal musculature weak; longitudinal layer partly sunk into the parenchyma, internal to the cutaneous nerve net, both ventrally and dorsally. Sensory border forming a thick turned edge around the anterior tip. Sensory pits of normal shape or obliquely elongated and internally branched. Testes are dorsal. Without adhesive musculo-glandular organs and sensory papillae. Copulatory apparatus without adenodactyls*" (Froehlich, 1978).

This diagnosis was later complemented with the following: "Color pattern with cross banding; mc:h value less than 4% (smaller than the smallest *Geoplana);* male antrum is very large, with penis papilla of small intra-antral type; female canal enters ventrally" (Ogren & Kawakatsu, 1990).

The four new species described here match this diagnosis. Nonetheless, the

sunken musculature is worthy of further comments. E. M. Froehlich (1978) considered the longitudinal layer in the inner side of the cutaneous nerve net as being cutaneous, i.e., the 'sunken' part of the longitudinal musculature. It follows that the sunken part is also cutaneous. Therefore, it should be considered to calculate the relative thickness of the cutaneous musculature. The relative muscle thickness in the four new species ranges between 16-23%, whereas this value is 21-24 % in *Gu. cruciata* as measured in Froehlich's material (FC, pers. obs.). Therefore, we suggest amending the diagnosis with the following "*The cutaneous musculature thickness relative to body height at the pre-pharyngeal region ranges between 16-24%*".

On the spermatophore. Spermatophores are rare in geoplaninids. They were observed in the Geoplaninae *Notogynaphallia sexstriata* (Graff, 1899) (see Froehlich, 1956), *Luteostriata muelleri* (Diesing, 1861) (see Froehlich, 1959), *Amaga righii* (Froehlich, 1972) and *Choeradoplana iheringi* Graff, 1899 (see Souza & Leal-Zanchet, 2004). Spermatophores were also reported for the Rhynchodeminae *Platydemus victoriae* (Dendy, 1890) (see Heinzel, 1929), *Platydemus manokwari* Beauchamp, 1962 (see Winsor, 1998), and *Pimea monticola* Winsor, 1991, and for the Microplaninae *Microplana aixandrei* Vila-Farré et al., 2008, *Microplana hyalina* Vila-Farré & Sluys, 2011 (see Vila-Farré et al., 2011), and *Othelosoma duplamaculosum* Sluys & Neumann, 2017. Leal-Zanchet & Froehlich (2006) observed that the four Geoplaninae species lack a penis papilla and possess a pleated male atrium. They suggested that the distal wall of the male atrium would be everted to transfer the sperm. As shown above, *Gusana lujanae* has a penis papilla and produces spermatophores, found in the male atrium. If sperm implantation into the recipient is a function of the male atrial fold, the penis papilla might address the sperm not into the partner's body but into its spermatophore.

References

Almeida, A. L., Francoy, T. M., Álvarez-presas, M., and Carbayo, F. (2021). Convergent evolution: A new subfamily for bipaliin-like Chilean land planarians (Platyhelminthes). Zoologica Scripta, 00, 1-9. DOI: 10.1111/zsc.12479

Beauchamp de, P. (1962). Platydemus manokwari n. sp., planaire terrestre de la Nouvelle-Guinée Hollandaise, Bulletin de la Société Zoologique de France, 87 (5-6), 609-615.

Blanchard, É. (1847). Sur lórganisation des vers. Chapitre IV. Annales des Sciences Naturelles. Troiseéme Série Zoologie, 8, 119-149.

Boll, P. K., Amaral, S. V. d., and Leal-Zanchet, A. M. (2019). Two new land planarian species (Platyhelminthes: Tricladida: Geoplanidae) from protected areas in southern Brazil. Zootaxa 4664 (4): 535–550.

Capella-Gutiérrez, S., Silla-Martínez, J. M., & Gabaldón, T. (2009). trimAl: A tool for automated alignment trimming in large-scale phylogenetic analyses. Bioinformatics, 25(15), 1972–1973. https://doi.org/10.1093/bioinformatics/btp348

Carbayo, F., Álvarez-Presas, M., Olivares, C. T., Marques, F. P. L., Froehlich, E. M., and Riutort, M. (2013). Molecular phylogeny of Geoplaninae (Platyhelminthes) challenges current classification: proposal of taxonomic actions. Zoologica Scripta 42(5), 508–528. doi:10.1111/zsc.12019

Cason, J. E. (1950). A rapid one-step Mallory-Heidenhain stain for connective tissue. *Stain Technology*, 25 (4), 225–226. http://dx.doi.org/10.3109/10520295009110996

Dendy, A. (1890). The Victorian land planarians. Transactions of the Royal Sociey of Victoria 65-81.

Diesing, K. M. (1861). Revision der Turbellarien. Abtheilung: Dendrocoelen. Sitzungsberichte der Mathematisch-Naturwissenschaftliche Classe, **44**, 486–578.

Ewing B, Green P. (1998). Base-calling of automated sequencer traces using Phred II. Error probabilities. *Genome Research* **8:** 186–194.

Ewing B, Hillier L, Wendl MC, Green P. (1998). Basecalling of automated sequencer traces using Phred I. Accuracy assessment. *Genome Research* **8:** 175-185.

Fetzner, J. (1999). Extracting high–quality DNA from shed reptiles skins: a simplified method. *BioTechniques*, **26**, 1052–1054.

Froehlich, C. G. (1956). Tricladida Terricola das regiões de Teresópolis e Ubatuba. Papéis Avulsos do Departamento de Zoologia 12(16), 313-344.

Froehlich, C. G. (1959). On geoplanids from Brazil. Boletim da Faculdade de Filosofia, Ciências e Letras da Universidade de São Paulo 22, 201–242.

Froehlich, C. G. (1967). A contribution on the zoogeography of neotropical land planarians. *Acta Zoologica Lilloana*, 23, 153-162.

Froehlich, E. M. (1978). On a collection of Chilean land planarians. *Boletins de Zoologia da Universidade de São Paulo*, 3, 7-80.

Froehlich, E. M. and Froehlich, C. G. (1972). land planarians fro mthe Amazonian region. Papéis Avulsos de Zoologia, 26(2), 29-45.

Gordon D, Abajian C, Green P. (1998). Consed: a graphical tool for sequence finishing. *Genome Research* **8:** 195-202.

Gordon D, Desmarais C, Green P. (2001). Automated finishing with autofinish. *Genome Research* **11:** 614-625.

Graff, L. v. (1896). Über das System und die geographische Verbreitung der Landplanarien. Verhandlungen der Deutschen Zoologischen Gesselschaft, 6, 61-75.

Hall, T. A. (1999). BioEdit: a user-friendly biological sequence alignment editor

and analysis program for Windows 95/98/NT. Nucleic Acids Symposium Series, 41, 95–98. https://doi.org/10.14601/Phytopathol_Mediterr-14998u1.29

Heinzel, L. (1929). Zur Kenntnis der Rhynchodemiden. *Zoologische Jahrbucher. Abteilung fur Systematik, Ökologie und Geographie der Tiere* **56**, 425–462.

Hyman, L. H. (1939). Land planarians from the Hawaiian Islands. Archives de Zoologie Expérimentale et Genérale, 80, 116-124.

Katoh, K., and Standley, D. M. (2014). MAFFT: Iterative Refinement and Additional Methods. In D. J. Russell (Ed.), Multiple Sequence Alignment Methods, Methods in Molecular Biology (pp. 131–146). Springer Science+Business Media, LLC. https://doi.org/10.1007/978-1-62703-646-7_8

Lanfear, R., Frandsen, P. B., Wright, A. M., Senfeld, T., and Calcott, B. (2017). Partitionfinder 2: New methods for selecting partitioned models of evolution for molecular and morphological phylogenetic analyses. Molecular Biology and Evolution, 34(3), 772–773. https://doi.org/10.1093/molbev/msw260

Leal-Zanchet, A. M. and Froehlich, E. M. (2006). A species complex in the genus Notogynaphallia Ogren and Kawakatsu (Platyhelminthes: Tricladida: Terricola) with a taxonomic revision of homonyms of Geoplana marginata Schultze & Müller and a reinterpretation of Notogynaphallia caissara (Froehlich) anatomy. Belgian Journal of Zoology 136(1), 81-100.

Marcus, E. (1954) Reports of the Lund University Chile Expedition 1948-1949. 11. Turbellaria. *Lunds Universitets Årsskrift,* 49(13), 3-114.

Minh, B. Q., Schmidt, H. A., Chernomor, O., Schrempf, D., Woodhams, M. D., Von Haeseler, A., … and Teeling, E. (2020). IQ-TREE 2: New Models and Efficient Methods for Phylogenetic Inference in the Genomic Era. Molecular Biology and Evolution, 37(5), 1530–1534. https://doi.org/10.1093/molbev/msaa015

Moseley, H. N. (1877). Notes on the Structure of several forms of Land Planarians, with a description of two new genera, and several new species, and a

list of all species at present known. Quarterly Journal of Microscopical Science, 17, 274-292.

Negrete, L., Álvarez-Presas, M., Riutort, M. and Brusa, F. (2020). Integrative taxonomy of land planarians (Platyhelminthes: Geoplanidae) from the Andean-Patagonian Forests from Argentina and Chile, with the erection of two new genera. Journal of Zoological Systematics and Evolutionary Research 00, 1-25. doi: 10.1111/jzs.12444

Negrete, L., Gira, R. D., and Brusa, F. (2019). Two new species of land planarians (Platyhelminthes, Tricladida, Geoplanidae) from protected areas in the southern extreme of the Paranaense Rainforest, Argentina. Zoologischer Anzeiger 279, 38–51. doi:10.1016/j.jcz.2019.01.002

Ogren, R. E., and Kawakatsu, M. (1990). Index to the species of the family Geoplanidae (Turbellaria, Tricladida, Terricola) Part I: Geoplaninae. *The Bulletin of Fuji Women's College*, 28, 79–166.

Puillandre, N., Brouillet, S., & Achaz, G. (2021). ASAP: assemble species by automatic partitioning. Molecular Ecology Resources, 21(2), 609–620. https://doi.org/10.1111/1755-0998.13281

Ronquist, F., Teslenko, M., van der Mark, P., Ayres, D. L., Darling, A., Höhna, S., … Huelsenbeck, J. P. (2012). MrBayes 3.2: Efficient Bayesian Phylogenetic Inference and Model Choice Across a Large Model Space. Systematic Biology, 61(3), 539–542. https://doi.org/10.1093/sysbio/sys029

Sandison, A. T. (1955). The histological examination of mummified material. *Stain technology*, 60(6), 227-283. https://doi.org/10.3109/10520295509114479

Sluys, R., Neumann, M., de Lima, R. F., and Drewes, R. C. (2017). Land flatworms (Platyhelminthes, Geoplanidae) of São Tomé: a first account on their diversity, with the description of five new species. Zootaxa 4221 (3), 291-322.

Souza, S. A. D., and Leal-Zanchet, A. M. (2004). Histological and histochemical

characterization of the secretory cells of Choeradoplana iheringi Graff, 1899 (Platyhelminthes: Tricladida: Terricola). Brazilian Journal of Biology 64(3), 511-522.

Stimpson, W. (1857). Prodromus descriptionis animalium evertebratorum, etc. *Proceedings of the Academy of Natural Sciences of Philadelphia*, 9, 19–31.

Vila-Farré, M., Mateos, E., Sluys, R., and Romero, R. (2008). Terrestrial planarians (Platyhelminthes, Tricladida, Terricola) from the Iberian Peninsula: new records and description of three new species. *Zootaxa* **1739**, 1–20.

Vila-Farré, M., Sluys, R., Mateos, E., Jones, H. D., and Romero, R. (2011). Land planarians (Platyhelminthes: Tricladida: Geoplanidae) from the Iberian Peninsula: new records and description of two new species, with a discussion on ecology. *Journal of Natural History* **45**, 869–891.

Von Graff, L. (1899). 'Monographie der Turbellarien II. Tricladida Terricola (Landplanarien). Atlas von Achtundfünfzig Tafeln zur Monographie der Turbellarien II. Tricladida Terricola (Landplanarien). Pls. I–LVIII.' (Wilhelm Engelmann: Leipzig, Germany.)

Winsor, L. (1991). A new genus and species of terrestrial flatworm from the central highlands of New Caledonia (Tricladida: Terricola).

Winsor, L. (1998). Aspects of taxonomy and functional histology in terrestrial flatworms (Tricladida: Terricola). *Pedobiologia* **42**, 412–432.

Chapter 3

Reassessing the systematics of the Neotropical land planarians (Platyhelminthes, Tricladida): the contribution of the Chilean component to the Geoplaninae

Reassessing the systematics of the Neotropical land planarians (Platyhelminthes, Tricladida): the contribution of the Chilean component to the Geoplaninae

Ana Laura Almeida[1], Marta Álvarez-Presas[2] & Fernando Carbayo[1,3]

[1] Museu de Zoologia da Universidade de São Paulo, Avenida Nazaré, 481, CEP 04263-000, Ipiranga, São Paulo, SP, Brazil

2 School of Biological Sciences, University of Bristol, 24 Tyndall Avenue, BS8 1TQ, Bristol, UK

[3] Laboratório de Ecologia e Evolução, Escola de Artes, Ciências e Humanidades, Universidade de São Paulo - USP, Av. Arlindo Bettio, 1000, CEP 03828-000, São Paulo, SP, Brazil

Abstract

Endemic to the Neotropical region, the land planarian subfamily Geoplaninae (Platyhelminthes, Tricladida, Geoplanidae) consists of 29 genera and 346 species, most of which from Brazil. The Chilean Timyminae (Geoplanidae) is sister to Geoplaninae and houses only the two-species rich genus *Timyma*. In this paper, a comprehensive systematic study of the land flatworms from Chile is addressed through morphology and molecular data of a sample of 24 specimens collected across that country. The molecular dataset consisted of the genes COI and 28S rDNA from 93 terminals, including those of ten new species herein described and the new Chilean taxa *Adinoplana* gen. n., *Harana* gen. n., *Mapuplana* gen. n., *Myoplana* gen. n., *Sarcoplana* gen. n., and *Transsandiplana* gen. n. The phylogenetic relationships inferred under the maximum likelihood optimality criterion retrieved nine main clades; these clades are composed of one to several species and/or genera. Morphologically, each clade can be recognized by putative morphological synapomorphies. Geoplaninae was composed of all species from east of the Andes plus one species from Chile, and is sister to a large

group composed by *Polycladus*, *Gusana*, *Inakayalia* (Geoplaninae), and *Adinoplana* gen. n. Timyminae was not sister to Geoplaninae but to *Harana*. Disagreement between the phylogenetic tree and the current classification substantiates the proposal of a new diagnoses for Geoplaninae, a down-ranking of the subfamily Timyminae to the tribe level and a proposal of new tribes for accommodating the known and new genera: Adinoplanini tribe n., Geoplanini, Gusanini tribe n., Haranini tribe n., Inakayaliini tribe n., Myoplanini tribe n., Polycladini tribe n., Sarcoplanini tribe n., and Timymini.

Introduction

The molecular phylogenetics has revolutionized the systematics of the animal phylogeny (see Aguinaldo et al., 1997; Adoutte et al., 2000; Halanych, 2004; Carranza et al. 1997; Ruiz-Trillo et al., 1999). This has been especially important for organisms that are morphologically simple and for those suffering from convergence and reversion of character states (e. g. McHugh, 2000; Smythe et al., 2019; Salvi et al., 2014; Gasmi et al., 2014), such as land planarians.

Land planarians or Geoplanidae (Platyhelminthes, Tricladida) are free-living and predator invertebrates (Hyman, 1951). They are distributed across all continents, except Antarctica, and regional species richness is attained in tropical forests (Sluys, 1999). Over 930 species are currently known (Sluys, 2016). Yet many species remain to be discovered. The systematics of these organisms is also a good example of the impact caused by the arrival of molecular phylogenetics. These soft-bodied organisms are relatively simple in their morphology and the classification of the group was constructed upon shared morphological similarities. Very few attempts explored the morphological attributes of land planarians in cladistic approaches (see Grau, 2010, Amaral, 2017). This situation may be due to the scarcity of morphological characters (Grau, 2010; Álvarez-Presas & Riutort, 2014).

The lack of a phylogenetic frame of the classification of Geoplanidae began to change when independent DNA-based tests of phyletic relationships came into the scene. Mitochondrial and nuclear markers were used and two of the old families Rhynchodemidae* and Geoplanidae* (the third family is Bipaliidae*; an asterisk is here used for referring to a former concept of the taxon quoted) were discovered to be

polyphyletic and paraphyletic, respectively (Baguñà et al., 2001). Geoplanidae* included two of the subfamilies of Rhynchodemidae* (namely Caenoplaninae* and Rhynchodeminae* - Microplaninae* is the third member of Rhynchodemidae*-) (Álvarez-Presas et al., 2008). As a result, Microplaninae* was set out of the Rhynchodemidae* and the major taxa of the Geoplanidae were re-ranked in the hierarchical classification (Sluys et al., 2009).

The current classification of Geoplanidae reflects these phylogenetic insights and consists of four subfamilies, namely Bipaliinae, Microplaninae, Rhynchodeminae, and Geoplaninae (Sluys, 2009) plus the very recent fifth subfamiliy Timyminae Almeida & Carbayo, 2021, which is sister of Geoplaninae (Almeida *et al*., 2021).

At less inclusive taxonomic levels, the classification of the land flatworms has also been impacted by the molecular phylogenetics. Most of the studies benefited from the combination of a morphological species recognition with independent tests of species delimitation based on molecular trees (e.g., Álvarez-Presas *et al*., 2015; Sluys *et al*., 2016; Carbayo *et al*., 2016; Amaral *et al*., 2018). Nonetheless, the ingroups of Geoplanidae have received uneven attention and many taxa are poorly represented in the phylogenetic inferences and entire speciose subfamilies were represented by only a couple of terminals in the abovementioned studies.

Among the subfamilies of land planarians, Geoplaninae is probably the taxon which has received more attention. The systematics of the group was re-shaped with molecular phylogenies (Carbayo *et al*., 2013): six new genera were added to the preexisting 17 genera; over 55 species were considered *incertae sedis* (in the sense that either they were retrieved in the phylogenetic trees out of the clade containing the type species of the genus and/or the morphology of the species does not match that of the diagnosis of the genus; herein those species are referred to with the genus name quoted, e.g. *"Pasipha" ercilla* (E. M. Frehlich, 1978)). However, deeper phylogenetic interrelationships remained elusive. More recently, the genera *Winsoria*, *Inakayalia* and *Wallmapuplana* were proposed (Negrete *et. al*., 2019, 2020).

Geoplaninae currently comprises 29 genera (including the collective genus *Pseudogeoplana* Ogren & Kawakatsu, 1990 to temporarily assign *species inquirendae* and *nomina dubia*), accounting for 346 species (http://planarias.each.usp.br/filtrar/caracteristica accessed on 21 June 2021). This

subfamily and its sistergroup Timyminae are exclusively Neotropical. Timyminae is represented by only two species of the genus *Timyma*, and is distributed only in Chile, as far as it is known. Most of the genera of Geoplaninae are from the eastern Andes and the phylogenies published so far considered overwhelmingly the species from the eastern Andes. Actually, from the western Andes only three species are present in the molecular phylogenies so far.

The Chilean component is particularly interesting for understanding the evolutionary framework of the Neotropical land planarians (Froehlich, 1967). Among the 29 genera of Geoplaninae, *Gusana, Inakayalia, Liana, Polycladus,* and *Wallmapuplana* are distributed across Chile or in the Argentinean Andean region (Blanchard, 1945; Graff, 1899; Marcus, 1954; E. M. Froehlich, 1978; Negrete *et al*., 2020). The purpose of this paper is to address a comprehensive systematic study of the Geoplaninae land planarians, with emphasis on the Chilean component through morphology and molecular data of a sample of specimens collected across Chile. Both the morphological putative synapomorphies found for the new taxa proposed here, and the phylogenetic trees underpin a new classification of the Geoplaninae.

Material and methods

Sampling and morphological plus histological procedures

The specimens were found in 2010 by active searching during the day and night in forests and open areas distributed along a latitudinal range from 25ºS to 41ºS, in Chile (Fig. 1).One-to-three collector spent 1-4 hours of sampling effort in each sampling site. The individuals collected were photographed and subsequently killed and fixed in 92% ethanol and stored at -20° C. In 2017, a small body portion of each individual was removed for DNA studies. The remaining main body portion was gradually rehydrated to 80% ethanol and maintained in this fluid for some months to reduce tissue hardness. Complementarily, some specimens, which were still hard, were immersed in Sandison solution for three days to soften the body (Sandison, 1955).

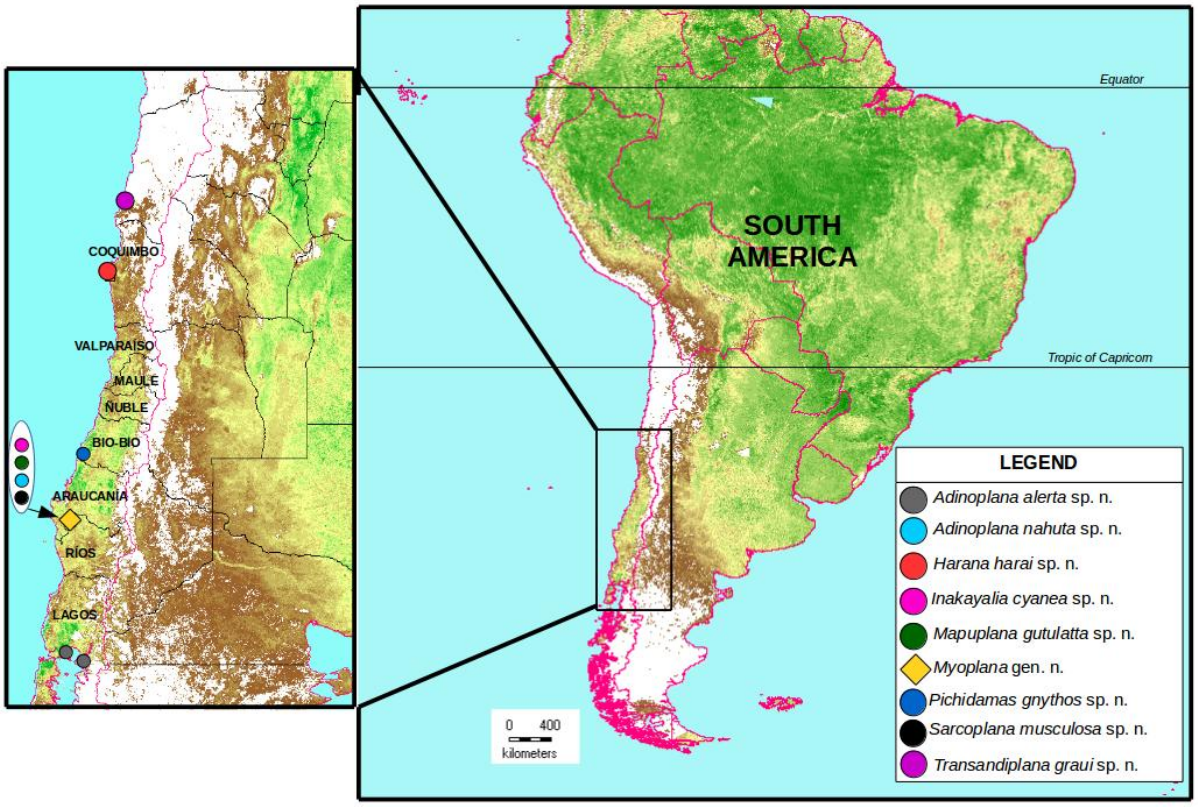

Fig. 1. Map of distrubuition of the new Chilean taxa.

For the histological preparation, the specimens were cut into several pieces, dehydrated, cleared in clove oil, and infiltrated and embedded in Paraplast® Tissue Embedding Medium. Tissue blocks were sectioned at 7 µm intervals using a retracting rotary microtome, and the produced sections were glued with albumin-glycerol (1:1) onto glass slides and subsequently stained following Cason (1950). Stained sections were dehydrated, cleared in xylene, and mounted in synthetic balsam (Synth). Sections were studied with an Olympus BX51 optical compound microscope. Diagrams of the copulatory apparatuses were drawn with the aid of a camera lucida attached to the microscope. Photomicrographs were taken with an Olympus DP72 digital camera attached to the microscope, and subsequently edited with GIMP (GNU Image Manipulation Program,versions 2.8.16 and 2.10.24; The GIMP team www.gimp.org, 1995-2021) to provide a whitish background or to enhance sharpness. Color descriptions of the body of live or fixed specimens follow online RAL palette colors (© RAL gemeinnützige GmbH, available at https://www.ral-farben.de/uebersicht-ral-

classic-farben.html?&L=1) through comparison with digital photomicrographs on a computer screen. Unless stated differently, figures were orientated so that the anterior extremity of the body is to the left. The holotype of each new species is deposited in the Museo Nacional de Historia Natural (MNHNCL), Santiago, Chile. The paratypes are deposited in the Museu de Zoologia da Universidade de São Paulo (MZUSP), Brazil.

DNA extraction, amplification, and sequencing

Genomic DNA extractions of the specimens (Table S1) were performed with an ammonium acetate protocol according to Fetzner, J. (1999). Polymerase Chain Reaction (PCR) was used to amplify partial sequences of the ribosomal 28S rDNA gene (herein 28S) and a fragment of the mitochondrial Cytochrome Oxidase I gene (COI). Amplifications were performed in a 25 µl volume containing 3 µl of DNA at a concentration of 50 ng/µl, 2.5 µl of 5x Phusion® Buffer HF (Thermo Scientific) mM Tris–HCl (pH 8.4), 50 mM KCl, 1 µl of lM dNTPs, 2 mM MgCl2, 1 µl of lM of each primer, 0.15 µl of GoTaq® DNA Polymerase (Promega), and 15.35 µl of ultrapure water. General PCR conditions included initial denaturation for 3 min at 94°C, 35 cycles of denaturation for 30 sec at 94°C, annealing for 30 sec at specific temperatures (Table S2), extension for 1 min at 72ºC, and a final extension for 3 min at 72°C. Amplification and sequencing were performed with the primer sets described in Table 2. PCR products were purified using an Agencourt AMPure XP DNA Purification and Cleanup kit (Beckman Coulter Inc.). Products were subsequently cycle-sequenced using BigDye Terminator v3.1 Cycle Sequencing Kit, cleaned with ethanol precipitation, and sequenced on an ABI 3730 DNA Analyzer automated sequencer (Life Technologies-Applied Biosystems). Sequence *reads* were assembled in contigs using the Consed/Phred/Phrap package (Ewing & Green 1998; Ewing *et al*. 1998; Gordon et al. 1998, 2001).

Molecular Datasets

Three different datasets have been used for the molecular phylogenetic analyses. The first one corresponds to the sequences from the 28S ribosomal gene

(from now on *28S dataset*) and consists of sequences from the public database Genbank (https://www.ncbi.nlm.nih.gov/genbank/) (Table S1) as well as the new sequences obtained specifically for this study. The second dataset corresponds to the sequences from the mitochondrial COI gene (from now on *COI dataset*) obtained for this study and sequences from the GenBank. Finally, the *Concatenated dataset* gathers all the sequences from the two markers concatenated.

Molecular Phylogenetic Analyses

The sequences of the 28S gene were aligned with the online version of MAFFT (Katoh *et al*., 2019) using the G-INS-i iterative refinement method. The COI gene sequences were aligned following the aminoacid translation guide with BioEdit (Hall, 1999), using the Equinoderm and Flatworm mitochondrial genetic code (number 9). Ambiguously aligned positions in the 28S alignment were excluded from the analyses by using TrimAl (Capella-Gutiérrez *et al.*, 2009) with the automated1 setting.

Phylogenies were inferred for the three datasets using Maximum Likelihood (ML) on the software IQ-Tree2 (Nguyen *et al*., 2015). 10,000 ultrafast bootstrap replicates (Hoang *et al*., 2017) were performed per analysis. ModelFinder (Kalyaanamoorthy *et al.*, 2017) was used to select the best model for each analysis. For the *Concatenated dataset* partitions by gene were applied.

All the datasets were also analysed with Bayesian Inference (BI) method using the software MrBayes v. 3.2 (Ronquist *et al.*, 2012). Two runs of Markov Chain Monte Carlo (MCMC) for 25 million generations were run in the Concatenated dataset and 5 million generations in the individual datasets (*28S* and *COI*), sampling every 1000 generations. 25% of the topologies were ignored as 'burn-in'. In order to check that both runs converged, the congruence of the topologies and model parameters of both runs were compared using the standard deviation of the split frequencies (SD < 0.01). Final summary trees were produced and viewed on the software FigTree v. 1.4.2 (http://tree.bio.ed.ac.uk/software/figtree/).

Abbreviations used in figures

(ac) adenodactyl cavity
(ad) adenodactyl
(bg) branched gland
(ce) common muscle coat
(cg) cerebral ganglia
(ci) circular muscle
(cm) cutaneous musculature
(cn) diagonal transverse fibers
(co) common glandular ovovitelline duct
(cv) common ovovitelline duct
(dc) diagonal cutaneous muscle
(dd) diagonal double muscle layer
(de) dorsal epidermis
(dp) diagonal parenchymatic muscle
(e) eye
(ej) ejaculatory duct
(ep) epithelium
(es) esophagus
(f) fold
(fa) female atrium
(fg) female genital canal
(g) gonopore
(gl) gland cells / gland
(i) intestine
(lc) longitudinal cutaneous muscle
(ls) sunken longitudinal cutaneous muscle
(lu) pharyngeal lumen
(m) muscle
(ma) male genital atrium
(mo) mouth
(nc) cutaneous peripheral nerve net
(np) nervous plate / orthogonal nervous system
(o) ovary
(oo) ootype
(ov) ovovitelline duct
(ph) pharyngeal pouch
(pi) sensory pit
(pp) penis papilla
(pv) prostatic vesicle
(px) pharynx
(sb) subintestinal transverse muscles
(sd) sperm duct
(sg) shell glands
(sh) sphincter
(sp) supraintestinal transverse muscles

(st) spermatophore
(t) testis
(tr) transneural parenchymal musle layer
(vd) subneural parenchymal musle layer
(ve) ventral epidermis
(vi) vitellaria

Results.

Molecular Results.

We obtained new sequences of the COI fragment from 18 specimens and 19 new sequences of the 28S gene fragment (Tabble S1, marked with an asterisk). The final datasets include 85 specimens for the *28S*, 91 for the *COI dataset*, and 93 for the *Concatenated*. Members of the Dugesiidae as well as representatives from all the Geoplanidae subfamilies have been used as outgroup. The final data matrices consisted of 753 nucleotide long sequences of COI and 1277 nucleotide long sequences of 28S (after trimming).

The results of this paper will impact on the classification of the current taxa. Therefore, for the sake of clarity, we advance the new classification in this section and use Geoplaninae* for the current concept of the subfamily (as re-diagnosed by Almeida *et al*., 2019), and Geoplaninae for the new concept of the taxon as proposed in this paper.

The general topologies of the phylogenies inferred from the *COI dataset* with both ML and IB are similar (Figs S5 and S6). Minor differences are concentrated in the relationships between the genera. Nevertheless, neither of the two methods show statistical support for groupings between genera. The more inclusive clades (subfamilies and tribes) are well grouped in both phylogenies.

The phylogenies inferred from the *28S dataset* with the two methods (Figs S3 and S4) also present some topological differences, but, as with COI, this occurs in clades that do not show statistical support for any of the phylogenies.

There are differences between the individual COI and 28S trees as well. For example, in the COI phylogenies, the most external group within the terrestrial planarians is the Rhynchodeminae subfamily, whereas Bipaliinae and Microplaninae are sister clades. On the other hand, in the 28S trees, Bipaliinae is recovered as the most ancestral subfamily of the land planarians, followed by Microplaninae and then Rhynchodeminae, which is the sistergroup of Geoplaninae.

Given the low resolution of the individual-gene phylogenies, from now on we will comment on the results of the phylogenies of the two genes concatenated, which present a better resolution and statistically supported clades.

In the ML tree inferred with the *concatenated dataset* (Fig. 2) Rhynchodeminae is sister to a clade including Bipaliinae and Microplaninae, which is at the same time sister to a clade including the rest of land planarians. The latter houses all Neotropical members, including Geoplaninae* (retrieved as a polyphyletic group), Timyminae and the new taxa sequenced for this study (Fig. 2 and Fig S1).

The re-rankink of Geoplaninae* (to Geoplanini) and Timyminae (to Timymini) follows the new classification of the Geoplaninae hereafter shown. The internal relationships of the Geoplaninae can be represented parenthetically as [({[(Inakayaliini +Adinoplanini) + Myoplanini] + (Polycladini + Gusanini)} + Geoplanini) + (Haranini + Timymini)] + Sarcoplanini]. Statistical support for these clades ranges between 82-100%.

Sarcoplanini includes the genera *Sarcoplana*, *Mapuplana*, *Pichidamas*, and *Wallmapuplana*. Geoplanini includes all members of the Geoplaninae from the East Andes plus the Chilean *Transandiplana*, which is nested within Geoplanini and sister either to *Geoplana* (Figs. 2, S1, S2; ML and BI, *concatenated dataset*) or to *Paraba* (Fig. S3, ML, *28S dataset*), both relationships with low support. The remaining seven new tribes are monogeneric.

The general topology of the concatenated BI tree matches that of the ML, and also recovered all the tribes, but differently from the ML tree the more comprehensive

clades (Myoplanini + [Inakayaliini + Adinoplanini]) and [Geoplanini [(Polycladini + Gusanini) (Inakayaliini + Adinoplanini)] are polytomic in the BI phylogeny (Fig. S2).

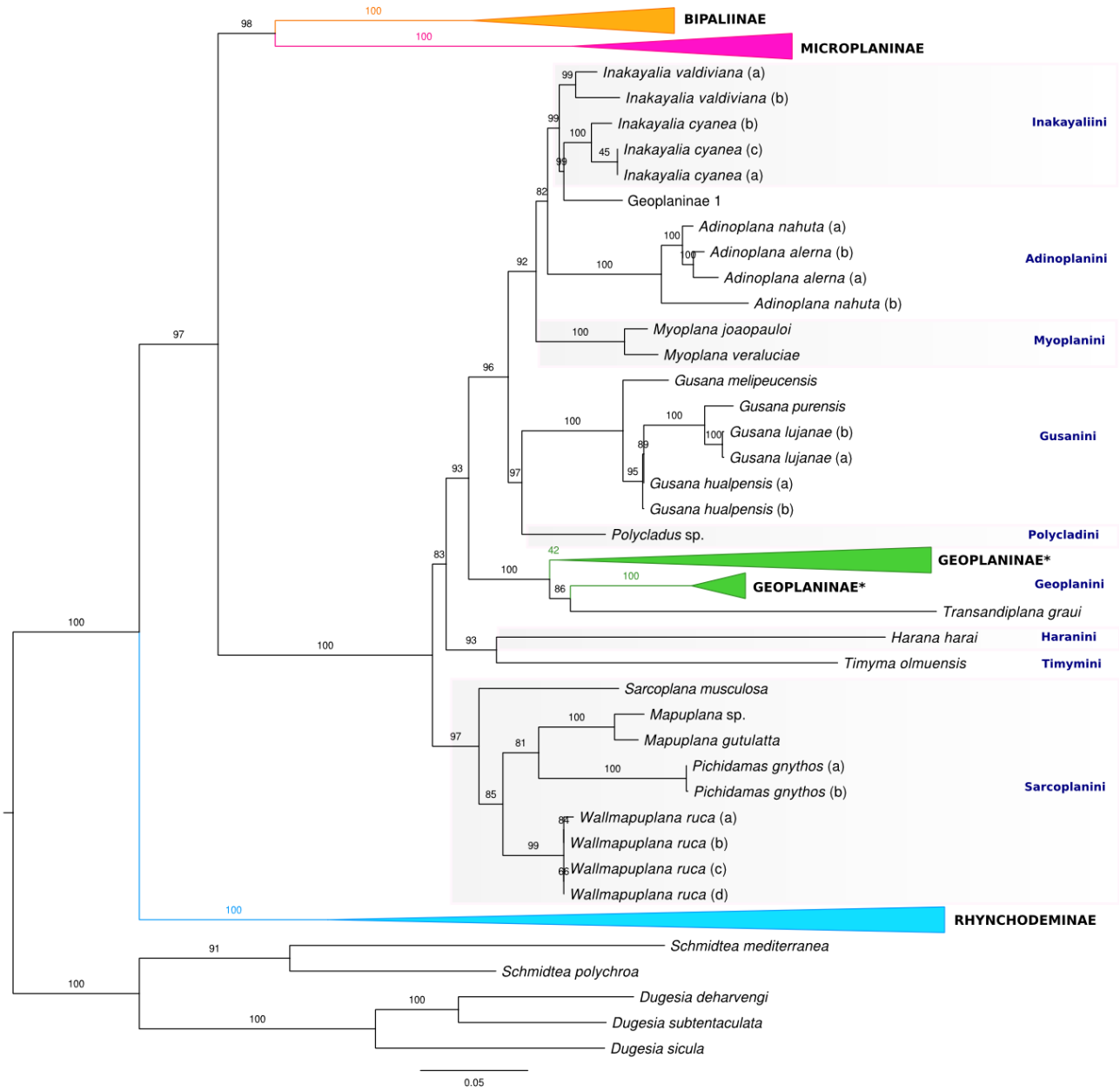

Fig. 2. Phylogenetic tree inferred from the concatenated genes (28S rDNA + COI) under maximum likelihood as the optimality criteria. With the exception of the Chilean terminals, the subfamily clades (colored) were collapsed. Numbers at the nodes correspond to ultrafast bootstrap values.

Morphological results.

Taxonomic account

Geoplanidae Stimpson, 1857

Geoplaninae Stimpson, 1857

Diagnosis. Geoplanidae with eyes encircling the anterior region of the body in a single row and extending until the posterior extremity of the body; creeping sole usually wide; usually dorsal testes.

Adinoplanini Carbayo & Almeida trib. n.

Diagnosis. Geoplaninae with the dorsal side of the body convex in the median zone and lateral zones flattened. The female atrium bears musculo-glandular organs.

The tribe includes only the genus *Adinoplana*.

Adinoplana Carbayo & Almeida gen. n.

Diagnosis. Adinoplanini with a mid-sized body, approximately 50 mm in length. The median zone of the dorsal side is convex, external to which the body is flattened. The creeping sole is wide. The eyes and sensory pits surround the entire cephalic region. The eyes are located dorsally. The thickness of the cutaneous muscle relatively to the body height is 10-16%. The prostatic vesicle is extrabulbar. The penis papilla is cylindrical. The male and female atria are long, both provided with musculo-glandular organs. The common ovovitelline duct is very long and dorsal to the female atrium. The female genital canal projects anteriorly from the dorsal region of the female atrium.

Type species. *Adinoplana alerna* Carbayo & Almeida sp. n.

Etymology. *Adinoplana* is derived from the Greek *adinos*, meaning crowded (regarding the numerous and varied musculo-glandular organs) and the Latin *plana,* meaning *flat* (regarding the body shape). The gender is female.

Adinoplana alerna Carbayo & Almeida sp. n.

Material examined. **Holotype** Museo Chile?? (Field code, F4925). Parque Nacional Alerce Andino, Región de Los Lagos, Chile, Coord. -41.58, -72.61, F. Carbayo, December 15th 2010. Transverse sections of cephalic region on 20 slides; horizontal sections of a body portion immediately behind on 27 slides; transverse sections of pre-pharyngeal region on 28 slides; sagittal sections of pharynx and male component of the copulatory apparatus on 113 slides; sagittal sections of the female component of the copulatory apparatus on 20 slides.

Type locality. Parque Nacional Alerce Andino, Región de Los Lagos, Chile.

Etymology. The specific epithet is an acronym composed from the first and last letters of the Alerce Andino, which is the name of the National Park where the species is found.

Diagnosis. Sensory pits distributed in a single row; extrabulbar prostatic vesicle; ejaculatory duct with a wide cavity close at the tip of the penis papilla; two types of adenodactyl present, one in the male and other in the female atrium.

Description

External aspect. The live specimen is approximately 50 mm in length and 6 mm in width. The preserved specimen measured 45 mm in length, 8 mm in width, and 2.5 mm in height. The living animal displays nearly parallel body margins throughout most of the body length (Fig. 3A-B). Close to extremities, the body tapers gradually towards the anterior, rounded tip and less gradually towards the posterior, obtuse tip. The dorsum is convex in the median zone, which is 50% of the body width. External to the median region, the dorsum is flattened (Fig. 3C-D). When the body contracts, body margins are undulate. The ventral side is flat.

The color of the dorsum is black grey with small green beige dots on the median region and larger, irregular green beige patches in the submarginal region (Fig. 3A, C-D). The

ventral side is of light grey color that passes into black grey in the extremities of the body. Additionally, there are numerous brown beige dots, that pass into black grey onto both extremities and body sides (Fig. 3B).

The eyes are of a single-cup with 50-70 µm in diameter. Each eye is placed in the middle of a round light grey halo (Fig. 3C). The eyes are present in a uniserial row round the anterior tip but 10 mm posteriorly they spread onto the dorsal surface to the extent of 27% of the width on either side.

The sensory pits are simple invaginations 50-57 µm deep, located ventro-marginally in a single row from the very anterior body tip up to pre-pharyngeal region (42% of body length). In the anterior tip, they occur in the middle of light grey halos (Fig. 3C). The relative position of the mouth : body length, is 47%; that of gonopore : body length, 68%

Epidermis and its secretions. In cephalic extremity, the epidermis is ciliated dorsally and ventrally. Behind this region, it is ciliated only on the creeping sole, this sole having 95% of the body width. Erythrophil granules and rhabdites are discharged through the dorsal and ventral epidermis, being much more abundant dorsally. A glandular margin is moderately developed. This margin is constituted of two types of gland cells, producing xanthophil and erythrophil granules, respectively (Fig. 4A).

Cutaneous musculature. The cutaneous musculature comprises three layers. A subepithelial, 5-µm-thick circular layer, a dense, double layer with decussate fibers (15 µm thick dorsally, 45 µm ventrally), and an innermost, well developed longitudinal muscle (Fig. 4A-D). The longitudinal muscle is 40 µm thick dorsally, and 145 µm ventrally. The ventral portion of this muscle becomes gradually thinner towards the body margins (Fig. 4A). The longitudinal muscle fibres laying immediately under the decussate ones run at a slight angle to the longitudinal axis (Fig. 4D). The muscle fibers are hollowed (Fig. 4C). The cutaneous musculature thickness relative to body height at the pre-pharyngeal region is 10%. A cephalic retractor muscle is absent.

Parenchymal musculature. Three parenchymal muscle layers are present throughout the body: a dorsal layer of decussate fibers (60-µm-thick, paratype), located to the

inside of the peripheral nervous plexus; a dense supra-intestinal layer of transverse fibers (60 µm thick); and a dense subintestinal layer of transverse fibers (70 µm thick) (Fig. 4A).

Digestive system. The mouth is situated at a distance from the root of the pharynx equivalent to 27% of the length of the pharyngeal pouch length. The pharynx is collar-shaped, with dorsal insertion backwards shifted by a distance equal to 70% of its length (Fig. 5A). An esophagus is absent. The outer pharyngeal musculature is composed of a subepithelial longitudinal muscle (10 µm thick), followed by a circular (20 µm) and a longitudinal one (30 µm thick). The inner pharyngeal musculature is composed of a 100 µm thick circular muscle followed by a 10-µm-thick longitudinal muscle (Fig. 5B).

Male reproductive system. The copulatory apparatus occupies 85% of the body height, and is 6 times longer than high. The testes are rounded, measuring about 180 µm in diameter. They are located dorsally, beneath the transverse supraintestinal parenchymal muscle, and between the intestinal branches (Fig. 4E). The anteriormost testes are placed at a distance equivalent to 38% of body length (that is, notably behind ovaries); the posteriormost testes at a distance equivalent to 59% of body length, i.e., at the level of the penis bulb.

The sperm ducts run above sub-intestinal parenchymal muscle and dorsally to the ovovitelline ducts (Fig. 4E). They contain sperm excepting for their distalmost portion which is very thin to open into the proximal, lateral section of the prostatic vesicle (Fig. 5C). The prostatic vesicle is tubular and sinuous. The anterior portion of the vesicle runs antero-dorsally, the posterior portion postero-dorsally to penetrate the anterior region of the well developed penis bulb. The prostatic vesicle is lined with a cuboidal, ciliated epithelium, which is pierced by gland cells producing erythrophil granules, and is surrounded by 30 µm-thick circular muscle. The ejaculatory duct crosses the center of the penis papilla to open into a small, irregular cavity at the tip of the papilla. The ejaculatory duct is lined with a cuboidal, ciliated epithelium, and is underlain by a 5 µm thick circular muscle. The small cavity is lined with a cuboidal, non-ciliated epithelium.

The penis papilla is conical, and slightly inclined and with the dorsal insertion slightly

posteriorly shifted. This papilla occupies the anterior 20% of the male atrium (Fig. 5C). The surface of the papilla is spinny due to small musculo-glandular organs. These organs are conical and 20-100 µm-high and 65-70 µm wide (Fig. 6A-D). The interior of the organs houses a blind cavity opening to the tip. The lumen receives fine erythrophil granules produced by gland cells located out of the penis bulb. A fine-granule cyanophil mass is beneath epithelium of the tip (Fig. 6B-D). The penis papilla is lined with a squamous epithelium, and is underlain by a circular muscle (8 µm thick), followed by a 10-µm-thick longitudinal muscle. These muscles seem to be organized in a concave net surrounding the basis of each organ, so that the organ has a pear-shaped aspect (Fig. 6B-D). Gland cells with 10-µm-thick necks, producing cyanophil granules also pierce penial epithelium, especially in its basal half.

These pear-shaped musculo-glandular organs extend to the anteriomost region of the male atrium (Fig. 6A-C). This atrium is long, and presents 2-3 large longitudinal, lateral folds (Fig. 5C) and a dorso-dorsal fold. Anterior and posterior regions of the roof of the male atrium also possess mgo, being different in their larger size, 80-120 µm high (Fig. 6A-D). Male atrium is lined with a columnar epithelium underlain by a 80-100 µm-thick muscle of circular and longitudinal fibers crossed. Epithelium of the anterior quarter of male atrium is pierced by gland cells secreting cyanophil granules. Opening of glands producing erythrophil granules piercing the entire epithelium of the male atrium cannot be distinguished with certainty.

Female reproductive system. The ovaries are rounded-to-ovoid, ca. 300 µm. They are incompletely developed. They are located 6.3 mm anterior to anteriormost testes (or the equivalent to 14% of body length), and located at a distance of 24% from anterior end of the body, lying immediately above the ventral nerve plate. The ovovitelline ducts emerge laterally from the dorsal side of the ovaries. They run between the subintestinal parenchymal muscle layer and the ventral nerve plate (Fig. 4E). Laterally to the female atrium, the ovovitelline ducts bend abruptly to the dorsal side and join dorsally to the female atrium, to form a 2-mm long, horizontal common ovovitelline duct (Fig. 7C). Shell glands are absent. The ovovitelline duct continues with the female genital canal (Fig. 7B). This canal is a forward dilated projection of the dorsal portion of the female atrium (Fig. 7B). The female genital canal and the female atrium are lined

with a columnar, ciliated epithelium. These cilia are 2 µm long. The female atrium is long, 1.2 times longer than male atrium. Its lumen is narrowed by 2-3 lateral, longitudinal folds (Fig. 5C, Fig. 7A, C). A large musculo-glandular organ is embedded in each of the lateral sides of the anterior section of the female atrium (Fig. 7A, 7C-D). These large organs project towards the midsagittal body plane and their size is approximately 500-700 µm in diameter at its base and 300 µm high.

A large musculo-glandular organ is embedded in each of the lateral sides of the anterior section of the female atrium (Fig. 7A, 7C-D). These large organs project towards the midsagittal body plane and their size is 500-700 µm in diameter at its base and approximately 300 µm high. The organ has an epitheliated, blind canal which opens at the tip of the organ. The epithelium is ciliated, columnar, and is pierced by two types of gland cells producing erythrophil and cyanophil granules, respectively. A cyanophil mass is in the canal (Fig. 7D). A well developed musculose ring followed by a layer of oblique fibers surrounds the organ. This double layer underlies the distal epithelium of the canal, but is 150 µm separated from the epithelium lining the bottom of the canal (Fig. 7D). The epithelium of the female atrium is also pierced by three types of gland cells producing xanthophil, erythrophil and cyanophil granules, respectively, the latter type being more abundant in mid-atrium. The epithelium of the female atrium is underlain by a 100-200-µm thick muscle layer of circular and longitudinal fibers. The common muscle coat comprises mainly longitudinal fibers, and envelops the male and female atria and the female genital canal.

Fig. 3. *Adinoplana alerna* Carbayo & Almeida, sp. n. Living holotype in dorsal (A-C) and ventral views (D). Scale not available.

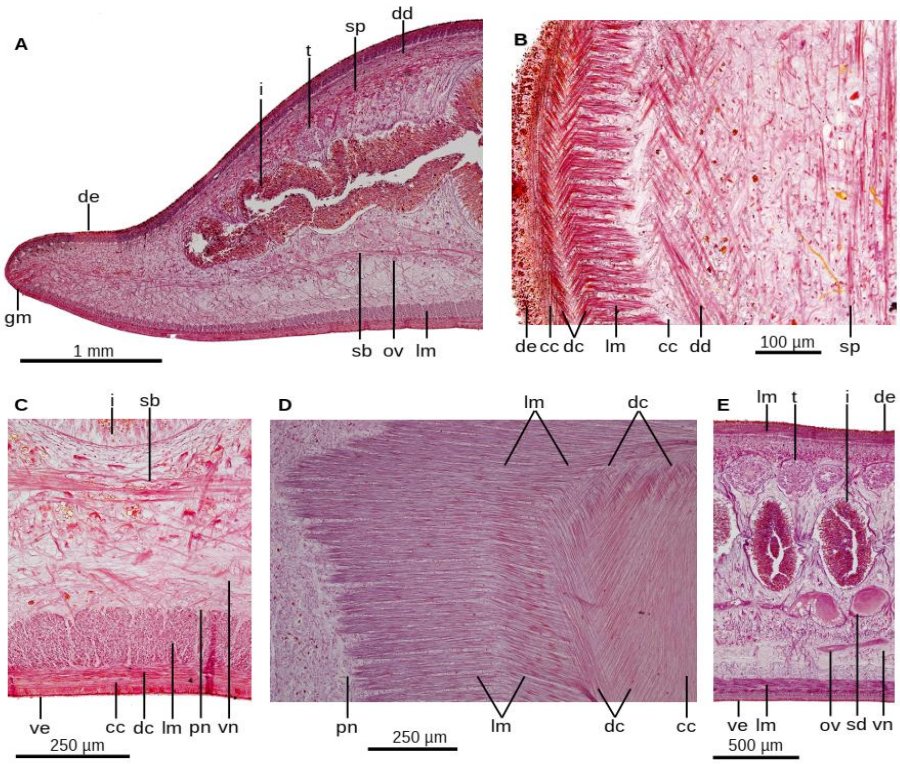

Fig. 4. *Adinoplana alerna* Carbayo & Almeida., sp. n. Photomicrographs of the holotype. A: Transverse section of the pre-pharyngeal region. B: Horizontal section of near dorsal epidermis. C: Transverse section of pre-pharyngeal region. D: Horizontal section of near ventral epidermis. E: Sagittal section of a region anterior to the penis bulb.

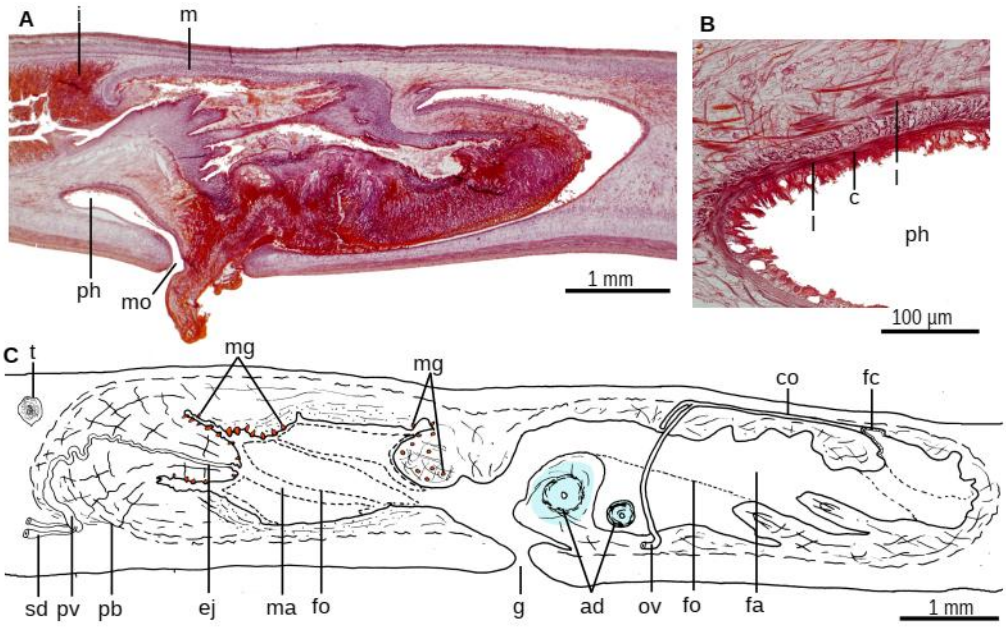

Fig. 5. *Adinoplana alerna* Carbayo & Almeida, sp. n. Holotype. A: Photomicrograph of a sagittal section of the pharynx. B: Photomicrograph of a sagittal section of the ventral insertion of the pharynx. C: Diagrammatic representation of the copulatory apparatus.

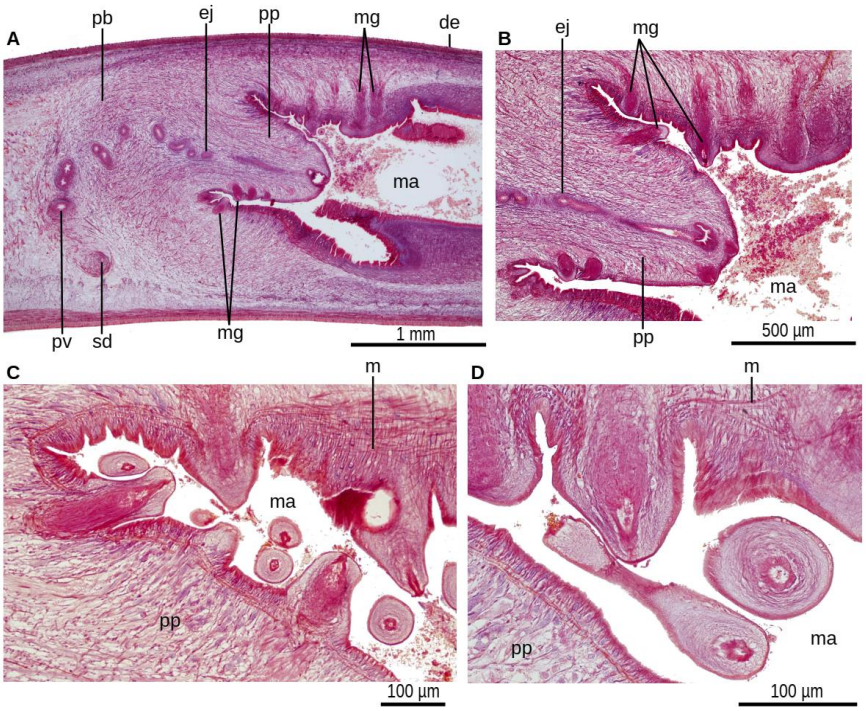

Fig. 6. *Adinoplana alerna* Carbayo & Almeida, sp. n. Holotype. Photomicrographs of sagittal sections of the male components of the copulatory apparatus showing musculo-glandular organs. A: Penis papilla and male atrium. B: Penis papilla. C: Dorsal insertion of the penis papilla. D: Musculo-glandular organs embedded in the dorso-anterior wall of the male atrium.

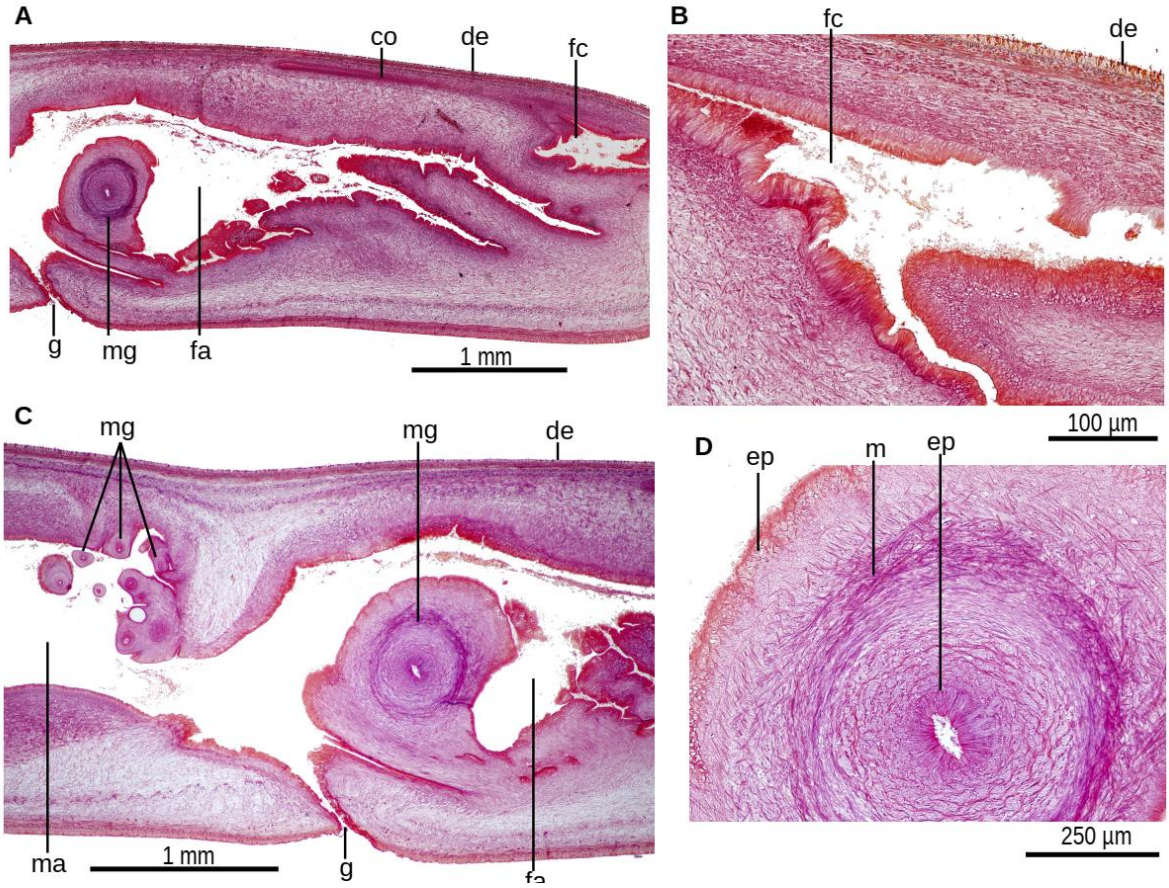

Fig. 7. *Adinoplana alerna* Carbayo & Almeida, sp. n. Holotype. Photomicrographs of sagittal sections of the female components of the copulatory apparatus. A: General view of the female atrium. B: Converging region of the female genital canal with the female atrium. C: Anterior region of the female atrium converging with the male atrium. B: Musculo-glandular organ.

Adinoplana nahuta Carbayo & Almeida, sp. n.

Material examined. Holotype MNHNCL PLAT-?? (Field code, F4911). Parque Nacional Nahuelbuta, Región de la Araucanía, Chile, Coord. -37.82756, -73.00972, F. Carbayo, December 15th 2010 F. Carbayo, December, 13th 2010. Transverse sections of the cephalic region on 25 slides; horizontal sections of a body portion immediately behind on 48 slides; transverse sections of pre-pharyngeal region on 24 slides; sagittal sections of pharynx on 37 slides; sagittal sections of the copulatory apparatus on 103 slides. **Paratype MZUSP PL ??** (Field code, F4877).

Type locality. Parque Nacional Nahuelbuta, Región de la Araucanía, Chile.

Etymology. The specific epithet is a free abbreviation of the Nahuelbuta mountains where the

species was found.

Diagnosis. Sensory pits distributed in 1-3 rows; small esophagus present; three types of adenodactyl present, two in the male atrium and other in the female atrium; female atrium large.

Description.

External aspect. The live specimen measured approximately 65 mm in length and 7 mm in width. The preserved specimen measured 57 mm long, 10 mm wide, and approximately 3 mm high. The body shape is as that of the type species of the genus (Fig. 8A-B).

The light grey color of the dorsum is covered with an irregular net of sized ink black (RAL 001500) marks and pear yellow (RAL 0808070) spots. The marks form an irregular paramedian band on each side of the body, whereas the sulfur yellow spots spread over the paramedian band and the space between them excepting for the anterior and posterior regions. The ventral side is light grey (RAL 0007000) covered with black grey spots the size of which is larger as they are closer to the posterior extremity of the body (Fig. 8B).

The eyes are 40-50 µm in diameter, and distributed as in type species. The sensory pits are simple invaginations 45-50 µm deep in the anterior extremity of the body, and 35 µm shortly behind. They are located ventro-marginally in a single-to-triple rows in the anterior body tip; behind this region, they are uniserial and extend behind up to level the posterior portion of the pharyngeal pouch (45% of body length). The relative position of the mouth : body length, is 51%; that of gonopore : body length, is 76%.

Epidermis and its secretions. In cephalic extremity, epidermis is ciliated dorsally and ventrally. Behind, ciliated only on the creeping sole, this with 88% of body width. Types and distribution of epidermal gland cells as in the type species.

Cutaneous musculature. Cutaneous musculature as in the type species, differing in the thickness as follows: circular muscle, is 5 µm thick; layer of decussate fibers, is 23-25 µm thick dorsally, 30 µm ventrally; longitudinal muscle, is 27 µm thick dorsally, and 92 µm ventrally (Fig. 9A-D). The longitudinal fibers lying immediately under the decussate fibers run slightly obliquely to the body margins (Fig. 9D). The cutaneous musculature thickness relative to body height at the pre-pharyngeal region ranges between 7-9%.

Parenchymal musculature as in the type species: dorsal layer of decussate fibers (25-40 µm

thick), supraintestinal transverse muscle (40-50 µm); and subintestinal transverse muscle (45-50 µm) (Fig. 9A).

Digestive system. The mouth is situated at a distance from the anterior region of the pharyngeal pouch equivalent to 23-25% of its length. The pharynx is collar-shaped, with dorsal insertion backwards shifted by a distance equal to 65-70% of its length (Fig. 10A). A short esophagus is 0.2 mm in length. The pharyngeal musculature is as in the type species. The components of the outer pharyngeal musculature are a longitudinal muscle (10 µm thick), a circular (25 µm) and a longitudinal (15 µm). Those of the inner pharyngeal musculature are a 60-100 µm thick circular muscle, and a 10-µm-thick longitudinal muscle (Fig. 9E).

Male reproductive system. The copulatory apparatus occupies 80-88% of the body height, and is 7.5 times longer than its height. The testes are rounded or pear-shaped, measuring approximately 200 µm in diameter. They are dorso-ventrally located as in the type species (Fig. 9E). The holotype possesses testes with sperm, whereas the paratype does not. The anteriormost testes are placed at a distance equivalent to 26% of body length (and 1.7 mm behind the ovaries); the posteriormost testes at a distance equivalent to 59% of body length, i.e., at the level of the penis bulb (Fig. 9E).

The sperm ducts run above sub-intestinal parenchymal muscle and lateral to the ovovitelline ducts (Fig. 9C). They contain spermatozoa except for their distal, thinner portion. This portion bends to the sagittal plane to open into the proximal, lateral section of the prostatic vesicle (Fig. 10A). The prostatic vesicle is tubular, and its proximal half is wider than the distal one. This vesicle is roughly C-shaped in lateral view, and is attached to the anterior region of the penis bulb. The dorso-anterior region of this bulb is crossed by the vesicle to communicate with the ejaculatory duct. The prostatic vesicle is lined with a cuboidal-to-columnar, ciliated epithelium, which is pierced by gland cells producing erythrophil granules. This epithelium is surrounded by a 25-µm-thick circular muscle. The proximal portion of the ejaculatory duct descends sinuously, whereas its distal portion runs horizontally within the penis papilla to open at its tip. The ejaculatory duct is lined with a cuboidal, ciliated epithelium, and is underlain by a 4 µm thick circular muscle.

The holotype presents a well developed penis papilla, the paratype does not. The penis papilla is cylindrical, and horizontal, with the anterior insertion anterior to the ventral. The papilla occupies the anterior 27% of the male atrium (Fig. 10A-B). This papilla is lined with a cuboidal, ciliated epithelium, and is underlain by a circular muscle (20 µm thick). The innermost fibers of

this muscle are interwoven with fibers of a 10-µm-thick longitudinal muscle. The epithelial lining of the penis papilla is crossed by two types of gland cells; one type produces an amorphous xanthophil secretion and is scarce; another type produces fine erythrophil granules and is abundant. The dorso-proximal portion of the papilla houses 6-7 musculo-glandular organs, herein abbreviated mg1. This mg1 is also found dorsally in the anterior half of the male atrium. A mg1 is a 100-125 µm-high and 100 µm wide, conical projection from the epithelium, so giving to the epithelial surface a spinny aspect (Fig 11A-C). The outer epithelium of the mg1 is ciliated and cuboidal proximally; the distal portion could not be discerned, but it might be squamous. The outer epithelium is pierced by gland cells producing fine erythrophil granules, and is strongly stained. The inner side of the mg1 houses a 30 µm wide and 90 µm deep blind-end canal which opens at the tip of the mgo. This canal is lined with a ciliated epithelium, that is columnar-to-cuboidal proximally and lower distally. Lining epithelium of the canal is so strongly erythrophil that its cells are hardly discernible, especially near the opening of the canal. Numerous gland cells pierce the epithelium of the canal. Bodies of these gland cells are out of the penis bulb and as they approach the canal, their contents pass from very fine pink granules to strongly reddish granules. The proximal half of the canal is also apparently pierced by gland cells producing very fine cyanophil granules. The bodies of these gland cells could not be observed. The canal contains erythrophil granules. Immediately underneath the outer and inner epithelium of the mg1 are a few muscle fibers. These gland cells are stained weakly in the paratype. Additional circular muscle fibers are between both outer and inner epithelia. Interwoven muscle fibers are located below the basis of the mgo, giving to the whole mg1 a pear-shaped aspect.

The male atrium is long, and ample, but shorter and narrower in the incompletely mature paratype. This atrium can be divided into a proximal, not-folded half and a distal, folded half. These halves are separated from each other by a large fold. The male atrium is lined with a cuboidal, ciliated epithelium; each cilium is 1-µm long. The atrial epithelium is pierced by two types of gland cells, producing fine erythrophil granules, and amorphous xanthophil secretion, respectively. The epithelium of male atrium is underlain by a 50-110 µm-thick muscle of circular and longitudinal fibers interwoven.

The dorsal wall of the anterior half and the large fold of the atrium are provided with numerous mg1, whereas the folds of the distal half are provided with four lateral musculo-glandular organs, mg2, pointing to the right side of the body.

A mg2 is a cone having a canal which opens at its tip. The anteriormost mg2 measures about

200 µm in diameter, 375 µm in height and the canal is 105 µm deep. The posteriormost mg2 measures 500 µm in diameter, 420 µm in height, and the canal is 280 µm deep. The outer epithelium of mg2 is ciliated, with 12 µm high at the base of the organ, and 3 µm at its tip. Gland cells discharge fine erythrophil granules through this epithelium, especially around the tip of the organ, so that its lining epithelium becomes strongly reddish. The inner epithelium, i.e, that of the canal, is ciliated, cuboidal-to-columnar at its bottom, and 10-12 µm high, and 3 µm high close to its opening at the tip of the organ. Two types of gland cells discharge their contents into the canal. One type produces cyanophil granules and occurs at its maximum density in the bottom of the canal. This type is progressively replaced by the second type which produces erythrophil granules. The gland cells of the mg2 are poorly developed in the paratype. The canal contains only cyanophil granular secretion. None of the cell bodies of these two types of glands were found. The space between outer and inner epithelia of the mg2 is occupied by a dense muscle of criss-crossed fibers.

The ovaries are rounded-to-ovoid, and are approximately 200 µm in size. They are located 3.3 mm (or the equivalent to 5.7% of body length) anterior to anteriormost testes, and at a distance of 23% from anterior extremity of the body. They lie immediately above the ventral nerve plate. The ovovitelline ducts contain sperm in their anteriormost portion. These ducts emerge from the dorsal aspect of the ovaries, and run between subintestinal parenchymal muscle and the ventral nerve plate (Figs. 9B-C).

Laterally to the mid-region of the female atrium, the ovovitelline ducts bend abruptly to the dorsal side and join the 2-mm long, horizontal common ovovitelline duct, the latter located dorsally to the female atrium (Figs. 9A-B; 12A). Shell glands, which are absent in the paratype, discharge their content only into the common ovovitelline duct, which continues with the female genital canal (Figs. 10A; 12B, D). This canal projects anteriorly from the postero-dorsal portion of the female atrium (proflex condition with dorsal approach) (Figs. 10A-B; 12A, D).

The female genital canal is lined with a columnar epithelium, the apical third of its cells is xanthophil (Fig. 12D). This epithelium is pierced by glands producing xanthophil granules. Scarce glands producing erythrophil granules are also discharged through this epithelium. The female atrium is long and folded, the largest folds being longitudinal (Figs. 10A-B; 12A). This atrium is smooth in the incompletely mature paratype. The female atrium is approximately as long as the male atrium. The female atrium is lined with a cuboidal-to-conical, xanthophil, ciliated epithelium. This epithelium is pierced by numerous glands producing fine erythrophil granules, less abundant glands producing xanthophil granules, and scarce glands producing

fine, cianophil granules. The female atrium epithelium is underlain by a dense muscle of circular and longitudinal fibers.

The female atrium presents four musculo-glandular organs of a third type, herein named mg3. In the sagittal sections the mg3 were longitudinally or obliquely sectioned. A mg3 is a conical projection with 200 µm in height, 100 µm in diameter and having an inner canal 350 µm deep. A muscle bulb extending 550 µm below the surface of the female atrial epithelium provides support to the mg3. The outer epithelium of the mg3 is squamous and stained pinkish, whereas that of the canal is ciliated and stained reddish. The canal contains pinkish granules produced by gland cells that pierce the inner epithelium of the mg3. The mg3 of the paratype lacks gland cells.

The common muscle coat is well developed, comprising mainly longitudinal fibers. It envelops the male and female atria and the female genital canal.

Remarks

Both type specimens are very similar to each other regarding the external and internal aspect except for the penis papilla, which is lacking in the paratype. The paratype presents signs of not being fully mature (musculo-glandular organs lacking gland cells; shell glands absent, male and female atria relatively narrower), but in our experience, juveniles of penis papilla-bearing species possess a penis papilla, more or less conspicuous. In view of the morphological similarities and the sistergroup relationships of the type specimens, we conclude for their conspecificity.

Adinoplana nahuta differs from *A. alerna* in that in *A. nahuta*: (a) The dorsal color exhibits yellowish marks medially (vs. lateral in *A. alerna* sp. n.; (b) the ventral side is covered with large black grey spots (vs. beige or black grey dots); (c) the prostatic vesicle enters the dorsal aspect of the penis bulb (vs. the ventral aspect); (d) the copulatory apparatus possesses two type of musculo-glandular organs (vs. three types); (e) the proximal portion of the ejaculatory duct runs ventrally (vs. dorsally); (f): the dorsal insertion of the penis papilla is anteriorly shifted (vs. posteriorly); and (g) the ejaculatory duct is widened distally (vs. not widened).

Fig. 8. *Adinoplana nahuta* Carbayo & Almeida, sp. n. Living holotype in dorsal (A) and ventral views (D). Scale not available.

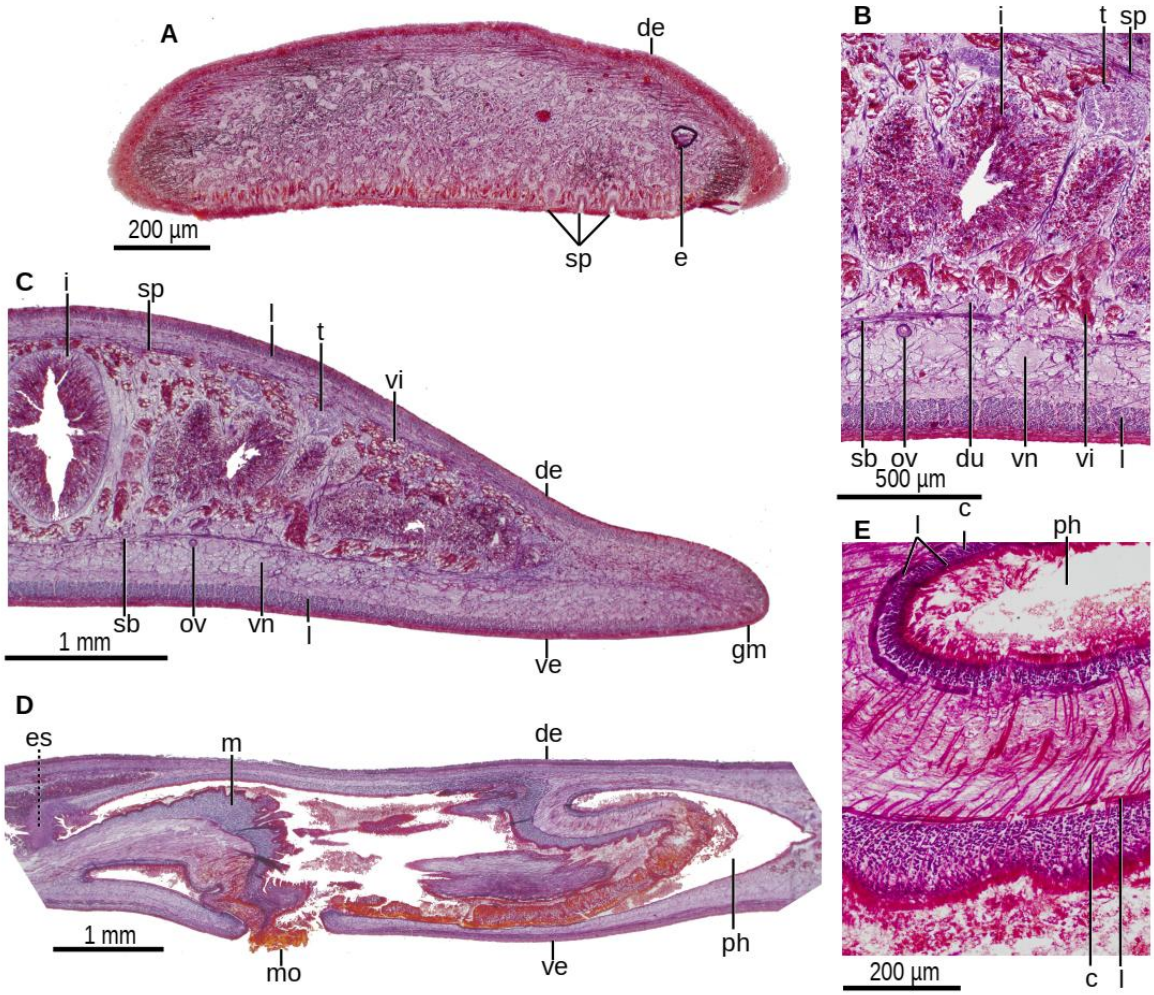

Fig. 9. *Adinoplana nahuta* Carbayo & Almeida, sp. n. Photomicrographs of histological sections of the holotype. A: Transverse section of the anterior tip of the body. B-C: Transverse sections of the prepharyngeal region. D-E: Sagittal sections of the pharynx (D) and its dorsal insertion (E).

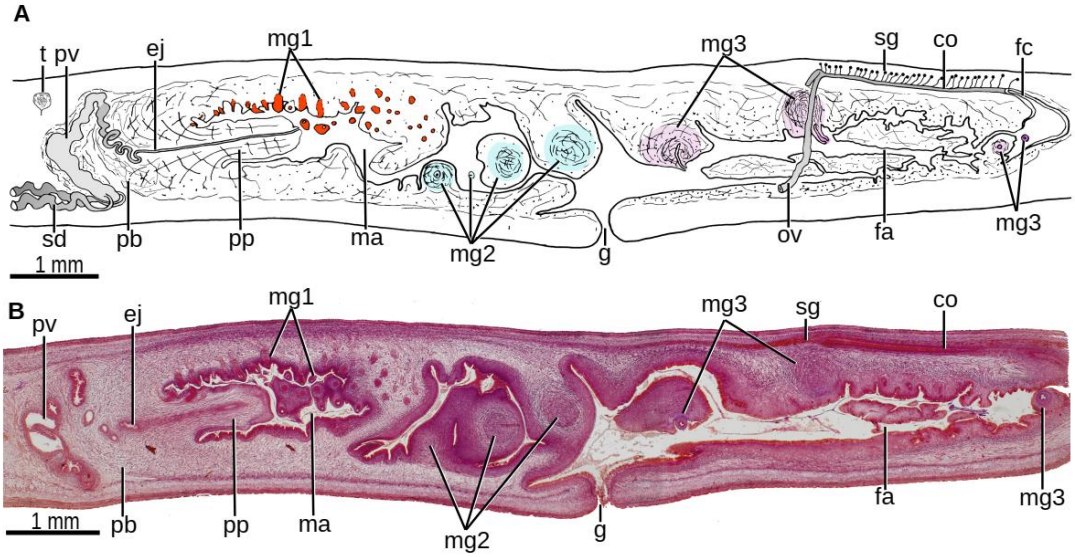

Fig. 10. *Adinoplana nahuta* Carbayo & Almeida, sp. n. A: Diagrammatic reconstruction of the copulatory apparatus. B: Photomicrograpah of a sagittal section of the copulatory apparatus.

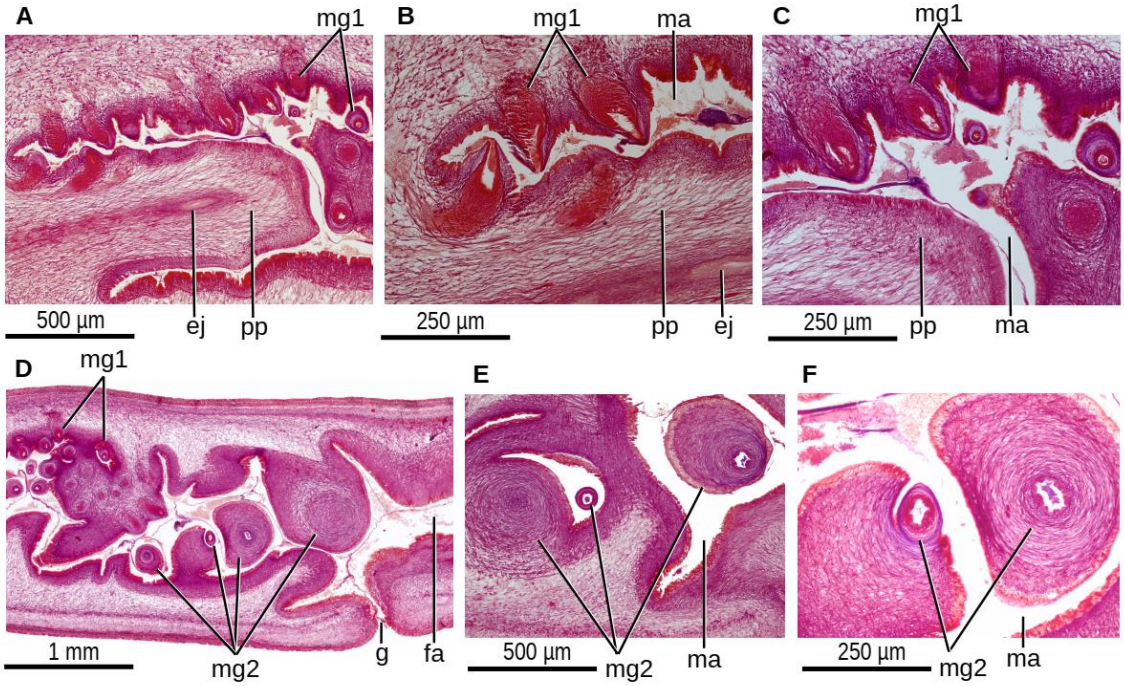

Fig. 11. *Adinoplana nahuta* Carbayo & Almeida, sp. n. Sagittal sections of the male components of the copulatory apparatus of the holotype. A-B: Penis papilla and dorsal wall of the male atrium. C: Dorsal wall of the male atrium. D: General view of the male atrium. E: Distal region of the male atrium. F: Musculo-glandular organs in the distal region of the male atrium.

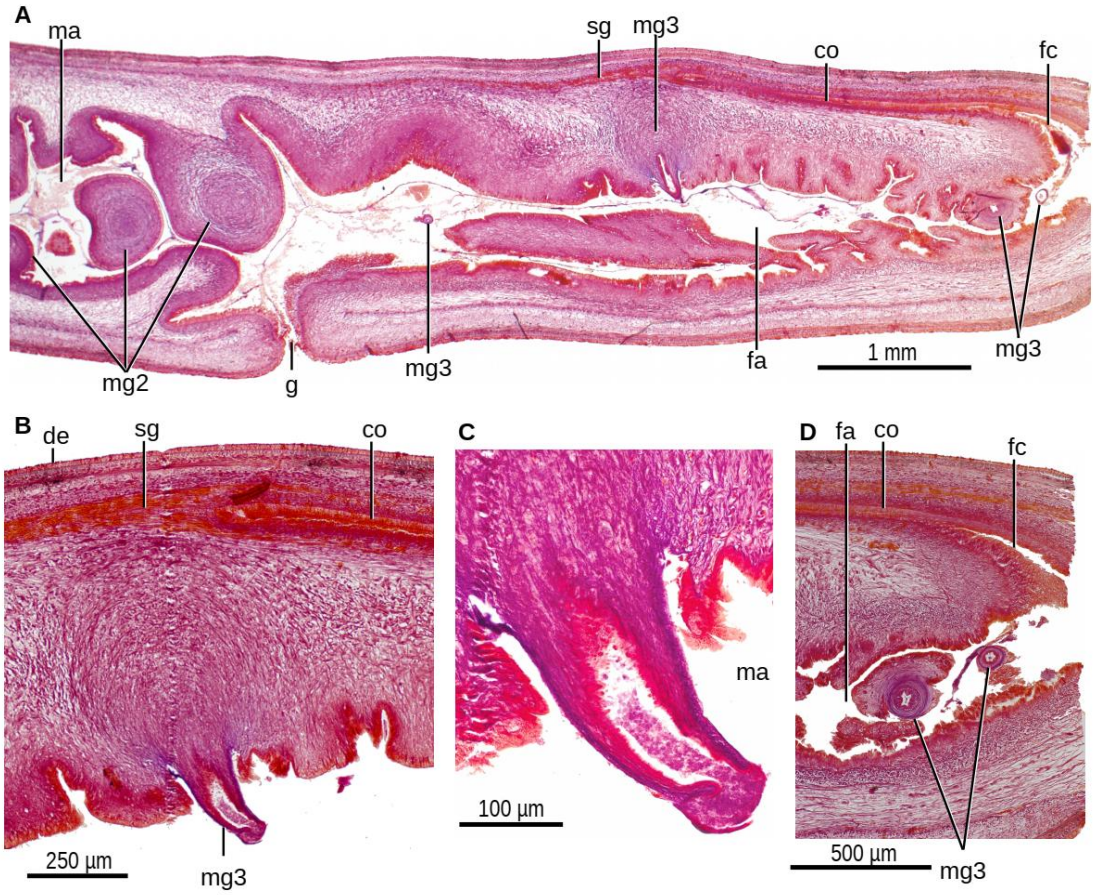

Fig. 12. *Adinoplana nahuta* Carbayo & Almeida, sp. n. Holotype. Photomicrographs of sagittal sections of the female components. A: General view of the female atrium. B-C: Dorsal wall of the female atrium (B) and musculo-glandular organ (C). D: Posterior region of the female atrium.

Geoplanini Stimpson 1857

Diagnosis. Geoplaninae with body ranging between subcylindrical and leaf-like body, in the latter case usually with dorsal eyes. Dorsum convex. Creeping sole usually wide. Dorsal longitudinal cutaneous muscle not insunk into the parenchyma. Pharyngeal pouch anterior to the copulatory apparatus; posteriormost testes anterior to the pharynx. Female genital ducts with even diameter. Female atrium without musculo-glandular organs.

This tribe comprises the new Chilean genus *Transandiplana* plus the 21 genera distributed out of Chile (except some species *incertae sedis* of *Amaga*, *Geoplana*, *Pasipha*).

***Transandiplana* Almeida & Carbayo, gen. n.**

Diagnosis. Geoplanini with a small-sized, slender body, approximately 25 mm in length. The creeping sole is wide. The eyes are located dorsally. Ventro-lateral sensory depressions are scarce. The thickness of the cutaneous muscle relative to the body height is 6.7%. The main nervous system comprises multiple longitudinal cords. The testes are surrounded by a dark pigment cup and are located anterior and away from the pharynx. The prostatic vesicle is extrabulbar. The penis papilla is well developed. The common ovovitelline duct is dorso-posterior to the female atrium. The female genital canal projects posteriorly from the dorso-posterior region of the female atrium.

Type species. *Transandiplana graui* Almeida & Carbayo, sp. n.

Etymology. *Transandiplana* refers to the Transandean location of the species with respect to the remaining members of the Geoplaninae, and the term *plana*, regarding the flattened body shape. The gender is female.

***Transandiplana graui* Almeida & Carbaio, sp. n**.

Material examined. **Holotype Museo Chile** (Field code, F4696). Huasco, Región de Atacama, Chile, Coord. -28.465931, -71.185961, F. Carbayo, December 2th 2010. Transverse sections of cephalic region on 13 slides; horizontal sections of the ovaries region on 4 slides; transverse sections of pre-pharyngeal region on 7 slides; sagittal sections of pharynx and copulatory apparatus on 13 slides.

Type locality. Huasco, Región de Atacama, Chile.

Etymology. The specific epithet pays homage to Dr. José Horácio Grau, for his friendship and contribution to the knowledge of the Chilean planarians.

Description.

External aspect. The live holotype (Fig. 13A) is approximately 25 mm in length and 2 mm in width. The body margins are parallel. The anterior extremity is rounded, and the posterior one pointed. The dorsum is convex, the ventral side is slightly convex. The dorsal color is graphite grey (RAL 7024), slightly clearer on the body margins, and ornated with a longitudinal median grey white (RAL 9002) stripe (Fig. 13A). The ventral surface is pure white (RAL 9010), darker in the cephalic region, and exhibits a median thin whitish stripe (Fig. 13B). Around the ventral

pores the color is also whitish. The preserved specimen measured 25 mm in length, 2.5 mm in width, and 1 mm in height.

The eyes are of a single-cup with 35-38 µm in diameter. The eyes are present in a uniserial row around the anterior 2 mm; behind this region, the spread onto the dorsal surface to the extent of a band 40% of the body width on either side. This band becomes progressively thinner to the posterior tip of the body, where the eyes are only marginal. Very scarce sensory depressions are located ventro-marginally in the anterior region of the body (Fig. 13C-E). These depressions are difficult to discern since their depth is 2/3th the height of the epithelium. This situation together with the suboptimal quality of the sections and the absence of a ventral body piece of the very anterior tip hindered the study of further details of their distribution. There are no sensory pits. The relative position of the mouth : body length, is 67.6%; that of gonopore : body length, 78.8%.

Internal Morphology

*Epidermis and its secretions.*The creeping sole occupies 85% of the ventral surface of the body. The dorsal epidermis of the pre-pharyngeal region is pierced by rhabtitogen cells and by two types of gland cells, producing erythrophil granules and xanthophil amorphous secretion, respectively. The ventral epidermis is pierced by gland cells producing cyanophil granules and a second type producing amorphous erythrophil secretion. A glandular margin is absent. In the cephalic region, the gland cells exhibit the same distribution, but are scarcer. The main nervous system is organized in approximately 24 longitudinal, crowded cords. The shape of each cord resembles a necklace of beads (Fig. 14A-B, D). Cerebral ganglia could not be discerned.

Cutaneous musculature. The cutaneous musculature comprises three layers, namely a subepithelial circular muscle (2-3 µm thick), followed by a double layer with diagonal fibers (4 µm), and then a longitudinal muscle (20-25 µm dorsally, 17-20 µm ventrally). Muscle fibers of the latter muscle are arranged into bundles with 6-15 fibers each (Fig. 14E-F). The cutaneous musculature thickness relative to body height at the pre-pharyngeal region is 6.7%. The musculature in the cephalic region maintains the organization found in the pre-pharyneal region.

Parenchymal musculature. The parenchymal musculature comprises a dorsal double layer (12-15 µm thick) of decussate fibers, a supraintestinal transverse muscle (40-50 µm) and a subintestinal transverse muscle (35-50 µm) (Fig. 14C-D). The three layers are relatively loose.

Digestive system. The mouth is situated at the end of the pharyngeal pouch (Fig. 15A). The esophagus : pharynx ratio is 24%. The pharynx is cylindrical (Fig. 15A). The esophagic musculature consists of a subepithelial circular muscle (40 µm thick), followed by a longitudinal muscle (25 µm thick). The pharyngeal epithelium is pierced by two types of cell glands producing cyanophil and erythrophil granules, respectively. The outer pharyngeal musculature is composed of a subepithelial longitudinal muscle (2.5 µm thick), followed by a circular muscle (7.5 µm thick). The inner pharyngeal musculature consists of a single muscle of circular and longitudinal fibers interwoven.

Male reproductive system. The copulatory apparatus occupies 87% of the body height, and is twice longer than high. The testes range between club- and pear-shaped and are approximately 180-230 µm in diameter. They are surrounded by a dark pigment cup (Fig. 14C, E-F). The testes are distributed into 1-2 rows at each side of the body. They are located dorsally, beneath the transverse supraintestinal parenchymal muscle, and between the intestinal branches. The anteriormost testes lay at a distance equivalent proximately to 10% of the body length; the posteriormost testes are 2 mm (8% of body length) anterior to the pharynx, i.e., at a distance equivalent to 52.4% of the body length.

The sperm ducts run dorsally to the ovovitelline ducts, and the distal portion of one of them is dilated to form a spermiducal vesicle filled with sperm. The distal portion of the sperm ducts bend dorsally and medially to open into the mid-dorsal portion of the prostatic vesicle (Fig. 15C). The prostatic vesicle presents an anterior, extrabulbar, dilated portion with folded wall and a canalicular distal portion which penetrates the dorso-anterior region of the penis bulb (Figs. 15B-D). The prostatic vesicle is lined with a columnar epithelium proximally; otherwise, the lining epithelium is cuboidal. Abundant gland cells discharge cyanophil granules in the prostatic vesicle (Figs. 15B, D). The dilated portion of the prostatic vesicle is surrounded by a single muscle (10-65 µm thick) of fibers intermingled, whereas the canalicular portion is surrounded by a single circular muscle (15 µm thick).

The prostatic vesicle passes to the ejaculatory duct in the penis papilla (Fig. 15C-D). This duct crosses the penis papilla medially to open at its tip. The ejaculatory duct is lined with a cuboidal, ciliated epithelium, and is pierced by two types of gland cells producing cyanophil and erythrophil granules, respectively. There are no apparent muscle fibers surrounding this duct.

The conical penis papilla presents its dorsal insertion shifted backwards and its entire basis is

dilated. This papilla occupies the entire length of the male atrium (Fig. 15C-D). The penis papilla is lined with a cuboidal-to-columnar epithelium which is pierced by numerous gland cells of two types producing erythrophil and cyanophil granules, respectively. The epithelium is underlain by a single circular muscle (10 µm thick). Numerous radial and longitudinal muscle fibers are in the stroma of the penis papilla.

The male atrium is smooth (Fig. 15C-D), and is lined with a low epithelium (10 µm high) proximally and tall (30 µm thick) in the other regions. The atrial epithelium is pierced by two types of gland cells. One produces cyanophil granules and is especially abundant proximally. The second type produces erythrophil granules. The atrial epithelium is underlain by a subepithelial circular muscle (7.5 µm thick), followed by a longitudinal muscle (5 µm thick).

Female reproductive system. The ovaries are ovoid, with 190 µm in maximum diameter (Fig. 16A), and are located at a distance from the anterior tip corresponding approximately to 11% of the body length. The ovovitelline ducts emerge from the dorso-posterior portion of ovaries (Fig. 16A). Laterally to the gonopore and the female atrium, the ovovitelline ducts run dorso-posteriorly and subsequently bend anteriorly to join the common ovovitelline duct. This unpaired duct runs dorso-anteriorly to join the postero-dorsal region of the female atrium, and a short diverticulum of this duct projects anteriorly (Fig. 15C).

The female atrium is approximately as long as the male atrium, and is slightly narrowed by a fold dorsal to the gonopore. The female atrium is lined with a columnar (150 µm high) epithelium with irregular surface and stratified appearance. It is irregularly ciliated and is pierced by two types of gland cells producing erythrophil and cyanophil granules, respectively. The epithelium presents some spaces with vacuolar aspect and filled with cyanophil secretion (Fig. 16B-C).

The lining epithelium of the female atrium is underlain by a subepithelial longitudinal muscle (2.5 µm thick), followed by a circular muscle (7.5 µm thick); ectally to this muscle is a 20 µm thick longitudinal loose muscle composing a coat of this atrium (Fig. 16B).

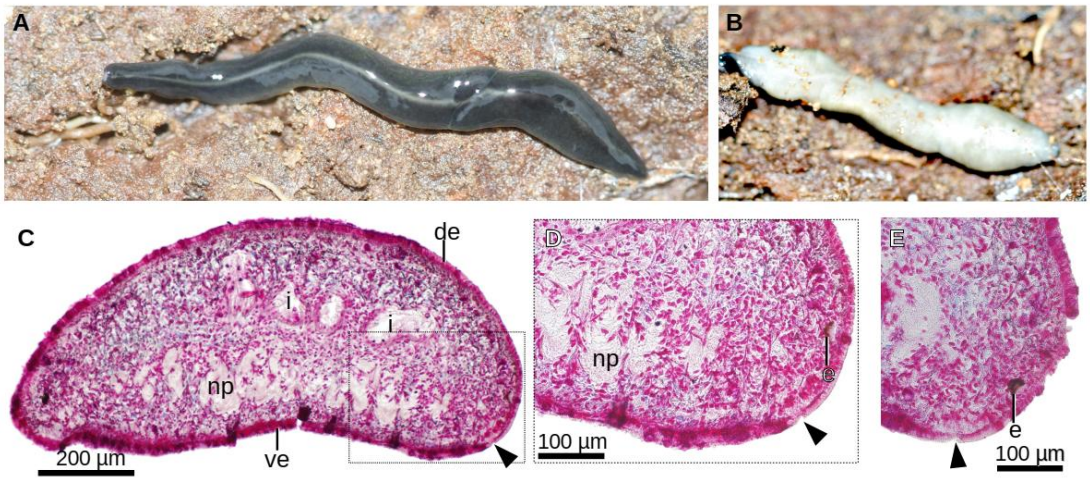

Fig. 13. *Transandiplana graui* Almeida & Carbayo, sp. n. Dorsal (A) and ventral (B) views of the living holotype. C-E: Photomicrographs of two transverse sections of the cephalic region. The arrowheads point to the sensory depressions. The inset in C is enlarged in D.

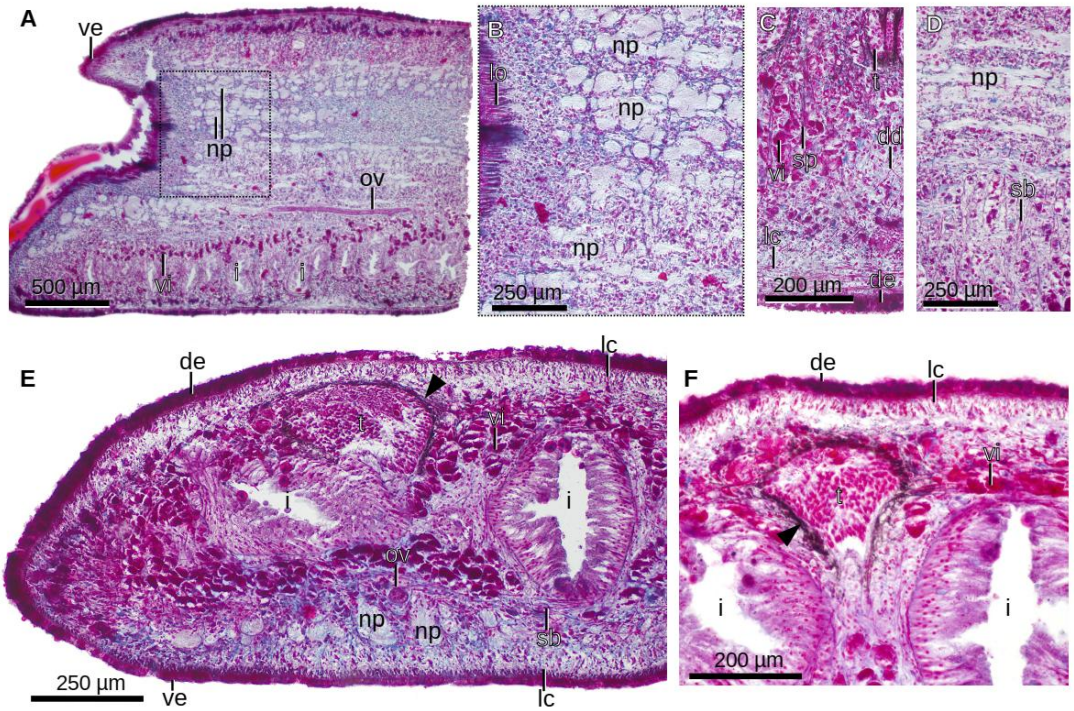

Fig. 14. *Transandiplana graui* Almeida & Carbayo, sp. n. Photomicrographs of horizontal sections of the anterior region of the body (A-D) and transverse sections of the pre-pharyngeal region (E-F). A-B: ventral region showing the main nerve system. The inset in A is enlarged in B. C: dorsal region showing cutaneous and parenchymal muscles. D: ventral region showing the subintestinal parenchymal muscle. E-F: Testes surrounded by dark pigment cup (arrowheads).

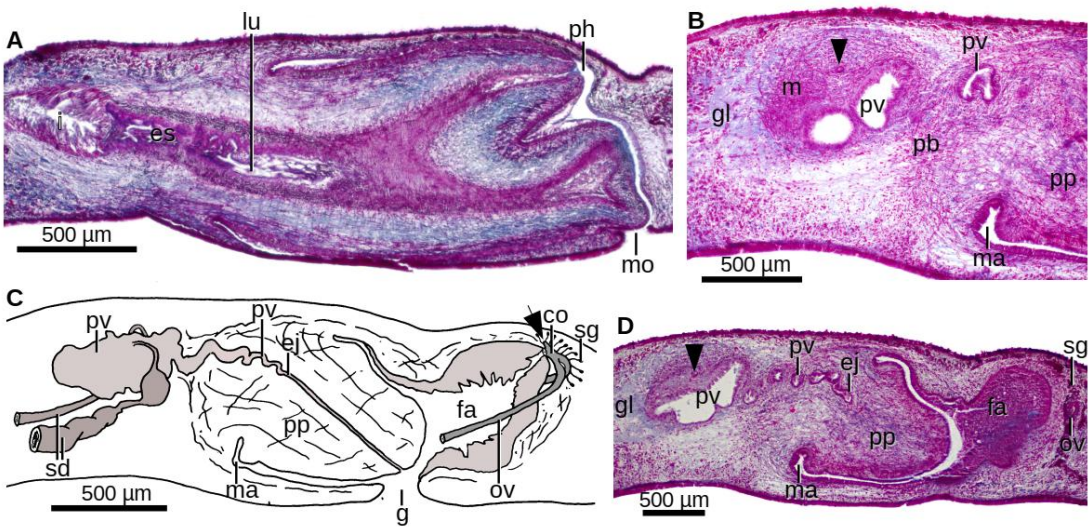

Fig. 15. *Transandiplana graui* Almeida & Carbayo, sp. n. **A**: Photomicrograph of a sagittal section of the pharynx. **B**: Photomicrograph of a sagittal section showing the prostatic vesicle. **C**: Diagrammatic reconstruction of the copulatory apparatus. **D**: Photomicrograph of a sagittal section of the copulatory apparatus. Arrowhead points to the entrance of a sperm duct into the prostatic vesicle. Arrow points to the diverticulum of the common glandular ovovitelline duct.

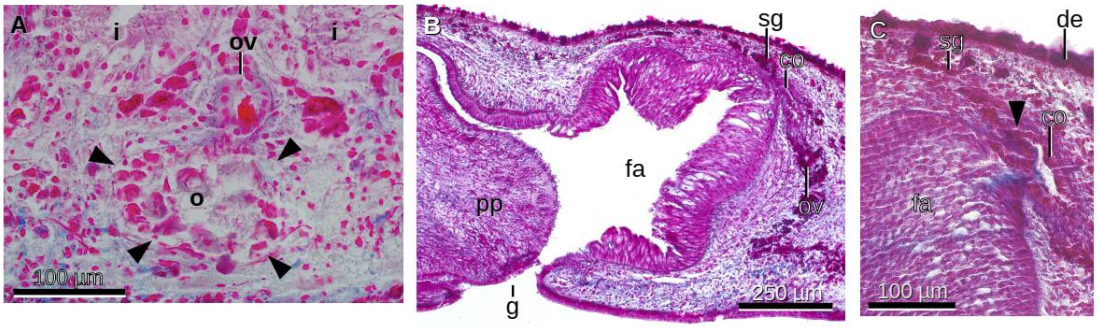

Fig. 16. *Transandiplana graui* Almeida & Carbayo, sp. n. Photomicrographs of a transverse section showing an ovary (A) and of sagittal sections showing the female atrium (B-C). Arrowhead points to the diverticulum of the common glandular ovovitelline duct.

Gusanini, trib. n.

Diagnosis. Geoplaninae with body broad and foliaceus, tapering very abruptly to the anterior end. Anterior end triangular. Longitudinal layer partly sunk into the parenchyma, internal to the cutaneous nerve net, both ventrally and dorsally. Sensory pits as a simple invagination or obliquely elongated and internally branched.

This tribe is monogeneric and currently houses three species, but see Chapter 2 of this thesis.

Haranini Almeida & Carbayo, trib. n.

Diagnosis. Small-sized Geoplaninae with a straight tube leveled with the subintestinal transverse parenchymatic muscle. Very long pharyngeal pouch, extending behind the copulatory apparatus.

This tribe includes only *Hara* Carbayo & Almeida, gen. n.

Geoplaninae Stimpson, 1857

***Harana* Almeida & Carbayo, gen. n.**

Diagnosis. Haranini with a subcylindrical, small-sized body, approximately 8 mm in length. The creeping sole is wide. The eyes and sensory pits surround the entire cephalic region. The eyes are located marginally. The thickness of the cutaneous muscle relative to the body height is 2.3%. A straight tube runs leveled with the subintestinal transverse parenchymatic muscle. The pharyngeal pouch is very long, extending dorsally behind the copulatory apparatus. The prostatic vesicle is extrabulbar. The penis papilla is cylindrical. The common glandular ovovitelline duct is ventro-posterior to the female atrium. The female genital canal projects posteriorly from the dorsal region of the female atrium.

Type species. *Harana harai* Almeida & Carbayo, sp. n.

Etymology. *Harana* is freely derived from Hara, and is a homage to Prof. Marcos Ryotaro Hara (USP), for his contributions to the scientific education of undergraduate and graduate students. The gender is female.

***Harana harai* Almeida & Carbayo, sp. n.**

Material examined. **Holotype MNHNCL PLAT-??** (Field code, F4738): Parque Nacional Bosque Fray Jorge (-30.662528, -71.682639), Coquimbo Region, Chile. F. Carbayo. 4 December 2010. Transverse-to-horizontal sections of the cephalic extremity on 2 slides; horizontal sections of a portion behind cephalic extremity on 3 slides; sagittal sections of the pharynx and copulatory apparatus on 8 slides.

Type locality. Parque Nacional Bosques de Fray Jorge, Chile.

Distribution. Only known from the type locality.

Etymology. The specific epithet pays homage to Prof. Marcos Ryotaro Hara (USP).

Description

External aspect. The live specimen measured approximately 8 mm in length and 1 mm in width when creeping, and 6.5 mm and 1.2 mm, respectively, after fixation. The body is elongate and subcylindrical, with the anterior tip rounded and the posterior tip pointed (Fig. 17A). The creeping sole is 78% of body width in the pre-pharyngeal region, as measured from sagittal sections. The mouth is positioned at a distance from the anterior extremity equal to 83% of the body length, and the gonopore is at 92%.

The dorsal coloration of the live specimen consists of numerous signal nigth brown (RAL 0502016) dots on the mustard brown (RAL 0605030) ground color of the dorsum (Fig. 17A). The ventral side is mustard brown, darker in the anterior tip.

The eyes are formed by one pigmented cup of 25 µm in diameter. Clear halos around the eyes are absent. The eyes are marginally distributed in a single row from the very anterior tip of the body backwards to the posterior end. The sensory pits are 25 µm deep and ventro-laterally distributed in a single row along approximately the anterior 8% of the body.

Internal Morphology

Epidermis and its secretions. Numerous rhabditogen cells, and two types of gland cells producing erytrophil and cyanophil granules, respectively, pierce the dorsal epidermis of the pre-pharyngeal region. The ventral epidermis is pierced by gland cells producing fine erythrophil granules. A glandular margin is absent.

Cutaneous musculature. The cutaneous musculature consists of a thin subepithelial circular muscle followed by a thin diagonal muscle of decussate fibers, and an innermost longitudinal muscle with fibers arranged in bundles of 2-4 fibers each. The longitudinal layer is 4 µm thick dorsally and 8 µm ventrally. The thickness of cutaneous muscle relative to the body height is 2.3%. These muscles are thinner in the cephalic region.

Parenchymal musculature. A parenchymal transverse subintestinal layer is relatively well developed (Fig. 18B). There are also some scattered dorsal diagonal fibers and some transverse supraintestinal fibers. The central nervous system is as two nerve chords (Fig. 18A).

A straight tube (Fig. 18A-B) runs medially among the muscle fibers of the subintestinal transverse parenchymatic muscle, from near anterior tip of the body to at least 1 mm behind. This tube is 25 µm in diameter, and is lined with weakly stained cuboidal cells. The tube is underlain by a thin longitudinal muscle. A body portion behind the cephalic region was denatured for DNA extraction and behind this region, namely the ovarian region, the tube is absent.

Digestive system. The pharyngeal pouch extends over the copulatory apparatus and continues 750 µm behind it (Fig. 19B-C), being approximately twice as long as the pharynx. The anteriormost portion of the pharynx is unavailable since it was denatured, but its general appearance is that of a cylindrical type (Fig. 18C). The posterior portion of the pharynx lays over the prostatic vesicle. The outer pharyngeal epithelium is underlain by a longitudinal muscle (5 µm thick) followed by a circular one (17 µm) and an innermost longitudinal muscle (8 µm); the inner pharyngeal epithelium is underlain by a circular muscle (12 µm), followed by a longitudinal muscle (5 µm) (Fig. 19A).

Male reproductive system. Testes were not found in the sections available. The sperm ducts run over the main nervous system. They contain sperm in their distal portion. Laterally to the prostatic vesicle, the sperm ducts curve dorsally, subsequently ventrally to communicate with the respective branch of the prostatic vesicle (Fig. 19B). The extrabulbar prostatic vesicle is tubular. The anterior portion of the vesicle runs dorsally and a short distal portion runs ventrally to penetrate the anterior region of a well-developed penis bulb. The prostatic vesicle is lined with a ciliated, cuboidal epithelium, which is pierced by gland cells producing erythrophil granules. This epithelium is surrounded by a circular muscle (10 µm thick). The ejaculatory duct is horizontal and slightly sinuous, and opens at the tip of the penis papilla. The ejaculatory duct is lined with a ciliated, cuboidal epithelium, and is surrounded by a 3 µm thick circular muscle.

The penis papilla is cylindrical, with a distal enlargement so as to resemble a club (Fig. 19B-E). Its is horizontally placed and occupies the entire male atrium. The proximal 2/3th of the penis papilla are lined with a columnar epithelium, whereas the epithelium of enlarged, distal third is cuboidal. The epithelium of this papilla is pierced by gland cells producing erythrophil granules, and these gland cells are especially abundant in the proximal 2/3th of the papilla. Some gland cells producing cyanophil granules cross the epithelium of the dorso-proximal region of the penis papilla. Additionally, other glands with light cyanophil granules open at the tip of the penis papilla. The lining epithelium of the penis papilla is underlain by a 5-µm-thick circular muscle followed by a 5-µm-thick longitudinal one.

The male atrium possesses small folds near the insertion of the penis papilla. The communication of the male atrium with the female atrium is very narrow by means of a thin fold dorsal to the level of the gonopore (Fig. 19B-E). The male atrium is lined with a squamous epithelium dorsally, and a columnar epithelium ventrally and distally. The epithelium is underlain by a 2-µm-thick circular muscle, followed by an additional 3-µm-thick longitudinal inner muscle, the latter only in the ventral side of the male atrium. The ventral epithelium of

the male atrium is pierced by gland cells producing eryhtrophil granules.

Female reproductive system. The ovaries were not found in the sections available. Vitellaria are abundant around the intestine. The ovovitelline ducts run backwards above the ventral nerve plate. These ducts ascend medially inclined behind the gonopore canal to unite with the common ovovitelline duct below the female atrium (Fig. 19B-C, E). This common duct ascends behind the female atrium to join the female genital canal. This canal is oriented postero-ventrally, and projects from the postero-dorsal portion of the female atrium (Fig. 19B) (postflex condition with dorsal approach). The female atrium : male atrium length ratio is 2.5 : 4. The female atrium is inclined towards the gonopore and distal narrow. This atrium is lined with a columnar, 100 µm high epithelium, the apical portion of which is erythrophil (Fig. 19E). Towards the gonopore canal, the epithelium passes gradually into a cuboidal type. Two types of gland cells producing fine cyanophil, and erythrophil granules, respectively, pierce the epithelium of the female atrium, the latter being scarcer. The epithelium is underlain by a 2-µm-thick longitudinal muscle followed by a 8-µm-thick circular one.

Remarks

Harana harai sp. n. does not fit in any of the current genera of Geoplaninae. Among the genera of this group, only *Gigantea, Gusana, Liana* (but the female genital canal is not developed), and *Pichidamas* share with the new species the presence of a penis papilla and the ventral location of the common glandular ovovitelline duct with respect to the female atrium. However, *Harana harai* sp. n. differs from these genera in other morphological attributes. *Gigantea* houses large and flat species (vs. small and subcylindrical in H*. harai* sp. n.) in which also the female genital canal projects from the posterior region of the female atrium (vs. from the dorsal region). *Gusana* characterizes species with a foliaceous body, tapering very abruptly to the anterior end, longitudinal layer partly sunk into the parenchyma, internal to the cutaneous nerve net, both ventrally and dorsally, and the sensory pits may be branched. *Liana* differs from the new species in that part of the longitudinal ventral cutaneous muscle is sunk into the parenchyma (vs. not sunken in *H. harai* sp. n.), and the female canal approaches from the horizontal or ventral aspect. Finally, *Pichidamas* distinguishes readily by the presence of a muscle retractor of the cephalic region (vs. absent) and the adenodactyls in the male part of the copulatory apparatus (vs. absent in the new species).

As a consequence, a new genus should be proposed for the new species. A synapomorphic character of Geoplaninae is the dorsal position of the testes, an attribute not unfortunately, an important attribute of the Geoplaninae could not be checked in the species, namely the position of the testes. Based on the phylogenetic position of the species (Fig. 1), it is assumed

that the testes are dorsally located and therefore, the species can be considered a member of Geoplaninae.

An interesting feature of the new species, namely the pharyngeal pouch extending behind the copulatory apparatus passing over it, is also found in the members of Timyminae (Almeida et al., 2021), also from Chile. *Harana* and Timyminae share a sistergroup relationship and it is reasonable to accept that the long extension of the pharyngeal pouches in both taxa are homologous.

Figure 17. *Harana harai* Almeida & Carbayo, sp. n. **A**: dorsal view of the living holotype. Scale not available. **B**: Preserved specimen on graph paper.

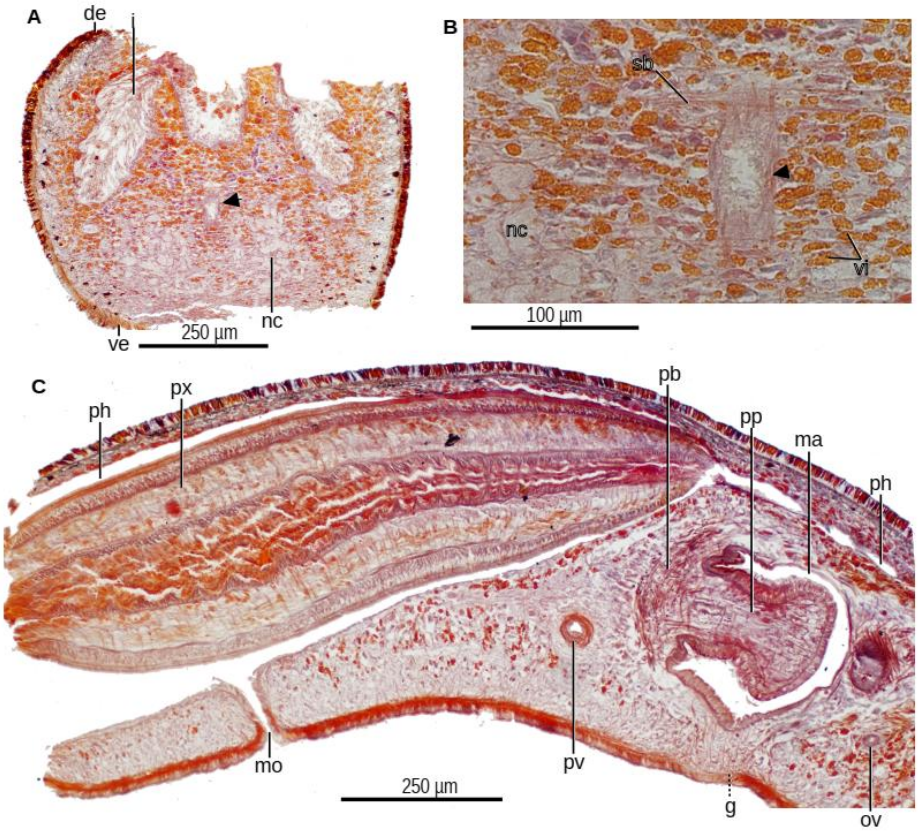

Figure 18. *Harana harai* Almeida & Carbayo, sp. n. Photomicrographs. **A-B**: transverse-horizontal sections of the anterior portion of the body, showing the longitudinal tube (arrowhead). **C**: sagittal section through the pharynx and copulatory apparatus.

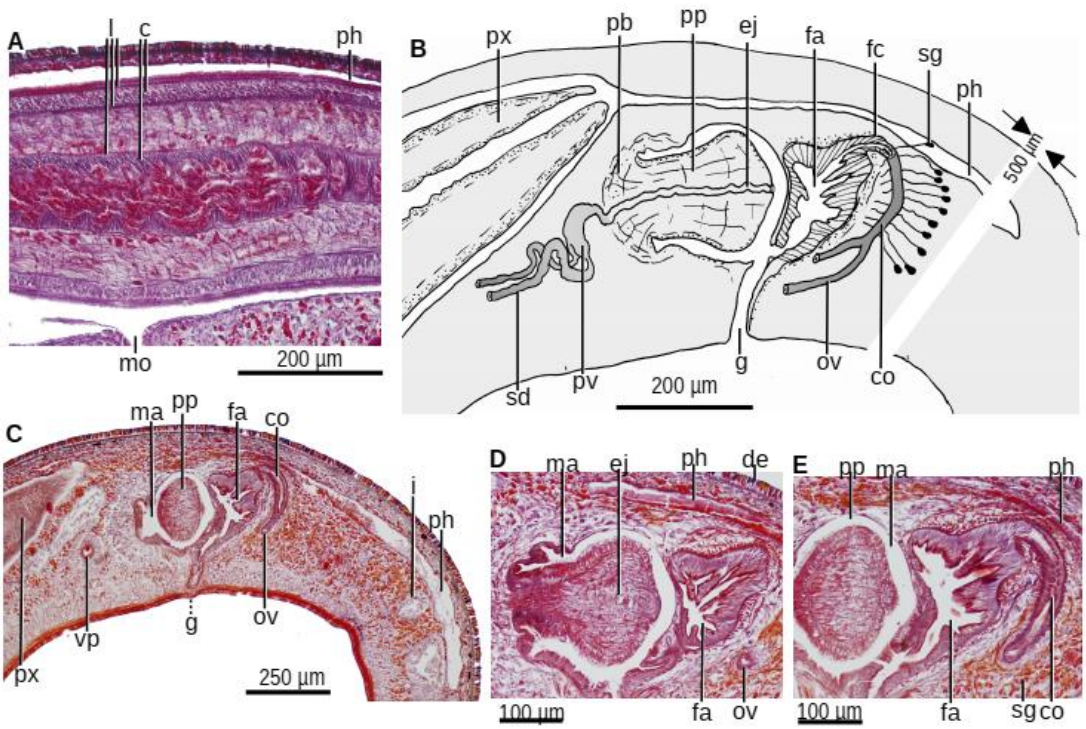

Figure 19. *Harana harai* Almeida & Carbayo, sp. n. **A**: Photomicrograph of a sagittal section through the pharynx, showing subepithelial muscles. **B**: diagrammatic reconstruction of the copulatory apparatus. **C**. Photomicrograph of a sagittal section through the copulatory apparatus and pharyngeal pouch extending behind it. **D-E**. Photomicrographs of sagittal sections through the copulatory apparatus.

Inakayaliini Almeida & Carbayo, trib. n.

Diagnosis. Geoplaninae with dilated female genital ducts.

This tribe is monogeneric and currently houses three species, including a new species described here.

Inakayalia cyanea Almeida & Carbayo, sp. n.

Material examined. Type material: Collected in Parque Nacional Nahuelbuta, Chile, Coord. -37.80, -73.00, F. Carbayo, 13 December 2010. **Holotype ?? MNHNCL F4912** (Field code F4912). Transverse sections of the anterior region of the body on 14 slides; horizontal sections of the ovarian region on 100 slides; transverse sections of the pre-pharyngeal region on 30 slides; sagittal sections of the copulatory apparatus on 122 slides. **Paratype MZUSP PL ??** (Field code F4914). Transverse sections of the cephalic region on 10 slides; horizontal sections of the ovarian region on 13 slides; transverse sections of a region behind that of the ovarian on 10

slides; sagittal sections of the pharynx and copulatory apparatus on 73 slides. **Paratype MZUSP PL ??** (field code F4917). Horizontal sections of the ovarian region on 12 slides; sagittal sections of the copulatory apparatus on 7 slides.

Type locality. Parque Nacional Nahuelbuta, Región de la Araucanía, Chile.

Etymology. The specific epithet derives from the Latin *cyano-*, meaning bluish, alluding to the color of the body.

Diagnosis. Species of *Inakayalia* with a very long and widened prostatic vesicle, branched in its proximal region, and provided with a long postero-dorsal diverticulum; very long unpaired and dilated common ovovitelline duct.

Description.

External aspect. The three animals are mature and measured between 23-27 mm in length and 6-8.3 mm in width at rest. The holotype was 63 mm long and 3 mm wide when creeping. The preserved specimens measured 28.5-44.5 mm long, 5-6 mm wide. The resting animals display a lanceolate body with wavy margins (Fig. 20). The cephalic region narrows to the rounded tip; the posterior narrows abruptly to the pointed tip. The dorsum is convex medially, and flat laterally. The ventral side is flat.

The cephalic region, with approximately 1/8th of the body length, exhibits two black blue (RAL 5004) bands, more or less separated from each other (Fig. 20A-C). This region is completely (Fig. 20A-B) or incompletely (Fig. 20C) separated from the remaining, posterior region of the body by a transverse, whitish-to-yellowish band. The margins of this band are irregular. Behind the transverse band the dorsum is covered with abundant fine black blue dots. These dots are more densely packed as a median band and a pair of paramedian bands (each with 12-16% of the body width). Large blue grey (RAL 7031) halos are over the dorsum except the median band.

The ground color of the ventral side is light gray (RAL 7035) (Fig. 20D-E). Towards the body margins of the cephalic region the color is progressively darker to black blue. A transverse whitish band is continued from the dorsal one so giving rise to a ring. Behind this transverse band, the ventral surface is covered by numerous dots either graphite grey (RAL 7024) or ochre brown (RAL 8001).

The eyes are of a single-cup type with 32-38 µm in diameter. The eyes are present in a

uniserial-to-biserial row around the anterior 1/8th of the body; behind this region, the spread onto the dorsal surface following the distribution of the halos.

The sensory pits are simple invaginations 50-57 µm deep, located ventro-marginally in a single row from the very anterior body tip up to 18% of body length. The relative position of the mouth : body length range between 63.4-66.3%; that of the gonopore : body length, 83.6-86.7%.

Internal morphology.

Epidermis and its secretions. The creeping sole is 95% of the body width. In the prepharyngeal region, the entire epidermis is pierced by 10-15 µm thick necks of gland cells producing coarse (1 µm gross) xanthophil granules and by scarcer gland cells producing erythrophil granules. The xanthophil type is more abundant towards the body margins. The glandular margin is constituted of xanthophil gland cells (Fig. 21A). Rhabditogen cells pierce the dorsal epidermis. As the creeping sole narrows towards the anterior extremity of the body, the xanthophil glands become scarce dorsally and abundant ventrally.

Cutaneous musculature. The cutaneous musculature comprises three layers, namely a subepithelial circular layer (5 µm thick), followed by a double layer (15-40 µm) with decussate fibers, and then a well developed innermost longitudinal layer (30-105 µm thick, dorsally and ventrally, respectively) (Fig. 21B-C). The cutaneous musculature thickness relative to body height is 13-15%. Towards the anterior region of the body, these muscle layers become thinner until they disappear.

Parenchymal musculature. There are three strong parenchymal muscle layers, namely dense dorsal layer of decussate fibers (30 µm thick), a supraintestinal layer of transverse fibers (100 µm thick) and a more dense subintestinal layer of transverse fibers (100 µm thick) (Fig. 21B-C). Towards the anterior region of the body, these muscle layers become thinner until they disappear.

Digestive system. The intestine consists of three main branches converging in the esophagus, namely an anterior main branch and two posterior ones. The paired branches may also connect to each other at the level of the prostatic vesicle. The esophagus : pharynx ratio is 31-33%. The mouth is situated at a distance from the root of the pharynx equivalent to 41-54% of the pharyngeal pouch length (Fig. 21D). The distal portion of the pharyngeal pouch is very close to the prostatic vesicle. The pharynx is bell-shaped, with its dorsal insertion slightly

anterior to the mouth. The epithelium of the distal portion of the pharynx is pierced by four types of gland cells, producing xanthophil, erythrophil and cyanophil granules, respectively, and amorphous secretion. The outer pharyngeal musculature consists of a subepithelial longitudinal muscle (5 µm thick), followed by a circular muscle (15 µm thick), and an innermost longitudinal muscle (5 µm thick). The inner pharyngeal musculature consists of a subepithelial circular muscle (75 µm thick), followed by a longitudinal muscle (10 µm thick) (Fig. 21E).

Male reproductive system. The rounded or irregular testes measure 325-450 µm in diameter. They are organized in 2-4 rows in two levels at each side of the body, and between the supraintestinal parenchymal muscle and the intestinal diverticula (Fig. 21A). The anteriormost testes lay at a distance from the anterior tip of the body equivalent to 17.3% of the body length; the posteriormost ones, the equivalent to 65% of body length, i.e, laterally to the pharyngeal root.

The sperm ducts run immediately above the subintestinal parenchymal muscle. Laterally to the pharyngeal pouch each duct opens into the antero-ventral region of the respective branch of the prostatic vesicle (Fig. 22A). The extrabulbar prostatic vesicle is very large and dilated. It occupies 2/3th of the body height and is as long as 2.7 times the length of the portion of the copulatory apparatus wrapped in the common muscle coat (Figs. 22B-C, 23A-C). The anterior 1/16th of the prostatic vesicle is branched and each branch is tubular; the following 8/16th of the vesicle is elongate and large, with dorsal and ventral folds filling its lumen. A long diverticulum projects over the distal portion of the vesicle, representing 7/16th of the total length of the organ (Fig. 22A, 23B-C). This third, distal portion is a long duct horizontally placed in the ventral region of the body, which penetrates the anterior section of the penis bulb to communicate with the ejaculatory duct. The prostatic vesicle is lined with a ciliated epithelium. This epithelium is cuboidal in the paired branches, and columnar in the remaining portions, and is pierced by abundant gland cells producing erythrophil granules. The epithelium is underlain by a decussate 25-100 µm thick muscle.

The ejaculatory duct is a horizontal canal opening at the tip of the penis papilla (Fig. 22A). This duct is lined with a cuboidal-to-columnar, ciliated epithelium which is surrounded by a 50 µm thick circular muscle. The penis papilla is cylindrical with rounded tip, and is horizontally located along most of the male atrial length (Figs. 22A-C, 23B). This papilla is lined with a columnar epithelium which is pierced by two types of gland cells producing erythrophil and cyanophil granules, respectively. This epithelium is underlain by a 15 µm thick muscle with circular and longitudinal fibers interwoven.

The male atrium is relatively short and not folded. It is lined with a cuboidal-to-columnar epithelium, which is crossed by gland cells producing erythrophil and cyanophil granules, respectively. This epithelium is underlain by a circular muscle followed by a longitudinal one, each 5 µm thick proximally, 30 µm distally

Female reproductive system. The ovaries are ovoid, with a maximum diameter of 400 µm in the longitudinal body axis. The ovaries are located immediately above the ventral nerve plate (Fig. 21C), and a distance from the anterior tip of the body corresponding to 9.6% of the body length. The ovovitelline ducts emerge from the lateral aspect of the ovaries and run ventrally above the nerve plate. At the level of the mid region of the prostatic vesicle, each ovovitelline duct opens laterally into the anterior portion of the dilated, long common ovovitelline duct (Figs. 22A, C; 23B-E). This long duct is six times wider than the ovovitelline ducts, and exhibits folded walls. The common ovovitelline duct ascends gradually to communicate with the common glandular ovovitelline duct dorsally to the penis papilla. In turn, this runs posteriorly to join the female genital canal, which is dorso-anteriorly flexed, and projects from the dorso-posterior region of the female atrium. The female atrium is slightly shorter than the male atrium and is elongated and slightly inclined towards the gonopore. The female atrium widens progressively towards the male atrium with which it communicates broadly.

The common ovovitelline duct is lined with a columnar epithelium, which is crossed by three types of gland cells producing xanthophil, erythrophil and cyanophil granules, respectively (Fig. 23E). This duct is surrounded by a single muscle layer (50 µm) of circular, diagonal and longitudinal mixed thin fibers. The female genital canal and the female atrium are lined with a 75-µm high columnar, non ciliated epithelium. This epithelium is pierced by gland cells producing erythrophil granules and its cells contain xanthophil granules in their subapical portion. This epithelium is underlain by a 50-120 µm thick muscle of longitudinal fibers with circular fibres interspersed.

Remarks

This new species matches nearly all diagnostic features of *Inkayalia* Negrete et al., 2020. Differences regard to the irregular walls of the penis papilla, and in the dilated portion of the female ducts. In the new species, the wall of the penis papilla is not irregular but smooth, and the dilated portion of the female ducts is not that the distal one of each ovovitelline duct but an unpaired, common ovovitelline duct.

Inakayalia cyanaea sp. n. distinguishes readly from the three species in the genus in the very

long prostatic vesicle and in the presence of a dilated common ovovitelline duct.

Fig 20. *Inakayalia cyanaea* Almeida & Carbayo, sp. n. Photographs of the live holotype (A, D), paratype F4917 (B), and paratype F4914 (C, E) in dorsal (A-C) and ventral (D-E) views. Scale bars not available.

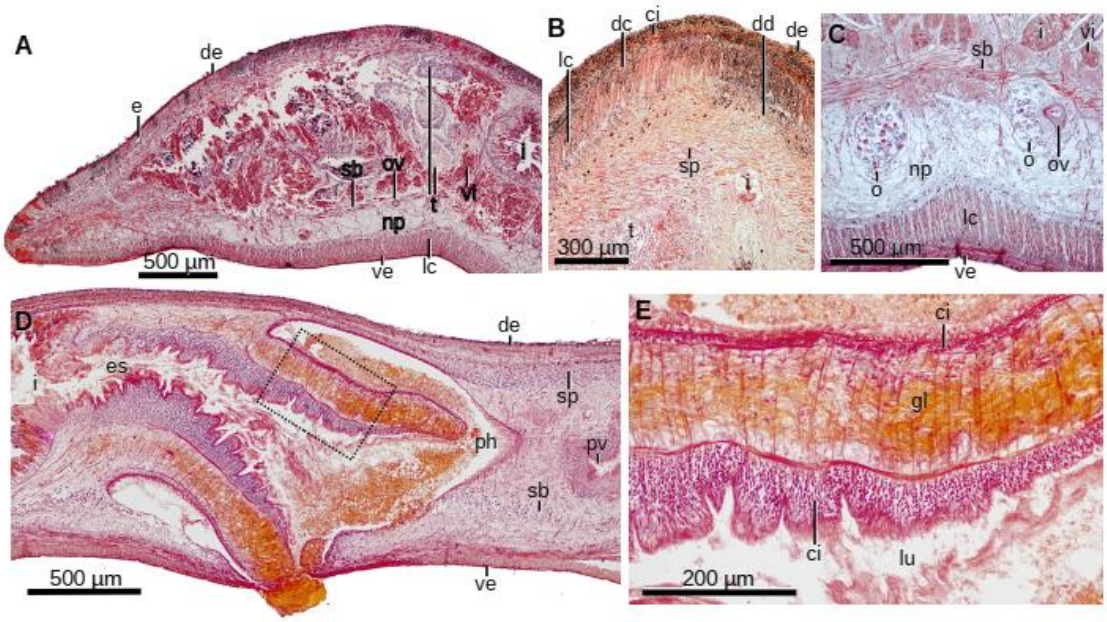

Fig. 21. *Inakayalia cyanaea* Almeida & Carbayo, sp. n. Photomicrographs of histological sections of holotype (A) and paratype F4914 (B-E). **A**: transverse section of the pre-pharyngeal region. **B**: horizontal section of the dorsal portion of the body showing cutaneous and parenchymal muscles. **C**: approximately transverse section showing the ovaries. **D**: sagittal section of the pharynx. **E**: sagittal section showing the outer and inner pharyngeal epithelia.

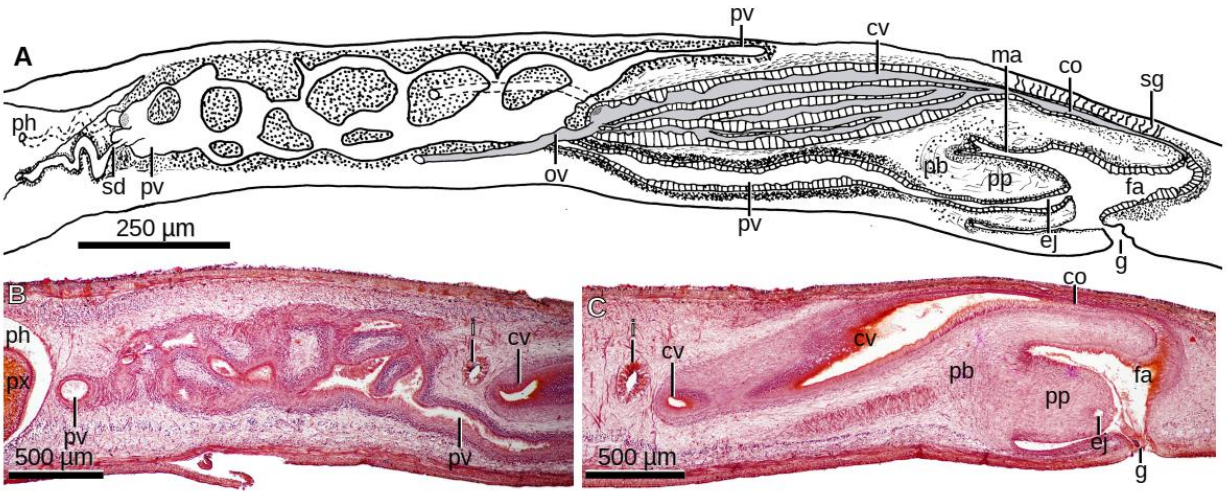

Fig. 22. *Inakayalia cyanaea* Almeida & Carbayo, sp. n. A: Diagrammatic reconstruction of the copulatory apparatus of the holotype. B-C: Photomicrographs of sagittal sections of the copulatory apparatus of the paratype F4914 showing the prostatic vesicle (B) and the male and female atria (C).

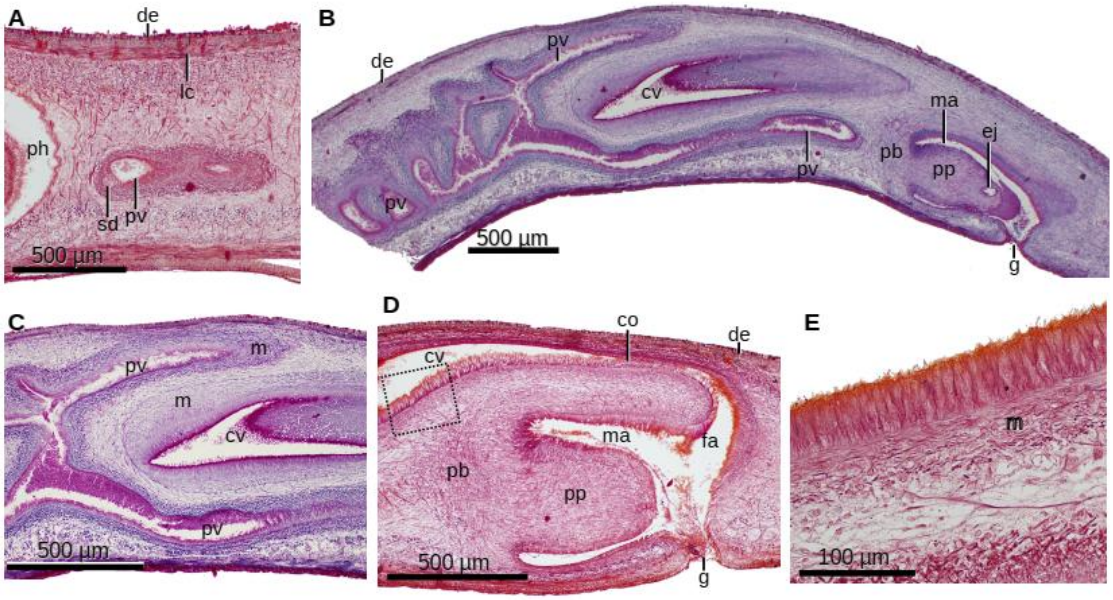

Fig. 23. *Inakayalia cyanaea* Almeida & Carbayo, sp. n. Photomicrographs of sagittal sections of the paratypes F4914 (A, D-E) and F4917 (B-C) showing the anterior region of the prostatic vesicle, the copulatory apparatus (B), the posterior region of the prostatic vesicle, the male and female atria (D) and the epithelium of the common ovovitelline duct.

Myoplanini Almeida & Carbayo, trib. n.

Diagnosis. Geoplaninae with transneural parenchymal muscle of diagonal fibers and four muscle layers underlying the inner pharyngeal epithelium.

This tribe includes only *Myoplana* Almeida & Carbayo, gen. n.

Myoplana Almeida & Carbayo, gen. n.

Diagnosis. Myoplanini with a small-sized, slender body, approximately 25 mm in length. The creeping sole is wide. The eyes are located marginally. Sensory pits present. Ventral peripheral nervous plexus is divided into two plexuses. Ventrally the longitudinal cutaneous musculature is divided in two layers, the inner one between the peripheral nerve plexuses. The thickness of the cutaneous muscle relatively to the body height is approximately 28%. A transneural parenchymal muscle is constituted of diagonal fibers. The inner pharyngeal musculature consists of four muscle layers. The prostatic vesicle is extrabulbar. The penis papilla is intra-penial. The common ovovitelline duct is dorsal to the female atrium. The female genital canal projects anteriorly from the anterior region of the female atrium.

Type species. *Myoplana veraluciae* Almeida & Carbayo, sp. n.

Etymology. *Myoplana* is composed of the Latin *myo* (*muscle*) and *plana* (*flat*), as a reference to the fact that the flatworm has complex muscular systems. The gender is female.

Myoplana veraluciae Almeida & Carbayo, sp. n.

Material examined. **Holotype** MNHNCL XXXX (Field code F4895). Monumento Nacional Contulmo, Chile, Coord. -38.014573, -73.18071, F. Carbayo, 12 December 2010. Transverse sections of the cephalic region on 10 slides; horizontal sections of the ovaries region on 7 slides; transverse sections of post-ovarian region on 7 slides; transverse sections of the pre-pharyngeal region on 6 slides; sagittal sections of the pharynx and copulatory apparatus on 28 slides.

Type locality. Monumento Nacional Contulmo, Purén, Malleco province, Región de la Araucanía, Chile.

Etymology. The specific name pays homage to Vera Lúcia Tenório Montes, teacher in the public school E. M. E. F. Henrique Souza Filho Henfil, and most influential in the humanistic formation of children.

Diagnosis. The pharynx is cylindrical; the inner muscle of the pharynx with four layers; male

atrium with four folds.

Description

External aspect. The preserved holotype is 25 mm in length and 4 mm in width. The body is elongated and flattened, with parallel margins (Fig. 24A). The anterior tip is slightly pointed and the posterior one rounded. The dorsal color is black brown (RAL 8022) with a median whitish stripe which is absent in the posteriormost region, representing 5% of the body length. The body margins are greyish. The ventral surface is whitish and provided, on each side of the body, with a paramedian greyish band with 25% of the body width (Fig. 24B). These ventral bands become sharper in the preserved holotype (Fig. 24C).

The eyes, monolobated and 38-50 µm in diameter, are placed inside halos (Fig. 24A, C). They are distributed in a marginal row contouring the entire body. The sensory pits are 22-25 µm deep; they contour the anterior region of the body and extend backwards ventro-marginally along a portion the body equivalent to 14%. The relative position of the mouth : body length is 60%; that of gonopore : body length is 76%.

Internal morphology.

Epidermis and its secretions. The creeping sole occupies the entire ventral surface. The epidermis is pierced by numerous rhabtitogen cells and by three types of cells producing erythrophil granules, xanthophil granules, and xanthophil amorphous secretion, respectively. Ventrally, the xanthophil secretion is much more abundant, whereas the erythrophil type is less abundant. The glandular margin is narrow (Fig. 25A), and mostly constituted by cells producing erythrophil granules. The main nervous system is a 200-220-µm-thick plate, representing approximately 16% of the body height (Fig. 25A). Ventrally, the peripheral nervous plexus is divided into two plexuses (Fig. 25C). These plexuses delimit externally and internally the sunken portion of the longitudinal cutaneous muscle (see below).

Cutaneous musculature. The cutaneous musculature comprises three strong layers, namely a subepithelial circular layer (7-10 µm thick), followed by a double layer (23-28 µm) with decussate fibers, and then a well developed innermost longitudinal layer (62-235 µm thick, dorsally and ventrally, respectively) (Fig. 25A-E). The ventral longitudinal layer is divided into two portions (Fig. 25C). One portion is external to the peripheral nerve plexus, and has 19% of the thickness of the layer. Another portion is internal to the plexus, i.e., sunken into the parenchyma and accounts for the remaining 81% of the thickness of the layer. Muscle fibers of

the external portion run at an angle to the longitudinal fibers of the sunken longitudinal fibers (Fig. 25D). The total cutaneous musculature thickness relative to body height is 28.4%. The musculature in the cephalic region maintains the organization observed in the pre-pharyngeal region.

Parenchymal musculature. Four parenchymal muscle layers are present: a strong dorsal layer of decussate fibers (35-43 µm thick. Fig. 25A-B), a supraintestinal (25-44 µm thick, Fig. 25A-B) and a subintestinal (43-72 µm thick, Fig. 25A, C) layers, both dense and composed of transverse fibers, and a fourth, loose transneural layer (Fig. 25A, C, F). This latter layer consists of diagonal muscle fibers approximately running in the transverse body plane and are situated beneath the subintestinal muscle layer and the cutaneous longitudinal muscle, i.e., they cross the ventral nerve plate (Fig. 25A, C, E-F). They are more abundant in the anterior half of the body. Dorso-ventral muscle fibers are abundant between the intestine branches.

Digestive system. The mouth is situated at a distance from the root of the pharynx equivalent to 27% of the length of the pharyngeal pouch (Fig. 26A). The pharyngeal pouch is very close to the prostatic vesicle. The esophagus : pharynx ratio is 28.7% (Fig. 26A). The pharynx is cylindrical, with the dorsal insertion shifted posteriorly the equivalent to 30% of the pharyngeal length. The epithelium of the distal portion of the pharynx is pierced by three types of cell glands producing erythrophil, xanthophil and cyanophil granules, respectively. The outer pharyngeal musculature consists of a subepithelial longitudinal muscle (15 µm thick), followed by a circular muscle (70 µm thick), and an innermost longitudinal one (25 µm thick, Fig. 26B). The inner pharyngeal musculature consists of four muscles, namely a subepithelial 42-50 µm thick longitudinal muscle, followed by a 22-35 µm thick decussate muscle partially mixed with a third 200 µm thick circular muscle, the latter followed by an innermost, 60 µm thick longitudinal muscle (Fig. 26B-C). Numerous radial muscle fibers run from the outer to inner pharyngeal epithelia (Fig. 26B).

Male reproductive system. The testes are rounded to pear-shaped. They measure 300-350 µm in diameter, and are distributed in 2-3 rows at each side of the body (Fig. 25A). They are dorsally located between the supraintestinal parenchymal muscle layer and the intestine. The anteriormost testes lay at a distance from the anterior tip of the body equivalent to 28% of the body length; the posteriormost ones the equivalent to 59% of body length, i.e, close to the pharyngeal root. The sperm ducts run dorsally to the ovovitelline ducts. Laterally to the anterior portion of the male atrium, these ducts bend dorsally and anteriorly to open laterally into the proximal portion of the prostatic vesicle (Fig. 26D). The sperm ducts are lined with a

squamous epithelium and are filled by spermatozoa.

The prostatic vesicle is pear-shaped and vertical (Fig. 26D-E). It is located anteriorly to the penis bulb and attached to it. The antero-dorsal region of the penis bulb is penetrated by the prostatic vesicle which continues with the ejaculatory duct (Figs. 26D-E). The prostatic vesicle is lined with a squamous-to-columnar epithelium. Ciliated epithelium was only discerned in the region converging with the ejaculatory duct. The epithelium of the prostatic vesicle is crossed by gland cells of two types, producing erythrophil and xanthophil granules, respectively. The proximal portion of the prostatic vesicle is surrounded by a 65 µm thick decussate muscle that gradually thins to a 12 µm thick layer of decussate fibers in its distal portion.

The ejaculatory duct runs sinuously ventro-posteriorly. The distal portion of this duct narrows to open into the anterior region of the male atrium (Fig. 26D-E). The duct is lined with a cuboidal, ciliated epithelium, and is pierced by gland cells producing cyanophil granules. This duct is surrounded by a one-fiber-thick circular muscle. An inconspicuous intra-penial penis papilla projects from the anterior atrial wall and is crossed by the ejaculatory duct (Figs. 26D-E). This papilla is constituted of radial muscle fibers and is lined with a columnar epithelium. This epithelium is underlain by a thin circular muscle.

The male atrium is long and provided with four transverse folds (Figs. 26D, 27A). The male atrium is lined with a columnar epithelium, which is pierced by three types of gland cells producing cyanophil, erythrophil and xanthophil granules, respectively. Additionally, gland cells producing amorphous xanthophil secretion pierce the distal region of the atrium. This epithelium is underlain by a layer (60-µm-thick) of circular and longitudinal intermingled muscles.

Female reproductive system. The ovaries are ovoid, and have a maximum diameter of 220 µm in the longitudinal body axis. The ovaries are located at a distance from the anterior tip of the body corresponding to 17.6% of the body length. The ovovitelline ducts emerge from the dorsal aspect of the ovaries and run ventrally onto the nerve plate. Anteriorly to the gonopore, these ducts ascend to join the common glandular duct, dorsally to the female atrium. This common duct runs postero-ventrally to communicate with the female genital canal (Figs. 26D, 27A-B). This canal, "C"-shaped in lateral view, is a wide projection of the posterior section of the female atrium. The female atrium is funnel-shaped. The lateral walls of the atrium present large folds projected in the lumen and continuing along the distal region of the male atrium. On each side of the gonopore canal is a longitudinal fold.

The female genital canal and the female atrium are lined with a columnar (57.5-µm high), non ciliated epithelium, which has gaps resembling vacuolar structures (Fig. 27A-B). The epithelium of the female atrium is pierced by two types of gland cells producing erythrophil and xanthophil granules, respectively. Underlying this epithelium is a circular muscle (30 µm thick) with longitudinal fibers interspersed. Towards the gonopore canal, this fibrilar organization turns gradually into two defined layers, namely a subepithelial circular muscle followed by a longitudinal muscle. The female atrium is wrapped by a weak muscle coat of longitudinal fibers (Fig. 27A-B).

Remarks

In the general aspect, *Myoplana veraluciae* distinguishes from *Myoplana joaopauloi* in that the latter species lacks a dorsal whitish median stripe. Internally, *M. veraluciae* differs from *M. joaopauloi* in the shape of the pharynx (cylindrical vs. bell-shaped in *M. joaopauloi*); the inner musculature of the pharynx (four muscle layers vs. three muscle layers in *M. joaopauloi*) and the number of folds of the male atrium (four folds vs. two folds in *M. joaopauloi*).

Fig. 24. *Myoplana veraluciae* Almeida & Carbayo, sp. n. A: Photograph of the live holotype in dorsal view. B: ventral view of the posterior half of the live holotype. C: Preserved holotype. Scale bars not available.

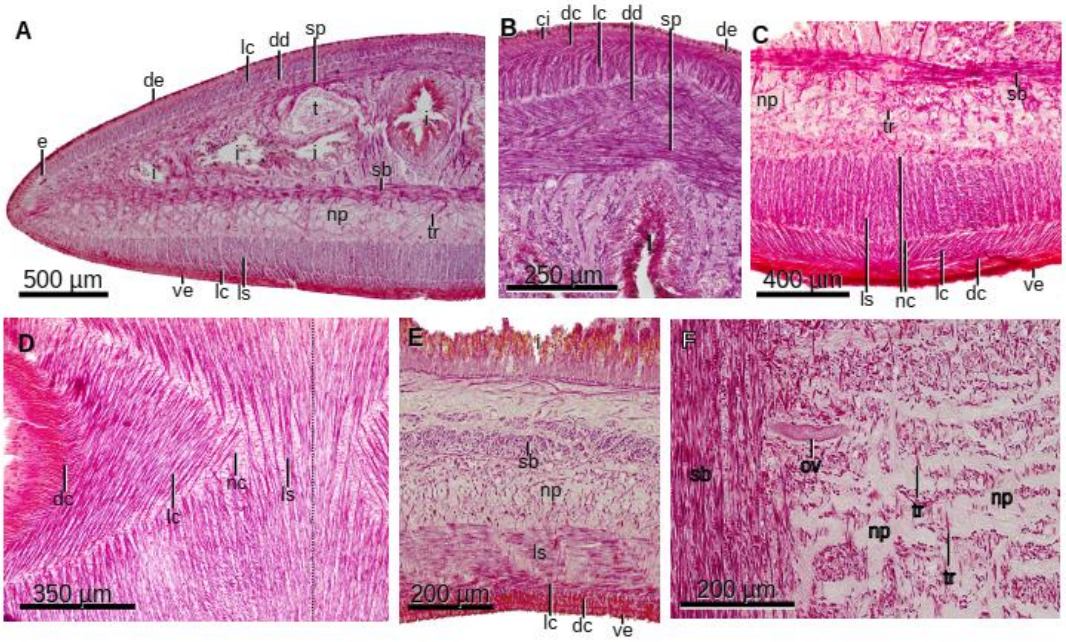

Fig. 25. *Myoplana veraluciae* Almeida & Carbayo, sp. n. Photomicrographs of histological sections. A: transverse section of the pre-pharyngeal region. B: horizontal section of the dorsal region of the body. C: transverse section of the ventral region in the pre-pharyngeal region. D: horizontal section of the ventral region; dotted line is in the longitudinal body axis. E: sagittal section of the ventral region in the pre-pharyngeal region. F: horizontal section of the ventral region.

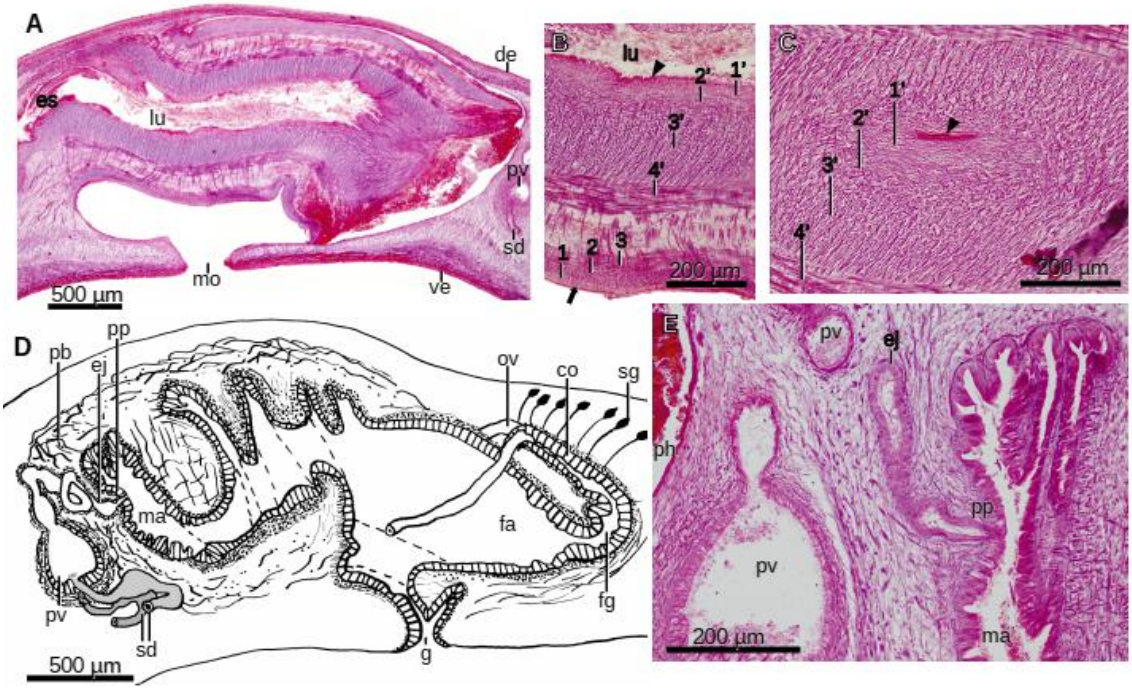

Fig. 26. *Myoplana veraluciae* Almeida & Carbayo, sp. n. Photomicrographs of sagittal sections. **A**: pharynx. **B**: Muscles underlying the outer (arrow) and inner (arrowhead) pharyngeal epithelia. **C**: tangentially sectioned musculature of underlying the inner pharyngeal epithelium (arrowhead). **D**: Diagrammatic reconstruction of the copulatory apparatus. **E**: prostatic vesicle and penis papilla. Numbers 1, 3, 1', and 4' point to longitudinal muscles; 2, and 3' point to circular muscles; 2' points to decussate muscle.

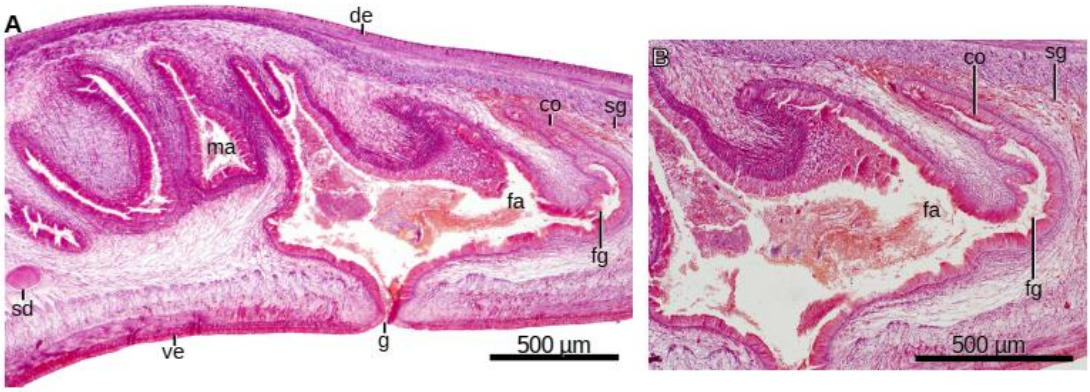

Fig. 27. *Myoplana veraluciae* Almeida & Carbayo, sp. n. Photomicrograph of sagittal sections. **A**: male and female atria. **B**: female atrium.

Myoplana joaopauloi Almeida & Carbayo, sp. n.

Material examined. Holotype F4875 (Museo Chile??). Parque Nacional Nahuelbuta, Región de Purén, Chile, Coord. -37.82756, -73.00972, F. Carbayo, Coll., 09 December 2010. Transverse sections of cephalic region on 13 slides; horizontal sections of the ovaries region on 27 slides; transverse sections of the anterior of the pre-pharyngeal region on 28 slides; sagittal sections of pharynx and copulatory apparatus on 32 slides.

Type locality. Parque Nacional Nahuelbuta, Región de la Araucanía, Chile.

Etymology. The specific name pays homage to João Paulo Gonzaga de Paula, teacher in the public school E. M. E. F. Henrique Souza Filho Henfil, and most influential in the humanistic formation of children.

Diagnosis. Species of *Myoplana* with a bell-shaped pharynx; the inner muscle of the pharynx with three layers; the male atrium with two folds.

Description.

External aspect. The fixed specimen presents 32 mm in length and 5.5 mm in width. The body is elongated and flattened, with the anterior end pointed and the posterior extremity rounded; the margins are nearly parallel (Fig. 28A). The dorsal color is black brown (RAL 8022) with the anterior extremity root brown (RAL 2152. Margins whitish. The ventral surface is whitish with brownish dots distributed close to the extremities of the body (Fig. 28B-C).

The eyes are monolobulate-shaped with 40 µm in diameter. They are distributed in a row contouring the cephalic region; since the initial 5 mm of the body length, they occupy 1-2 rows in the margins of the body until the tail, more spaced. There are halos evolved the eyes, situated in external limits of the dorsal dark pigmentation (Fig. 28C). Sensory pits are approximately 45 µm deep; they contour the anterior region of the body and extend backwards ventromarginally along a portion the body equivalent to 28%. Relative position mouth : body length, 75%. Relative position gonopore : body length, 87.5%.

Internal morphology.

Epidermis and its secretions. The creeping sole occupies the entire ventral surface. The dorsal and the ventral epidermis region of the body are abundantly pierced by rhabtitogen cells and by three types of cells producing erythrophil amorphous secretion, xanthophil amorphous secretion and erythrophil granules, respectively. Ventrally, granular erythrophil secretion is much more abundant, whereas xanthophil is less abundant than dorsally. Glandular margin narrow, constituted by two types of gland cells, producing erythrophil and xanthophil granules, respectively. Nervous system organized in a 220-µm-thick plate, representing approximately 13.5% of the body height (Fig. 29A-B).

Cutaneous musculature. The cutaneous musculature comprises three layers, namely a subepithelial circular layer (5 µm thick), followed by a double layer (20 µm) with diagonal fibers, and then a well developed innermost longitudinal layer (55-145 µm thick, dorsally and ventrally, respectively). 78% of thickness of the ventral layer is insunk into the parenchyma (Fig. 29A-B). The cutaneous musculature thickness relative to the body height at the medial length of the body is 15%.

Parenchymal musculature. Four parenchymal muscle layers present: a dorsal layer of decussate fibers, a supraintestinal and a subintestinal layers of transverse fibers, and a subneural layer of diagonal fibers, the latter extending into the ventral nerve plate. Medially, dorso-ventral muscle fibers are abundant between the intestine branches. In the body sides, the fibers are obliquely arranged (Fig. 29A-B).

Digestive system. The mouth is situated at a distance from the root of the pharynx equivalent to 33% of pharyngeal pouch length (Fig. 29C). The pharyngeal pouch is close to the prostatic vesicle. The esophagus is present, with esophagus : pharynx ratio representing 42%. The pharynx is bell-shaped (Fig. 29C). The epithelium of the distal portion of the pharynx is pierced by three types of gland cells producing xanthophil, erythrophil and cyanophil granules,

respectively. The outer pharyngeal musculature consisting of a subepithelial layer (20 µm thick) of longitudinal fibers, followed by a layer (67.5 µm thick) of circular fibers, and a layer (40 µm thick) of a longitudinal fibers. The inner pharynx musculature consists of a subepithelial 40-µm-thick layer of diagonal fibers, followed by a layer of 200 µm thick circular muscle, followed by a 72.5 µm thick longitudinal muscle.

Male reproductive system. The testes are approximately 330 µm in diameter, distributed into 2-3 rows at each side of the body. They are dorsally located between the supraintestinal parenchymal muscle layer and intestine (Fig. AB). The anteriormost testes are at a distance equivalent to 15.5% of the body length; the posteriormost testes are placed at a distance equivalent to 70% of the body length, i.e, lateral to the pharyngeal root.

The sperm ducts run posteriorly and lateral to the male atrium, they bend dorsally and anteriorly to open laterally into the proximal region of the prostatic vesicle (Fig. 30A-B). The sperm ducts are lined with squamous epithelium and are filled by spermatozoa mass, excepting at their distal section. The prostatic vesicle is extrabulbar and located anteriorly to the penis bulb. The anterior half of this vesicle is pear shaped and runs dorso-posteriorly. The posterior half of the prostatic vesicle is an intrabulbar canalicular portion that penetrates the penis bulb and runs sinuously ventro-posteriorly to open into the ejaculatory duct (Fig. 30A, C). The prostatic vesicle is lined with an epithelium varying from squamous to columnar; only the epithelium of the canalicular portion is ciliated. This epithelium is crossed by gland cells producing erythrophil, xanthophil, and cyanophil granules. The prostatic vesicle is surrounded by a single layer of decussate fibers in its extrabulbar portion and circular fibers in its intrabulbar portion, with 25-µm thick and 7.5-µm-thick, respectively. The ejaculatory duct crosses the medial region of the penis papilla and opens at its tip. This duct is lined with a cuboidal, ciliated epithelium, and is pierced by gland cells producing cyanophil granules; it is surrounded by a one-fiber-thick circular muscle. The penis papilla is short, horizontal and cylindrical. It occupies approximately the anterior 1/10th of the male atrium and is placed in the ventral portion of the penis bulb (Fig. 30A, C). The penis papilla is lined with a columnar epithelium, which is pierced by gland cells producing cyanophil and erythrophil fine granules. The epithelium is underlain by a 4-µm-thick muscle of spaced circular fibers.

The male atrium is long and folded. The anterior section of the male atrium is narrowed and houses the penis papilla. Its 'subdistal' portion is narrowed by two large folds, one dorsal and the other ventral. Distally, a dorso-lateral fold is continued with a fold of the female atrium (Fig. 30A); it is lined with a columnar epithelium which is rugged in some sections. This

epithelium is pierced by gland cells producing fine erythrophil granules; additionally, glands producing cyanophil granules pierce mid dorsal section of this atrium, just before the two large folds. This epithelium is underlain by a circular muscle (5 µm thick) followed by a longitudinal one (10 µm thick) in the anteriormost and posteriormost section of the male atrium; in the central section these two muscles are intermingled.

Female reproductive system. The ovaries are ovoid, with a maximum diameter of 280 µm. The ovaries are located at a distance from the anterior tip of the body corresponding to 8.5% of the body length. The ovovitelline ducts emerge from the dorsal portion of the ovaries and run ventrally above the nerve plate. Anteriorly to the gonopore, these ducts ascend dorso-posteriorly to join the common glandular duct. This common duct runs poterio-ventrally to communicate with the apparent female genital canal. This canal, "C"-shaped in lateral view is a projection from the posterior section of the female atrium. This atrium is a spacious funnel-shaped and presents a lateral fold continued from that of the male atrium (Fig. 30A). The female genital canal and female atrium are lined with a columnar (60-µm high), non ciliated epithelium, with the distal half portion of its cells is reddish stained. Underlying this epithelium there is a circular muscle (25-µm thick) with longitudinal fibers interspersed; posterior to the female genital canal, there is a ectal reinforcement of longitudinal fibers. Close to the gonopore canal, these two types of muscle fibers are separated into two layers, each 7 µm thick.

Fig. 28. *Myoplana joaopauloi* Almeida & Carbayo, sp. n. A: Photograph of the live holotype in dorsal view. B: dorsal and ventral view of the posterior region of the live holotype. C: convolute live holotype, showing halos in the anterior margin. Scale bars not available.

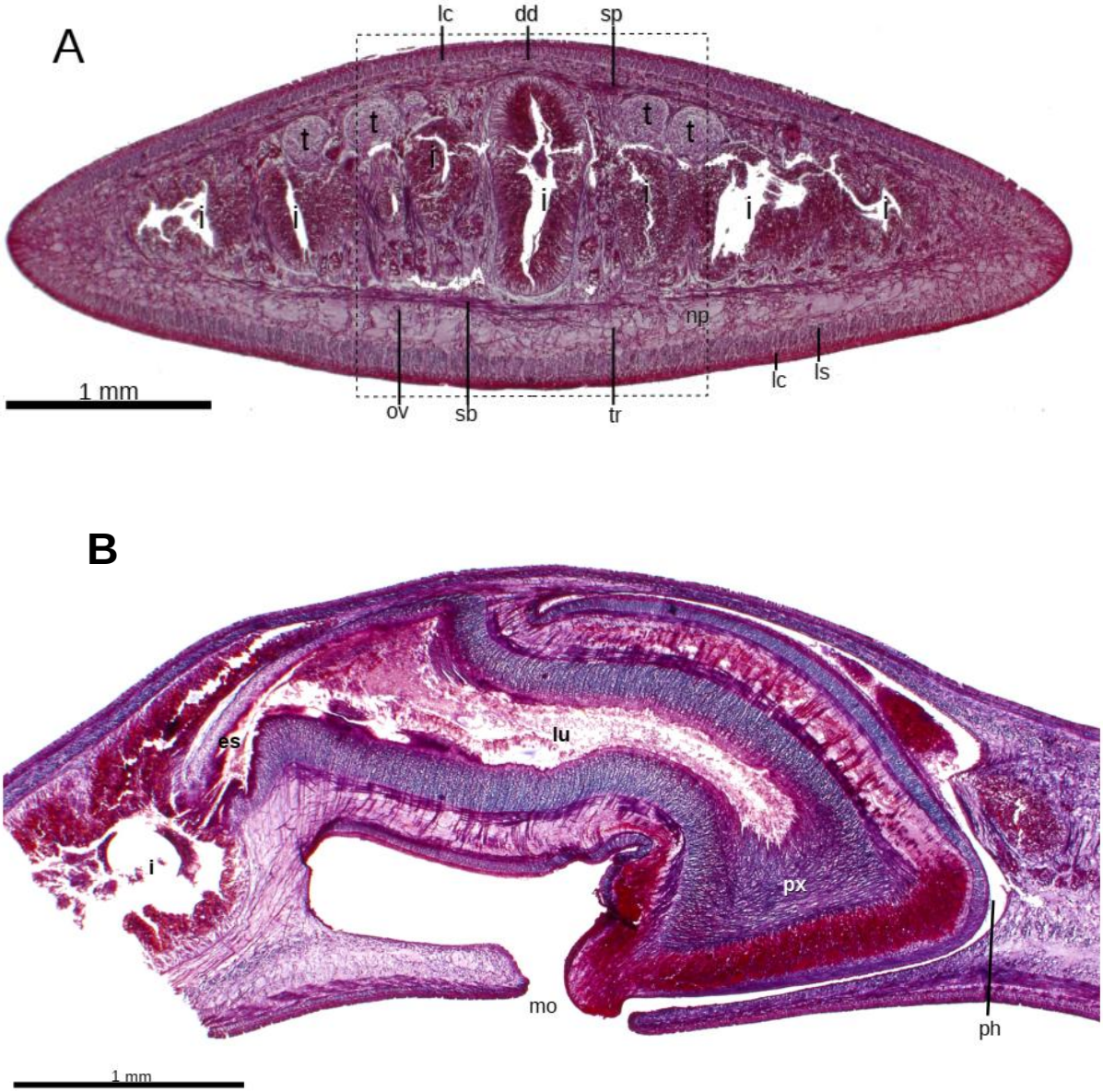

Fig. 29. *Myoplana joaopauloi* Almeida & Carbayo, sp. n. Photomicrographs of histological sections. A: transverse section of the pre-pharyngeal region. B: sagittal section of the pharynx.

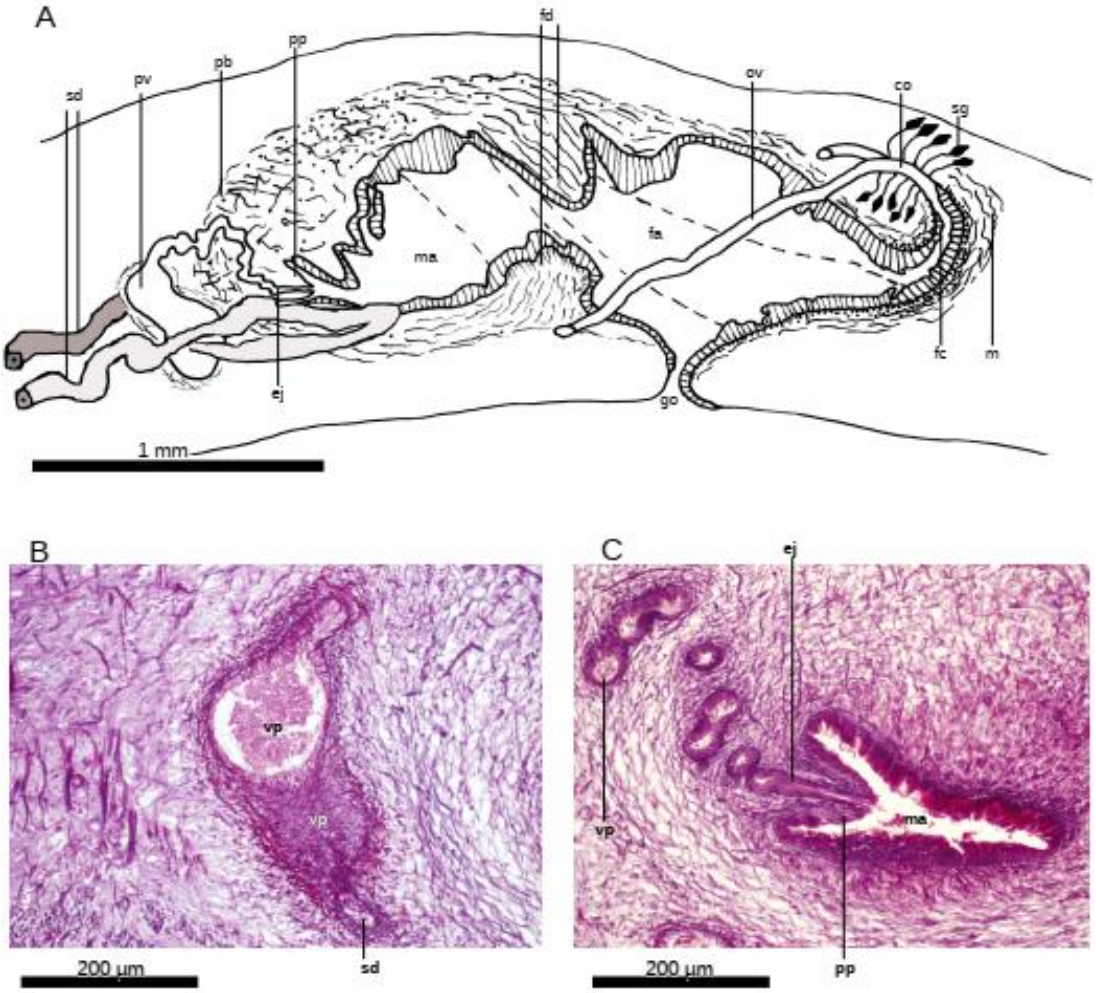

Fig. 30. *Myoplana joaopauloi* Almeida & Carbayo, sp. n. **A**: Diagrammatic reconstruction of the copulatory apparatus. **B**: prostatic vesicle receiving a sperm duct. **C**: penis papilla and ejaculatory duct.

Polycladini Carbayo & Almeida, trib. n.

Diagnosis. Geoplaninae with extraordinarily wide and flattened body, marginal eyes, a transverse subneural parenchymatic muscle and a longitudinal transneural parenchymatic muscle.

This tribe is monogeneric and the only one known species is *Polycladus gayi* Graff, 1899.

Sarcoplanini Almeida & Carbayo, trib. n.

Diagnosis. Geoplaninae with creeping sole with narrow-to-wide creeping sole;

eyes marginal; sensory depressions and a subneural parenchymatic decussate muscle; generally provided with a cephalic retractor muscle, multicellular glands associated with the prostatic vesicle and genital musculo-glandular organs.

This tribe includes the genera *Liana*, *Mapuplana*, *Pichidamas*, *Sarcoplana*, and *Wallmapuplana*.

Mapuplana **Grau, Almeida, Sluys & Carbayo, gen. n.**

Diagnosis. Sarcoplanini with flattened, slightly lanceolate body, ranging between 40-50 mm in length. Sensory depressions contour the cephalic region. The thickness of the cutaneous muscle relatively to the body height is 12.5-22%. The ventral longitudinal cutaneous muscle is partially sunken into the parenchyma. A cephalic retractor muscle present. The subneural parenchymal muscle is constituted of diagonal decussate fibers, and is intermingled with the sunken portion of the ventral longitudinal cutaneous muscle. Multicellular glands open into the prostatic vesicle. The penis papilla is small and conical. A blind canal opening sideways into the female atrium. The common glandular ovovitelline duct is postero-dorsal to the female atrium. The gonopore canal opens into the mid-ventral female atrium. The female genital canal projects posteriorly from the postero-dorsal region of the female atrium.

Type species. *Mapuplana guttulata* Almeida & Carbayo, sp. n.

Distribution: Southern Chile

Etymology: The generic epithet refers to the native Mapuche nation of Southern South America plus -*plana* meaning flat.

Mapuplana guttulata **Almeida & Carbayo sp. n.**

Material examined. Holotype F4906 (MNHNCL XXXX). Monumento Natural Contulmo, Región de La Araucanía, Central Chile, Coord. -38.014573, -73.18071, F. Carbayo, December, 12th 2010. Transverse sections of the cephalic and ovarian region on 31 slides; horizontal sections of a portion behind cephalic region on 25 slides; transverse sections of the pre-pharyngeal region on 17 slides; sagittal sections of the pharynx and copulatory apparatus on 62 slides.

Diagnosis. Species of *Mapuplana* with 50 mm in length; yellowish dorsum with a dark reticular

pattern. Proximal portion of the prostatic vesicle is dorsal. Distal portion of the prostatic vesicle helicoidal. Male atrium is twice as long as the female atrium. Entire length of the female common duct receives shell glands.

Type locality. Monumento Natural Contulmo, Southern Chile.

Etymology. The specific epithet derives from the Latin *guttula*, droplet, and alludes to the dots and marks adorning the dorsum.

Description.

External aspect. The live specimen measured approximately 50 mm in length and 5 mm in width, and after fixation 30.5 mm long, 6 mm wide, and 2.8 mm thick. The body is slightly lanceolate, with the dorsum convex and the ventral side slightly convex. The anterior tip is rounded and the posterior is obtuse (Fig. 31A-C). At rest, the dorsum is slightly rough. The ground color of the dorsum is pastel yellow (RAL 1034), and is ornate with scarce yellow orange (RAL 2000) dots and numerous red orange (RAL 2001) small marks forming a reticular pattern (Fig. 31A-B). A median stripe (1/9th of body width) passes from yellow orange in mid-body to red orange in the extremities of the body. This median stripe is divided into two thinner lines in some regions of the body. The ventral surface bears the dorsal color pattern, but the median band is lighter (Fig. 31C).

The eyes are monolobated, ranging between 45-82 µm in size. They are distributed in a single-to-double marginal row from the very anterior tip of the body to the posterior one. Sensory pits are absent. Instead, spots of cilia in slight epithelial depressions are located in the ventro-lateral region of the cephalic region (Fig. 32A). These depressions are rare and inconspicuous, and were not observed in the anteriormost body region.

The width of the creeping sole is difficult to measure in the pre-pharyngeal region because of the abundant erythrophil secretion adhered to the ventral surface. The creeping sole occupies 57% of the body width in the cephalic region. Mouth and gonopore located behind midbody. The relative position of the mouth : body length, is 60.6%; that of the gonopore : body length, 77.7%.

Epidermis and its secretions. The epidermis is pierced by three types of gland cells producing erythrophil, cyanophil and xanthophil granules, respectively. The erythrophil type is very abundant ventrally. Rhabditogen cells pierce the dorsal and marginal epidermis. All types of glands are scarcer in the cephalic region. A glandular margin is absent (Fig. 32B).

Cutaneous musculature. The cutaneous musculature comprises three layers, namely a subepithelial circular layer (5-7.5 µm thick in the pre-pharyngeal region), followed by a double layer (12.5-20 µm) with decussate fibers, and a strong, innermost longitudinal muscle (Fig. 32C-F). The longitudinal musculature is 80 µm thick, dorsally and 400 µm ventrally. The ventral portion of the longitudinal muscle is divided into a normal, 65 µm thick portion, and a sunken portion with 335 µm in thickness (Fig. 32D, F). The cutaneous musculature thickness relative to the body height in the pre-pharyngeal region corresponds to 12.5% in the mid-sagittal plane. This value increases to 20% in para-sagittal planes due to an increase in the thickness of this muscle (Fig. 32D, F).

Parenchymal musculature. There are four parenchymal muscle layers, namely a dorsal layer of decussate fibers (30 µm thick, 1.0% of the body height), a supraintestinal transverse muscle (70-80 µm), a subintestinal transverse muscle (65-83 µm), and fourth subneural layer with diagonal decussate fibers (90-120 µm); the decussate fibers and those of the insunk ventral cutaneous muscle layer are intermingled (Fig. 32D). Additionally, arched transverse muscle fibers run obliquely among the muscle fibers of these two decussate parenchymal and cutaneous muscles from one side of the ventral epidermis to the other side.

Musculature in cephalic region. The cutaneous and parenchymatic muscles are organized in another way in the cephalic region (Fig. 33). At 1 mm from the anterior tip of the body, the ventral sunken longitudinal muscle occupies 67% of the body width, whereas the normal portion represents 63% (Fig. 33A). Here, the MCI is 35%. The width of the longitudinal muscle relatively to the body width and the MCI diminish to 58% and 33.9%, respectively, at 460 µm from the tip of the body (Fig. 33C-D). Here, the arched transverse muscle fibers are relatively more abundant than in the pre-pharyngeal region, whereas the subneural muscle fibers are restricted to the mid-body. In this region the sunken fibers are oriented obliquely towards the

dorsal and body sides, but the path of these fibers were not seen beyond the central nerve system (Fig. 33C-F). At 100 µm from the tip, only the normal ventral muscle remains.

Digestive system. In the specimen with the pharynx protracted out of the body, the mouth is situated in the posterior end of the pharyngeal pouch. The esophagus is 0.5 mm long. The pharynx is cylindrical (Fig. 34A). Pharyngeal pouch musculature is composed of subepithelial longitudinal muscle fibers, followed by circular muscle fibers. The outer pharyngeal musculature consists of a subepithelial longitudinal muscle layer (8 µm thick), followed by a layer of circular musculature (20-25 µm thick). Underneath this muscle layer is a 200 µm thick layer of longitudinal and circular muscle fibers extending anteriorly out of the pharynx. The inner pharyngeal musculature consists of a single subepithelial layer (120-225 µm thick of circular and longitudinal mixed fibers (Fig. 34B). Radial muscle fibers present. Granular erythrophil and xanthophil secretions run through the parenchyma of the pharynx and open through the tip of the pharynx.

Male reproductive system. The testes are globular in shape and measure 210-320 µm in diameter, and are distributed in 2 rows at each side of the body between the supra-intestinal transversal parenchymatic muscle layer and the intestinal diverticula (Fig. 32C). The anteriormost testes lay at a distance from the anterior tip of the body equivalent to 22% of the body length; the posteriormost ones, the equivalent to 50% of body length, i.e, they are anterior to the pharyngeal root.

The sperm ducts run immediately above the sub-intestinal parechymal musculature and slightly external to the oviducts. Posterior to the pharynx, these ducts are sinuous, dilated and full of spermatozoa. The distal portion of these ducts narrows run towards the dorsum (Figs. 34C, 35A). The sperm ducts communicate with the respective ramified and tubular gland of the prostatic vesicle through a transitional, epitheliated canal which is surrounded by 10 a µm thick circular muscle. These two glands consist of numerous ramified ducts which collect erythrophil and xanthophil granular secretions produced by gland cells located around them. The branches are 15-37 µm in diameter and are lined with a ciliated epithelium (Fig. 35C-D). The tubulous glands join before opening into the very proximal portion of the prostatic vesicle

(Fig. 34C).

The prostatic vesicle is a very long, unpaired duct, with 35-50 µm in diameter proximally, and 10-18 µm distally (Fig. 34C, 35B-C). The prostatic vesicle is extrabulbar; its anterior most portion is dorsally located. Roughly the proximal ⅔ portion of this vesicle exhibits large loops, whereas the loops are smaller in its ⅓ distal, ascending portion. The prostatic vesicle penetrates the antero-dorsal region of the penis bulb to open into the ejaculatory duct. This prostatic vesicle is lined with a cuboidal, ciliated epithelium which is surrounded by a 50-75 µm thick circular muscle. Additionally, the distal portion is embedded in a loose muscle attached to the anterior face of the penis bulb. On its way through the penis papilla, the ejaculatory duct doubles its diameter to 60 µm before narrowing to open at the tip of the papilla through a pit with 5 µm in diameter. The ejaculatory duct is lined with a ciliated epithelium, which is underlain by a 30 µm thick circular muscle.

The small and conical penis papilla is as long as 9% of the male atrium length (Fig. 35E). This papilla projects from the antero-dorsal portion of the male atrium and points postero-ventrally. This papilla is lined with an infranucleated epithelium, which is pierced by two types of gland cells producing xanthophil and cyanophil granules, respectively. The epithelium is underlain by 17-20 µm thick circular muscle, and followed by a 15-33 µm thick longitudinal one.

The male atrium is long and folded (Figs. 34C, 35A-B). Two large, transverse flap-shaped folds occupy the anterior half of the male atrium. One flap is ventral to the penis papilla, another posterior to it. The distal half of the male atrium is occupied by two oblique folds, the proximal one being narrower than the distal one. The male atrium is lined with a low epithelium. The basal lamina underlying the converging epithelium of the flaps and the dorsal converging epithelium of the oblique folds are thickened to 5 µm. The entire atrial epithelium of the male atrium is crossed by gland cells producing erythrophil granules, and is underlain by a 18-35-µm-thick circular muscle layer. Transverse and longitudinal muscle fibers are abundant in the flaps and oblique folds. Additionally, the oblique, narrow fold is reinforced with a 75-85 µm thick muscle of circular and longitudinal fibers. Between the oblique folds is a strongly

xanthophil clump, 250 x 350 µm in size attached to the wall. The atrial surface where the clump is attached lacks epithelium (Figs. 35B, 36A).

Female reproductive system. The ovaries are roughly round, and measure 250 µm in diameter. They lay above the ventral nerve plate, and are at a distance from the anterior tip of the body corresponding to 23% of the body length, and are located underneath the transversal sub-intestinal parenchymal muscle layer. The ovovitelline ducts emerge from the dorsal aspect of the ovaries and subsequently run ventrally above the nerve plate. Posteriorly to the gonopore, these ducts ascend to open into the common glandular duct behind the female atrium. This duct is 120 µm wide and runs antero-dorsally to communicate with the female genital canal (Fig. 34C). The converging portion of this canal with the dorso-posterior section of the female atrium is narrow (Figs. 34C, 36B). The female genital canal is lined with a columnar epithelium, the subapical portion of which contains xanthophil granules.

The gonopore canal opens in the mid-region of the female atrium. The female atrium is spacious and more or less ovoid (Figs. 34C, 36B-C). The length of this atrium is half of that of the male atrium. The female atrium is lined with a columnar (100 µm high) epithelium, the subapical portion of it is xanthophil. This epithelium is surrounded by a 25-µm thick circular muscle, ectally to which is a loose muscle coat of longitudinal fibers. The surface of the epithelium is irregular and presents some recesses sunken into the surrounding parenchyma (Fig. 36D). A blind canal with 140 µm in width and 520 µm in length opens into the antero-lateral region of the female atrium (Figs. 34C, 36E-F). This canal is lined with a cuboidal epithelium, which is pierced by two types of gland cells producing erythrophil and cyanophil granules, respectively. This epithelium is surrounded by a 20-µm thick circular musculature. The female atrium houses a spermatophore of roughly 550 x 300 µm in size. This is composed of a strongly xanthophil secretion -similar to the clump in the male atrium-, and is amorphous centrally and fibrous in its periphery. Small areas of the innermost region of the spermatophore contain sperm.

The common muscular coat is constituted of longitudinal and oblique muscle fibers, and surrounds the male atrium, the female atrium and the female genital canal.

Remarks

The most outstanding feature of this species is the tubulous nature of the ramified glands associated with the prostatic vesicle. This type of gland is only present in *Pichidamas* and *Wallmapuplana*. However, only *Pichidamas* and *Mapuplana* present a cephalic retractor muscle. Nonetheless, this muscle differs in the details since in *Pichidamas* the retractor muscle is less developed relative to the body height and the muscle fibers and mainly concentrated in the sagittal plane, whereas in *Mapuplana*, the retractor is very strong and relatively wider. There are other differences distinguishing *Mapuplana* from *Pichidamas*, namely a subneural transverse muscle is absent in *Mapuplana* (vs. present in *Pichidamas*), part of the ventral longitudinal cutaneous muscle is sunken into the parenchyma (vs. not sunken), the copulatory apparatus is devoid of adenodactyl (vs. provided with), and the female atrium is provided with a blind canal (vs. lacking).

Fig. 31. *Mapuplana guttulata* Almeida & Carbayo, sp. n. Photographs of the live holotype in dorsal (A-B) and ventral (C) views. Scale bars not available.

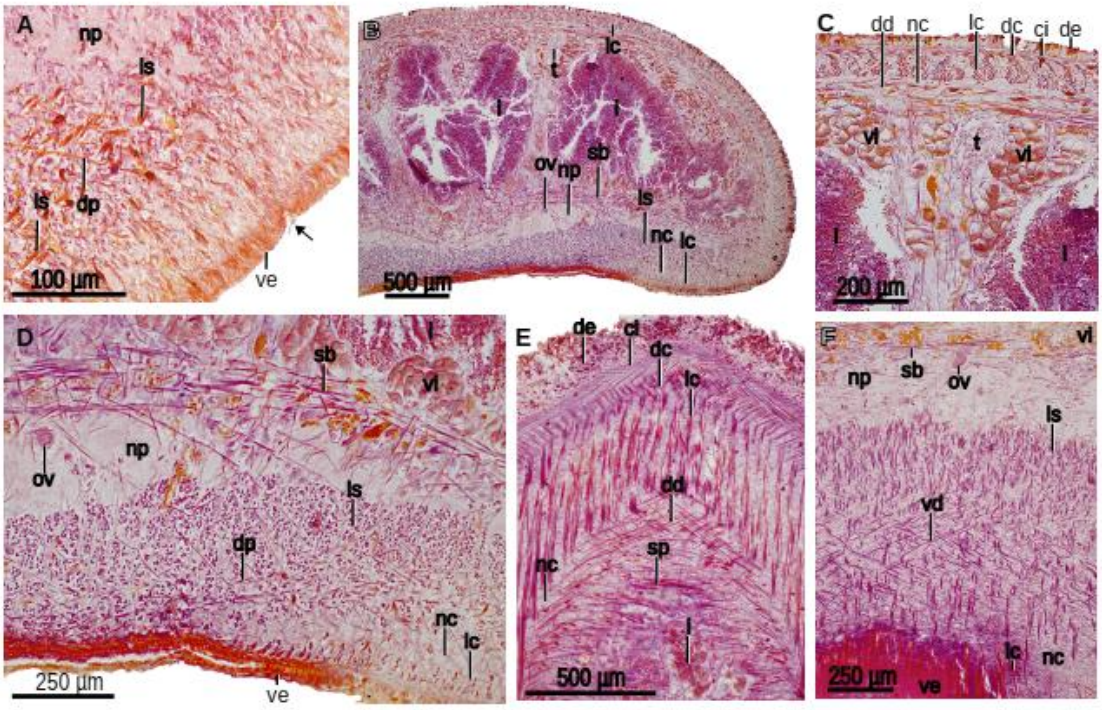

Fig. 32. *Mapuplana guttulata* Almeida & Carbayo, sp. n. Photomicrographs of histological sections. A: transverse section of the cephalic region showing the epithelial depression (arrow). B-D: transverse of the pre-pharyngeal region. E-F: horizontal sections showing cutaneous and parenchymal muscles.

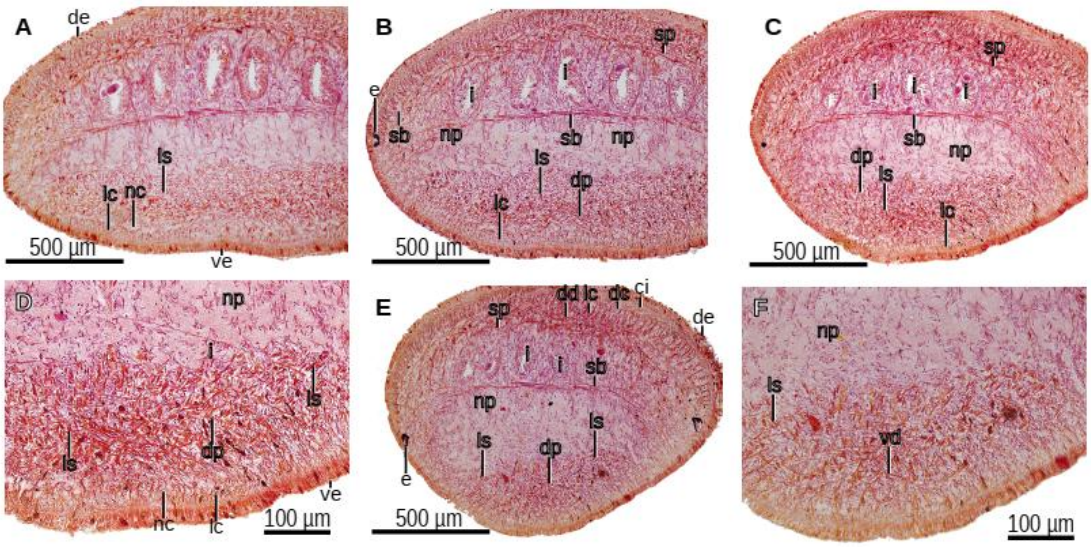

Fig. 33. *Mapuplana guttulata* Almeida & Carbayo, sp. n. Photomicrographs of transverse sections of the anterior region of the body, at 1000 (A), 900 (B), 500 (C-D), and 400 µm (E-F) from the anterior extremity, respectively.

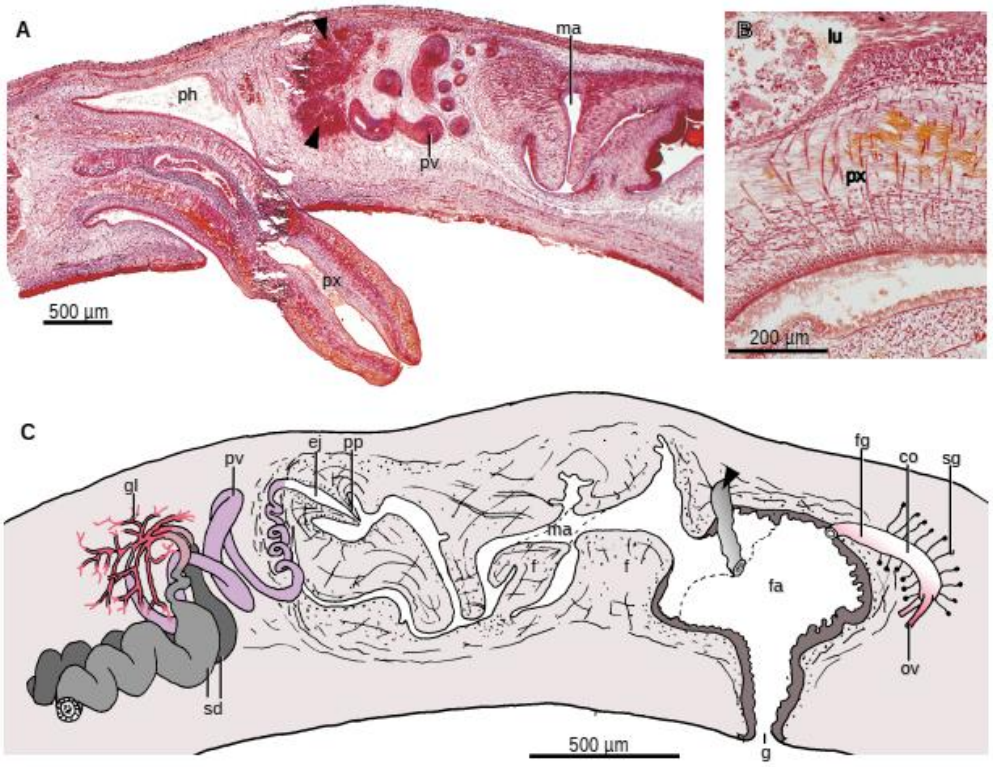

Fig. 34. *Mapuplana guttulata* Almeida & Carbayo, sp. n. Photomicrograph of a sagittal section of the pharynx (A) and detail of the outer and inner pharyngeal musculature of the paratype (B). Diagrammatic reconstruction of the copulatory apparatus.

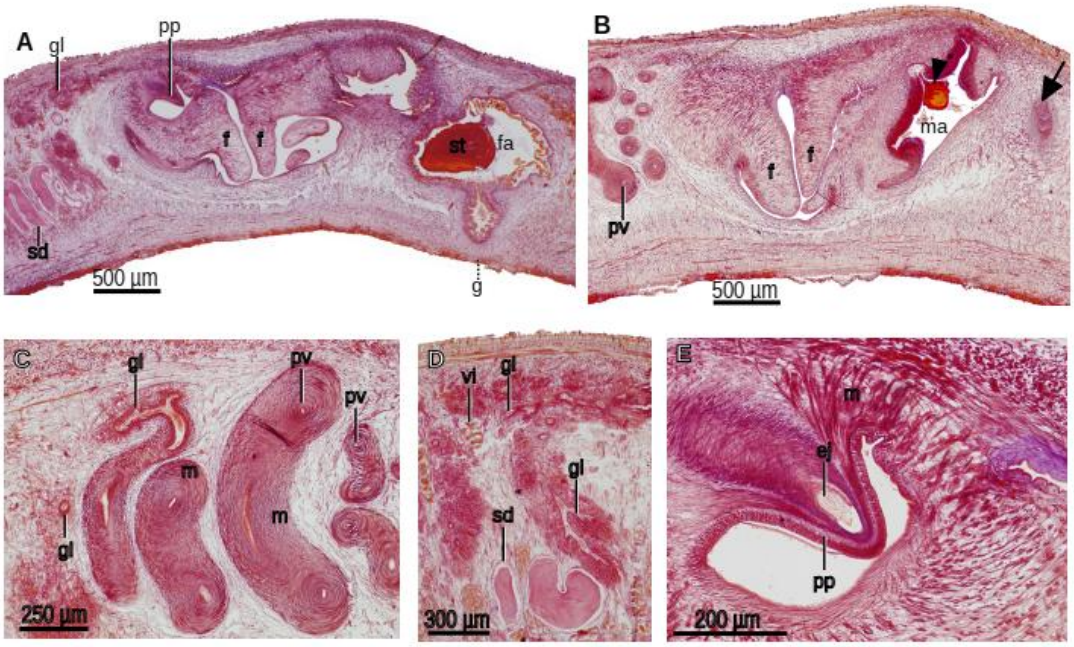

Fig. 35. Mapuplana guttulata Almeida & Carbayo, sp. n. Photomicrographs of sagittal sections of the copulatory apparatus (A), male atrium (B), prostatic vesicle (C), tubulous gland of the prostatic vesicle (D), and penis papilla (E). Note the xanthophil clump in the male atrium (arrowhead) and the blind canal opening into the female atrium (arrow, in B).

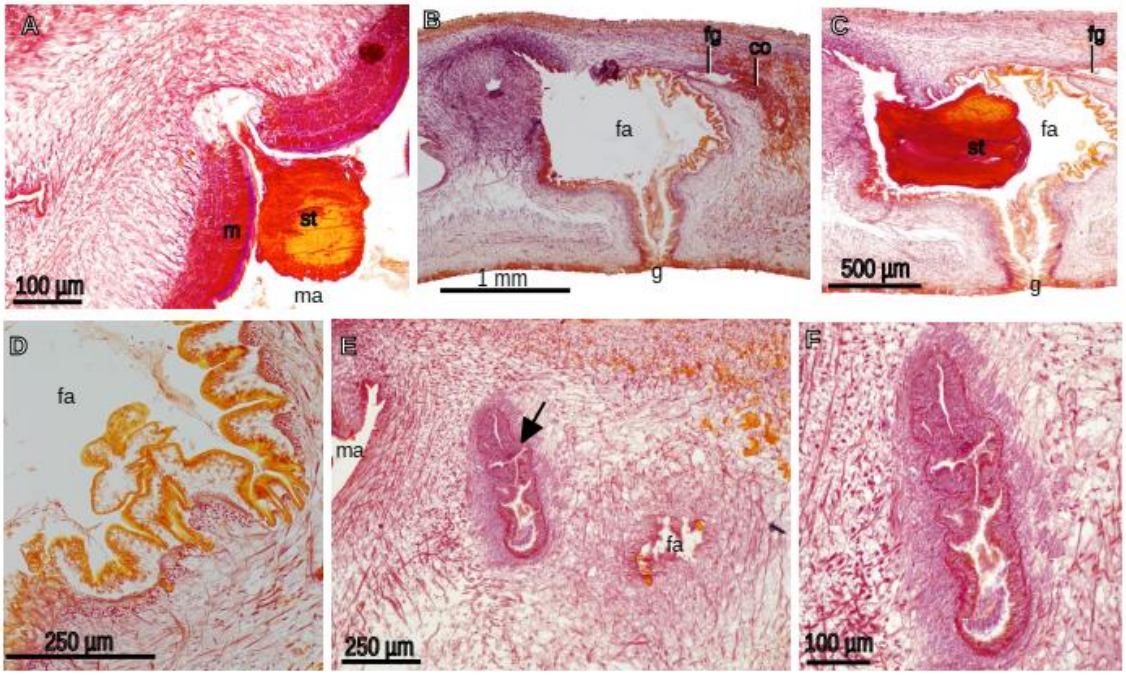

Fig. 36. *Mapuplana guttulata* Almeida & Carbayo, sp. n. Photomicrographs of sagittal sections of the male atrium and the xanthophil clump (A), the female atrium (B-C, spermatophore lost in B), epithelium of the female atrium (D), and blind canal opening into the female atrium (E-F).

***Pichidamas gnythos* Almeida & Carbayo, sp. n.**

Material examined. Both specimens were found in Reserva Nacional Los Ruiles, Cauquenes, Chile, Coord. -35.8335, -72.5102, F. Carbayo, October, 7th 2010. **Holotype MNHNCL PLAT-??** (Field code F4840). Horizontal sections of cephalic region on 24 slides; horizontal sections of a body portion immediately behind on 9 slides; transverse sections of pre-pharyngeal region on 9 slides; sagittal sections of the pharynx and copulatory apparatus on 30 slides. **Paratype** MZUSP PL XXXX (Field code F4847). Transverse sections of cephalic region on 3 slides; horizontal sections of a body portion immediately behind on 3 slides; transverse sections of pre-pharyngeal region on 4 slides; sagittal sections of pharynx and copulatory apparatus on 6 slides.

Type locality. Reserva Nacional Los Ruiles, Cauquenes, Región del Maule, Chile.

Etymology. The epithet *gnythos* is a Greek noun meaning *pit, hollow*, alluding to the fact that the adenodactyl is hollowed.

Diagnosis. Species of *Pichidamas* with part of the bundles of the ventral cutaneous muscle bipartite. The mouth is located in the end of the pharyngeal pouch. The pharyngeal pouch is contiguous to the prostatic vesicle. The penis papilla is postero-dorsally oriented. The posterior

region of the male atrium possesses a large dorso-lateral fold, the apical portion which is flap-shaped and placed in the anterior section of the male atrium. The common ovovitelline duct is relatively short.

Description

External aspect. The live specimens measured approximately 20-30 mm in length and 2-3 mm in width. The body exhibits more or less parallel body margins throughout most of its length. The anterior extremity is rounded, and the posterior tip is pointed (Fig. 37A-C). The dorsal and side are convex, the body margins are rounded. The size of the preserved specimens ranged between 13.5-28 mm long, 2.5-3 mm wide, and 1-2 mm thick.

The dorsal background color is olive yellow (RAL 1020), covered with chocolate brown (RAL 8017) pigment, excepting for oval patches (Fig. 37A-C). A tenuous median darker band (1/7 of body width) is more apparent over the pharynx and copulatory apparatus, and in a submarginal line (1/8 on each side of the body), external to it is a rind of olive yellow color. The olive yellowish body margins are darker along a line rimming the anterior region of the body (Fig. 37D). The ventral side is also olive yellowish, darker in both extremities of the body.

The eyes vary in size between 25 µm and 75 µm. They are distributed in a single-to-double irregular, marginal row from the very anterior tip of the body to the posterior one (Fig. 37D). The eyes are packed in the cephalic region and scattered towards the posterior tip. Sensory pits are absent. Instead, spots of cilia in very slight epithelial depressions are located in the ventro-lateral region of the cephalic region. The creeping sole occupies 51-54% of the body width. The relative position of the mouth : body length, is 48-57%; that of the gonopore : body length, 67-73%.

Internal Morphology

Epidermis and its secretions. The epidermis is 30 µm thick in the anterior tip of the body, and 17-25 µm in the pre-pharyngeal region. Rhabditogen cells and two types of gland cells discharge erythrophil and cyanophil granules, respectively, through the entire body surface. Rhabditogen cells and erythrophil gland cells are more abundant in the dorsal epithelium of the cephalic region. There is no glandular margin.

Cutaneous musculature. The cutaneous musculature comprises three layers, namely a subepithelial, one-fiber-thick circular muscle, a 15-µm-thick double layer with decussate fibers,

and an innermost longitudinal muscle of dense muscle bundles. The latter muscle is 45-65 µm thick dorsally (Fig. 38A-D), and 130-185 µm ventrally (Fig. 38A, C). To the inner side of the creeping sole, bundles of this muscle tend to be bipartite so that those immediately beneath the epithelium of the creeping sole are somewhat separate from the remaining fibers (Fig. 38C). The space between these two portions is occupied by nervous tissue. The cutaneous musculature thickness relative to body height at the pre-pharyngeal region ranges between 16.3-18.1%.

Parenchymal musculature. Five parenchymal muscle layers are present throughout the body: a dorsal layer of decussate fibers (10-15 µm thick), located to the inside of the peripheral nervous plexus; a dense supra-intestinal layer of transverse fibers (25-32 µm); a dense sub-intestinal layer of transverse fibers (35-40 µm); a weak subneural layer (10 µm thick) of thin transverse fibers; and a weak ventral layer (5 µm thick) of thin decussate fibers, located to the inside of the peripheral nervous plexus underlying the ventral body wall (Fig. 38A-E). A small number of fibers of this muscle layer pierce the peripheral nervous plexus.

Musculature in cephalic region. The muscular organization changes in the anterior region of the body with respect to that of the pre-pharyngeal region. All the cutaneous muscles are relatively thinner at a distance equivalent to 10% of the body length, excepting for the longitudinal, ventral muscle, which is relatively thick under the creeping sole. At 3% of the body length (or one millimeter), the muscle fibers of the ventral longitudinal muscle are gathered medially, giving rise to the cephalic retractor muscle. In this region, the retractor muscle is lens-shaped (Fig. 39A), and the relative thickness of the cutaneous musculature reaches 23.2% of the body height. At 300 µm from the tip, fibers of the retractor muscle are concentrated even more medially (Fig. 39B-C). From this point towards the anterior tip of the body, the muscle fibers of the retractor detach from it and run obliquely towards the dorsum and body margins (Fig. 39D). Here, fibers of the parenchymatic subneural layer seem to run parallel to fibers detached from the retractor muscle. Additionally, parenchymatic dorso-ventral muscle fibers intersect those of the retractor muscle.

Digestive system. The mouth is located in the posteriormost portion of the pharyngeal pouch (Fig. 40A). The relatively short pharynx is cylindrical, and placed horizontally. The esophagus is 100 µm long. The outer pharyngeal musculature (Fig. 40B) consists of a one-fiber-thick longitudinal muscle followed by a circular muscle (10 µm). The inner pharyngeal musculature (Fig. 40C) consists of a 100-150 µm thick circular muscle with longitudinal fibers intermingled.

Male reproductive system. The testes are pear-shaped, and measure about 150 µm in height. They are located dorsally, beneath the transverse supraintestinal parenchymal muscle, and between the intestinal branches (Fig. 39A). The anteriormost testes are placed at a distance equivalent to approximately 14.8-18.9% of body length; the posteriormost testes at a distance equivalent to 46.0-52.5% of body length and 0.2-0.3 mm before the pharyngeal root.

The copulatory apparatus occupies 80-82% of the body height, and is 3.0-3.6 times longer than its own height. Sperm ducts run immediately above the subintestinal parenchymal muscle and dorsal to the ovovitelline ducts. They contain spermatozoa. Laterally to the distal section of pharyngeal pouch, the sperm ducts ascend to the sagittal plane in a spiral course before bending downwards to open into the proximal section of the prostatic vesicle, and very close to each other (Fig. 41A). The prostatic vesicle is extrabulbar (Fig. 41A-B). This vesicle is tubular, very long, and repeatedly recurved. The vesicle is lined with a squamous-to-cuboidal, ciliated epithelium, and is surrounded by a very dense and 70 µm-thick circular muscle. The prostatic vesicle and its musculature are surrounded by a mass of scattered thin fibers of collagen. Very close to the communicating point of the sperm ducts to the prostatic vesicle, two-three multi-branched canals open into the prostatic vesicle (Figs. 41-42). These canals are lined with a ciliated epithelium and receive openings of numerous gland cells producing erythrophil granules with 2.5 µm in diameter. The distal portion of the prostatic vesicle communicates with the ejaculatory duct at the point of penetrating the ventro-anterior section of the penis bulb. The ejaculatory duct is a wide canal, 3/4th if its length is located in the penis papilla (Fig. 41A). This duct is lined with a columnar, ciliated epithelium, the free surface of it is strongly undulate. This epithelium is underlain by a 12 µm thick circular muscle. Fibers of this muscle immediately underlying the epithelium are intermingled with bodies of gland cells producing fine erythrophil granules. These gland cells discharge their contents into the ejaculatory duct. The conical penis papilla is well-defined and small. This papilla projects obliquely from the ventro-anterior wall of the male atrium and is lined with a squamous epithelium constituted of cells, bodies of which are seemingly sunken. The epithelium of the papilla is underlain by a circular muscle (15 µm thick), followed by a longitudinal muscle which occupies most of the stroma of the papilla. The penis bulb comprises a moderate number of muscle fibers, part of which penetrates the basis of the penis papilla.

The male atrium is a long cavity divided into two sections (Figs. 41-42). The anterior section is oval and corresponds approximately to a third of the total atrial length. The posterior section is long and narrower and possesses three structures, namely a large dorso-lateral fold (Fig. 41),

an adenodactyl (Fig. 43B-D) behind this fold, and a transverse annular fold, or sphincter (Figs. 41, 43B, C, E). The apical portion of the large fold is flap-shaped and is placed in the anterior section of the male atrium (Figs. 41, 42C).

The male atrium is lined with a very low (1 µm high) squamous, non-ciliated epithelium, excepting that of the flap which is irregularly ciliated. The epithelium of the male atrium is underlain by a circular muscle (25 µm thick), followed by a longitudinal muscle (50-90 µm). Around the base of the penis papilla, these two muscles are penetrated by radial bundled muscles originating in the penis bulb (Fig. 43A). The flapped portion of the atrial fold also possesses numerous dorso-ventral muscle fibers.

Two types of gland cells discharge weakly cyanophil granules and erythrophil granules, respectively, into the male atrium. The epithelium of the flap receives three types of gland cells producing abundant erythrophil granules, erythrophil, amorphous secretion, and cyanophil granules, respectively. All these types of gland cells are progressively more abundant towards the tip of the flap, especially those producing erythrophil granules.

The adenodactyl (Figs. 43B-D, 44A) projects ventro-anteriorly from the dorsal or dorso-lateral wall of the male atrium. This adenodactyl is a 1-mm-long conical or finger-like structure, lined with a squamous infranucleated epithelium. This epithelium is underlain by a 5µm thick longitudinal muscle, followed by a 40 µm thick circular muscle; the longitudinal muscle is only present in the basal, innermost portion of the adenodactyl. The tip of adenodactyl presents an opening leading to a non epitheliated canal as long as 2/3 of the length of the adenodactyl. This canal is surrounded by gland cells producing fine cyanophil granules. The stroma of the adenodactyl presents circular muscle fibers, and scarce longitudinal ones.

As spermatophore is attached to the fold of the distal portion of the male atrium of the holotype (Fig. 43B-C). The spermatophore is irregular in shape and measures 600 x 200 µm. It consists of a main strongly erythrophil mass of erythrophil secretion, in some parts with the aspect of strands, scarce cyanophil granules, and small quantity of sperm attached to indentations located in the surface oriented to the gonopore canal. The lining epithelium of the fold is absent where the spermatophore is attached, and two types of gland cells producing amorphous erythrophil secretion and cyanophil granules, respectively, are in the stroma of the fold. Another spermatophore, 120 x 40 µm in size, is in the gonopore canal of the paratype (Figs. 43E, 44B). This spermatophore has no sperm.

Female reproductive system. The ovaries are rounded, 150 µm in diameter, and lay at a

distance from the anterior tip equivalent to 20% of body length. The ovovitelline ducts emerge from the dorso-lateral portion of the ovaries and run ventrally above the nerve plate. Behind the female atrium and the female genital canal, they bend dorsally and to the sagittal plane to enter the common ovovitelline duct (Fig. 41A). This duct runs dorso-anteriorly and communicates with the female genital canal. The female genital canal is dilated and long, and projects backwards from the posterior wall of the female atrium. This canal is located outside of the common muscle coat (Fig. 43E). The ventro-anterior region of the female atrium converging with the gonopore canal is bulky (Figs. 41, 43E, 44B).

The common ovovitelline duct is lined with a cuboidal, ciliated epithelium and is surrounded by a 7 µm thick circular muscle.

The female genital canal is lined with a cuboidal-to-columnar or squamous epithelium. This epithelium is pierced by two types of gland cells producing erythrophil and cyanophil, fine granules, respectively, the latter being very abundant. The epithelium is underlain by a 10 µm thick layer of thin circular fibers (<0.5 µm), followed by a loose layer of longitudinal fibers. No shell gland cells were found. The female atrium is approximately rounded, and is provided with a ventral bulk which continues on either side of the body with gonopore canal. The female atrium is lined with a cuboidal epithelium, and is pierced by gland cells producing fine erythrophil granules. The bulk is lined with a columnar, irregularly ciliated epithelium. This epithelium has poor affinity for the stain. The lining epithelium of the female atrium is underlain by a 2 µm thick longitudinal muscle, followed by a 12 µm thick circular one.

Remarks

Pichidamas gnythos Almeida & Carbayo, sp. n. matches all the diagnostic features of the genus, excepting for the shape of the posterior tip of the body. With regard to this trait, the diagnosis of the genus reads "posterior end rounded", whereas the posterior tip of the new species is pointed. One could argue that the type species of the genus is only known from a preserved specimen and that this extremity of the body could be pointed in the live specimen, but the two type specimens of *P. gnythos* sp. n. do present this extremity pointed in the live and preserved animals as well. So variation in this character within the genus should be accepted.

On other hand, *P. gnythos* Almeida & Carbayo, sp. n. presents a very rare feature, namely

multi-cellular glands. As shown above, these glands produce secretions discharged into the prostatic vesicle. They were not reported for *P. piru.* However, *P. piru* does have this type of glands as revealed from additional photomicrographs taken by the authors (FC) before deposition in the Museum für Naturkunde Berlin, Germany.

According to these observations, an emendation of the genus is proposed as follows: Geoplaninae with small to medium-sized body, sub-cylindrical, slender with nearly parallel margins, anterior extremity rounded. Eyes monolobulated distributed along the body margins. Sensory pits absent. Cephalic retractor muscle present, derived from ventral longitudinal cutaneous musculature. Five parenchymatic muscle layers, ventralmost layer of decussate fibres and located to the inside of the peripheral nervous plexus. Prostatic vesicle extrabulbar and receiving secretions from multicellular glands. Distal portion of male atrium with an adenodactyl. Penis eversible. Ovovitelline ducts ventral, opening to the common ovovitelline duct from posteroventral.

The general body size and color pattern of *Pichidamas gnythos* sp. n. resembles that of *P. piru*, the latter known from a preserved specimen only. However, the internal morphology of both species differ in the following aspects: In *P. gnythos* sp. n., (a) the posterior tip of the body is pointed (*vs*. rounded in *P. piru*); (b) part of the bundles of the ventral cutaneous muscle are bipartite (*vs*. non bipartite in *P. piru*); (c) the mouth is located in the end of the pharyngeal pouch (*vs*. the equivalent to 66% of the length of the pouch); (d) the pharyngeal pouch is contiguous to the prostatic vesicle (*vs.* separated from it); (e) the penis papilla is more developed and postero-dorsally oriented (*vs*. posteriorly); (f) the anterior region of the male atrium lacks a large tongue-like fold (vs. fold present); (g) the common ovovitelline duct is shorter than in *P. piru*.

Fig. 37. *Pichidamas gnythos* Almeida & Carbayo, sp. n. Photographs of live specimens. Holotype (A, D) and paratype (B-C). Scale bars not available.

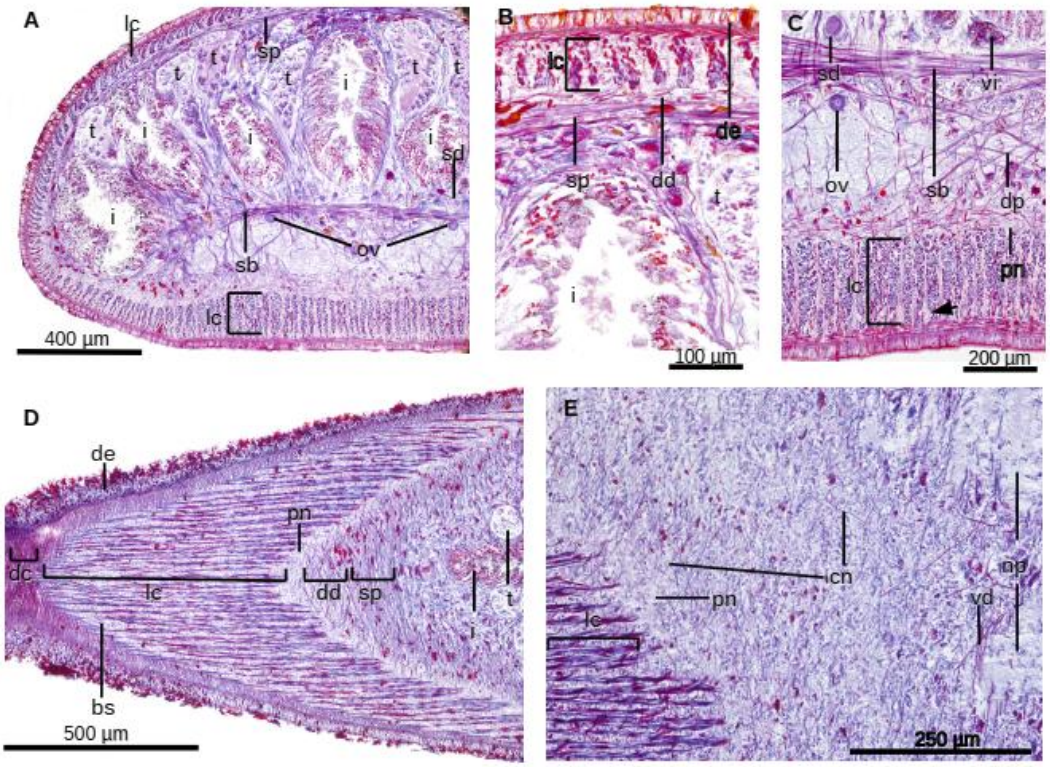

Fig. 38. *Pichidamas gnythos* Almeida & Carbayo, sp. n. Photomicrographs of histological sections of holotype (C) and paratype (A-B, D-E). A-C: transverse sections of the pre-pharyngeal region. D-E: horizontal sections showing cutaneous and parenchymal muscles. Note the nervous tissue (arrowhead) dividing the ventral longitudinal muscle into two portions.

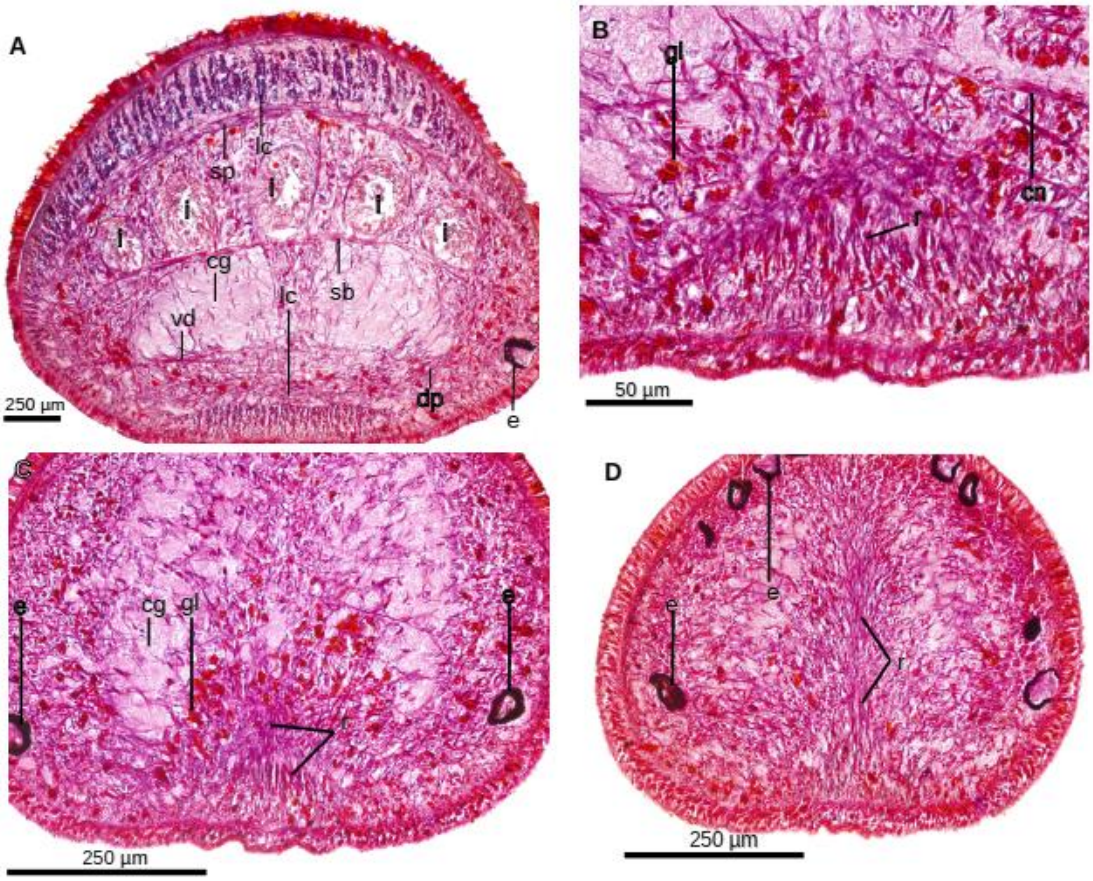

Fig. 39. *Pichidamas gnythos* Almeida & Carbayo, sp. n. Holotype. Photomicrographs of transverse sections of the anterior region of the body, at 1000 (A), 300 (B), 240 (C), 125 µm (D) from the anterior extremity, respectively.

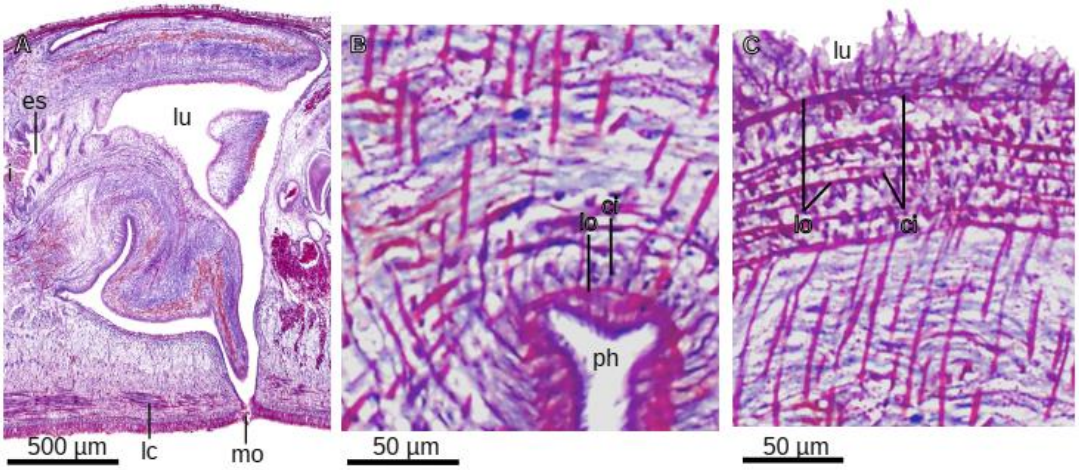

Fig. 40. *Pichidamas gnythos* Almeida & Carbayo, sp. n. Photomicrograph of a sagittal section of the pharynx (A) and detail of the outer (B) and inner (C) pharyngeal musculature of the paratype.

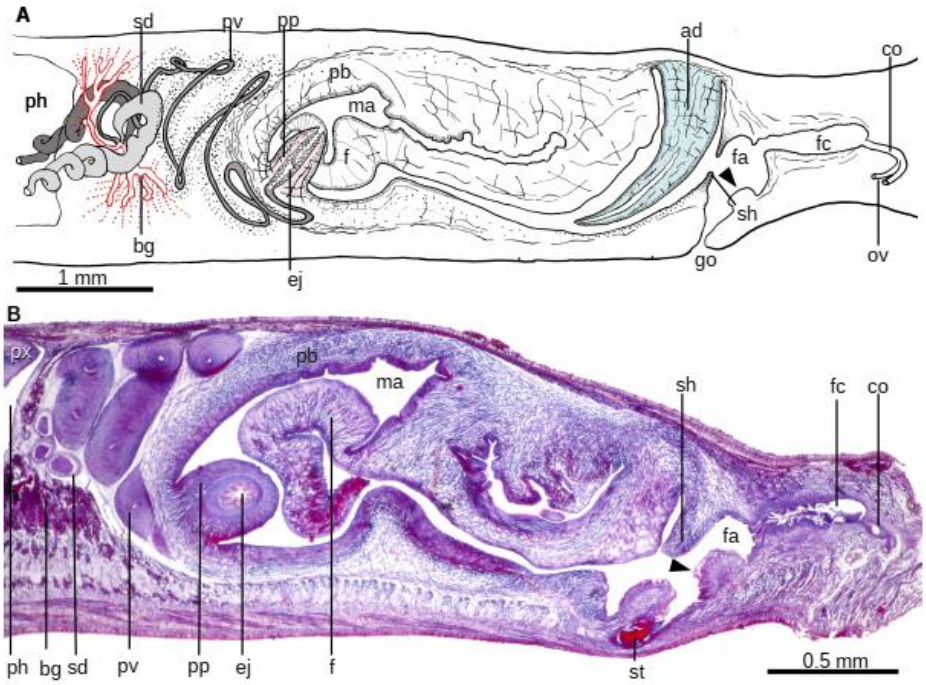

Fig. 41. *Pichidamas gnythos* Almeida & Carbayo, sp. n. A: Diagrammatic reconstruction of the copulatory apparatus of the holotype. B: Photomicrographs of a sagittal section of the copulatory apparatus of the paratype. Note the bulky region (arrowhead) of the female atrium.

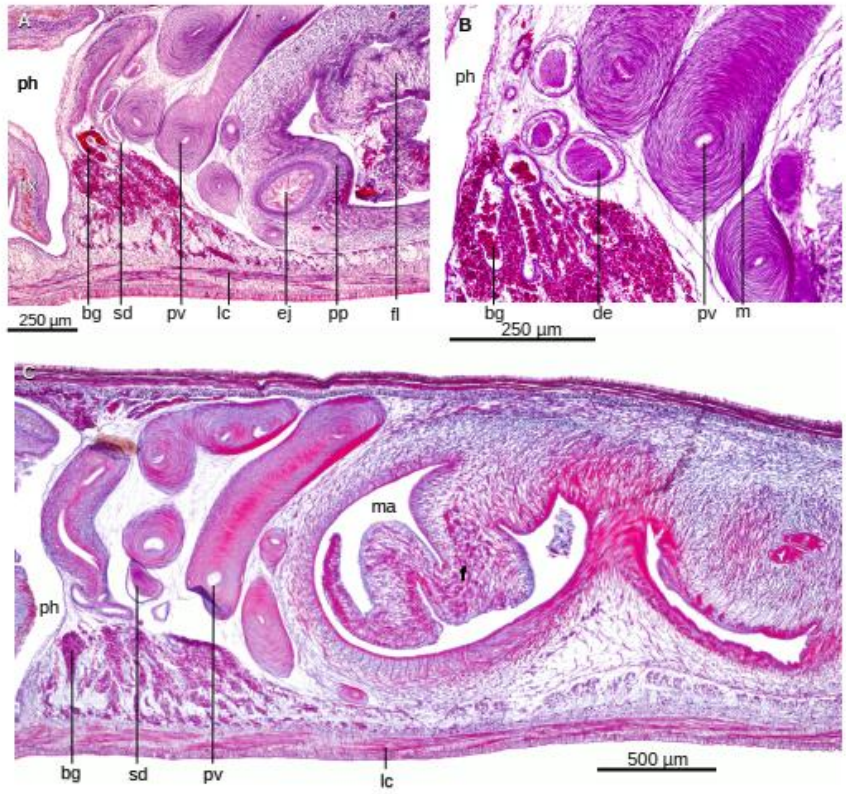

Fig. 42. *Pichidamas gnythos* Almeida & Carbayo, sp. n. Photomicrographs of sagittal sections of the paratype the prostatic vesicle and its glands of the paratype (A-B) and prostatic vesicle and male atrium of the holotype (C).

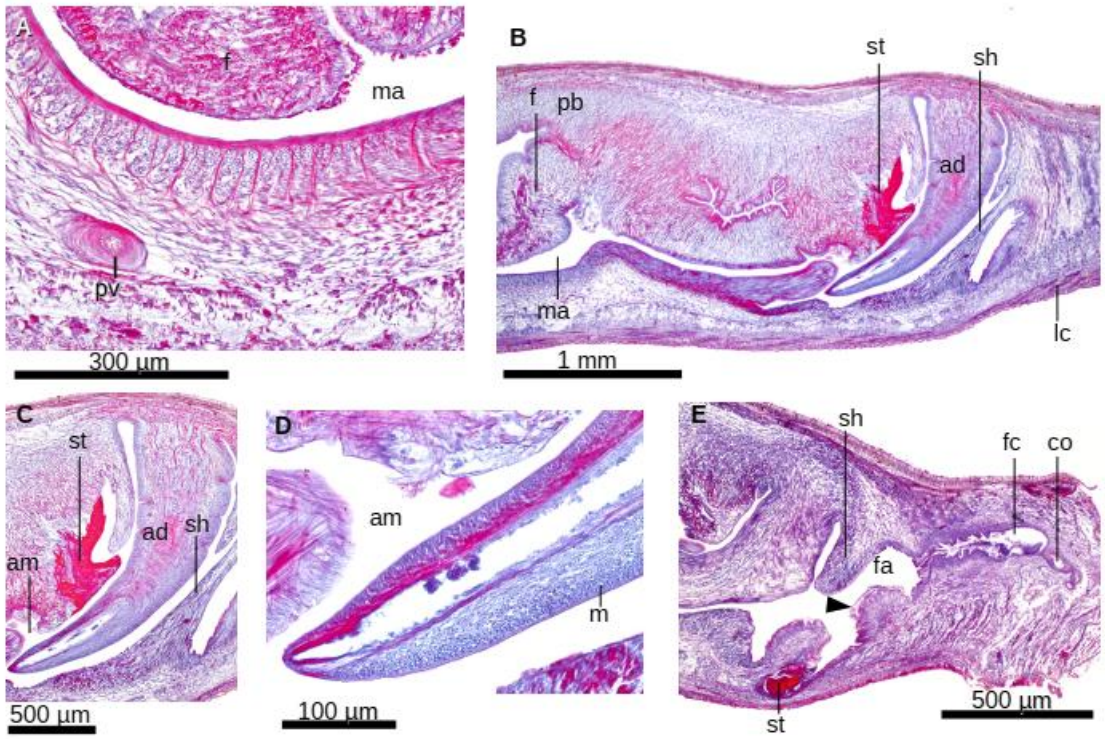

Fig. 43. *Pichidamas gnythos* Almeida & Carbayo, sp. n. Photomicrographs of sagittal sections of the holotype (A-D) and paratype (E) showing the anterior region of the male atrium (A), the male atrium (B), the adenodactyl (C-D) and the female atrium (E). Note the bulky region (arrowhead) of the female atrium.

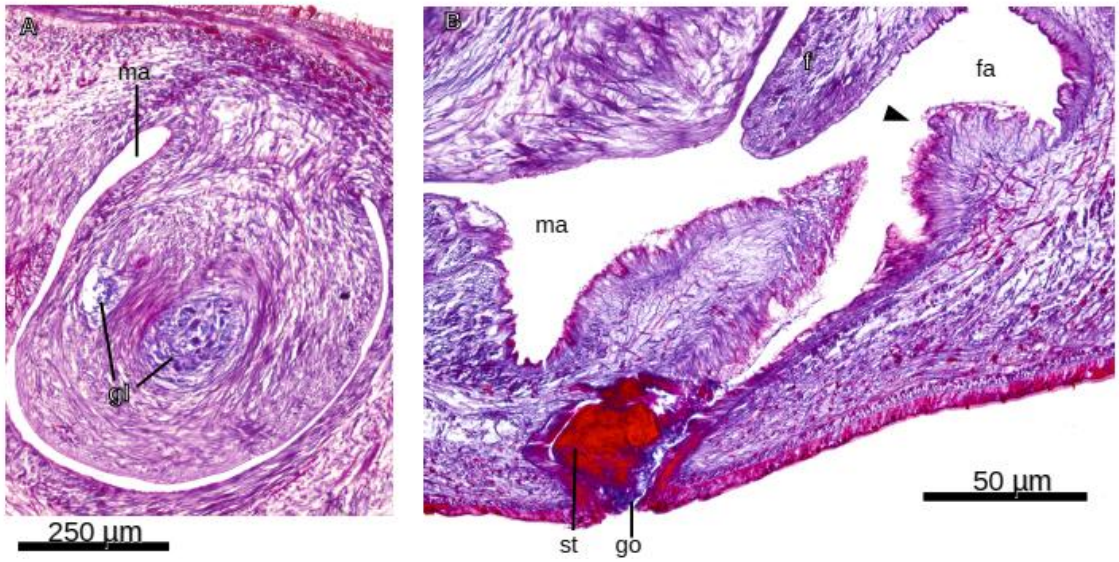

Fig. 44. *Pichidamas gnythos* Almeida & Carbayo, sp. n. Photomicrographs of sagittal sections of the paratype. A: adenodactyl. B: female atrium and gonopore. Note the bulky region (arrowhead) of the female atrium.

Sarcoplana Almeida & Carbayo, gen. n.

Diagnosis. Sarcoplanini with a small-sized body, approximately 18 mm in length. The creeping sole is wide. Sensory depressions along the anterior region of the body, but are absent in the tip. The thickness of the cutaneous muscle relatively to the body height is approximately 19%. The ventral, longitudinal cutaneous muscle forms a cephalic retractor muscle. A subneural parenchymatic layer of decussate fibers is present. The prostatic vesicle is extrabulbar. The penis papilla is conical. The common genital atrium is provided with musculo-glandular organs. The common ovovitelline duct is posterior to the female atrium. The female genital canal projects posteriorly from the posterior dorsal region of the female atrium.

Type species. *Sarcoplana musculosa* Almeida & Carbayo, sp. n.

Etymology. *Sarcoplana* is derived from the Latin terms *sarco-*, meaning flesh, and *plana,* alluding to the flattened body. It alludes to the strong cutaneous and parenchymatic muscles. The gender is female.

Sarcoplana musculosa Almeida & Carbayo, sp. n.

Material examined. Holotype MNHNCL PLAT-?? (Field code, F4886). Parque Nacional Nahuelbuta, Purén, Región de La Araucanía, Chile, Coord. -37.827, -73.009, F. Carbayo, December, 11th 2010. Transverse sections of cephalic region on 11 slides; horizontal sections of a portion immediately behind on 6 slides; transverse sections of pre-pharyngeal region on 17 slides; sagittal sections of pharynx and copulatory apparatus on 4 slides.

Type locality. Parque Nacional Nahuelbuta, Región de La Araucanía, Chile.

Etymology. The specific epithet alludes to the thick cutaneous musculature.

Description.

External aspect. The live specimen measured approximately 18 mm in length and 3 mm in with. The body length doubles when crawling. The body possesses parallel body margins. The anterior tip is rounded, and the posterior tip is pointed (Fig. 45A-C). The dorsum is convex, and the ventral side is flat. The preserved specimen measured 17.5 mm long, 2.5 mm wide, and approximately 1.5 mm high.

The dorsum displays a pure orange (RAL 2004) median stripe with 21% of the body width. This stripe is divided longitudinally by a thin carmin red (RAL 3002) midline (2.3% of the body width; Fig. 45A-B). The median stripe is absent in both extremities of the body. External to each side of the median stripe is a black red (RAL 3007) band with 37% of the body width, the margins of which are darker. Some pure orange spots occur in the bands. In the cephalic region, these bands merge and external to them is a short longitudinal beige grey line. The body margins are pure orange. The ventral side is pure orange with a pair of bands with 26% of body width, constituted of brown red (RAL 3011) dots. The inner and outer margins of the bands are crowded with these dots (Fig. 45C).

The eyes, measuring between 45-50 µm in diameter, are distributed in an irregular row contouring the cephalic region and extending marginally to the posterior tip of the body. Sensory pits are absent. Instead, the ventro-marginal epithelium of the cephalic region possesses depressions reaching the underlying basal lamina and provided with spots of cilia

(Fig. 46A). These depressions are absent in the very anterior tip of the body. The relative position of the mouth : body length is 66%; that of gonopore : body length is 77%.

Internal Morphology

Epidermis and its secretions. The epidermis is ciliated only on the creeping sole, this having 83% of the body width. Gland cells producing erythrophil granules and cells producing rhabdites pierce the entire epidermis. The former type of cells are more abundant in the body margin, whereas the rhabditogen cells are more numerous in the ventral surface of the cephalic region (Fig. 46A). Gland cells producing weakly cyanophil granules also pierce ventral and marginal epithelium. A glandular margin is absent.

Cutaneous musculature. The cutaneous musculature comprises three layers, namely, a subepithelial, one-fiber-thick circular layer, followed by a double layer with decussate fibers (13 µm thick), and an innermost longitudinal muscle the fibers of which are gathered in bundles (Fig. 46B). This longitudinal muscle is 70 µm thick dorsally, and 160 µm ventrally. It is thinner than the body margins but still very conspicuous (Fig. 46B). The bundles of the dorsal longitudinal muscle are cylindrical, whereas those of the ventral muscle are narrow and high. The ventral longitudinal muscle is divided into a thin, outer muscle, and a thick, inner muscle. These outer and inner ventral longitudinal muscles are separated by a secondary peripheral nerve net (Fig. 46B-E). The relative thickness of the cutaneous musculature is 19.5% of body height.

Musculature in cephalic region. The muscular organization changes in the anterior region of the body with respect to that of the pre-pharyngeal region. At 1.9 millimeters from the anterior tip of the body, the longitudinal cutaneous muscle is 40 µm thick dorsally, and 180 µm ventrally. In this region, the relative thickness of the cutaneous musculature is 21.6%, this index being highest in this region of the body (Fig. 46F). All cutaneous and parenchymatic muscles are thinner at 1.35 mm from the body tip. At 0.6 mm, the inner ventral cutaneous longitudinal muscle concentrates medially so that 1/4th of the body width on each side of the body is devoid of this muscle. In this point, a cephalic retractor muscle is recognizable (Fig. 47A). At 0.4 mm from the anterior tip, the secondary peripheral cutaneous nerve net is inconspicuous so that the cutaneous ventral muscle is no longer divided into an outer and an inner layer. Here, this longitudinal layer is roughly lens-shaped in cross section (Fig. 47B). Towards the anterior tip, the retractor muscle becomes progressively smaller as muscle fibers progressively detach from it to run obliquely to the dorsum and body margins (Fig. 47C-D).

Parenchymal musculature. The parenchymatic musculature mainly comprises four layers along the entire body: a dorsal layer of decussate fibers (30-µm-thick), located to the inside of the peripheral nervous net; a dense supraintestinal transverse muscle (40 µm thick); a dense subintestinal transverse muscle (75 µm thick); and a subneural layer of decussate fibers (40 µm thick) (Fig. 46B). Additionally, abundant diagonal muscle fibers run in the transverse body plane along the body.

Digestive system. The mouth is located at a distance from the anterior region of the pharyngeal pouch equivalent to 65% of its length. The pharynx is cylindrical (Fig. 48A-B). The ventro-anterior portion of the pharynx was cut off for DNA extraction, so the presence of an

esophagus could not be ascertained. The outer pharyngeal musculature consists of a subepithelial longitudinal muscle (5 µm thick), followed by a circular muscle (8 µm thick). The inner pharyngeal musculature consists of a single subepithelial circular muscle with longitudinal fibers interspersed (40 µm). A 35-45 µm thick muscle of circular and longitudinal fibers is in the stroma of the pharynx (Fig. 48A).

*Male reproductive system.*The testes are pear-shaped, and measure approximately 400 µm in height. They are dorsally located dorsally, beneath the transverse supraintestinal parenchymal muscle layer, and between the intestinal branches (Fig. 48C). They are distributed in a row of 1-2 testes on each side of the body. The anteriormost testes are placed at a distance equivalent to approximately 35% of body length, that is, 1.2 mm behind the ovaries; the posteriormost testes at a distance equivalent to 44% of body length, i.e, 100 µm anterior to the pharynx.

The copulatory apparatus occupies 50-55% of the body height, and is four times longer than its own height. The sperm ducts run above subintestinal parenchymal muscle and approximately dorsally to the ovovitelline ducts. The distal portion of the sperm ducts bends to the dorsally and to the sagittal plane to open into the proximal section of the respective branch of the prostatic vesicle (Fig. 48C). The prostatic vesicle is a sinuous tube with a proximal portion bifurcate. The vesicle is roughly C-shaped in lateral view and penetrates the anterior region of the penis bulb to join the ejaculatory duct. The penis bulb is well developed, and is mainly constituted of longitudinal fibers. Most of the ejaculatory duct is sinuous and located in the penis bulb. The distal portion of the duct is straight and crosses centrally the penis papilla. The penis papilla is 300 µm long, and is horizontally placed. This papilla is conical and presents some folds (Fig. 48C, 49A). One of these folds is located at the tip of the papilla and receives the ejaculatory duct.

The prostatic vesicle is lined with a cuboidal epithelium, apparently not ciliated. This epithelium is pierced by gland cells producing fine (0.5 µm) erythrophil granules, and is surrounded by a 10 µm-thick circular muscle. The ejaculatory duct is lined with a cuboidal, ciliated epithelium. The basal half of the penis papilla is lined with a columnar epithelium which is pierced by numerous gland cells producing erythrophil granules. The distal half of the papilla is lined with a cuboidal epithelium pierced by a smaller quantity of the same type of gland cells. Underlying the epithelium of the penis papilla are only some longitudinal muscle fibers.

The male atrium is elongated, roughly smooth (Fig. 48C). This atrium is lined with a cuboidal-to-columnar epithelium, the apical surface of which is erythrophil. This epithelium is pierced by numerous gland cells producing erythrophil granules and is underlain by a 10 µm-thick circular muscle, followed by a 10 µm thick longitudinal one.

The atrial wall dorsal to the gonopore canal presents the opening of two different glandulo-muscular organs, one located behind another (Fig. 48C). The anterior organ, (Fig. 49B) herein named mg1, consists of a 310 µm long and 30 µm wide, bowed, and vertical canal. This canal is lined with a 10 µm high columnar epithelium, the cells of which contain 0.5 µm erythrophil granules produced by gland cells located outside the mg1. The epithelium of the canal is underlain by a 10-µm-thick circular muscle followed by a 50-µm-thick muscular mass of fibers variously oriented, most of them being circular. Beneath epithelium of the innermost portion of the canal is a cyanophil, granular mass. The lumen of the canal contains some erythrophil

granules.

The posterior musculo-glandular organ, herein named mg2, is ampulla-shaped, the dilated portion being 120 µm in diameter and the canal 130 µm long (Fig. 48C, 49C). Cells of the lining epithelium of the dilated portion are not discernible. Instead, there is a mass of fine cyanophil granules produced by gland cells located outside the organ. Some muscle fibers are present among this mass. Surrounding this dilated portion of the mg2 is a 30-µm thick muscle net, followed by a 30-µm-thick longitudinal muscle. The canalicular portion of the mg2 is lined with cuboidal, strongly erythrophil cells. This epithelium is underlain by a 30-µm-thick longitudinal muscle. The lumen of mg2 contains cyanophil granules.

Female reproductive system. The ovaries are rounded-to-ovoid, with approximately 100 µm in diameter; they are incompletely developed. These ovaries are located at a distance from the anterior tip of the body corresponding to 28% of the body length, and 1.2 mm anterior to anteriormost testes, lying immediately above the ventral nerve plate. The ovovitelline ducts emerge laterally from the dorsal side of the ovaries. Subsequently, these ducts run posteriorly above the nervous plate and immediately underneath the transverse subintestinal parenchymal muscle (Fig. 46C). Just behind the level of the gonopore, one ovovitelline duct ascends gradually to enter the common ovovitelline duct behind the female atrium. This duct is short and oriented dorsally, and communicates with the female genital canal. This canal projects postero-ventrally from the posterior wall of the female atrium (Fig. 48C). Suboptimal quality of the sections did not allow examination of the second ovovitelline duct, nor the type of epithelium lining the common ovovitelline duct and the female genital canal.

The female atrium is elongated and narrow. Its dorsal wall is more or less smooth, whereas the ventral wall is provided with three tenuous recesses, each with 100-200-µm in size. The female atrium is lined with a columnar, 35-45 µm high epithelium, the free surface of it is erythrophil and with an aspect of brushes (Fig. 49D). Gland cells producing erythrophil fine granules pierce this epithelium. The bottom of the recesses is lined with a low epithelium. The female atrium contains clumps of xanthophil granules. The lining epithelium of the female atrium is surrounded by a 5-µm thick longitudinal muscle followed by a 10 µm thick circular one. The male atrium : female atrium ratio is 84%. A common muscle coat wraps the distal half of the prostatic vesicle, and male and female atria. This coat is constituted by abundant longitudinal fibers.

Fig. 45. *Sarcoplana musculosa* Almeida & Carbayo, sp. n. Photographs of living holotype. A: dorsal view, in rest. B: dorsal view, while creeping. C: ventral view. Scale bars not available.

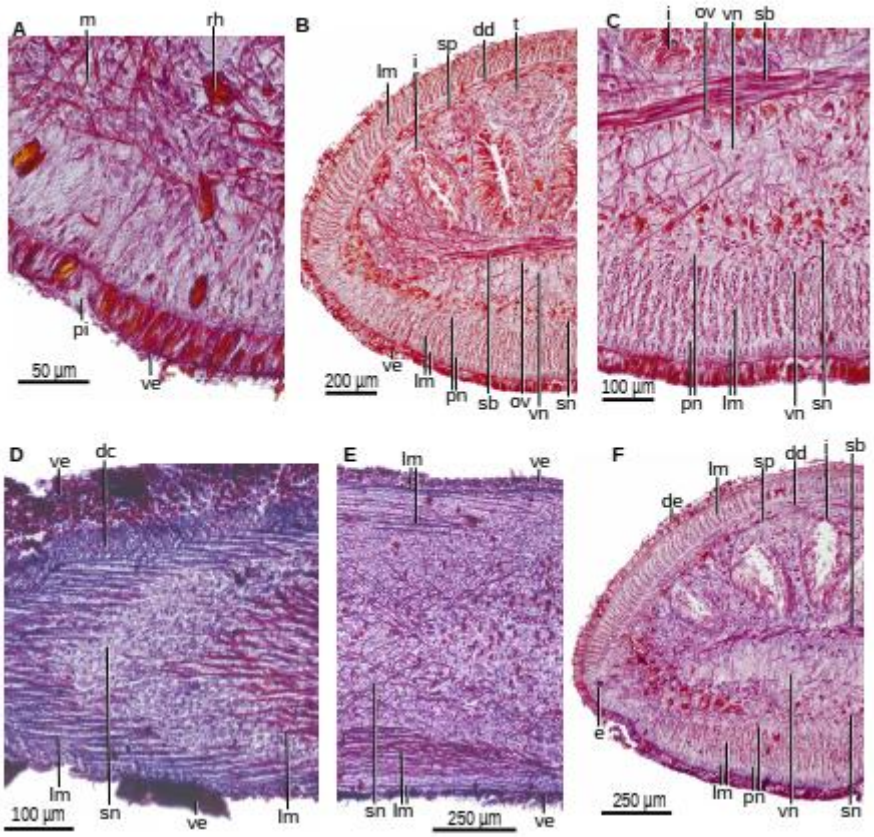

Fig. 46. *Sarcoplana musculosa* Almeida & Carbayo, sp. n. Photomicrographs of histological sections of holotype. A, transverse section at 0.88 µm from the anterior tip of the body. B-C: transverse sections of pre-pharyngeal region. D-E: horizontal sections of a region behind the cephalic region. F: transverse section at 1.9 mm from anterior tip of the body.

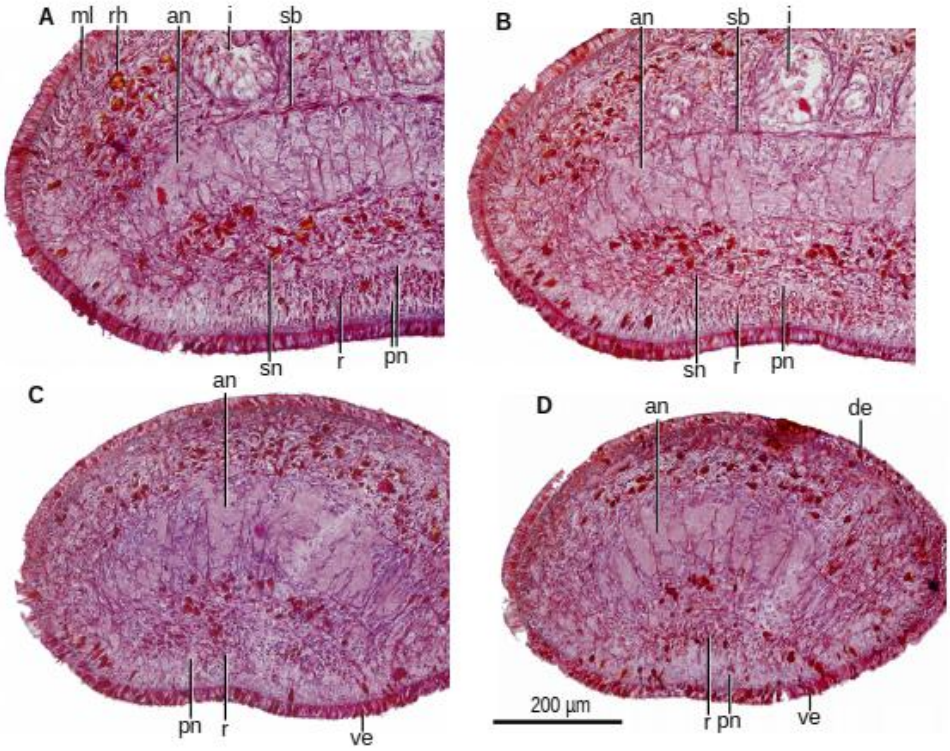

Fig. 47. *Sarcoplana musculosa* Almeida & Carbayo, sp. n. Holotype. A-D: Photomicrographs of transverse sections of the anterior section of the body, at 600, 400, 200 and 160 µm from the anterior extremity, respectively. Same scale.

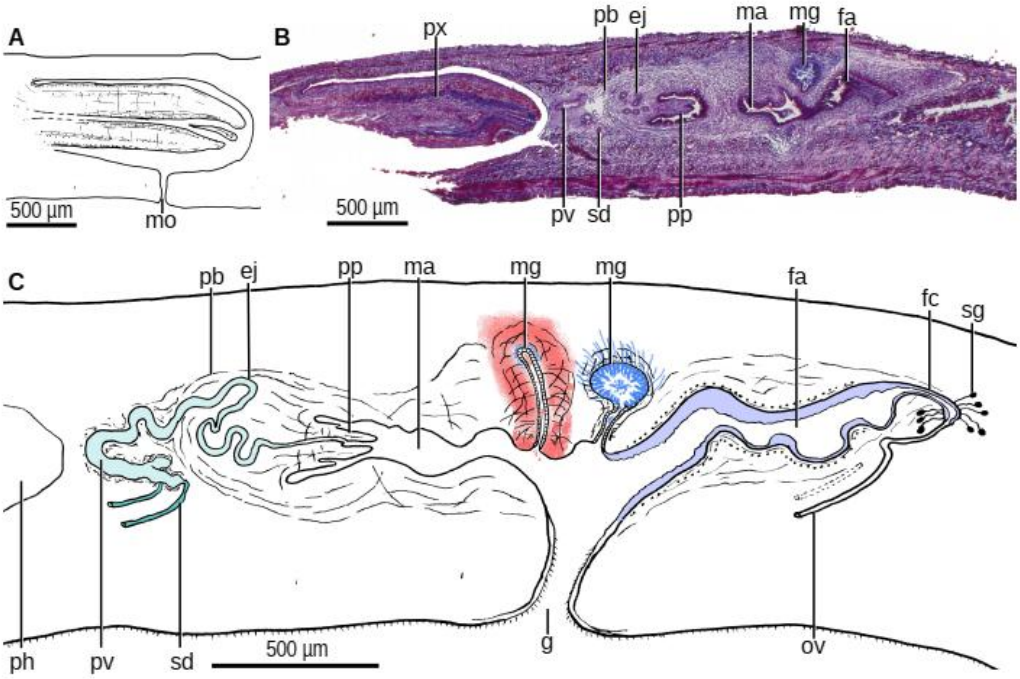

Fig. 48. *Sarcoplana musculosa* Almeida & Carbayo, sp. n. A: Diagrammatic representation of the pharynx from sagittal sections. B: Photomicrograph of a sagittal section of the pharynx and copulatory apparatus. C: Diagrammatic representation of the copulatory apparatus.

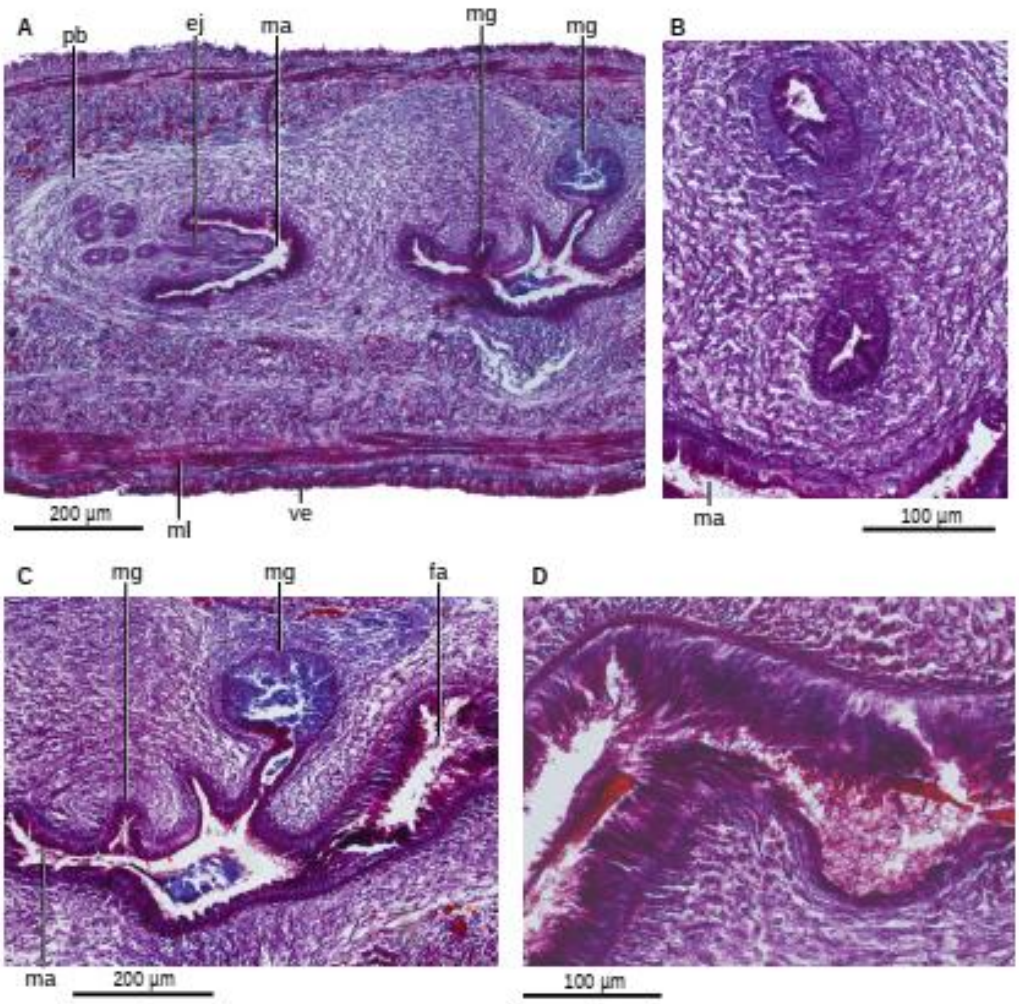

Fig. 49. *Sarcoplana musculosa* Almeida & Carbayo, sp. n. Photomicrographs of sagittal sections of holotype. A: copulatory apparatus. B: Anterior musco-glandular organ. C: Posterior musculo-glandular organ and female atrium. D: Female atrium.

Timymini Almeida & Carbayo, 2021

Diagnosis. Geoplaninae with a semi-lunate head plate, which is provided with sensory pits intercalated with sensory papillae, and ventral testes.

This monogeneric taxon is the former subfamily Timyminae here down-ranked and re-diagnosed.

Discussion

Monophyly of Geoplanini. Without considering the new taxa described here, Geoplaninae* is a monophyletic group, as in previous molecular studies (Álvarez-Presas et al., 2008; Carbayo et al., 2013; Álvarez-Presas & Riutort, 2014). However, the sistergroup of Geoplaninae* is unstable. This sistergroup is either Caenoplaninae + Rhynchodeminae (Álvarez-Presas et al., 2008) or Bipaliinae + Microplaninae (this study; Álvarez-Presas & Riutort, 2014), and accordingly the statistical support for the interrelationships of the taxa was low independently from the genes used in the phylogenetic inferences. This situation is probably due to the old age of these lineages and that hitherto, molecular markers with an adequate phylogenetic signal were not yet discovered(Álvarez-Presas & Riutort, 2014).

Putative synapomorphies of the new and the re-ranked taxa

The molecular phylogeny shows congruence with the morphology. Furthermore, most of the tribes can unequivocally be distinguished from each other by one or more putative synapomorphic characters (see table S3) as discussed below. Next, the taxa are presented and discussed in alphabetical order within each taxonomic rank.

Subfamily Geoplaninae Stimpson, 1857. Before this study, the majority of the genera of Geoplaninae* were distributed to the East of the Andes. In the new classification, the eastern component became only a fraction of the taxonomic diversity of the group and Geoplanini is proposed for the clade including only species from the east of the Andes plus *Transandiplana* (see below), whereas Geoplaninae embrace the entire group including all the nine tribes.

Geoplaninae members can be recognized by means of three putative synapomorphies: (a) the eyes encircle anterior region of the body in a single row and extend until the posterior extremity of the body, frequently spreading onto the dorsum; (b) the creeping sole is wide; and (c) the testes are dorsal. Carbayo et al., (2013) pointed out the progressive fragility of the diagnostic traits of Geoplaninae* as new taxa are being discovered. For instance, some ingroups of Geoplaninae* do not have eyes at the anterior region of the body, namely *Cephaloflexa* and *Choeradoplana*, and *Geobia* lacks eyes, while *Xerapoa* Froehlich, 1955 (Geoplaninae) and *Difroehlichia* Leal-Zanchet & Marques, 2018 have a narrow creeping sole,

with 50% of the body width. Furthermore, the New Zealand Anzoplanini Winsor, 2006 (Rhynchodeminae) bears dorsal and ventral testes simultaneously (Winsor, 2006).

Adinoplanini trib. n. Members of this group share the following three synapomorphies: the median zone of the dorsal side of the body is convex, and the lateral zones are flattened. The female atrium bears musculo-glandular organs.

Geoplanini Stimpson, 1857. As proposed here, this group comprises all the current members of Geoplaninae* geographically distributed to the East of the Andes plus the genus *Transandiplana*. Geoplanini is the richest tribe in terms of genera (22) and species (about three hundred). Discovering synapomorphies in Geoplanini is elusive. Important taxonomic attributes vary among the genera, such as cephalic retractor muscle (present vs. absent), eyes distribution (dorsal vs. marginal only), sensory depressions (present vs. absent), subneural parenchymal muscle (present. vs. absent), position of the prostatic vesicle (intrabulbar vs. extrabulbar), penis papilla (present vs. absent), condition of the female genital canal (proflex, vs. postflex). Hopefully, future morphological studies addressed with other techniques (micro-computed tomography, transmission electron microscopy) will reveal taxonomically valuable details of the organs such as those of eyes, lining epithelium of the genital atria, etc.

What concerns the current available knowledge of the flatworms, the only feature present almost exclusively in leaf-shaped species of Geoplanini is the dorsal distribution of the eyes. It is true that some species of Geoplanini with such a body exhibit only marginal eyes (e.g. *Bogga*, *Amaga*). However, the phylogenetic position of these two genera has not yet been assessed based on molecular data. Furthermore, these species are distributed across Andean regions, which leads to expect some geographical isolation of the lineages they represent. An additional problem is that most diagnoses do not mention eye allocation along the body. Therefore, a comprehensive revision of all Geoplanini is to be addressed.

Nonetheless, Geoplanini planarians without a leaf-shaped body are not covered by this diagnostic character. For this reason, the diagnosis of the tribe needs further characters. Given that there are no synapomorphies, we need to propose an exclusive combination of attributes. Among Geoplaninae, only Inakayaliini, Adinoplanini and Geoplanini comprise

species with dorsal eyes, but the female genital ducts are dilated in Inakayaliini (vs. not dilated in the remaining Geoplaninae), and species of Adinoplanini exhibit a wide median convex zone of the dorsal side, external to which the body is flattened (vs. dorsum convex). In Geoplanini, the dorsal longitudinal cutaneous muscle is not sunken into the parenchyma (*Choeradoplana gladismariae* excepted) (vs. sunken in *Gusana*). The pharyngeal pouch is located anteriorly to the copulatory apparatus (vs. extending posteriorly over the copulatory apparatus in Haranini and Timymini). The female atrium does not bear glandulo-muscular organs. Together with eye pattern distribution, these negative traits allow the diagnosis of Geoplanini.

Transandiplana, gen. n. (Geoplanini). Three morphological traits might be synapomorphic, namely the main nervous system consisting of multiple longitudinal cords, testes provided with dark pigment cup and the relatively anterior position of the testes with respect to the pharynx. The main nervous system in Geoplaninae consists of either two longitudinal cords (usually in small and thin species) or it exhibits the aspect of an even plate, especially in large and flat organisms. An exception is the new taxa *Transandiplana*, which presents a main nervous system consisting of multiple cords. Records of dark pigment around the testes are anecdotal because it is uncommon to mention absent structures in taxonomic papers (but see dark spots covering testes in *Obama ladislavii* (Graff, 1899) in Álvarez-Presas *et al.*, 2015). In any case, such a conspicuous pigment cup has previously never been recorded in our experience with the morphological study of Geoplaninae.

Gusanini trib. n. This clade includes only *Gusana*. The body shape, broad, foliaceous, with the anterior triangular tip is a synapomorphic and unmistakable trait among land planarians. Other putative synapomorphy is a transverse light stripe as a ring in the cephalic region or only a transverse stripe in the ventral side of the head (convergent in *Barreirana barreirana* and in some species of *Obama, Paraba*, *Pasipha, Piima and Pseudogeoplana*), the dorsal longitudinal cutaneous muscle sunk into the parenchyma (convergent in *Choeradoplana gladismariae*) and sensory pits internally branched.

Haranini trib. n. The straight tube leveled with the subintestinal transverse parenchymal muscle might represent a synapomorphy of this tribe. The extraordinarily long pharyngeal

pouch, which extends even behind the copulatory apparatus, is apparently a symplesiomorphy, since it is also shared with the sistergroup Timymini.

Inakayaliini trib. n. This tribe presents one putative synapomorphic character, namely dilated female genital duct(s), either the paired ovovitelline ducts, or the common (glandular) ovovitelline duct. This trait is unique among land planarians.

Myoplanini trib. n. Two apparent synapomorphies support morphologically this clade, namely a transneural parenchymal muscle of diagonal fibers (convergent in *Sarcoplana*), and the four-layer inner pharyngeal muscle. This latter muscle is unique among land planarians.

Polycladini, trib. n. This group encompasses only *Polycladus gayi*. Most conspicuous characteristic of this species is the extraordinarily wide (2.4 times as long as wide) and flattened body (Graff, 1899), provided with marginal eyes only (Graff, 1899; Schmidt, 1902). The musculature of the species is not clearly understood. Graff (1899) described the species and illustrated the cutaneous and parenchymal muscles (Plate 30, Figs 3, 4 in Graff, 1899). The cutaneous musculature is described as constituted of three muscle layers, namely a circular, a diagonal and an innermost longitudinal one. In a drawing of a transverse section of the body (Plate 30, Fig. 3) the parenchymal musculature is depicted as formed by "Obere Transversalmuskeln", "Mittlere Transversalmuskeln", and "Ventrale Transversalmuskeln". The two latter muscles are crossed by fibers of "Ventrale Longitudinalmuskeln". Other drawing showing a sagittal section (Plate 30, Fig. 4), depicts only "Dorsale Longitudinalmuskeln" and "Dorsoventrale Muskeln". The "Dorsale Longitudinalmuskeln" are drawn as dashed lines, suggesting that they might not be longitudinal but diagonal. Although Graff (1899) stated that in land planarians the parenchymal musculature is composed of longitudinal, transverse and dorso-ventral fibers, all Geoplaninae (*Timyma* excepted) do present a diagonal parenchymal muscle.

Summing up, apart from the dorso-ventral muscle fibers, the parenchymal musculature in Polycladini comprises a dorsal layer of decussate fibers ("Dorsale Longitudinalmuskeln"), a transverse supraintestinal muscle ("Obere Transversalmuskeln"), a transverse subintestinal muscle ("Mittlere Transversalmuskeln"), a transverse subneural muscle ("Ventrale Transversalmuskeln") and a longitudinal transneural muscle ("Ventrale

Longitudinalmuskeln") which is intermingled with fibers of the subintestinal and subneural muscles. The longitudinal transneural parenchymal muscle is a synapomorphic character of the Polydanini.

Sarcoplanini, trib. n. The members of this group share three putative synapomorphies, namely sensory depressions, a cephalic retractor muscle (secondarily lost in *Wallmapuplana*), and a subneural parenchymal decussate muscle (but in *Wallmapuplana* the fiber orientation of this muscle is unknown). Additional traits shared by all species in Sarcoplanini and which might have convergently evolved in other lineages of Geoplanidae are: marginal distribution of the eyes (also present in Adinoplanini, Myoplanini, Haranini, Caenoplanini (Rhynchodeminae), and some Geoplanini)), a small penis papilla (e. g. *Amaga*, *Gusana,* but in *Liana* is large), copulatory apparatus provided with musculo-glandular organs (secondarily lost in *Mapuplana*; also present in Australasian taxa, such as some *Bipalium, Artioposthia* (see Fyfe, 1937), *Coleocephalus* (see Winsor, 1998)), and female genital canal in the postflex condition (e. g. *Pasipha*, *Gigantea*, *Gusana*). Furthermore, the ingroup constituted by *Mapuplana* + *Pichidamas* + *Wallmapuplana* evolved multicellular glands associated with the prostatic vesicle. This is also true for *Pichidamas piru* Bulnes et al., 2018. These glands were not reported in the original description. However, after being observed in *Pichidamas gnythos* sp. n., led us to a reexamination of our records of the species. Unpublished photomicrographs of histological sections revealed that, although the quality of the sections is suboptimal, *P. piru* also bears this glands (pers. obs.).

Sarcoplana (Sarcoplanini) stands apart from the remaining sarcoplaninin genera by means of an autapomorphic trait, namely a secondary peripheral nerve net in the ventral side of the body (convergent in *Myoplana*). *Mapuplana* and *Liana* are the only genera with part of the ventral longitudinal cutaneous muscle sunken into the parenchyma, but in *Mapuplana* the penis papilla is small (vs. large in *Liana*), whereas *Wallmapuplana* is the only genus lacking a cephalic retractor muscle. Finally, *Pichidamas* presents a large musculo-glandular organ of adenodactyl type.

The genus *Liana* E. M. Froehlich, 1978 deserves a deeper discussion. This monotypic genus was proposed for *L. guasa* E. M. Froehlich, 1978. The species was described from incompletely mature individuals. The main diagnostic features of the genus are: elongated

body, broad creeping sole, with sensory depressions ('minute sensory pits'), longitudinal ventral cutaneous muscle partially sunken into the parenchyma, cutaneous muscle thickness relatively to the body height is 10%, testes are dorsal; copulatory apparatus without adenodactyls; penis papilla short and blunt; female canal approaches from horizontal or ventral aspect. The species also has a subneural decussate parenchymal muscle ("a layer of fibres obliquely oriented to the right and to the left" in E. M. Froehlich, 1978, p. 21) interwoven with fibers of the sunken longitudinal cutaneous muscle. The relative thickness of the cutaneous musculature increases to 21% when the sunken muscle portion is also considered (see Fig. 24 in E. M. Froehlich, 1978).

There are no gene sequences of the species. Among the geoplanin tribes, *Liana* fits best Sarcoplanini: the creeping sole is wide; the eyes marginal; sensory depressions and subneural parenchymatic decussate muscle are present. Original description does not mention a cephalic retractor muscle, but it describes modification of the musculature organization in the cephalic region which is compatible with a retractor organ ("*At the anterior end, the dorsal longitudinal [ventrally?] cutaneous fibres bend dorsally to end on the basement membrane. Laterally, towards the ventral sensory border the cutaneous musculature progressively loses height becoming minimal if not absent. Ventrally it regains height towards the median line, attaining a little more than half the height of the dorsal portion. [...] The ventral longitudinal parenchymal [cutaneous?] musculature progressively disappears towards the anterior extremity. At the same time it appears there a layer of diagonal fibres interspersed with rarer and rarer longitudinal fibres. Presumably the longitudinal fibres change direction anteriorly but it cannot be discerned*", p. 22). The presence of the remaining two diagnostic traits of Sarcoplanini (i. e. multicellular glands associated with the prostatic vesicle and genital musculo-glandular organs) cannot be adequately studied since the individuals are only partially mature. *Liana* does not fit better in any of the remaining tribes, as for they present features precluding transferring the genus to them: Adinoplanini (median zone of the body convex, and lateral zones flattened; the female atrium bears musculo-glandular organs); Geoplanini (body leaf-like and with dorsal eyes); Gusanini (anterior region of the body triangular, ventral and dorsal longitudinal cutaneous muscle sunken into the parenchyma; sensory pits present); Haranini (very long pharyngeal pouch); Inakayaliini (dilated female genital ducts); Myoplanini (transneural

parenchymal muscle of diagonal fibers); Polycladini (extraordinarily wide and flattened body, marginal eyes, transverse subneural parenchymatic muscle and a longitudinal transneural parenchymatic muscle); Timymini (semi-lunate head plate). Therefore, we transfer the genus to Sarcoplanini.

Timymini Almeida & Carbayo, 2021 (or subfamily Timyminae here down-ranked). Distinct putative synapomorphies of Timymini are the semi-lunate head plate (independently evolved in the Asian Bipaliinae, see Almeida et al., 2021), sensory pits intercalated with sensory papillae, and the ventral position of the testes (as in all non-Geoplaninae species; but Eudoxitopoplaninae Winsor, 2009 (Rhynchodeminae) has dorsal and ventral testes) (see Froehlich, 1978; Winsor, 2009; Almeida et al., 2021).

On re-ranking of the current taxa and proposal of new tribes

It could be thought that the new classification proposed is over splitting the number of taxa, from genera to tribes, each represented by a few or only one taxon. However, two reasonable motives to do that. One motive is related to the restrictions imposed by the current classification of Geoplanidae. Before this study, there were two subfamilies, Geoplaninae* and Timyminae, both sharing a sistergroup relationship (Almeida *et al.*, 2021). However, it became evident that the concept of Geoplaninae* had to be expanded to house all the species within the subfamily together with Timyminae and the new taxa described in this paper. Consequently, (a) Timyminae must be down-ranked to the level of the tribe; and (b) the clade constituted by the genera from the East to the Andes plus *Transandiplana* necessitated to be assigned a Linnean category below the family level, i.e., the tribe Geoplanini. Therefore, the Chilean and Argentinean endemic genera would have to be considered *incertae sedis* unless a tribe is erected for them, as done here.

The second motive complements the first one. The morphological diversity embodied in the new taxa here described is great: cephalic retractor muscle, sensory depressions, main nervous system organized in multiple nerve cords, subneural and transneural parenchymal muscles, multicellular glands, only to mention some of them. All this morphological variety is distributed across the taxa in a way that most of the tribes and nested genera, reflecting the phylogenetic interrelationships, can by be diagnosed by putatives synapomorphies.

Biogeography

Currently, the representatives of Geoplaninae are distributed across the Neotropical region, with some species most probably dispersed outside this region through human activity (Jones & Sterrer, 2005; Carbayo *et al.*, 2016; Justine *et al.*, 2020). Eight tribes of Geoplaninae are distributed across Chile and the Argentinean Andes, whereas only the ninth tribe (Geoplanini) mostly occur to the west of the Andes. In principle, this biogeographic distribution could be explained as the ancestral of Geoplaninae having been originated in a region to the West of the Andes, with subsequent diversification, followed by the dispersal of the ancestral lineage of the Geoplanini to the East of the Andes. Subsequently, the lineage of the Chilean genus *Transandiplana*, nested within Geoplanini, might have dispersed back to West of the Andes. Disjunct distributions of taxa in the Eastern Andes and Western Andes are well known among plants (e.g., Kunzmann, 2007; Murillo-A. et al., 2012), and animals (e.g., Ferreti, 2015; Fachin et al., 2018). These patterns were related to climatic and geological changes, which caused vicariant events. However, there are no records of an ingroup of the Eastern component (Geoplanini) being distributed in the Western Andes (Transandiplana) However, this hypothesis of a secondary dispersal through the Andes back to the West must be considered only tentative because of the low statistical support of *Transandiplana* as a member of Geoplanini.

Concluding remarks

This study signifies a contribution to expand the scarce knowledge of the systematics of the Neotropical land planarians, especially those of the West Andean region. Numerous supra-specific taxa were proposed from a handful of species sampled across Chile in an only two-week long field campaign. Presumably, a large fraction of the species dwelling in the sampling areas must have been overlooked, since the sampling effort in each locality was clearly insufficient, especially for small detecting individuals (see Carbayo et al., 2016).

Congruence between distribution of the morphological synapomorphic traits of the new taxa and their phylogenetic interrelationships suggests that the new classification proposed for Geoplaninae is natural. Hopefully new samplings and new systematic studies will support

the classification of Geoplaninae and expand the knowledge of the morphological and taxonomic richness of this Chilean invertebrate fauna.

Overview of the new classification of Geoplaninae (new taxa in bold; only new species are mentioned)

Geoplanidae Stimpson, 1857

Geoplaninae Stimpson, 1857

Adinoplanini Carbayo & Almeida, trib. n.

Adinoplana Carbayo & Almeida, gen. n.

***Adinoplana alerna* Carbayo & Almeida, sp. n.**

***Adinoplana nahuta* Carbayo & Almeida, sp. n.**

Geoplanini Stimpson, 1857

Amaga Ogren and Kawakatsu, 1990

Barreirana Ogren & Kawakatsu, 1990

Bogga Grau & Sluys, 2012

Cephaloflexa Carbayo and Leal-Zanchet, 2003

Choeradoplana Von Graff, 1896

Cratera Carbayo et al., 2013

Difroehlichia Leal-Zanchet & Marques, 2018

Geobia Diesing, 1861

Geoplana Stimpson, 1857

Gigantea Ogren and Kawakatsu, 1990

Imbira Carbayo et al., 2013

Issoca C. G. Froehlich, 1955

Luteostriata Carbayo, 2010

Matuxia Carbayo et al., 2013

Notogynaphallia Ogren and Kawakatsu, 1990

Obama Carbayo et al., 2013

Paraba Carbayo et al., 2013

Pasipha Ogren and Kawakatsu, 1990

Piima Carbayo, 2020

Pseudogeoplana Ogren and Kawakatsu, 1990

Supramontana Carbayo and Leal-Zanchet, 2003

***Transandiplana* Almeida & Carbayo, gen. n.**

Transandiplana graui **Almeida & Carbayo, sp. n.**

Winsoria Negrete *et al*., 2019

Xerapoa C. G. Froehlich, 1955

Gusanini Almeida & Carbayo, trib. n.

Gusana E. M. Froehlich, 1978

Haranini Carbayo & Almeida, trib. n.

Harana **Carbayo & Almeida, gen. n.**

Harana harai **sp. n.**

Inakayaliini Almeida & Carbayo, trib. n.

Inakayalia Negrete *et al.*, 2020

Inakayalia cyanea **Almeida & Carbayo, sp. n.**

Myoplanini Almeida & Carbayo, trib. n.

Myoplana **gen. n.**

Myoplana veraluciae **Almeida & Carbayo, sp. n.**

Myoplana joaopauloi **Almeida & Carbayo, sp. n.**

Polycladini Carbayo & Almeida, trib. n.

Polycladus Blanchard, 1845

Sarcoplanini Almeida & Carbayo, trib. n.

Liana E. M. Froehlich, 1878

Mapuplana **Grau, *et al*., gen. n.**

Mapuplana guttulata **Almeida & Carbayo, sp. n.**

Pichidamas Bulnes et al., 2018

Pichidamas gnythos **Almeida & Carbayo, sp. n**

Sarcoplana **Almeida & Carbayo, gen. n.**

Sarcoplana musculosa **Almeida & Carbayo, sp. n.**

Wallmapuplana Negrete *et al.,* 2020

Timymini Almeida & Carbayo, 2021

Timyma E. M. Froehlich, 1978

Acknowledgements

To Corporación Nacional Forestal (Chile) for licensing field work (#27/2010). To Fernando Portella de Luna Marques (USP) and Francisco Cádiz for their help with sampling. Ítalo Silva de Oliveira Sousa, Geison Castro da Silveira, and Lucas Beltrami for histological processing. Bianca Lujan, Beatriz Vieira Freire, Manuel Antunes Junior and Sabrina Baroni (USP) are thanked for their kind assistance during molecular work. Adriano Kury (UFRJ) and Marcos Hara (USP) are kindly thanked for their help to interpret the Code. This study was financed in part by the Coordenação de Aperfeiçoamento de Pessoal de Nível Superior - Brasil (CAPES) - Finance Code 001 (Proc. 88882.378126/2019-01). FC has financial support from São Paulo Research Foundation - FAPESP (Proc. 2019/12357-7).

References

Adoutte, A., Balavoine, G., Lartillot, N., Lespinet, O., Prud'homme, B., & de Rosa, R. 2000. The new animal phylogeny: reliability and implications. *Proceedings of the National Academy of Sciences of the USA, 97*(9), 4453-4456.

Halanych, K. M. 2004. The new view of animal phylogeny. *Annual Review of Ecology, Evolution and Systematics, 35*, 229-256.

Aguinaldo, A. M. A., Turbeville, J. M., Lindford, L. S., Rivera, M. C., Garey, J. R. & Raff, R. A.1997. Evidence for a clade of nematodes, arthropods and other moulting animals. *Nature, 387*, 489-493.

Almeida, A. L., Marques, F. P. L., & Carbayo, F. 2019. 'Endless forms most beautiful': Taxonomic revision of the planarian Geoplana vaginuloides (Darwin, 1844) and discovery of numerous congeners (Platyhelminthes: Tricladida). Zoological Journal of the Linnean Society, 185(1): 1-65. https://doi.org/10.1093/zoolinnean/zly022

Almeida, A. L., Francoy, T. M., Álvarez-presas, M. &Carbayo, F. 2021. Convergent evolution: A new subfamily for bipaliin-like Chilean land planarians (Platyhelminthes). *Zoologica Scripta*, 00: 1-9. DOI: 10.1111/zsc.12479

Álvarez-Presas, M.; Baguñà, J. & Riutort, M. 2008. Molecular phylogeny of land and freshwater planarians (Tricladida, Platyhelminthes): From freshwater to land and back. Molecular Phylogenetics and Evolution 47: 555-568.

Álvarez-Presas & Riutort, M. 2014. Planarian (Platyhelminthes, Tricladida) Diversity and Molecular Markers: A New View of an Old Group. Diversity 6: 323-338; doi:10.3390/d6020323

Álvarez-Presas, M.; Amaral, S.V.; Carbayo, F.; Leal-Zanchet, A. M. & Marta Riutort. 2015. Focus on the details: morphological evidence supports new cryptic land flatworm (Platyhelminthes) species revealed with molecules. Organism Diversity and Evolution 15(2): 379-403. DOI 10.1007/s13127-014-0197-z

Amaral, S. V. do. 2017. Taxonomia e filogeni de espécies de Geoplaninae (Plathyelminthes) com ênfse nos gêneros Pasipha Ogren & Kawakatsu, 1990 e Imbrira Carbayo, et al., 2013. PhD Thesis. Unisinos. São Leopoldo.

Amaral. S. V.; Ribeiro, G. G.; Müller, M. J.; Valiati, V. H. & Leal-Zanchet. A. M. 2018. Tracking the diversity of the flatworm genus Imbira (Platyhelminthes) in the Atlantic Forest. Organisms Diversity & Evolution 18: 87-99. https://doi.org/10.1007/s13127-018-0358-6

Baguñà, J.; Carranza, S.; Paps, J.; Ruiz-Trillo, I. & Riutort, M., 2001. Molecular taxonomy and phylogeny of Tricladida. In: Littlewood, D.T.J., Bray, R.D. (Eds.), The Interrelationships of the Platyhelminthes. Taylor & Francis, UK, CL, pp. 49-56.

Blanchard, E. 1845. Recherches sur l'organisation des vers. *Annales des Sciences Naturelles, Zoologie, 3e série*. 8: 119-149. doi:10.5962/bhl.title.51506.

Bulnes, V. N., Grau, J. H., & Carbayo, F. 2018. A new Chilean genus and species of land planarian (Platyhelminthes: Tricladida, Geoplaninae) with cephalic retractor muscle and adenodactyl. *Journal of Natural History,* 52: 2553-2566. https://doi.org/10.1080/00222933.2018.1538468

Capella-Gutiérrez, S., Silla-Martínez, J. M. & Gabaldón, T. 2009. trimAl: A tool for automated alignment trimming in large-scale phylogenetic analyses. *Bioinformatics*, 25(15): 1972-1973. https://doi.org/10.1093/bioinformatics/btp348

Carbayo, F., Álvarez-Presas, M., Olivares, C. T., Marques, F. P. L., Froehlich, E. M. & Riutort, M. 2013. Molecular phylogeny of Geoplaninae (Platyhelminthes) challenges current classification: proposal of taxonomic actions. *Zoologica Scripta* 42(5): 508-528. doi:10.1111/zsc.12019

Carbayo, F.; Junior, O. M. & Jucá, M. 2016. Relative and absolute density estimates of land planarians (Platyhelminthes, Tricladida) in urban rainforest patches. *Papéis Avulsos de Zoologia,* 56(3): 27-32.

Carbayo, F., Álvarez-Presas, M., Jones, H. D. & Riutort, M. 2016. The true identity of *Obama* (Platyhelminthes: Geoplanidae) flatworm spreading across Europe. Zoological Journal of the Linnean Society 177: 5-28.

Carranza, S., Baguñà, J., & Riutort, M. 1997. Are the Platyhelminthes a monophyletic primitive group? An assessment using 18S rDNA sequences. *Molecular Biology and Evolution, 14*(5), 485-497.

Cason, J. E. 1950. A rapid one-step Mallory-Heidenhain stain for connective tissue. *Stain Technology*, 25 (4), 225-226. http://dx.doi.org/10.3109/10520295009110996

Ewing, B. & Green, P. 1998. Base-calling of automated sequencer traces using Phred II. Error probabilities. *Genome Research* 8: 186-194.

Ewing, B., Hillier, L., Wendl, M. C. & Green P. 1998. Basecalling of automated sequencer traces using Phred I. Accuracy assessment. *Genome Research* 8: 175-185.

Fachin, D. A.; Santos, C. M. D.; Amorim, D. d. S. 2018. First two species of Austroleptis Hardy (Diptera: Brachycera: Austroleptidae) from Brazil. Zootaxa 4369 (4): 557–574. https://doi.org/10.11646/zootaxa.4369.4.6

Ferreti, N. 2015. Cladistic reanalysis and historical biogeography of the genus Lycinus Thorell, 1894 (Araneae: Mygalomorphae: Nemesiidae) with description of two new species from western Argentina. Zoological Studies 54:11. DOI 10.1186/s40555-014-0083-6

Fetzner, J. 1999. Extracting high–quality DNA from shed reptiles skins: a simplified method. *BioTechniques*, 26: 1052-1054.

Froehlich, C. G. 1967. A contribution on the zoogeography of neotropical land planarians. *Acta Zoologica Lilloana*, 23: 153-162.

Froehlich, E. M. 1978. On a collection of Chilean land planarians. *Boletins de Zoologia da Universidade de São Paulo*, 3: 7-80.

Gasmi, S., Nve, G. & Pech, N. 2014. Evolutionary history of Chaetognatha inferred from molecular and morphological data: a case study for body plan simplification.*Front Zool.* 11: 84. https://doi.org/10.1186/s12983-014-0084-7

Gordon, D., Abajian, C. & Green P. 1998. Consed: a graphical tool for sequence finishing. *Genome Research* 8: 195-202.

Gordon, D., Desmarais, C. and Green, P. 2001. Automated finishing with autofinish. *Genome Research* 11: 614-625.

Graff, L. 1899. 'Monographie der Turbellarien II. Tricladida Terricola (Landplanarien). Atlas von Achtundfünfzig Tafeln zur Monographie der Turbellarien II. Tricladida Terricola (Landplanarien). Pls. I–LVIII.' (Wilhelm Engelmann: Leipzig, Germany).

Grau, J. H. & Carbayo, F. 2010. Panorama de la diversidad de planarias terrestres (Platyhelminthes: Tricladida) de Chile. *Boletín de Biodiversidad de Chile* 2: 41-54.

Hall, T. A. 1999. BioEdit: a user-friendly biological sequence alignment editor and analysis program for Windows 95/98/NT. *Nucleic Acids Symposium Series*, 41: 95-98. https://doi.org/10.14601/Phytopathol_Mediterr-14998u1.29

Hoang, D. T., Chernomor, O., von Haeseler, A., Minh, B. Q., & Le, S. V. 2017. UFBoot2: Improving the Ultrafast Bootstrap Approximation. *Molecular Biology and Evolution*. https://doi.org/10.1093/molbev/msx281

Hyman, L. H. 1941. Terrestrial flatworms from the Canal Zone, Panama. *American Museum Novitates*, 1105: 1-11.

Justine J-L, Gey D, Thévenot J, Gastineau R, Jones HD. 2020. The land flatworm Amaga expatria (Geoplanidae) in Guadeloupe and Martinique: new reports and molecular characterization including complete mitogenome. PeerJ 8:e10098 DOI 10.7717/peerj.10098

Jones, H. D. & Sterrer, W. 2005. Terrestrial planarians (Platyhelminthes, with three new species) and nemertines of Bermuda. *Zootaxa,* 1001: 31-58.

Kalyaanamoorthy, S., Minh, B. Q., Wong, T. K. F., Von Haeseler, A., & Jermiin, L. S. 2017. ModelFinder: Fast model selection for accurate phylogenetic estimates. *Nature Methods*, 14(6): 587-589. https://doi.org/10.1038/nmeth.4285

Katoh, K., Rozewicki, J., & Yamada, K. D. 2019. MAFFT online service: Multiple sequence alignment, interactive sequence choice and visualization. *Briefings in Bioinformatics* 20(4): 1160-1166. https://doi.org/10.1093/bib/bbx108

Kunzmann, L. 2007. Araucariaceae (Pinopsida): Aspects in palaeobiogeography and palaeobiodiversity in the Mesozoic. Zoologischer Anzeiger, 246: 257–277. https://doi.org/10.1016/j.jcz.2007.08.001

Marcus, E. 1954. Reports of the Lund University Chile Expedition 1948-1949. 11. Turbellaria. *Lunds Universitets Årsskrift,* 49(13): 3-114.

McHugh, D. 2000. Molecular phylogeny of the Annelida. *Canadian Journal of Zoology,* 78(11), 1873-1884. doi:10.1139/z00-141.

Murillo, J., Ruiz, E., Landrum, L.R., Stuessy, T.F. & Barfuss, M.H.J. 2011. Phylogenetic relationships in Myrceugenia (Myrtaceae) based on plastid and nuclear DNA sequences. Molecular phylogenetics and evolution, 62, 764–776. https://doi.org/10.1016/j.ympev.2011.11.021

Negrete, L., Álvarez-Presas, M., Riutort, M. & Brusa, F. 2020. Integrative taxonomy of land planarians (Platyhelminthes: Geoplanidae) from the Andean-Patagonian Forests from Argentina and Chile, with the erection of two new genera. *Journal of Zoological Systematics and Evolutionary Research,* 00: 1-25. doi: 10.1111/jzs.12444

Negrete, L., Gira, R. D., & Brusa, F. 2019. Two new species of land planarians (Platyhelminthes, Tricladida, Geoplanidae) from protected areas in the southern extreme of the Paranaense Rainforest, Argentina. *Zoologischer Anzeiger,* 279: 38-51. doi:10.1016/j.jcz.2019.01.002

Nguyen, L-T., Schmidt, H. A., von Haeseler, A. & Minh, B. Q. 2015. IQ-TREE: A fast and effective stochastic algorithm for estimating maximum likelihood phylogenies. *Molecular Phylogenetics and Evolution* 32: 268-274.

Ogren, R. E. & Kawakatsu, M. 1990. Index to the species of the family Geoplanidae (Turbellaria, Tricladida, Terricola) Part I: Geoplaninae. *The Bulletin of Fuji Women's College*, 28: 79-166.

Ogren, R. & Kawakatsu, M. 1990. Index to the species of the family Geoplanidae (Turbellaria, Tricladida, Terricola). Part II: Caenoplaninae and Pelmatoplaninae. *Bulletin of the Fuji Women's College,* 29(2): 25-102.

Ronquist, F., Teslenko, M., van der Mark, P., Ayres, D. L., Darling, A., Höhna, S. & Huelsenbeck, J. P. 2012. MrBayes 3.2: Efficient Bayesian Phylogenetic Inference and

Model Choice Across a Large Model Space. *Systematic Biology*, 61(3): 539-542. https://doi.org/10.1093/sysbio/sys029

Ruiz-Trillo, I., Riutort, M., Littlewood, D. T. J., Herniou, E. A., & Baguñà, J. 1999. Acoel flatworms: earliest extant bilaterian Metazoans, not members of Platyhelminthes. *Science, 283*(5409), 1919-1923.

Salvi, D., Macali, A. & Mariottini P. 2014. Molecular Phylogenetics and Systematics of the Bivalve Family Ostreidae Based on rRNA Sequence-Structure Models and Multilocus Species Tree. *PLoS ONE,* 9(9): e108696. https://doi.org/10.1371/journal.pone.0108696

Sandison, A. T. 1955. The histological examination of mummified material. *Stain technology*, 60(6): 227-283. https://doi.org/10.3109/10520295509114479

Schmidt, 1902. Zur Kenntnis der Tricladenaugen und der Anatomie von Polycladus gayi. *Zeitschr. Wiss. Zool.* 72: 545-564.

Sluys, R. 1999. Global diversity of land planarians (Platyhelminthes, Tricladida, Terricola): a new indicator taxon in biodiversity and conservation studies. *Biodivers. Conserv.*, 8:1663-1681.

Sluys, R., Kawakatsu, M., Riutort, M. & Baguñà J. 2009. A new higher classification of planarian flatworms. *Journal of Natural History* 43 (29-30): 1763-1777.

Sluys, R.; Mateos, E.; Riutort, M. & Álvarez-Presas, M. 2016. Towards a comprehensive, integrative analysis of the diversity of European microplaninid land flatworms (Platyhelminthes, Tricladida, Microplaninae), with the description of two peculiar new species. Systematics and Biodiversity 14(1): 1-23.

Smythe, A.B., Holovachov, O. & Kocot, K.M. 2019. Improved phylogenomic sampling of free-living nematodes enhances resolution of higher-level nematode phylogeny.*BMC Evol Biol.* 19: 121. https://doi.org/10.1186/s12862-019-1444-x

Stimpson, W. 1857. Prodromus descriptionis animalium evertebratorum, etc. *Proceedings of the Academy of Natural Sciences of Philadelphia*, 9: 19-31.

Winsor, L. 2006. New and revised terrestrial flatworm taxa (Platyhelminthes: Tricladida: Terricola) of Australia and the Subantarctic Islands of New Zealand. *Tuhinga*, 17: 81-104.

Supplementary material

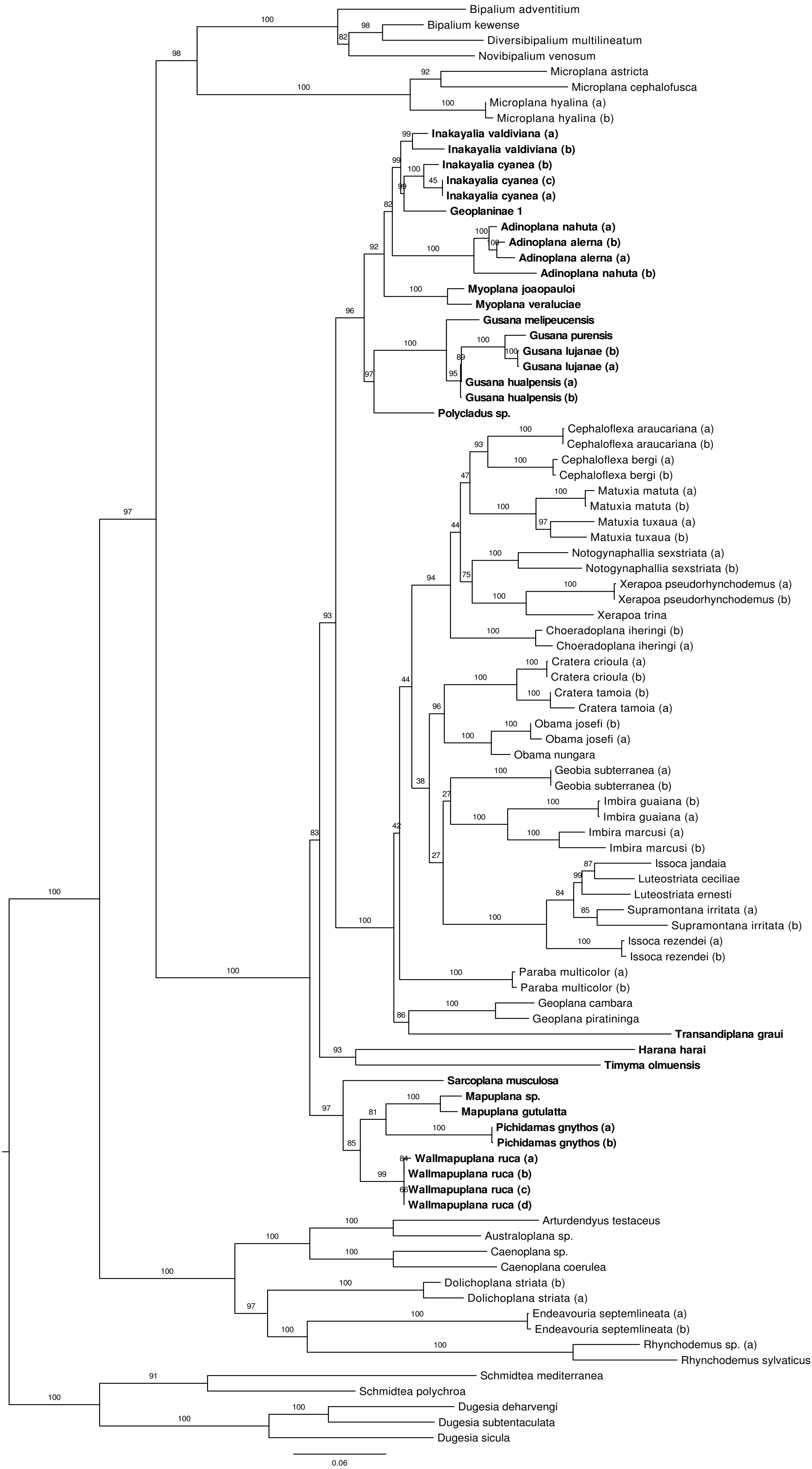

Fig. S1. Phylogenetic tree inferred from the concatenated genes (28S rDNA + COI) under maximum likelihood as the optimality criteria. Numbers at the nodes correspond to ultrafast bootstrap values. Chilean terminals are written in bold.

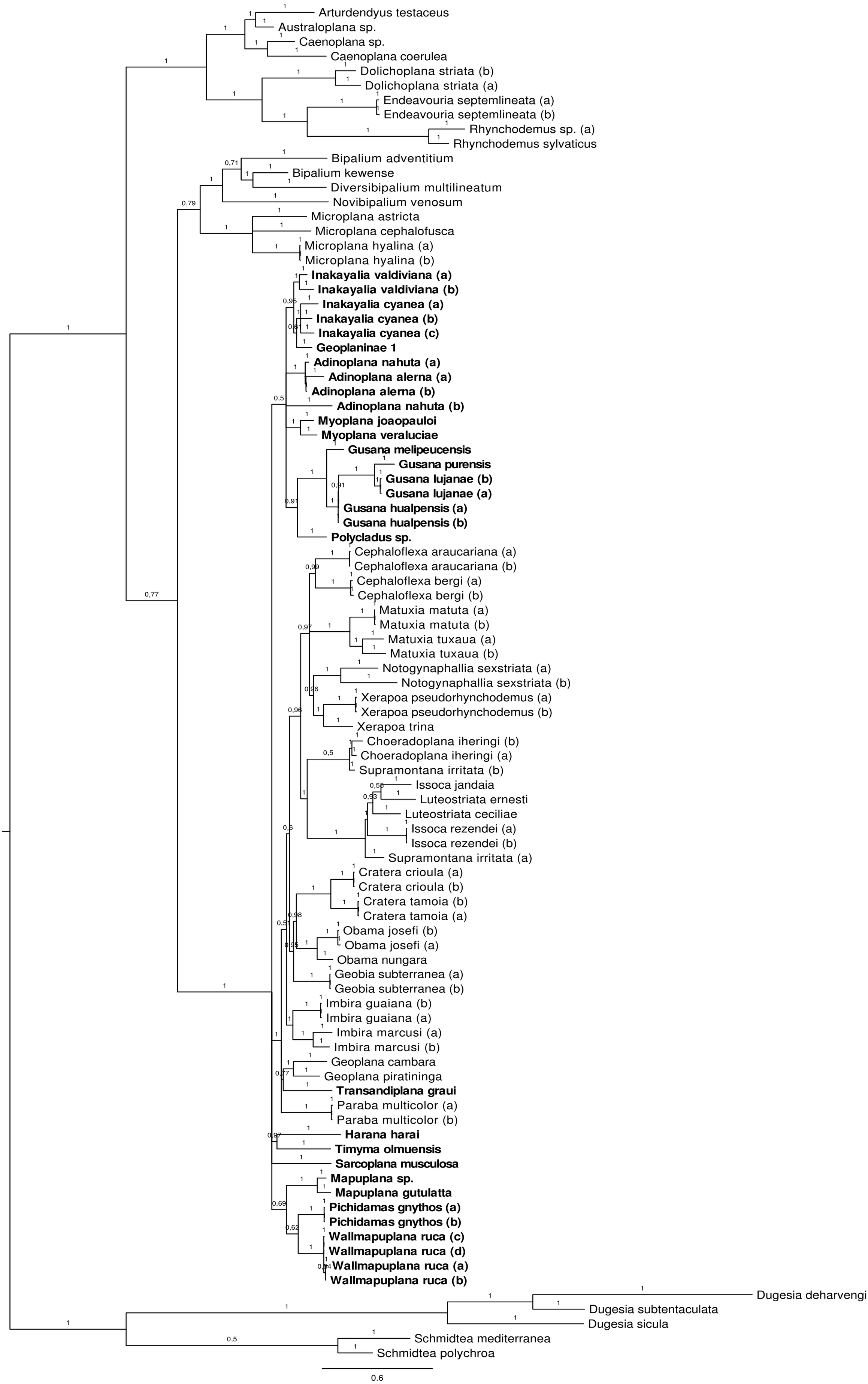

Fig. S2. Phylogenetic tree inferred by Bayesian inference from the concatenated genes (28S rDNA +COI). Numbers at the nodes correspond to posterior probabilities. Chilean terminals are written in bold.

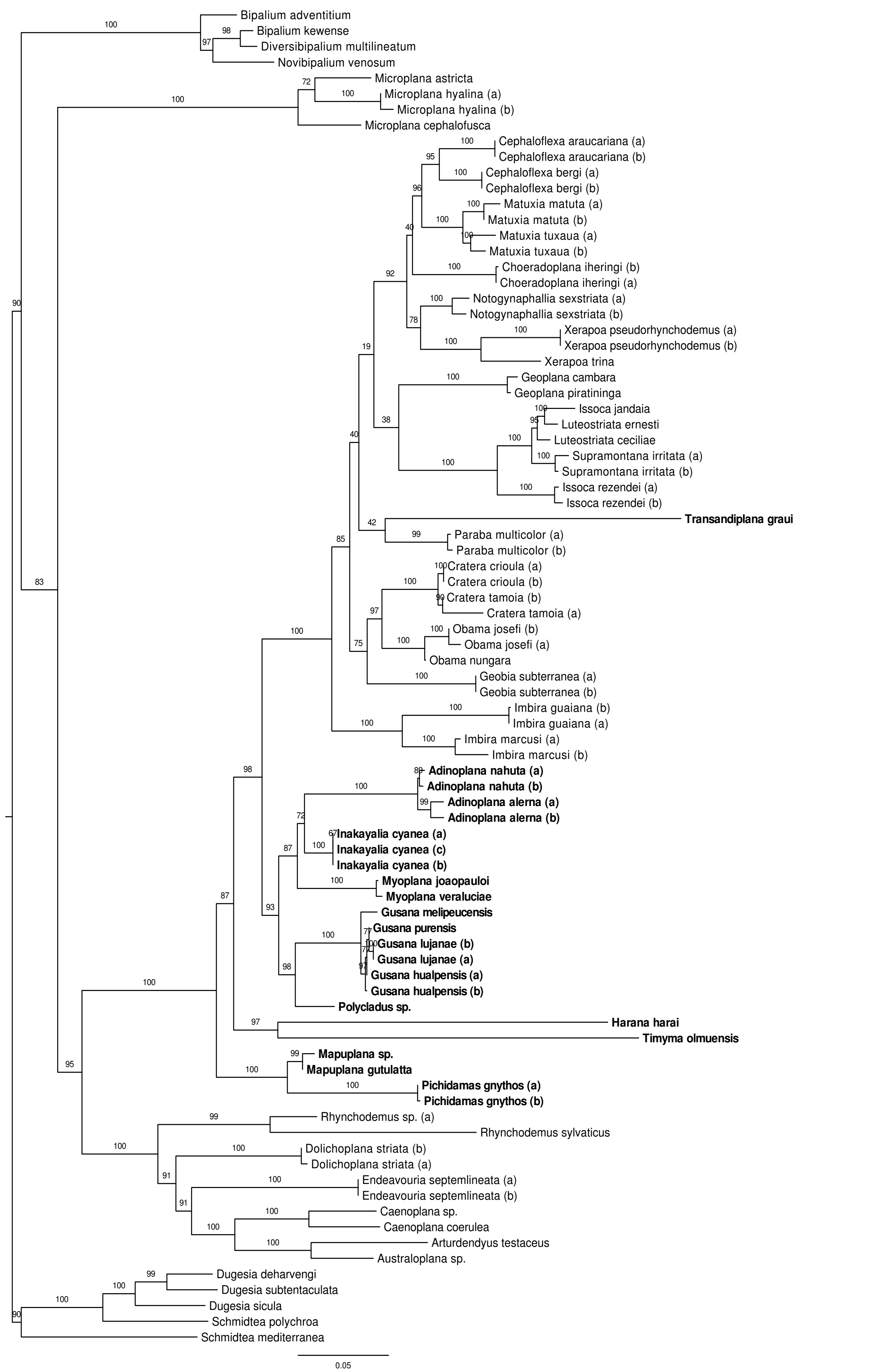

Fig. S3. Phylogenetic tree inferred by Bayesian inference from the 28S rDNA gene. Numbers at the nodes correspond to posterior probabilities. Chilean terminals are written in bold.

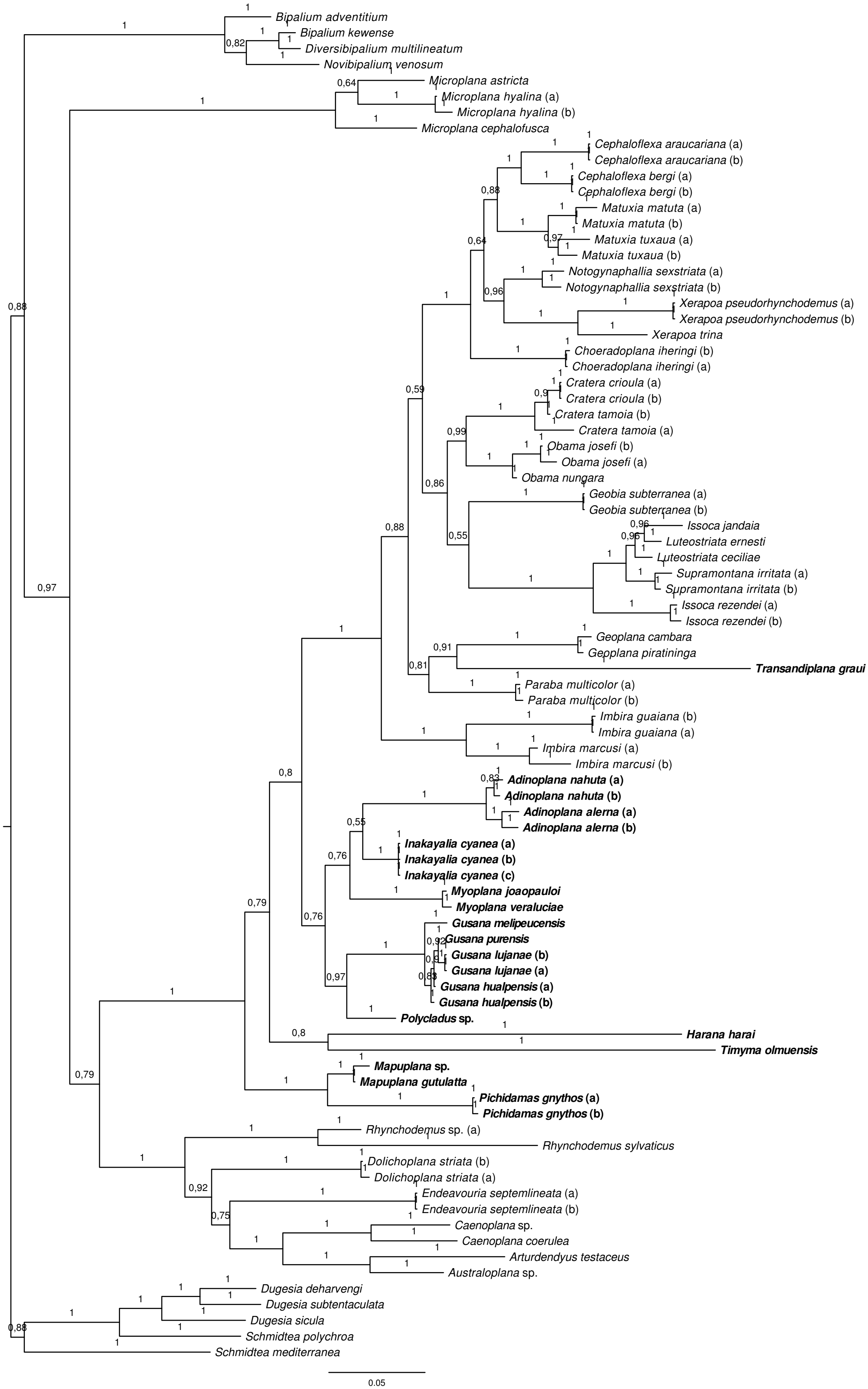

Fig. S4. Phylogenetic tree inferred by Bayesian inference from the 28S rDNA gene. Numbers at the nodes correspond to posterior probabilities. Chilean terminals are written in bold.

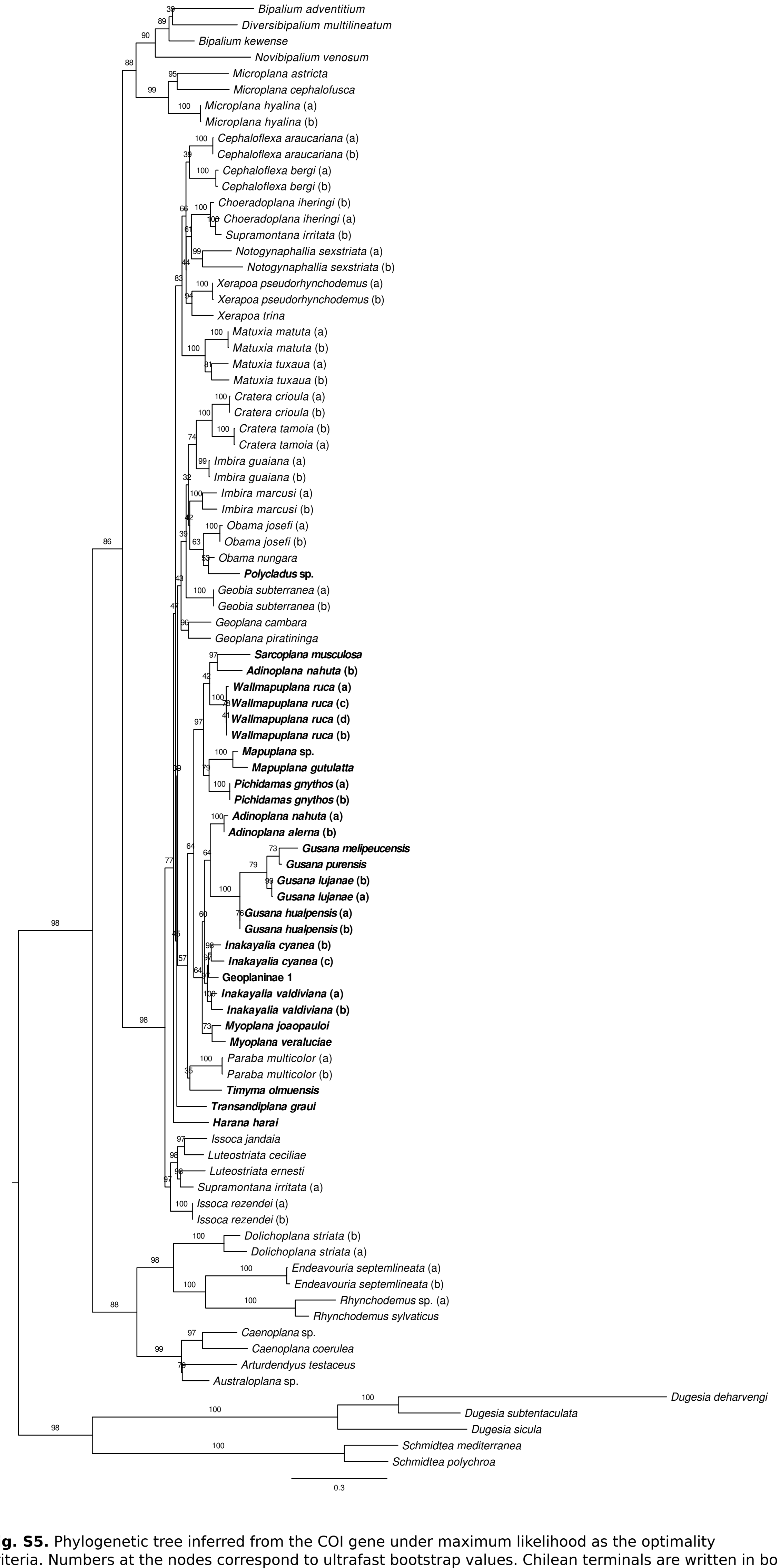

Fig. S5. Phylogenetic tree inferred from the COI gene under maximum likelihood as the optimality criteria. Numbers at the nodes correspond to ultrafast bootstrap values. Chilean terminals are written in bold.

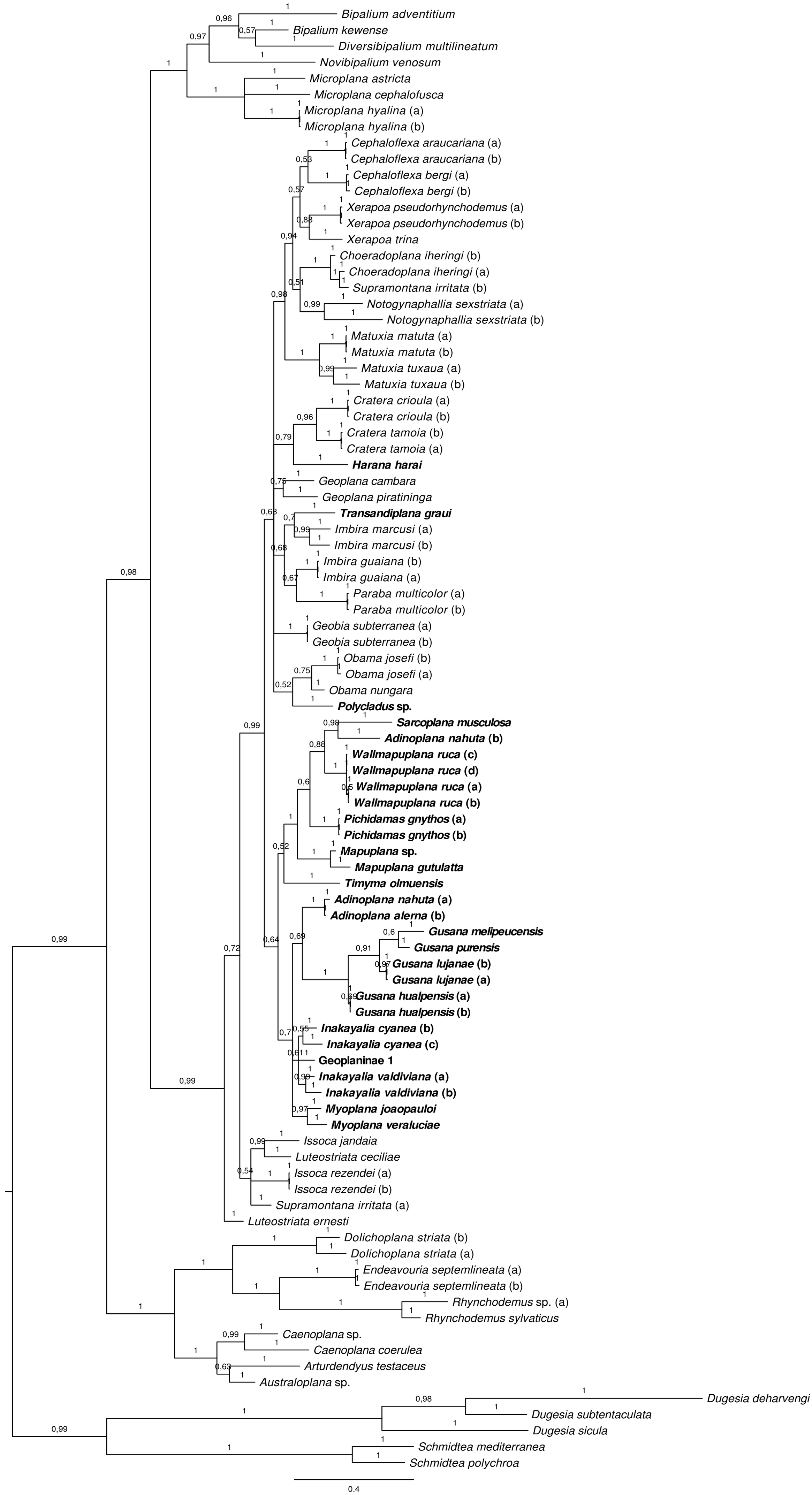

Fig. S6. Phylogenetic tree inferred by Bayesian inference from the COI gene. Numbers at the nodes correspond to posterior probabilities. Chilean terminals are written in bold.

Table S1. Individuals used in the study with their corresponding sequence's GenBank accession numbers. Sequences generated for this study are indicated with *.

Family	Subfamily	Tribe	Terminal name	Formal species name	28S rDNA - Accession Number	COI – Accession Number
Dugesidae Ball, 1974			*Dugesia deharvengi*	*Dugesia deharvengi* Kawakatsu & Mitchell, 1989	KF907824	KF907820
			Dugesia subtentaculata	*Dugesia subtentaculata* (Draparnaud, 1801)	MK712520	MK712622
			Dugesia sicula	*Dugesia sicula* Lepori, 1948	DQ665969	KF308800
			Schmidtea mediterranea	*Schmidtea mediterranea* Benazzi, Baguna, Ballester & del Papa, 1975	MG457267	JF837062
			Schmidtea polychroa	*Schmidtea polychroa* (Schmidt, 1861)	DQ665993	FJ647021
Geoplanidae Stimpson, 1857	Bipaliinae Stimpson, 1857		*Bipalium adventitium*	*Bipalium adventitium* Hyman, 1943	AF022758	AF178306
			Bipalium kewense	*Bipalium kewense* Moseley, 1878	KJ659703	KJ659609
			Diversibipalium multilineatum	*Diversibipalium multilineatum* (Makino & Shirasawa, 1983)	KU245357	KU245358
			Novibipalium venosum	*Novibipalium venosum* (Kaburaki, 1922)	DQ665981	DQ666048
	Geoplaninae Stimpson, 1857	Adinoplanini trib. n.	*Adinoplana alerna* (a)	*Adinoplana alerna* Carbayo & Almeida sp. n.	*	*
			Adinoplana alerna (b)	*Adinoplana alerna* Carbayo & Almeida sp. n.	*	*
			Adinoplana nahuta (a)	*Adinoplana nahuta* Carbayo & Almeida sp. n.	*	*
			Adinoplana nahuta (b)	*Adinoplana nahuta* Carbayo & Almeida sp. n.	*	*
		Geoplanini Stimpson, 1857	*Cehaloflexa araucariana* (a)	*Cephaloflexa araucariana* Carbayo & Leal-Zanchet, 2003	KC608436	KC608319
			Cephaloflexa araucariana (b)	*Cephaloflexa araucariana* Carbayo & Leal-Zanchet, 2003	KC608433	KC608316
			Cephaloflexa bergi (a)	*Cephaloflexa bergi* Graff, 1899	KC608355	KC608240
			Cephaloflexa bergi (b)	*Cephaloflexa bergi* Graff, 1899	KC608353	KC608238
			Choeradoplana iheringi (a)	*Choeradoplana iheringi* Graff, 1899	KC608437	KC608320
			Choeradoplana iheringi (b)	*Choeradoplana iheringi* Graff, 1899	MF802624	MF802642
			Cratera crioula (a)	*Cratera crioula* (Froehlich, 1955)	KC608441	KC608324
			Cratera crioula (b)	*Cratera crioula* (Froehlich, 1955)	KC608440	KC608323
			Cratera tamoia (a)	*Cratera tamoia* (Froehlich, 1955)	KC608369	KC608254
			Cratera tamoia (b)	*Cratera tamoia* (Froehlich, 1955)	KC608361	KC608246
			Geobia subterranea (a)	*Geobia subterranea* Schultze & Müller, 1857	KC608340	KC608225
			Geobia subterranea (b)	*Geobia subterranea* Schultze & Müller, 1857	KC608370	KC608255
			Geoplana cambara	*Geoplana cambara* Almeida & Carbayo, 2018	KC608377	KC608262
			Geoplana piratininga	*Geoplana piratininga* Almeida & Carbayo, 2018	KC614479	KC608247
			Imbira guaiana (a)	*Imbira guaiana* Leal-Zanchet & Carbayo, 2001	KC608431	KC608314
			Imbira guaiana (b)	*Imbira guaiana* Leal-Zanchet & Carbayo, 2001	KC608344	KC608229
			Imbira marcusi (a)	*Imbira marcusi* Carbayo et al., 2013	KC608406	KC608291
			Imbira marcusi (b)	*Imbira marcusi* Carbayo et al., 2013	KC608356	KC608241
			Issoca jandaia	*Issoca jandaia* Froehlich, 1954	KC608385	KC608270

			Issoca rezendei (a)	*Issoca rezendei* (Schirch, 1929)	KC608378	KC608263
			Issoca rezendei (b)	*Issoca rezendei* (Schirch, 1929)	KC608363	KC608248
			Luteostriata ceciliae	*Luteostriata ceciliae* (Froehlich & Leal-Zanchet, 2003)	KC608438	KC608321
			Luteostriata ernesti	*Luteostriata ernesti* (Leal-Zanchet & Froehlich, 2006)	KC608430	KC608313
			Matuxia matuta (a)	*Matuxia matuta* Froehlich, 1954	KC608392	KC608277
			Matuxia matuta (b)	*Matuxia matuta* Froehlich, 1954	KC608391	KC608276
			Matuxia tuxaua (a)	*Matuxia tuxaua* Froehlich, 1954	KC608419	KC608302
			Matuxia tuxaua (b)	*Matuxia tuxaua* Froehlich, 1954	KC608368	KC608253
			Notogynaphallia plumbea (a)	*Notogynaphallia plumbea* (Froehlich, 1956)	KC608420	KC608303
			Notogynaphallia sexstriata (a)	*Notogynaphallia sexstriata* (Graff, 1899)	KC608372	KC608257
			Notogynaphallia sexstriata (b)	*Notogynaphallia sexstriata* (Graff, 1899)	KC608347	KC608232
			Obama josefi (a)	*Obama josefi* Carbayo & Leal-Zanchet, 2001	KT714098	KU564143
			Obama josefi (b)	*Obama josefi* Carbayo & Leal-Zanchet, 2001	KC608435	KC608318
			Obama nungara	*Obama nungara* Carbayo, Alvarez-Presas, Jones & Riutort, 2016	KT714094	KT714108
			Paraba multicolor (a)	*Paraba multicolor* Graff, 1899	KC608386	KC608271
			Paraba multicolor (b)	*Paraba multicolor* Graff, 1899	KC608415	KC608299
			Pasipha pasipha	*Pasipha pasipha* (Marcus, 1951)	KC608410	-
			Supramontana irritata (a)	*Supramontana irritata* Carbayo & Leal-Zanchet, 2003	KC608451	KC608334
			Supramontana irritata (b)	*Supramontana irritata* Carbayo & Leal-Zanchet, 2003	KC608439	KC608322
			Xerapoa hystrix	*Xerapoa hystrix* Froehlich, 1954	KC608418	-
			Xerapoa pseudorhynchodemus (a)	*Xerapoa* pseudorhynchodemus (Riester, 1938)	KC608352	KC608237
			Xerapoa pseudorhynchodemus (b)	*Xerapoa* pseudorhynchodemus (Riester, 1938)	KC608350	KC608235
			Xerapoa trina	*Xerapoa trina* Marcus, 1951	KC608365	KC608250
		Gusanini trib. n.	*Gusana hualpensis* (a)	*Gusana hualpensis* Cabayo	KC608448	KC608331
			Gusana hualpensis (b)	*Gusana hualpensis* Carbayo	KC608449	KC608332
			Gusana melipeucensis	*Gusana melipeucensis* Almeida & Carbayo	MW854310	MW865707
			Gusana lujanae (a)	*Gusana lujanae* Almeida & Carbayo	MW854313	MW865709
			Gusana lujanae (b)	*Gusana lujanae* Almeida & Carbayo	MW854312	MW865708
			Gusana purensis	*Gusana purensis* Bolonhezi, Almeida & Carbayo	MW854311	MW881250
		Haranini trib. n.	*Harana harai*	*Harana harai* Carbayo & Almeida sp. n.	*	*
		Inakayaliini trib. n.	*Inakayalia valdiviana* (a)	*Inakayalia valdiviana* (Grau & Carbayo) comb. n.	-	MT649093
			Inakayalia valdiviana (b)	*Inakayalia valdiviana* (Grau & Carbayo) comb. n.	-	MT649094
			Inakayalia cyanea (a)	*Inakayalia cyanea* Almeida & Carbayo sp. n.	*	*
			Inakayalia cyanea (b)	*Inakayalia cyanea* Almeida & Carbayo sp. n.	*	*
			Inakayalia cyanea (c)	*Inakayalia cyanea* Almeida & Carbayo sp. n.	*	*
		Myoplanini trib. n.	*Myoplana veraluciae*	*Myoplana veraluciae* Almeida & Carbayo sp. n.	*	*
			Myoplana joaopauloi	*Myoplana joaopauloi* Almeida & Carbayo sp. n.	*	*
		Polycladini trib. n.	*Polycladus* sp.	*Polycladus* sp. Blanchard,	KC608343	KC608228

				1845		
		Sarcoplanini trib. n.	*Mapuplana gutulatta*	*Mapuplana gutulatta* Almeida & Carbayo sp. n.	*	*
			Mapuplana sp. 1	*Mapuplana* sp. 1	*	*
			Pichidamas gnythos (a)	*Pichidamas gnythos* Almeida & Carbayo sp. n.	*	*
			Pichidamas gnythos (b)	*Pichidamas gnythos* Almeida & Carbayo sp. n.	*	*
			Sarcoplana musculosa	*Sarcoplana musculosa* Almeida & Carbayo sp. n.	*	*
			Wallmapuplana ruca (a)	*Wallmapuplana ruca* (Marcus, 1954) comb n.	-	MT649095
			Wallmapuplana ruca (b)	*Wallmapuplana ruca* (Marcus, 1954) comb n.	-	MT649096
			Wallmapuplana ruca (c)	*Wallmapuplana ruca* (Marcus, 1954) comb n.	-	MT649097
			Wallmapuplana ruca (d)	*Wallmapuplana ruca* (Marcus, 1954) comb n.	-	MT649098
		Timymini Almeida & Carbayo, 2021	*Timyma olmuensis* sp. nov.	*Timyma olmuensis* sp. nov.	MW354692	MW331438
	Microplaninae Pantin, 1953		*Microplana astricta*	*Microplana astricta* Sluys, Álvarez-Presas & Mateos, 2017	KU872619	KU867128
			Microplana cephalofusca	*Microplana cephalofusca* Sluys, Álvarez-Presas & Mateos, 2017	KU872620	KU867133
			Microplana hyalina (a)	*Microplana hyalina* Vila-Farré & Sluys, 2011	KU872630	KU867167
			Microplana hyalina (b)	*Microplana hyalina* Vila-Farré & Sluys, 2011	KU872631	KU867168
	Rhynchodeminae Graff, 1896	Caenoplanini Ogren & Kawakatsu, 1991	*Arturdendyus testaceus*	*Arturdendyus testaceus* (Hutton, 1880)	DQ665952	MN990643
			Australoplana sp.	*Australoplana* sp. Winsor, 1991	DQ665955	DQ666028
			Caenoplana coerulea	*Caenoplana coerulea* Moseley, 1877	DQ665961	DQ666030
			Caenoplana sp.	*Caenoplana* sp. Moseley, 1877	DQ665964	DQ666031
			Endeavouria septemlineata (a)	*Endeavouria septemlineata* (Hyman, 1939)	KC608348	KC608233
			Endeavouria septemlineata (b)	*Endeavouria septemlineata* (Hyman, 1939)	KC608337	KC608222
		Rhynchodemini Heinzel, 1929	*Dolichoplana striata* (a)	*Dolichoplana striata* Moseley, 1877	KC608341	KC608226
			Dolichoplana striata (b)	*Dolichoplana striata* Moseley, 1877	KJ659698	KJ659679
			Rhynchodemus sp. (a)	*Rhynchodemus* sp. Leidy, 1851	KJ659697	KJ659676
			Rhynchodemus sp. (b)	*Rhynchodemus* sp. Leidy, 1851	KJ599733	-
			Rhynchodemus sylvaticus	*Rhynchodemus sylvaticus* (Leidy, 1851)	KJ659706	KJ659686

Table S2. List of primers used to amplify and sequencing the DNA fragments.

Gene region	Primer name	Utilization	Sequence (5' to 3')	Reference	Annealing temperature
28S rDNA	LSU 5F (Forward)	Amplification and sequencing	TAGGTCGACCCGCTGAAYTTAAGCA	Littlewood *et al.* (1997)	56-58ºC
	Rob1 (Forward)	Sequencing	GTCCAATAGCAAACAAGTCCCG	Heneberg et al. (2013)	-
	LSU 330F (Forward)	Sequencing	CAAGTACCGTGAGGGAAAGTTG	Williams & Ozawa (2006)	-
	Rob2 (Reverse)	Sequencing	CACGYACTRTTTACCTC	Chisholm et al., (2001)	-
	ECD-2 (Reverse)	Sequencing	CCTTGGTCCGTGTTTCAAGACGGG	Littlewood *et al.* (1997)	-
	LSU 1500R (Reverse)	Amplification and sequencing	GCTATCCTGAGGGAAACTTCG	Tkach *et al.* (1999)	56-58ºC
COI	BarS (Forward)	Amplification and sequencing	GTTATGCCTGTAATGATTG	Álvarez-Presas *et al.* (2011)	45ºC
	FlatwormCOIF (Forward)	Sequencing	GAGCAACAACATAATAAGTATCATG	Sunnucks *et al.* (2006)	-
	COIR (Reverse)	Amplification and sequencing	CCWGTYARMCCHCCWAYAGTAAA	Lázaro *et al.* (2009)	45ºC

References:

Álvarez-Presas M, Carbayo F, Rozas J, Riutort M. 2011. Land planarians (Platyhelminthes) as a model organism for finescale phylogeographic studies: understanding patterns of biodiversity in the Brazilian Atlantic Forest hotspot. *Journal of Evolutionary Biology,* 24: 887-896.

Chisholm, L.A., Morgan, J.A.T., Adlard, R.D., Whittington, I.D., 2001. Phylogenetic analysis of the Monocotylidae (Monogenea) inferred from 28S rDNA sequences. *International Journal for Parasitology,* 31: 1253-1263.

Heneberg, P. & Literák, I. 2013. Molecular phylogenetic characterization of Collyriclum faba with reference to its three host-specific ecotypes. *Parasitology International*, 62: 262-267.

Lázaro, E. M., Sluys, R., Pala, M., Stocchino, G. A., Baguña, J. & Riutort, M. 2009. Molecular barcoding and phylogeography of sexual and asexual freshwater planarians of the genus Dugesia in the Western Mediterranean (Platyhelminthes, Tricladida, Dugesiidae). *Molecular Phylogenetics and Evolution*, 52: 835-845.

Littlewood, D. T. j.; Rohde, K. & Chough, K. A. 1997. Parasite speciation within or between host species? - Phylogenetic evidence from site-specific polystome monogeneans. *International Journal for Parasitology,* 27: 1289-1297.

Sunnucks P, Blacket MJ, Taylor JM, Sands CJ, Ciavaglia SA, Garrick RC, Tait NN, Rowell DM, Pavlova A. 2006. A tale of two flatties: different responses of two terrestrial flatworms to past environmental climatic fluctuations at Tallaganda in montane southeastern Australia. *Molecular Ecology,* 15: 4513-4531.

Tkach, V.; Grabda-Kazubska, B.; Pawlowski, J. & Swiderski, Z. 1999. Molecular and morphological evidence for close phylogenetic affinities of the genera *Macrodera*, *Lepdophallus*, *Metaleptophallus* and *Paralepoderma* (Digenea, Plagiorchiata). *Acta Parasitologica*, 44: 170-179.

Williams, S. T. & Ozawa, T. 2006. Molecular phylogeny suggests polyphyly of both the turban shells (family Turbinidae) and the superfamily Trochoidea (Mollusca: Vetigastropoda). *Molecular Phylogenetics and Evolution*, 39: 33-51.

Table S3. Selected diagnostic traits for the main new clades and genera. +: present; -: absent, (C+L): one layer with circular and longitudinal mixed muscles; C-L: one muscular layer with circular fibers, folowed by a layer of longitudinal fibers.

	Semilunate headplate	Eyes dorsal	Sensory depressions	Creeping sole	Main nervous system organized in nerve cords	Cephalic retractor muscle	Dorsal longitudinal cutaneous muscle sunken	Ventral long. cut. muscl sunken	Subneural parencymatic muscle	Transneural parenchymatic muscle	Ventralparenchymatic muscle	Pharyngeal pouch over cop. app.	outer pharyngeal musculature with a third innermost longitudinal muscle	Inner pharyngeal muscle organization	Multicellular glands	Ventral testes	Musculo-glandular genital organs	(Common) ovovitelline duct dilated	Ootype	Blind canal in the female atrium
Sarcoplanini																				
Sarcoplana	-	-	+	wide	-	+	-	-	decussate	-	-	-	-	(C+L)	-	-	In common atrium	-	-	-
Mapuplana	-	-	+	wide	-	+	-	+	decussate	-	-	-	-	(C+L)	+	-	-	-	-	+
Pichidamas	-	-	+	narrow	-	+	-	-	decussate	-	+	-	-	(C+L)	+	-	In male atrium	-	-	-
Wallmapuplana	-	-	+	wide	-	-	-	-	+	-	-	-	-	(C+L)	+	-	-	-	-	-
Haranini											-									
Harana	-	-	-	wide	+	-	-	-	-	-	-	+	+	C-L	-	?	-	-	-	-
Timymini																				
Timyma	+	-	-	wide	-	-	-	-	-	-	-	+	+	C-L	-	+	-	-	+	-
Geoplanini																				
Transandiplana	-	-	+	wide	+	-	-	-	-	-	-	-	-	(C+L)	-	-	-	-	-	-
Polycladini											-									
Polycladus	-		-	wide	+	-	-	-	transverse	longitudinal	-	-	?	?	-	-	-	-	-	-
Gusanini																				
Gusana	-	-	-	wide	-	-	+	+	-	-	-	-	+	(C+L)	-	-	-	-	+	-
Myoplanini																				
Myoplana	-	-	-	wide	-	-	-	+	decussate	decussate	-	-	+	variable	-	-	-	-	-	-
Inakayalini																				
Adinoplana	-	+	-	wide	-	-	-	-	-	-	-	-	+	C-L	--	-	In male and female atria	-	-	-
Inakayalia	-	+	-	wide	-	-	-	-	-	-	-	-	+	variable	-	-	-	+	-	-